PARAMETRIC STUDIES OF DOWNDRAFT GASIFIER ALONG WITH TAR CRACKING

A Thesis Submitted in Partial Fulfillment of

the Requirements for the Award of the Degree of

DOCTOR OF PHILOSOPHY

By

GAJANAN NAMDEORAO SHELKE

DEPARTMENT OF MECHANICAL ENGINEERING
INDIAN INSTITUTE OF TECHNOLOGY GUWAHATI
GUWAHATI – 781039, INDIA
DECEMBER 2016

This thesis is dedicated to

My Parents

Mr. Namdeorao Mahipatrao Shelke

and Mrs. Chandrakala N. Shelke

My Wife

Mrs. Sunita Gajanan Shelke

My Children

Aumkar Gajanan Shelke

Hrucha Gajanan Shelke

Declaration

I hereby certify that the information presented in this thesis is entirely my own account of research and contains as its main content work expect where otherwise stated, which has not previously been submitted for a degree or diploma at this institute or any tertiary educational institution.

Gajanan Namdeorao Shelke
Roll No.-10610331
Department of Mechanical Engineering
Indian Institute of Technology Guwahati
Guwahati – 781039, India
December 2016.

Certificate

It is certified that the work contained in the thesis entitled **Parametric Studies of Downdraft Gasifier Along With Tar Cracking** by **Gajanan Namdeorao Shelke**, a student in the Department of Mechanical Engineering, Indian Institute of Technology Guwahati, India, for the award of the degree of **Doctor of Philosophy** has been carried out under my supervision and this work has not been submitted elsewhere for the degree.

Dr. Pinakeswar Mahanta
Professor
Department of Mechanical Engineering
Indian Institute of Technology Guwahati
Guwahati – 781039, India

Abstract

The world reserve of the fossil fuel is drastically reducing and there is a need for replacing the same with alternative fuel to meet the demand of electricity and thermal power. With rapid industrialization and improvement in standard of living, demand of energy is increasing rapidly. The supply and demand of energy is mismatching in major energy generating systems.

Amongst all the renewable sources of energy, use of biomass for power generation is gaining attention by researchers as biomass is abundantly available and is compatible to the environmental pollution. Considering country like India whose economy is based on agriculture with more than 70% of the population engaged in the sector, enough biomass is generated to produce electricity and thermal power. However, state of the technology to convert biomass into power is limited. Power obtained from biomass gasification is a promising technology but limited with generalized design.

In the present investigation the feasibility of loose biomass in the form of briquette and pellets in an existing downdraft gasifier designed to operate with woodchips is tested. Performance evaluation of the gasifier in terms of temperature profile, gas quality and gas yield are carried out with various equivalence ratios. Comparison is made for the aforementioned parameters for biomass briquettes, pellets and woodchips as feedstock. Further, an innovative study is carried out on the in-situ treatment of the tar using the biomass-dolomite pellets.

The parametric studies of downdraft gasifier are carried out with the various equivalence ratios and feedstock. It is observed that performance at equivalence ratio of 0.32 is comparatively good for all the three feedstock used in the experiments. The pellets with 20% dolomite give good gas composition.

A liquid gas bubbling fluidized bed set-up is developed for thermal cracking of tar obtained from the biomass gasification. Tar is a heavy hydrocarbon. It is cracked using fluidization under high temperature and using dolomite as catalyst.

The performance analysis of the tar cracking unit is carried out using various percentage of dolomite as catalyst. The cracked gas composition is found to be better with 10-15 % dolomite mixture by weight. In the present experiments tar is converted into cracked gas by fluidizing with air at flow rate 0.0015 m^3/h and followed by heating at temperature

above 800^0 C and converted into cracked gas. The tar cracking unit can be retrofitted in conventional gasifier system to get better performance and yield of gas.

Thus the present methodology with in-situ tar cracking in downdraft gasifier and novel liquid-gas bubbling fluidized bed technique is found effective for cracking of tar coming out from gasification.

Acknowledgement

First of all I give my sincere thanks to Almighty God for his blessings throughout my research work. I wish to express my profound sense of gratitude to my supervisor, Professor Pinakeswar Mahanta for his invaluable guidance and inspiration in bringing out this work to the present shape. His mentorship was eminent in planning implementation of my long term goals. I can never forgot the vigour and attention bestowed by him in taking my research ahead. His innovative idea and acumen helped me truly understanding research and to bring it in practical. He encouraged me to grow as a researcher as well as an instructor and independent philosopher also. His personal character combined with professional ethics will remain a source of inspiration for the rest of my life.

I would like to thank my doctoral committee members, Prof. A. K. Das, Dr. Vinayak Kulkarni and Dr. G. Pugazhenthi for their valuable suggestions, insightful comments and encouragement at different stages of research.

I am thankful to Head of Department Prof. A.K. Das, Prof. P. Mahanta and Prof. D. Chakraborty for providing all kind of facilities in Department of mechanical Engineering.

I would like to acknowledge Dr. Pradip Kumar Chatterjee, chief scientist and Dr. Malay kr. Karamkar, senior scientist of Central Mechanical Engineering Institute, Durgapur for arranging a visit to Hara Parbati Rice Mill Private Ltd Dhanbad, for case study of 25 kW downdraft Gasifier. I am also thankful to Mr. Santosh Rateria Chairman M/S Synergy Ltd. Jogigopa, Assam for allowing me for Case Study of Bamboo Char Plant.

I wish to express my thank to, Mr. Dilip Chatri, Mr. Mrinal Sarma, Mr. Dipak kr Deka, Mr. Upen Gohain and other staff members of Central Workshop for helping me in various stages of fabrication of the experimental setup. Without their timely support this work could not be accomplished.

I express my thank to Mr. Sanjaykumar Yadav, Mr. Anil Kumar Halvi, Mr. Gopal Kumar Verma, Mr. Biren Barman, Mr. Dipankar Kalita, Mr. Deepjyoti , Mr. Akash Bhowmick, Mr. Deep Bora and Mr. Tapan Das for their help throughout the experimental investigation.

I am very much thankful to Dr. Sibashankar Mohapatra. Dr. Ranjit Patil, Dr. A. Muthuraja, Dr. Satish, Mr. Dhiren Huzuri, Mr. Sanjib Sarma, Mr. Rituraj Saikia, Mr. Nip Bora, Mr. Devarshi Kashyap, Mr. Chilka Ravichandra, Mr. Ashish Chaudhari Mr. Jnyana Pati, Mr. Pavitra Singh. Mr. Santosh Hotta, Mr. Abinash Mohapatra, Ms. Dipti Yadav, Mr. Jonmani Kalita and all the friends for their encouragement and help.

Hearty thanks to Mrs. Anita Mahanta for her kind support and encouragement in my social life which is unforgettable. She memorizes the Indian history of 'Gurukul' system with her kindness.

Sincere thanks to my brother Mr. Dnyaneshwar Shelke, Sister Mrs. Mandakini Cheke, brother in law Mr. Vinayak Cheke, Dr. Mohan Bajad and Dr. Mahesh Bajad for motivation and support.

At last but not least, I am highly indebted to my wife Sunita for her patience, endless support, sacrifice, love and inspiration towards the completion of my PhD thesis. My heartfelt love and appreciations go to my daughter Hrucha and son Aumkar for bearing me through the research period. I extend my sincere gratitude to my parents and parents-in-law for their constant encouragement and moral support.

Place: IIT Guwahati
Date: (Gajanan Namdeorao Shelke)

Contents

Nomenclature

BPV	:	By pass valve
CV_1	:	Control valve at compressor pipe compressor in TCC
CV_2	:	Control valve for aeration pipe in TCC
CV_3	:	Control valve for sampling port compressor in TCC
CV_4	:	Control valve for tar inlet compressor in TCC
CV_5	:	Control valve for residue outlet compressor in TCC
FV	:	Flare valve
S_1	:	Surface temperature at the top of the downdraft gasifier
S_2	:	Surface temperature at drying zone
S_3	:	Surface temperature at pre pyrolysis zone
S_4	:	Surface temperature at pyrolysis zone
S_5	:	Surface temperature at pre combustion zone
S_6	:	Surface temperature at combustion zone
S_7	:	Surface temperature at reduction zone
S_8	:	Surface temperature at reduction zone
S_9	:	Surface temperature at reduction zone
S_{10}	:	Surface temperature at Ash chamber
S_{11}	:	Surface temperature at producer gas line at the exit of reduction chamber
T_1	:	Temperature in drying zone at a distance 44 mm from vertical axis of gasifier
T_2	:	Temperature in drying zone at a distance 122 mm from vertical axis of gasifier
T_3	:	Temperature in drying zone at a distance 158 mm from vertical axis of gasifier
T_4	:	Temperature in drying zone at a distance 168 mm from vertical axis of gasifier
T_5	:	Temperature in pre pyrolysis zone at a distance 30 mm from the vertical axis of gasifier
T_6	:	Temperature in pre pyrolysis zone at a distance 112 mm from the vertical axis of gasifier

T_7 : Temperature in pre pyrolysis zone at a distance 152 mm from the vertical axis of gasifier

T_8 : Temperature in pre pyrolysis zone at a distance 210 mm from the vertical axis of gasifier

T_9 : Temperature in pyrolysis zone at a distance 100 mm from the vertical axis of gasifier

T_{10} : Temperature in pyrolysis zone at a distance 110 mm from the vertical axis of gasifier

T_{11} : Temperature in pyrolysis zone at a distance 152 mm from the vertical axis of gasifier

T_{12} : Temperature in pre combustion zone at a distance 110 mm from the vertical axis of gasifier

T_{13} : Temperature in pre combustion zone at a distance 110 mm from the vertical axis of gasifier

T_{14} : Temperature in combustion zone at a distance 130 mm from the vertical axis of gasifier

T_{15} : Temperature combustion zone at a distance 130 mm from the vertical axis of gasifier

T_{16} : Temperature in reduction zone at a distance 86 mm from the vertical axis of gasifier

T_{17} : Temperature in reduction zone at a distance 86 mm from the vertical axis of gasifier

T_{18} : Temperature in Ash chamber at a distance 130 mm from vertical axis of gasifier

T_{19} : Raw producer gas temperature (subsequent to reduction chamber and before scrubbing)

T_{20} : Producer gas temperature after scrubbing and before filtrations

T_{21} : Producer gas temperature after filtrations

T_{22} : Producer gas flame temperature at flare

T_{23} : Temperature of water inlet to scrubbing

T_{24} : Temperature of water outlet from scrubbing

T_{25} : Atmospheric temperature

Abbreviations

ADF	:	Acid Detergent Fibre
ADL	:	Acid Detergent Lignin
ADS	:	Acid Detergent Solution
BMG	:	Biomass Gasifier
DSC	:	Differential Scanning Calorimetry
DTG	:	Differential Thermogravimetric
EDS		Energy Dispersive X-Ray Spectroscopy
ER	:	Equivalence Ratio
FA	:	Fibre Analysis
FC	:	Fixed Carbon
FESEM		Field Emission Scanning Electron Microscope
FTIR		Fourier Transform Infrared Spectroscopy
GC	:	Gas Chromatography
GCMS	:	Gas Chromatography And Mass Spectroscopy
IRI	:	Impact Resistance Index
MNRE	:	Ministry Of New And Renewable Energy
NDF	:	Neutral Detergent Fibre
NDS	:	Neutral Detergent Solution
TCC	:	Tar Cracking Chamber
TCU	:	Tar Cracking Unit
TG	:	Thermo Gravimetric
TGA	:	Thermo Gravimetric Analysis
VM	:	Volatile Matter
WC	:	Wood Chip

List of Figures

List of Tables

CHAPTER 1

INTRODUCTION

1.1 MOTIVATION

With scintillating growth of industry, agriculture and transport sectors a proportionate demand for energy in the present day world is increasing. Currently most of the energy required in the major sectors is harnessed from fossil fuel. However, fossil fuel reserve is limited and use of the same affects severe environmental pollution. Agarwal (2007) indicates the exploration and utilization of fossil fuel. Accordingly, coal, petroleum oil and natural gas may be harnessed effectively for 218 years, 41 years and 63 years, respectively. Thus major attention has shifted towards utilization of alternative sources of energy in the last two decades. Focus is concentrated amongst the researchers to utilize the renewable form of energy such as solar, wind, hydropower and biomass. Solar energy is expensive and wind energy is site specific. However, biomass is abundantly available throughout the world.

Biomass can be utilized for generation of biogas through anaerobic digestion or producer/syn-gas through thermo-chemical conversion. The significant amount of energy requirement can be full field through biomass gasification technology. Gas produced from this processes is clean and safe in comparison to the conventional energy sources. India is an agriculture country which presently produces around 500 million metric tones agro waste per year. The 70% population of the country depends upon energy derived from biomass. The principal energy need full field through the biomass is projected about 32% of total energy. The production of producer/syn-gas from biomass thermo chemical gasification process is a mature technology. Many biomass gasifier are developed and been tested in field. But it is found that there is a lack of standard process in which different biomass can be used as feed stock in same biomass gasifier. Moreover, processes involved in gasification are not understood for all type of gasifier. Even, a gasifier designed to operate with one kind of feed stock is hardly known whether will operate with other type of feed stock. Another problem, especially for downdraft gasifier

is to reduce the unwanted tar. This motivated to take up the challenges encountered in a down draft gasifier for the present work.

1.2 PRINCIPLE OF GASIFICATION

The biomass materials like wood, agro waste and coal are converted into burnable gas by partial combustion. The burnable gas is known as producer gas and thermochemical process of conversion is called gasification. The producer gas is composition of Hydrogen (H_2), Carbon monoxide (CO), Methane (CH_4) and waste products like tar and ash as shown in Fig. 1.1.

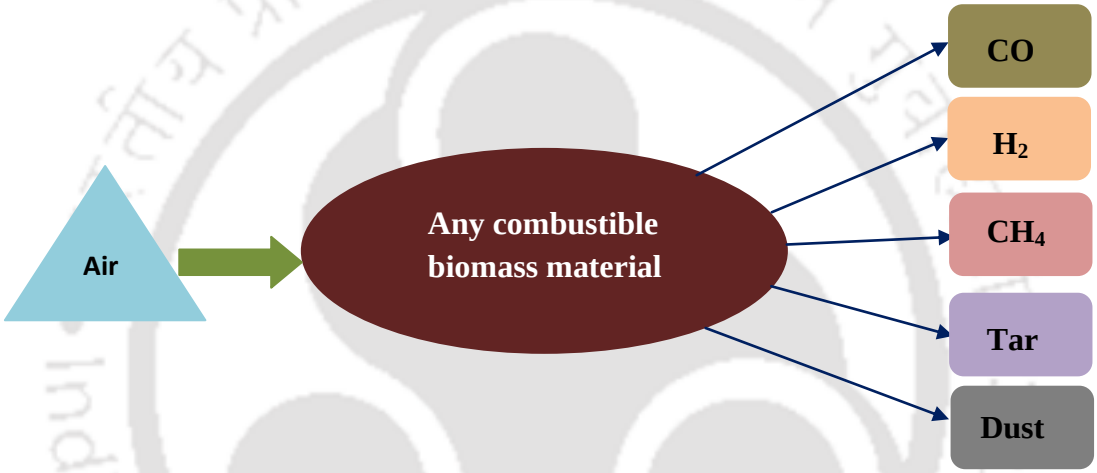

Fig.1.1 Products of gasification

If the combustion is held at stochiometric air instead of restricted air supply then complete combustion of biomass takes place and it produces carbon dioxide, water vapor, nitrogen oxides and additional amount of oxygen.

1.3 HISTORICAL DEVELOPMENT OF GASIFICATION

The gasification is matured technology since seventeenth century. It is developed with various views and aspects. The history of the growth of gasification in the course of time is as enumerated below [Turare (2002)].

1669-The first research on gasification was carried out by Thomas Shirley. He performed experiment with carbureted hydrogen.

1699-Dean Clayton carried out experiment on pyrolysis of biomass and produced coal gas.

1788-The first patent on gasification is acquired by Robert Gardner.

1792-William Murdoc produced producer gas from coal which is known as town gas and used this gas for lighting his room. Afterward this gas is utilized for cooking and lighting.

1801-Lampodium confirmed use of waste gases generated by conversion of wood in to char.

1804-Fourcroy carried out reaction of water with hot carbon and produced water gas.

1812-The first gasifier is developed in which oil is used as feedstock.

1840-The first commercial gasifier is developed in the France.

1861-Siemens gasifier unit is commenced which is treated as first successful unit.

1878-Gasifiers are used effectively for power production through engines.

1900-The first gasifier with 600 hp power generation capacity was presented in an exhibition held at Paris. Afterward higher capacity engine up to 5400 hp was developed and brought into utilization.

1901-A passenger vehicle was run with the producer gas by J.W. Parker.

1901-1920 -The numerous gasifier coupled with engine and generator were developed for the production of electricity and put on the market.

1930 -Nazi Germany converted oil used vehicles into producer gas feed vehicles. In this year production of automotive and portable gasifier was started. British and French Government realized that gasoline and wood were limited and charcoal feed gasifiers are more suitable for the power generation.

1939 -In Sweden 2, 50,000 vehicles were registered from which 90 % were converted to producer gas drive and nearly 20,000 tractors were worked on producer gas. The fuel used for the production of the producer gas was 40 % wood and rest was charcoal.

1945-The abundant amount of gasoline and diesel was available at low-priced rate after finishing Second World War which decreased the magnificence of gasification technology.

1950-1970 Europe governments thought that the utilization of wood produce environmental troubles. So the gasification technology becomes less attention.

The gasification technology comes in limelight after the year 1970´s in concern with decentralized power generation. Researchers are also working on utilization of alternative fuel instead of wood and charcoal.

1.4 GASIFICATION PROCESS

Gasification is a composite thermo chemical process. It is difficult to divide gasifier into various processes. For the simplicity of understanding theoretically it is divided into four processes namely are drying, pyrolysis, oxidation and reduction in which biomass is converted into producer gas as shown in Fig. 1.2.

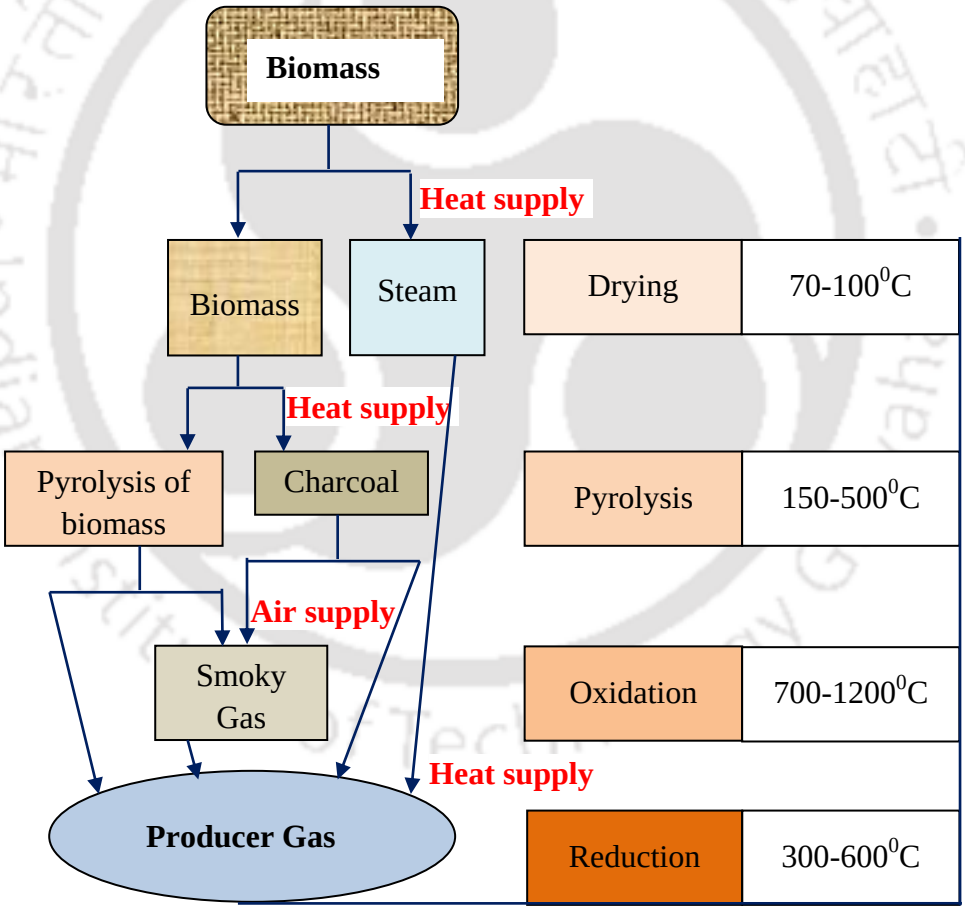

Fig.1.2 Conversion of biomass into producer gas

1.4.1 DRYING

Biomasses have 10-30% moisture content. The moisture in biomasses is reduced up to 10-15% to utilize in gasification process. The process of removing moisture from the

biomass without any decomposition is known as drying. The drying of the feedstock is takes place at the temperature 70-100°C. The zone in which drying of biomass occurs is called as drying zone. The required heat for the drying is accomplished from the other zones. The time required for drying is depending upon various parameters like surface area of feedstock material, temperature in drying zone, inside diffusivity of moisture, speed of drying medium, internal diffusivity of moisture, association of moisture to that material and heat transfer rate. The chemical reaction is not occurred in this zone [Devi etal. (2005 b)]. Some time biomass releases organic acids in drying process which causes corrosion of inside surface of gasifiers [Sadka (http://www.bioweb.sungrant.org)].

1.4.2 PYROLYSIS

The process of heating biomass or carbonaceous material in absence of oxygen is called as pyrolysis process. Pyrolysis takes place at temperature 150 to 500^0C and thermally decomposes biomass into solid, liquid and gaseous products as shown in Fig.1.3.

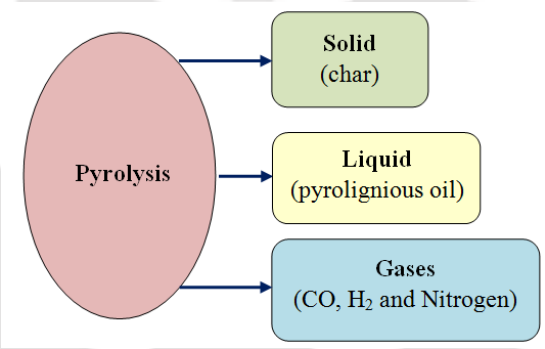

Fig.1.3 Pyrolysis Products

It is decomposed in solid carbon like char, condensable gases like pyrolignious oil, methyl alcohol, tar and non condensable gases like CO, H_2, CO_2 and nitrogen. At more temperature gas production reduces and it mainly contains hydrogen.

1.4.3 OXIDATION REACTION

The atmospheric air consists of oxygen, water vapors and nitrogen. The oxygen in the air reacts with biomass and produces carbon dioxide, water vapors and heat. The oxidation reaction takes place at temperature about 700-1200^0C. In oxidation two reactions takes place. In first reaction carbon in the biomass fuel reacts with the oxygen in air and produces carbon dioxide and released 393.8 MJ of heat as given in Eq. 1.1.

$$C + O_2 \rightarrow CO_2 + 393.8\left[\frac{MJ}{Kmol}\right] \quad (1.1)$$

Hydrogen in biomass fuel reacts with oxygen in air and produces water vapors and released 242 MJ heat as given in Eq. 1.2.

$$H_2 + \frac{1}{2}O_2 \rightarrow H_2O + 242\left[\frac{MJ}{Kmol}\right] \quad (1.2)$$

1.4.4 REDUCTION REACTION

The heat generated in the combustion zone is propagated to the upward side which is utilized for the pyrolys is and drying and the heat propagated in the reduction zone is utilized for the reduction reaction. In reduction zone, various high temperature chemical reduction reactions exist in absence of oxygen. The main reactions that take place in reduction zone are stated below in Eq. 1.3-1.6.

Boudouard reaction

In Boudourad reaction carbon dioxide produced in combustion reacts with the carbon by absorbing 176 MJ heat and produces carbon monoxide as given in Eq. 1.3.

$$CO_2 + C \rightarrow 2CO - 176\left[\frac{MJ}{Kmol}\right] \quad (1.3)$$

Water-gas reaction

In water gas reaction carbon reacts with the water vapors produced in combustion absorbing heat and produces carbon monoxide and hydrogen as given in Eq. 1.4. .

$$C + H_2O \rightarrow CO + H_2 - 131.4\left[\frac{MJ}{Kmol}\right] \quad (1.4)$$

Water shift reaction

In water shift reaction carbon dioxide and hydrogen reacts by absorbing heat 41.2 MJ and produces carbon monoxide and water vapors as given in Eq. 1.5.

$$CO_2 + H_2 \rightarrow CO + H_2O + 41.2\left[\frac{MJ}{Kmol}\right] \quad (1.5)$$

Methane production reaction

In this reaction carbon and hydrogen reacts by absorbing heat 75

MJ and produces methane as given in Eq. 1.6.

$$C + 2H_2 \rightarrow CH_4 + 75\left[\frac{MJ}{Kmol}\right] \quad (1.6)$$

In reduction process heat is required for completion of reaction which reduces temperature of producer gas in the reduction zone. The various reduction reactions produce carbon monoxide, hydrogen, methane, a combustible gas. The carbon is either burned completely or reduced to carbon monoxide during complete gasification. Some amount of char (unburned carbon) and ash is obtained.

1.4.5 TAR CRACKING

Tar is a condensable byproduct of gasification process. It is obtained by scrubbing the producer gas after coming out from the reduction zone. This tar can be cracked by different processes like reforming, thermal cracking, and steam cracking as shown in Fig.1.4 [Delgado et al. (1996)]. During this processes tar is converted into smaller hydrocarbons.

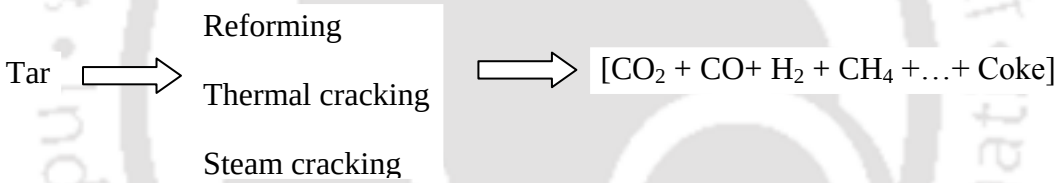

Fig.1.4 Tar Cracking

Tar reforming: The tar reforming reaction exists in gasification of feedstock with steam. In this case the steam cracks the tar (C*n*H*x*) into lighter molecules like H_2 and CO as shown in Eq.1.7.

$$C_nH_x + n\,H_2O \longrightarrow (n+x/2)\,H_2 + n\,CO \quad (1.7)$$

Dry tar reforming: The dry reforming reaction exists in the gasification of feedstock with CO_2 as shown in Eq. 1.8. In this reaction tar is cracked intoH_2 and CO.

$$C_nH_x + n\,CO_2 \longrightarrow (x/2)\,H_2 + 2\,n\,CO \quad (1.8)$$

Thermal cracking: The thermal cracking of the tar required high temperature. In this case tar is reduced into lower hydrocarbon at temperature above 1100 °C and also produces soot [Dayton (2002)]. The temperature required for cracking is more than temperature of producer gas at outlet. So the heat requirement is fulfilled by either external heat supply or producing more amount of heat with additional supply. The both processes are expensive than the steam reforming.

Steam cracking: The tar is cracked in steam cracking in absence of oxygen. In this method at first tar is diluted with the steam and then heated in a furnace. The higher hydrocarbons are cracked into lower hydrocarbon and small molecules.

1.5 VARIOUS TYPES OF FIXED BED GASIFIERS

Fixed bed gasifiers are classified according to the direction of gas produced during the gasification process. It is classified as

(a) Updraft Gasifier
(b) Cross-draft Gasifier
(c) Downdraft Gasifier

1.5.1 UPDRAFT GASIFIER

In updraft gasifier feedstock is fed from the top side and air enters from downward side of the gasifier as shown in Fig. 1.5. Feedstock is loaded from the top of the gasifier while fresh air enters the gasifier from the bottom. The producer gas generated is collected from the top of the gasifier.

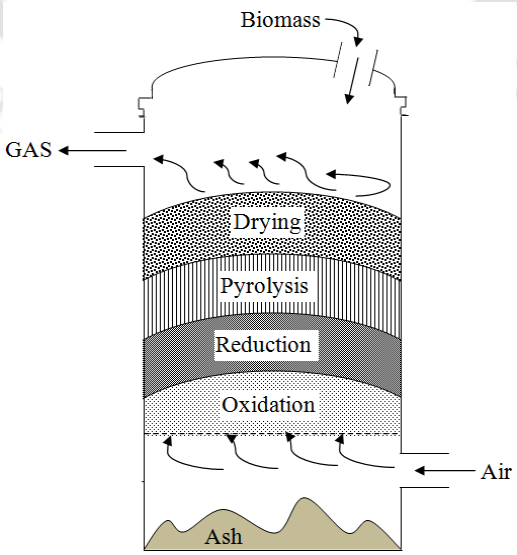

Fig. 1.4 Updraft gasifier

The combustion (oxidation) of the feedstock takes place close to the grate. The heat generated in the combustion is transmitted from the bottom to the top of the gasifier. The reduction reactions occur above combustion/oxidation zone followed by the pyrolysis and drying as observed from the bottom. The producer gas along with tar and volatiles are discharged from the top while ash is released to the bottom through the grate. The updraft gasifier has advantages like it has small pressure drop, good thermal efficiency and slight tendency towards the slag formation. However, it is having serious drawbacks like channeling of the equipment leading to oxygen break-through leading to explosions. Further, it requires necessary arrangements for condensing tar to separate from the product gas.

1.5.2 CROSS DRAFT GASIFIER

In the cross-draft gasifier the feedstock is fed from the top of the gasifier similar to the updraft gasifier. However, air and final gas produced enters and leaves along the same line along the combustion zone at the bottom. An air nozzle is used to inject air to the combustion zone at relatively high velocity. The combustion takes place in front of nozzle and produces heat at high temperature above 1500°C. At this temperature feedstock undergoes pyrolysis, reduction and generates the producer gas. The schematic of cross-draft gasifier is as shown in Fig.1.6.

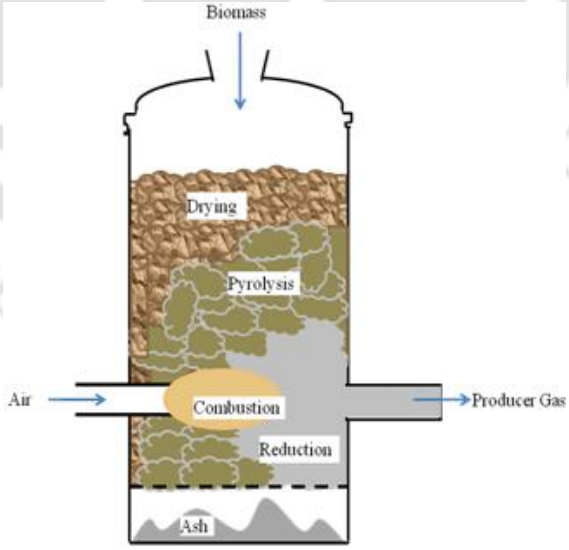

Fig.1.5 Cross-draft gasifier

The cross draft gasifier has some advantages like it has small height and it is sensitive towards load flexible gas production. It has limitations towards high slag formation and high pressure drop. Tar cracking capability of this type of gasifier is reported to be poor.

1.5.3 DOWNDRAFT GASIFIER

In downdraft gasifier the feedstock is filled from top of the gasifier unit. The air is entering just above the combustion zone. The pyrolysis and drying zone are located above the combustion zone and reduction zone is located below the combustion zone. The heat generated in combustion zone is transmitted towards upward side to pyrolysis and drying zone and towards downward side to reduction zone. The products of pyrolysis passes through the glowing bed of charcoal and reduced the hydrocarbon to carbon dioxide, carbon monoxide and methane depending upon temperature and residence time of feedstock in various zones of the gasifier. The producer gas comes out from bottom ofthe reduction zone as shown in Fig. 1.7.

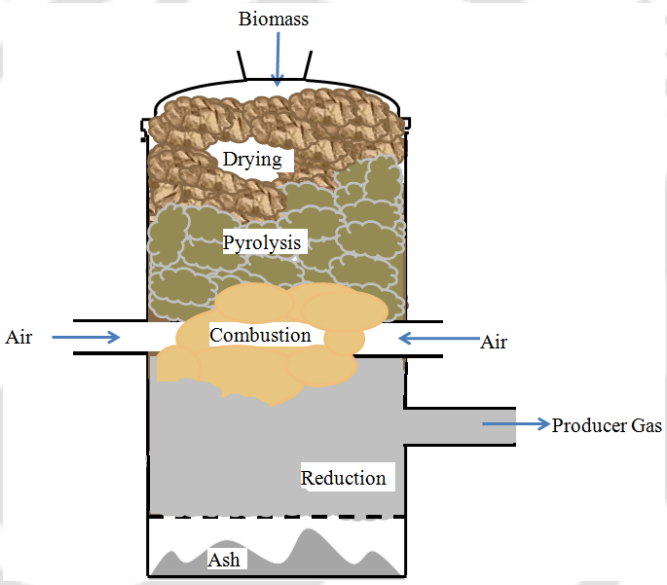

Fig. 1.6 Downdraft gasifier

The downdraft gasifier is flexible in gas with the load. It is having low sensitivity towards charcoal dust formation. However, this type of gasifier is not feasible for the feed materials with small particle size. The size of the gasifier is larger in comparison to the other two type of gasifers described. Tar produced in this gasifer comes out with the producer gas.

1.6 CRACKING OF TAR

Production of tar along with gasification process is undesirable as the same leads to blocking of the gas filters, piston-cylinder assembly of power generating unit and damage

of valves, etc. Tar is a complex mixture of heavy hydrocarbon mainly containing poly-aromatics. Cracking of tar has been reported by Devi et al. c (2005), Roche et al. (2014). There are many methods for reducing tar from producer gas including in-situ tar cracking and post gasification treatment. Use of catalyst at high temperature has been reported by Dayton D. (2002), Myren et al. (2002). Development of an improved method for in-situ tar cracking or post gasification tar cracking are challenges in fix bed gasifiers.

1.7 AIM AND OBJECTIVES

The objectives of the present work under consideration are as follow.

1. Use of loose biomass in the present 5kW downdraft gasifier designed for wood chips
2. Development of liquid-gas bubbling fluidized bed tar cracking unit.

The scope of the work is given as

1. Performance evaluation of biomass gasifier in terms of feedstock properties, zone temperatures, equivalence ratio, producer gas composition, Producer gas production rate. Comparison of gas yield quality in terms of different feed materials such as wood chips, biomass briquettes, pellets and biomass-dolomite pellet
2. Improvement in gas composition through inline treatment by biomass-dolomite pellet.
3. Thermal cracking of the tar gained from biomass gasification. Experimentation with various blends of tar with dolomite as catalyst.

The above objectives are accomplished with parametric study of the downdraft gasifier integrated with liquid-gas bubbling fluidized bed tar cracking unit. Experiments are carried out in two setups. First, experiments are performed on gasification with various feedstock in downdraft gasifier and second, experiments are done on thermal cracking of tar (obtained from biomass gasification) in liquid-gas bubbling fluidized bed.

1.8 OUTLINE OF THE THESIS

This thesis comprises of seven Chapters. **Chapter 2** includes an exhaustive review of literature pertaining to the biomass gasification and performance characteristics of various gasifiers. A few case studies conducted in field are also described in this Chapter. **Chapter 3** deals with characterization of biomass, combustion characteristics, thermo

gravimetric analysis and Fibre analysis. **Chapter 4** describes the experimental setup, procedure and instrumentation of the downdraft gasifier. It also presents the measurement technique of the various parameters. It also explains material and methodology for feed stocks preparation. **Chapter 5** deals with the results and discussion of the experimental investigation on performance analysis of downdraft gasifier, thermal behavior, gas yield, tar yield, gas chromatography analysis of the producer gas with various feedstock and innovative in-situ tar cracking with biomass dolomite pellet. Development of a novel liquid-gas bubbling fluidized bed tar cracking unit followed by its performance evaluation are presented in **Chapter 6**. Conclusions and scope for future work are presented in **Chapter 7**.

CHAPTER 2

LITERATURE REVIEW

2.1 INTRODUCTION

A literature review on biomass gasification (BMG) reports the current status of biomass gasification, feasibility of the gasifier with various feed stocks, tar destruction. It identifies loopholes in the gasification processes, near research scope and collects reliable information for proposed planning as clean gas energy technology.

2.2 REVIEW OF BIOMASS GASIFICATION

The biomass gasification plays an important role in renewable energy generation. It is a proficient energy production technology. Biomass is converted into producer gas through thermo-chemical process. The various types of gasifier are used for conversion of biomass. The biomass undergoes combustion process and produces water vapor, carbon dioxide and surplus of oxygen. When there is partial combustion it generates hydrogen, carbon monoxide, methane and distrustful products like tar and dust (Rajvanshi, 1986). The producer gas produced during gasification process replace with fossil fuels for effective power generation, heat and/or CHP applications (Maniatis, 2001, Balat et al., 2009). Biomass gives bio oil through pyrolysis process which has similar chemical properties like crude petroleum oil. This can be used for the transportation after the refinement. The hydrogen generated in pyrolysis process can be used in fuel cell. The low grade biomass is transformed into high grade charcoal through carbonization process (Panwara et al., 2012). In India gasifier manufactured had 5- 500 kW power generation capacities. Biomass gasification is encouraged by the Ministry of New and Renewable Energy (MNRE) by providing subsidies. Current installed capacity is 1410.20 MW. The gasification technology is found cost-effective and stable than petroleum fuel for thermal applications (Varshney, 2010). The low- or medium heating value producer gas generated in gasification can be used as fuel gas in an internal combustion engine for power production (Balat et al., 2009). Typically, the dual fuel engines are used for power generation which replaced the 50- 60 % fossil fuel (Varshney, 2010). In India a large

amount of agro-waste is available. In general, it is burnt or dumped due to limitation of space. This agro-waste can be used for power generation through gasification (Varshney, 2010). The solid biomass is preferable to use directly due to its more than 76% carbon content (Balat et al., 2009). In industries downdraft gasifier is found suitable for the heating and drying appliances of agriculture and industrial products. The biomass gasification protects environment and ecology as well (Panwara et al., 2012).The low price of biomass attracts the gasification as energy-economic technology (Babu, 2005). In IGCC plant it is noticed that the coal gasification along with biomass not only increased the power output of plant but also decreased the emission. In this case decrease in carbon dioxide is observed by 30% (Long, 2011). There is large scope in the improvement of the biomass gasification technology for efficient and economic development with clean producer gas (Kirkels et al., 2011). The selection of gasification technology for desirable purpose is depend upon various factors consisting of availability of feed stock, environmental degradation, awareness about technology, economy of the project , local politics, gasification process and requirement (Ahrenfeldt et al., 2012).

2.3 PERFORMANCE ANALYSIS OF BIOMASS GASIFIER

Researchers performed various experiments with downdraft gasifier and used several feed stocks to obtain the good composition producer gas. Table-1 enumerates some of the studies carried out on performance of downdraft gasifier with the various parameters.

Table-2.1 Various experimental comparative studies on downdraft gasifier

Investigator (s)	Experimental variables	Observations
Vyarawalla et al., (1984)	• Gasifier-downdraft 9 kW Size- Hearth opening- 90 mm • Feedstock- Sawmill waste, cotton stalk, toor stalk size- 90 mm, random	✓ Producer gas composition- CO%- 16.5% H_2%- 17.2% ✓ Temperature in various zones Combustion- 950^oC Exit temperature- 147^oC
Khater et al., (1992)	• Gasifier-downdraft Size- Drying zone height 800mm Drying zone diameter- 350mm Combustion zone-height 300 mm Combustion zone diameter- 50mm Ash chamber height- 300mm Ash chamber diameter- 400mm • Feedstock- rice hull	✓ Optimum equivalence ratio (ER) -0.55. ✓ optimum gas composition- CO%- 13.67% H_2%- 5.13% CH_4%- 2.42% ✓ Maximum temperature in gasifier – 750^oC.

	size- approx. 50mm cube • Equivalence ratio- 0.26-0.55	✓ Percentage of CO increased with increase in ER and temperature
Zainal et al., (2002)	• Gasifier-downdraft Size- Cone structure Height 400mm Top diameter- 600mm Bottom diameter- 200 mm • Feedstock- Furniture wood and woodchip size- approx. 50mm cube • Equivalence ratio- 0.268-0.43	✓ Optimum equivalence ratio- 0.388. ✓ Average gas composition- CO%- 14.05% H_2%- 24.04% CH_4%- 0.01% ✓ Temperature in various zones Pyrolysis - 200-250^oC Combustion- 700-1200^oC Reduction - 600-700^0C Exit temperature- 20-200^oC
Dogru et al., (2002)	• Gasifier-downdraft Size- Diameter of drying hopper zone-305 mm, Height of bed - 810 mm, Diameter oxidation zone- 450 mm, Diameter of throat (d) = 135 mm. • Feedstock- hazelnut shells size-Approx.- 17.9×16.5×8.5 mm^3 • Equivalence ratio- 0.165-0.355	✓ Optimum air/fuel ratio-1.46. ✓ Average gas composition- CO %- 20.66% H_2 %- 13.13% CH_4 %- 2.18% ✓ Maximum Temperature Drying zone- 125^oC Pyrolysis zone – 566^oC Throat- 1206^oC Throat (optimum) – 1015^oC ✓ Tar output rate- 0.023 kg/h.
Sheth and Babu (2009)	• Gasifier-downdraft Size- Height of the gasifier-1.1 m Diameter (pyrolysis zone)- 310 mm Diameter (reduction zone)-150 mm. Height (reduction zone)- 100 mm Height (oxidation zone)- approx.53 mm. • Feedstock- Furniture waste of sesame size- approx. 50mm • Equivalence ratio- 0.16-0.355	✓ Optimum ER-0.205 ✓ Gas composition in (vol. %) (approx.)- CO - 22% H_2 - 14% CH_4 - 3% ✓ Temperature Pyrolysis zone – 260-550^oC Combustion zone-900-1050^oC Tar output rate- 0.023 kg/h.

The portable downdraft gasifier can be the good solution for the demonstration and awareness among the public. The gasifier can be taken to various cotton gins and agriculture industry for the heat and power generation (Powell et al., 2007). The moisture content of the feedstock is directly related to its consumption. If moisture content of feedstock is higher the consumption rate decreases and temperature in the gasifier also

reduces. While increase in the air flow rate increase the consumption of the feedstock and results into the higher temperature in the gasifier (Sheth and Babu, 2009). A low superficial velocity of the air entering into the gasifier decreases the pyrolysis and increased the production of the coal and tar. If superficial velocity is increased speedy pyrolysis occurred. This decreased the production rate of the coal as well as tar and increases the gas flow rate. In an experiment increase in superficial velocity from 0.05 m/s to 0.26 m/s results into increased gas production rate from 102 to 679 cm^3/s (Reed et al., 1999). The modified rectangular throat in 125 kg/h downdraft gasifier gives more stable thermal profile and reduces hot and cold spots inside gasifier. The rectangular throat design is more efficient for the short term experiment. At the same time uneven thermal expansion is observed which deteriorate performance of gasification system. (Pathak et al., 2008).The open core downdraft gasifier with feed rate of 90 kg/hr produces the heat up to 850 MJ/hr which has potential of replacement of 20 L/hr light diesel oil for industrial thermal application. The producer gas coming at exit has the temperature 400-650^0C. This is an economical biomass gasification technology and used for increasing the concentration of Phosphoric acid (Rathore et al., 2009). The temperature increased in the gasifier with increase in gas flow rate increases air biomass ratio. The higher temperature in bed results into the better conversion of CO_2 and H_2O into CO and H_2 which improves calorific value of product gas and cold gas efficiency (Sharma, 2009, Sharma, 2011). The shell biomass material like Coconut shell, Groundnut shell and Rice husk converted into combustible gas at 800^oC with gasification technique. The gas quality for the coconut shell is found good which has the calorific value 23 % higher than Ground nut shell and 45 % higher than Rice husk (Sivakumar and Mohan, 2010). The gasification experiments with 12 kW downdraft gasifier using Coal, Charcoal and Corn piths as feedstock generates $39m^3$, $41m^3$ and $35m^3$ producer gas respectively for equal weight of 18 kg (Ahmad et al., 2011). The OK wood shavings are used as feedstock in the throat-less gasifier with flow rate of 18.7 kg/h. The gas produced has the composition 20.8–23.6 % CO, 8.7–13.2 % H_2, 3.6–5.2 % CH_4, 9.3–14.5 % CO_2 and 47.2–53.6 N_2 (Patil et al., 2011). The 48 g/Nm^3 average tar is obtained during the gasification (Dogru et al., 2002) which is higher than hazelnut shell $3g/Nm^3$ and sewage sludge 6.3 g/Nm^3. These values are less due to use of throated gasifier, non fluffy feedstock and experimental conditions. Wei et al., (2011) performed experiment by blending glycerol with the woodchip with various feed rate in pilot level downdraft gasifier. The increase in amount of glycerol in glycerol-woodchip blend increased CO, CH_4, tar and decreased particle concentration.

The 20 (wt %) of glycerol can be significantly used in the blend. Antonopoulos et al. (2012) produced tar free synthesis gas from municipal solid waste and biomass in three stage steady bed gasifier. The first stage includes the pyrolysis of the feedstock, second stage consists of combustion of pyrolysis gas obtained from first stage and third stage consists of gasification of the coal obtained from the first stage. The preheated air is supplied for the combustion and gasification. The combination of two gasifier updraft and downdraft is used and in between space is nominated as the buffer zone. The buffer zone plays an important role in the tar cracking due to presence of temperature up to 1100 ^{o}C. At this temperature tar is almost cracked. This gasifier is also useful for low calorific and high moisture content feedstock. However the operating conditions like equivalence ratio has direct relation with the temperature in the gasification and the composition of the producer gas. The higher or lower values of the equivalence ratio are not desirable. It is preferable to operate the gasifier at the ER 0.28-0.32 for the better composition of the gas (Gai and Dong, 2012). The temperature increased in the gasifier results in increase in composition of CO and H_2 and decrease in CO_2 and H_2O (Li et al., 2001, Shabbar and Janajreh, 2013, Kulkarni et al. 2016). The higher gasifier temperature throughout length instead of only in combustion zone increased two times composition of the CO and H_2 (Adeyemi, 2017). Increase in the equivalence ratio increased gas production rate and decreased the heating value and conversion efficiency. The quality of the gas deteriorates due to the increase I the oxygen with equivalence ratio (Singh et al. 2016).The supply of preheated air up to 500^{o}C is significant and increases the volume percentage of H_2, CO and CH_4 from 8.47, 22.87 and 2.03% to 10.53, 24.94 and 2.04 % respectively (Guangul et al., 2014). The sizes of the feedstock play an important role in the gasification. As the size of feedstock increased the consumption rate reduces. However the producer gas generation rate increases. As well as the higher temperature in the reduction zone increases concentrations of CO and H_2 in the producer gas composition with the increase in the size of the feedstock (Patel et al., 2014). Jorapur and Rajvanshi (1997) obtained HHV 3.56 - 4.82 MJ Nm^3 produces char, which is about 24% by weight. Patel et al. (2016) performed experiment with lignite as feedstock in downdraft gasifier. The clinker formation , bridging or channel burning, erosion and corrosion due to high ash content of lignite, etc. was observed during operation of gasifier The co-gasification of lignite with waste wood minimize these issues and given higher heating value of the producer gas.

2.4 PERFORMANCE ANALYSIS OF GASIFIER WITH BRIQUETTE AND PELLET

The detailed descriptions of the biomass briquette/pellet gasification process are reported in the several published literature. The loose biomass can be used in the gasifier by converting it into pellet or briquette (Asadullah, 2014). The bridging problem of the gasifier can be solved by pelleting the biomass (Kjellstorm et al., 2005). The socioeconomic development can be achieved by linking the gasification unit to the pelletizing unit in rural areas (Erlich, 2009). Sivakumar et al., (2012) performed experiment with various sizes of saw dust: cow dung briquettes which are in proportion 75:25. The size of the briquette plays an important role in the gasification. The increase in the size of the briquette results in the increase of volumetric percentage of CO, CH_4. CO_2 and decrease in the volumetric percentage of H_2 and N_2. The size 40 mm diameter × 60mm length is found more suitable in terms of gas composition. Varshney et al., (2010) evaluated the performance of 20 kW throat-less downdraft gasifier with cylindrical briquettes of pigeon pea, lantana and soybean stalks. The optimum length of the briquette was found to be 8-12 mm with minimum choking during the flow of briquettes during the operation. Pongamia de-oiled cake pellets of 17 mm and 11.5 mm diameter and length in the range of 10-68 mm were gasified by Prasad et al., (2014, 2015) in a 20 kWe downdraft wood gasifier. Thermal degradation occurred between 166– 480^{o}C. It was reported that complete gasification is not possible due to the larger thermal gradient within the pellets (Prasad et al., 2014). The gasification efficiencies were reported to be 73% and 95% for 17 mm and 11.5 mm diameter pellets, respectively (Prasad et al., 2015). Briquettes made with leather residues with nominal size of 70 - 50 mm and bulk density of 537.30 kg/m^3 were successfully gasified in a 10 kWe downdraft gasifier by Dogru et al. (2004). The temperatures of combustion, pyrolysis, and oxidation zone were found to be 1050^{o}C, 530^{o}C, and 290^{o}C, respectively. The bridging of the leather briquettes is observed in the throat zone of the gasifier. Sridhar et al., (2005) reported severe ash fusion problem at high loading rate with fine biomass like rice husk or sugarcane trash, peanut shell or coir pith and same was overcome by use of briquettes. The gasification of refuse-derived fuel briquette gives the produced gas with heating value 1.76 MJ/m^3, cold gas efficiency of 66% (Chiemchaisri et al., 2010). The pellets from the palm oil residue are not found suitable due to its poor efficiency for the gasification (Erlich and Fransson, 2011). The ricehusk briquette gives the heating value 1300 kcal/Nm^3 and cold gas

efficiency 70% with the air flow rate of 50-75 Nm^3/h and fuel feeding rate of 40-60 kg/h at temperature range 600-850^oC (Sang et al., 2012). Simone et al., (2012) performed experiment with sawdust and sunflower seeds pellets in a 200 kW downdraft gasifier. He observed the gasification process form the wet ash. At the same time good gas quality with gas composition H_2 -17.2%, N_2 -46.0%, CH_4 -2.5%, CO -21.2%, CO_2 -12.6%, and C_2H_4 -0.4% is yielded. Evelyn et al., (2014) received the composition of NO, CO and SO_2 higher than wood pellet with gasification of Brazil nut shells and sunflower husks. The temperature in the gasifier reaches to the 1100^oC with wood pellet. Whereas this temperature reduces in the range 800 and 850^oC due to the pressure drop caused inside the gasifier with the pellets prepared from saw dust rape straw, poultry litter, and dried sewage sludge. Striugas Nerijus et al., (2014).

2.5 GAS CLEANING

The biomass-derived tar is very hard to crack by thermal treatment alone. In order to effectively decompose the tar, the following ways were suggested: (1) increasing residence time, such as using a fluidized bed reactor freeboard, but this method is only partially effective; (2) direct contact with an independently heated surface, which required a significant energy supply and decreases the overall efficiency. At the same time, this method is also partly effective and depends on good mixing; and (3) partial oxidation by adding air or oxygen that could increase CO levels at the expense of decrease in conversion efficiency and increase in operational cost (Bridgwater, 1995). Dolomites and limestones can be used as effective tar decomposing catalysts at lower pressures and around 900°C temperatures, where they stay in calcined form (Simell et al., 1996). Velegol et al., (1997) catalytically cracked the coal derived tar from coal in a fluid bed reactor fluid catalytic cracking system LZ-Y82 cracked most effectively in the temperature range 500-530^oC.

The producer gas from gasifier consists of particle and tar. This causes harm to I C engines when used as diesel substitute. Hasler and Nussbaumer, (1999) experimented on tar and particle collection efficiencies with sand bed filter, wash tower, two different fabric filters, and a rotational particle separator in different test runs with fixed bed gasifier. Tar adsorption on coke has been studied in a fixed bed batch reactor. It is observed that 90% particle removal is easier to achieve than 90% tar removal. The higher amount of tar can be removed with the utilization of catalytic tar crackers. It is seen that

none of the investigated gas cleaning systems were capable of reducing tar more than 90%. So new methodologies for tar removal has to be investigate.

Rapagna et al., (2000) reported that naturally occurring catalytic substances are employed in biomass steam-gasification processes to enhance the yield of fuel gas and reduce its tar content by cracking and reforming the high molecular weight organic components. Calcined dolomite is widely used for this purpose; it exhibits good catalytic activity under the operating conditions of the gasifier. However, due to its poor mechanical strength, it gives rise to a large production of fines in a fluidized-bed environment. He investigated the catalytic behavior of olivine, common, naturally occurring mineral containing magnesium, iron oxides and silica: iron is known to play a positive role in tar decomposition reactions. The gasification runs, performed with a laboratory scale, biomass gasification unit, show that the olivine activity is close to that exhibited by dolomite under comparable operating conditions. Olivine has the additional advantage, however, that its resistance to attrition in the fluidized bed is much greater, similar to that of sand. Parametric sensitivity studies of a gasification process, utilizing olivine as fluidized-bed inventory, indicate an optimum gasification temperature of just above $800^{o}C$.

Sutton et al., (2001) explained that Dolomite is a suitable catalyst for the removal of hydrocarbons, which are evolved in the gasification of biomass. Dolomites increase gas yields at the expense of liquid products. With suitable ratios of biomass feed to oxidant, almost 100% elimination of tars can be achieved. The dolomite catalyst deactivates due to carbon deposition and attrition; however, dolomite is cheap and easily replaced. The catalyst is most active if calcined and placed downstream of the gasifier in a fluidized-bed at temperatures above $800^{o}C$. The reforming reaction of tars over dolomite occurs at a higher rate with carbon dioxide than steam. Dolomite activity can be directly related to the pore size and distribution. A higher activity is also observed when iron oxide is present in significant amounts. Dolomites are not active for reforming the methane present in the product gas and hence they are not suitable catalysts if syngas is required. The main function of dolomite is to act as a guard bed for the removal of heavy hydrocarbons prior to the reforming of the lighter hydrocarbons to produce a product gas of syngas quality.

Dayton, (2002) described the fact that dolomites are quite inexpensive and an abundant material makes them very attractive as tar cracking catalysts. On the other hand, calcined dolomites are rather soft and therefore erode quickly as a result of attrition phenomena in fluidized bed reactors. Another disadvantage of using dolomites is that they are not very active for tar elimination and as a result, they are often used in guard beds, in conjunction with highly active and more expensive Ni-based catalysts.

Dou et al., (2003) evaluated five catalysts to tar component removal from high-temperature fuel gas in a fixed-bed reactor. The cracking removal of tar component in high-temperature fuel gas cleanup is one of the most crucial problems in developing cleanest advanced power technology. 1-Methylnaphthalene was chosen as a model of tar component. The Y-zeolite and NiMo catalysts were found to be the most effective catalysts. Two catalysts almost removed 100% tar component at 550^{o}C. The process variables, temperature and space velocity, have very significant effects on tar component removal with catalysts. The long-term durability shows that two catalysts maintain more than 95% removal conversion at 550^{o}C in 168 h. He carried out combustion study of coke deposited on catalysts by thermal gravimetric analysis technology showing that very small amount build up of coke appears on two catalysts surface.

El-Rub et al. (2004) explained that there are many types of catalysts used for tar removal, minerals like calcined rocks, olivine, clay minerals and iron ores or synthetic catalysts like zeolites, activated alumina, alkali metal-based or transition metal based catalysts. In particular Ni-based catalysts are 8-10 times more active than dolomite, are able to attain complete tar elimination at 900°C and to increase the yield of CO_2 and H_2. The problem is their rapid deactivation due to sulphur and high tar content in the feed.

Devi et al. (2005) considered olivine as a prospective in-bed tar removal catalyst for fluidized bed biomass gasifiers. The catalytic activity of olivine is investigated via steam reforming reaction of naphthalene as a model biomass tar compound. It is observed that the calcination of olivine improves the performance of the catalyst. Calcination of olivine is done with air at 900^{o}C for different treatment times. With increasing calcination time, tar conversion increases; more than 80% naphthalene conversion is observed with 10 h of calcination time for olivine, which is found to be an optimum as further increase in time up to 20 h does not improve the naphthalene conversion.

Thomas et al., (2006) described that tar formation is a major drawback when biomass is converted in a gasifier to obtain gas. Catalytic cracking is an efficient method to diminish the tar content in the gas mixture. Metallic iron, small grains of hematite (Fe_2O_3) were placed in a secondary reactor downstream the gasifier and reduced in-situ prior to catalytic operation. The fuel used in the atmospheric fluidized bed gasifier with a moisture content of approximately 7 wt %. The influence of temperature in the range 700–900^{o}C and ER values (i.e. equivalence ratio, ER) between 0 and 0.20 has been investigated. In essence, the results show that raising the temperature in the catalytic bed to approximately 900^{o}C yields almost 100% tar breakdown. Moreover, increasing ER value also improves the overall tar cracking activity.

Bhave et al., (2008) developed the producer gas cooling–cleanings compact unit, in which the gas cooling and cleaning take place effectively in one vertical tower, unlike other systems which have several chambers for these tasks. It is easy to operate, and has a low pressure drop. The unit will give a clean gas with tar and dust content below the limit of 150 mg/Nm3 as long as the inlet gas tar and dust content is below about 600 mg/Nm3.

Pathak et al., (2008) described that engine quality producer gas must be almost free of solid particulate matters and organic contaminants (Tar) to minimize engine wear and maintenance. Except for the catalytic tar crackers, none of the gas cleaning systems commercially available can securely meet a tar removal exceeding 90 % and hence new concepts for tar removal are required. This paper presents a design and development work of sand filter for upgrading producer gas to IC engine quality fuel. The experimental investigations show that percentage reduction in tar and particulate matters is above 90 % before and after filter respectively. Regenerative sand bed filters to clean producer gas.

Post cleaning the gas is achieved by passing through cyclone where major amount of particulates are collected in dry form. The gas is cooled with water spray and scrubbed subsequently, the gas is also sub cooled to condense the saturated moisture. In the process of moisture precipitation, fine particulate matter is also trapped. The clean dry gas is inducted to a blower and discharged to fabric filter before it can enter in to the engine (Dassapa et al., 2010)

Higher temperature was beneficial to lower the amount of tar while the soot yield showed a peak of 56.7 g/kg fuel at 1200^{o}C. With steam addition, the producer gas yield and in

particular the H_2 yield increased gradually, while the CO yield decreased slowly. Gas cleaning for tar and particle removal is necessary (Qin et al., 2012).

The Fe/g-Al_2O_3 exhibited good performances for H_2 production from biomass. The gaseous products stream consisted in 30-35% H_2. Comparison of the pyrolysis of biomass (empty reactor) with the catalytic cracking revealed that processes of thermal decomposition and catalytic reformation were co-existent. Catalyst improve biomass pyrolysis, decompose bio-oil into gaseous products and increase hydrogen production by steam reforming (Xiwei et al., 2012).

2.6 TAR GENERATION AND CRACKING

Tar is a complex mixture of condensable hydrocarbons, including, among others, oxygen-containing, 1- to 5-ring aromatic and complex polyaromatic hydrocarbons. It is defined as "all organic contaminants with a molecular weight larger than 78, which is the molecular weight of benzene." It is a thick, black, highly viscous liquid that condenses in the low-temperature zones of a gasifier, clogging the gas passage and leading to system disruptions. Tar is an unavoidable by-product of the thermal conversion process (Basu, 2010). Various attempts are made to remove and crack the tar but till it is awaited. Tar cracking can be defined as a process that breaks down the larger, heavier and more complex hydrocarbon molecules of tar into simpler and lighter molecules by the action of heat and aided by the presence of a catalyst but without the addition of hydrogen (Abu et al., 2004).

Catalysts accelerate the two main chemical reactions steam-reforming and dry-reforming reaction of tar reduction. Dry reforming is more effective than steam reforming when dolomite is used as the catalyst (Sutton et al., 2001). Catalysts can facilitate tar reduction reactions either in the primary reactor (gasifier) or downstream in a secondary reactor. In either of the case, dolomite, olivine, alkali, nickel, and char found successful as catalysts for tar reduction.

Dolomite

Dolomite ($MgCO_3$, $CaCO_3$) is relatively inexpensive and is readily available. It is more active if calcined and used downstream in the secondary reactor at above 800 °C (Sutton et al., 2001).The reforming reaction of tar on a dolomite surface occurs at a higher rate with CO_2 than with steam. Under proper conditions it can entirely convert the tar, but

cannot convert methane if that is to be avoided for syngas production. Carbon deposition deactivates dolomite, which, being less expensive, may be discarded.

The Dolomite is a calcium magnesium ore with general chemical formula CaMg $(CO_3)_2$ with some minor impurities. In order for dolomite to become active for tar conversion, it has to be calcined. Calcination involves decomposition of the carbon and mineral, eliminating CO_2 to form MgO-CaO, at high temperatures (usually 800-900°C). The effective use of dolomite as a catalyst is restricted by relatively high temperatures and the partial pressure of CO_2 (Simell et al., 1995). The dolomites composition for catalytic activity has been shown that an increased content of iron in dolomites, i.e.Fe_2O_3, can raise its activity towards tar elimination by 20% (Orio et al., 1997).

Olivine

Olivine is a magnesium-iron silicate mineral (Mg, Fe_2) SiO_4 that comes in sizes (100-400 micron) and density ranges (2500–2900 kg/m3) similar to those of sand. Thus, it is conveniently used with sand in a fluidized-bed Gasifier. The catalytic activity of olivine is comparable to that of calcined dolomite. When using olivine, Mastellone and Arena, (2008) noted a complete destruction of tar from a fluidized-bed gasifier for plastic wastes, while Rapagnà et al., 2000 obtained a 90% reduction in a biomass-fed unit.

Alkali

Alkali metal catalysts are premixed with biomass before they are fed into the gasifier. Some of them are more effective than others. For example, the order of effectiveness of some alkali catalysts can be shown as follows

$K_2CO_3 > Na_2CO_3 > (Na_3H(CO_3)_2 \times 2H_2O) > Na_2B_4O_7 \times 10H_2O$

Unlike dolomite, alkali catalysts can reduce methane in the product gas, but it is difficult to recover them after use. Furthermore, alkali cannot be used as a secondary catalyst. Its use in a fluidized bed makes the unit prone to agglomeration.

Nickel

Many commercial nickel catalysts are available in the market for reduction of tar as well as methane in the product gas. They contain various amounts of nickel. For example, catalyst R-67-7H of Haldor Topsoe has 12 to 14% Ni and Mg/Al_2O_3 support (Sutton et

al., 2001) Nickel catalysts are highly effective and work best in the secondary reactor. Use of dolomite or alkali as the primary catalyst and nickel as the secondary catalyst has been successfully demonstrated for tar and methane reduction. Catalyst activity is influenced by temperature, space–time, particle size, and composition of the gas atmosphere. The optimum operating temperature for a nickel catalyst in a downstream fluidized bed is 780 °C (Sutton et al., 2001). Steam-reforming with nickel catalysts for heavy hydrocarbons are effective for reduction of tar while nickel catalysts for light hydrocarbons are effective for methane reduction. Deactivation due to carbon deposition and particle growth is a problem for nickel-reforming catalysts.

Char

Char, a carbonaceous product of pyrolysis, also catalyses tar reforming when used in the secondary reactor obtained a nearly total reduction in tar with this. As a major gasification element, char is not easily available in a gasifier's downstream. Design modification is needed to incorporate char as a catalyst

Milne et al., (1998) described that, "The organics, produced under thermal or partial-oxidation regimes (gasification) of any organic material, are called "tar" and are generally assumed to be largely aromatic. A common perception about tar is that it is a product of gasification and pyrolysis that can potentially condense in colder downstream sections of the unit. The amount of tar in product gas depends on the gasification temperature as well as on the gasifier design. Typical tar levels in gases from downdraft and updraft biomass gasifiers are 1 g/Nm^3 and 50 g/Nm^3, respectively (Table 2.2). Tar levels in product gas from bubbling and circulating fluidized-bed gasifiers are about 10 g/Nm^3. Table 2.2 also shows that the amount of tar produced varies from 1 to 20% of the feed of the biomass.

TABLE 2.2 Typical levels of tar in various types of gasifier biomass (Milne et al., 1998).

Gasifier Type	Average Tar Concentration In Product Gas (g/Nm^3)	Tar as % of Biomass Feed
Downdraft	<1.0	<2.0
Fluidized bed	10	1-5
Updraft	50	10-20
Entrained flow	negligible	-

The amount of tar reduced with temperature, is as shown in Figure 2.1.

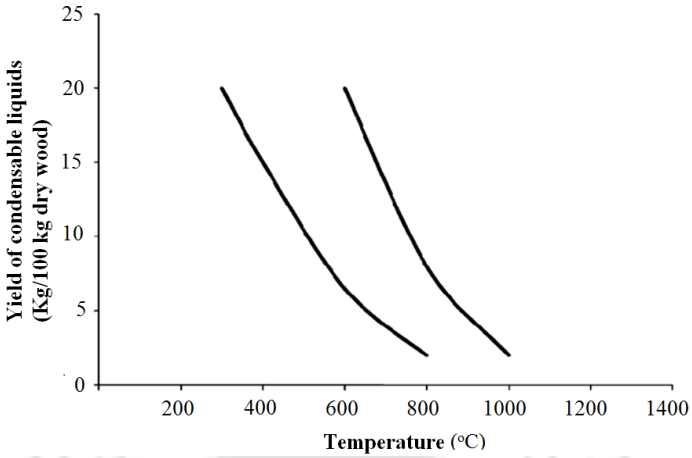

Fig. 2.1 Effect of maximum gasification temperature on tar yield (Milne et al.,1998)

As we can see in Table 2.3, tar is a mixture of various hydrocarbons. The yield and composition of tar depends on the reaction temperature, the type of reactor, and the feedstock. Table 2.3 shows that benzene is the largest component of a typical tar.

Table 2.3 Typical composition of tar (Milne et al.,1998)

Component	Weight (%)
Benzene	37.9
Toluene	14.3
Other 1-ring aromatic hydrocarbons	13.9
Other 2-ring aromatic hydrocarbons	7.8
3-ring aromatic hydrocarbons	3.6
4-ring aromatic hydrocarbons	0.8
Naphthalene	9.6
Phenolic compounds	4.6
Heterocyclic compounds	6.5

Dayton D, (2002), the fact that dolomites are quite inexpensive and abundant materials makes them very attractive as tar cracking catalysts. On the other hand, calcined dolomites are rather soft and therefore erode quickly as a result of attrition phenomena in fluidized bed reactors. Another disadvantage of using dolomites is that they are not very active for tar elimination and as a result, they are often used in guard beds, in conjunction with highly active and more expensive Ni-based catalysts.

Myren et al., (2002) investigated the catalytic effects of dolomite and silica on biomass tar decomposition. The concentration of naphthalene is of particular interest since it is the most difficult compound to decompose when dolomite is used as catalyst. The two catalysts were tested in different combinations to see whether synergetic effects on the cracking of naphthalene could be found. Thermal and catalytic cracking were carried out at 700–900°C under ambient pressure in a fixed bed reactor using a tar-rich gas obtained from pyrolysis of different biomass materials. Characterization of light components of tars using the solid phase adsorption method was also performed. Experimental results indicate that when pure silica is placed in a layer above the dolomite, considerably less naphthalene and total light tar remains after cracking.

Corella et al. (2004) conducted a study of several in-bed additives in biomass gasification with air and made the conclusion that calcined dolomite is more effective for in-bed tar removal (~1.40 times) than untreated olivine but at the same time generates more particulates in the producer gas (~4-6 times) Abu et al., (2004), explained that the dolomite and olivine tar cracking catalysts are naturally occurring minerals. Another type of material that has been recognized as a tar cracking catalyst is the Fluid Catalytic Cracking (FCC) catalyst. Unlike dolomite; olivine is a nonporous material that has an extremely low surface area and negligible pore volume. The main advantage of olivine, in comparison to dolomite is its resistance to attrition. Price levels of olivine and dolomite are approximately the same,

Devi, et al., (2005a) explained that the tar removal technologies can be divided into two approaches: treatments inside the gasifier (primary methods) and hot gas cleaning after the gasifier (secondary methods). Although primary methods theoretically eliminate the need for downstream clean-up creating tar-free gas at the exit of the gasifier, they have not yet resulted in satisfactory low level of tar

Kannaiyan et al. (2016) used the downstream catalytic post treatment to scrubbed producer gas for removal of the tar. The fixed bed catalytic tar cracking unit was wound with electrical resistance coils for maintaining required temperatures. Unit was consisting of tar cracking reactor filed with bimetallic Ni-Co/Si-P nano catalyst an guard bed reactor filled with dolomite stones. Dolomite captures fine particle and convert heavy tar while Ni-Co/Si-P reforms the lighter tar into CO and H_2. The 99% tar removal is obtained at

optimum bed temperature 800 °C. The H_2 and CO compositions increased by 24 vol % and 16 vol % , respectively while CO_2 and CH_4 compositions decreased.

Jankeset et al., (2012) suggested that gas clean-up problems can be largely avoided if biomass gasifier is coupled to the combustion chamber and tar cracking columns. As a small portion of oxygen will be introduced into the combustion chamber, a portion of gas will be combusted in order to reach gas temperature of 800 °C. The combustion chamber is coupled with the regenerative heat exchanger of which two columns are filled with Al_2O_3 pebbles where thermal decomposition of tar takes place. Tar free gas exits the combustion chamber at the temperature of approximately 700 °C. After tar cleaning, the syngas is carried through gas to water and gas to air heat exchangers for cooling. The purpose of gas cooling is to lower gas temperature which should meet the requirements of gas treatment equipment and provide optimal operation conditions.

Sun, (2012) developed and tested a bimetallic dolomite based tar cracking catalyst. It was enriched in Ni and Fe. The catalytic characterizations were tested with tar simulated by naphthalene, and with tar produced by biomass and coal co-pyrolysis. 93% naphthalene was decomposed at 950 °C. A first order apparent kinetic model was developed. Activation energy of 63.96 kJ/mol and pre exponential factor of 396.2/s were calculated. The reduction in char yield was observed 7%, when the catalyst was used in the biomass–coal co-pyrolysis.

Grieco, et al., (2013) studied two perovskites ($LaCrO.7NiO.3O_3$ and $LaCrO.5NiO.5O_3$) as possible catalysts for cracking of tar produced by pyrolysis and gasification of biomass and wastes. Naphthalene and n hexadecane were chosen as model compounds for tar. The catalysts containing chromium are much more stable although less active than $LaFeO.7NiO.3O_3$; in all tests an almost constant conversion of the hydrocarbons was found.

Jordan and Akay, (2013) investigated the impact of granular calcium oxide used in syngas conditioning on tar composition, concentration, dew point and syngas yield during gasification of fuel cane bagasse (FCB). The results showed that the use of 2, 3 and 6 wt. % in-bed CaO promoted the conversion of Class1, 4 and 5 tars to Class 3 tars to varying degrees. Overall, this resulted in a decrease in tar yield ranging from 16 to 35%, a decrease in the tar concentration in syngas of 44–80%, an increase in syngas yield of 17–

37%, and a decrease in tar dew point of 37–60 °C as the CaO concentration was increased from 2 to 6 wt.% .

Laksmono, et al., (2013), studied of valorization of tar from biomass gasification. Thermal cracking of biomass gasification tar gave a yield of biodiesel 73.67 wt. % of feed. The cracking process in the presence of zeolite, magnesium oxide, and aluminum oxide catalysts gave a yield of biodiesel 62–75 wt. %, 55–66 wt. %, and 67–71 wt. % respectively. The produced bio-oil density and heating value were close to the conventional diesel fuel with slightly higher viscosity and acidic value.

Raman et al. (2013) designed a dual fired downdraft gasifier system to produce clean gas from biomass fuel. The system is equipped with dry gas cleaning and indirect gas cooling equipment. The dry gas cleaning system completely eliminates wet scrubbers that require large quantities of water. With dual firing system, tar level in raw gas is less than 100 mg Nm^{-3}. Cold gas efficiency has improved to 89%.

Berrueco et al. (2014) conducted experiments in a fluidized bed reactor using two different types of feedstock material Norwegian spruce and Norwegian forest residues torrefied at 275 ^{o}C ,under a constant pressure of 0.5 MPa and at two temperature levels (750^{o}C and 850^{o}C). The catalytic effect of dolomite promoted tar cracking towards gas products and thus higher gas yield. Higher production of gas was detected at 850^{o}C. Tar destruction reactions in presence of catalyst (dolomite) shifted to higher composition of H_2, CO_2, CO and CH_4 whereas hydrocarbons decreased an effect that was slightly more relevant at 850^{o}C.

Roche et al. (2014) investigated the influence of throughput (TR), steam and the use of dolomite (as primary catalyst) over the sewage sludge gasification products. According to the obtained results, higher TRs decreased the H_2 content of the produced gas and clearly increased the gravimetric tar production. The use of air with steam, especially in the presence of dolomite, increased the H_2 content (between 20% and 36%) and decreased the gravimetric tar production.

2.7 CASE STUDY OF VARIOUS PLANTS

Case Study is carried out for two plants namely Hara Parbati Rice mill Dhanbad, West Bengal and M/S Synergy Ltd. Jogigopa, Assam.

2.7.1 CASE STUDY OF HARA PARBATI RICE MILL PRIVATE LTD DHANBAD, WEST BENGAL

The salient points of the visit to Hara Parbati Rice Mill are as follow:

- The Rice mill is named as 'Hara Parbati Rice Mill Private Ltd Dhanbad, West Bengal. Downdraft gasifier is used to supply power to rice mill. Gasifier is manufactured by Ankur Seeds (P) Ltd. Barodara. Rice husk which is byproduct of rice mill is used as feedstock. The feed rate is controlled with pocket elevator.
- Gasifier is fired from top by powering the quantity of the diesel from lead of the gasifier. Afterward feedstock is continued from the pocket elevator. Air is supplied from the lead. The gas is coming out from the reaction chamber which is cooled by the water to remove the tar (Fig.2.2)
- The gas is sucked by ID fan which create the pressure drop. Afterword gas is passed through various filters which contain rice husk, saw dust and filter bag. Filtered producer gas is used in duel fuel mode CI Engine for power generation.

Fig. 2.2 Pictorial view of Hara Parbati rice mill private Ltd Dhanbad

Drawback of the gasifier

- The producer gas consists of measurable amount tar even if after the post treatment to the raw producer gas. Though there is gas clean up system, the producer gas consists of sticky Tar.

- Tar is sticky in nature and clogged coupled duel fuel engine. The frequent maintenance of the engine is required.
- This is the main headache to the owner.

2.7.2 CASE STUDY OF M/S SYNERGY PRIVATE LTD JOGIGOPA, ASSAM

The salient points of the visit to M/S Synergy Private Ltd Jogigopa, Assam

- M/S Synergy is a 100 ton biomass-char unit in which charcoal is produced from biomass (Fig. 2.3).
- The principal of updraft gasifier is used for the conversion of biomass to coal.
- Large amount of tar and liquor is generated as a byproduct of unit.
- Tar and liquor is separated from the hot gas with cyclone separators. Afterward large amount of tar is separated from liquor by natural sedimentation method.
- Presently tar collected in plant is used for the construction of roads.
- There is a large scope for waste-to energy from tar.

Fig.2.3 Pictorial view of M/S Synergy Private Ltd Jogigopa, Assam

2.8 RESEARCH GAP

An extensive literature review was conducted on the performance of gasifier, effect of feedstock, shape of the feedstock and various input parameter are studied. Excellent remarks are given by the researchers on the use of feedstock into gasifier. Fixed bed gasifiers are more suitable for solid fuels like woodchip. It has the limitation of fluffy

biomass and low density materials. Use of these materials as feedstock gives rise to flow problems and excessive pressure drop in the gasifier. The bridging of the feedstock was observed in the throat zone of the gasifier (Dogru et al., 2004). Sridhar et al.,(2005) reported severe ash fusion problem at high loading rate with loose biomass. The loose biomass can be used in the gasifier by converting it into pellet or briquette which solve bridging problem of gasifier (Asadullah, 2014, Kjellstom, et al., 2005). The larger size of the briquette gives the more amount of yield gas (Shivkumar, et al., 2012). However most of the studies were confined to the effect of geometry of briquettes and pellets on gas production. Production of tar is another severe problem causing clogging or soaking the downdraft gasifier. Very few results on tar formation and remedial solutions to reduce or crack tar during gasification has been reported in the literature (Catharina, 2011). Tar removal is approached in two type of treatments inside the gasifier (primary methods) and hot gas cleaning after the gasifier (secondary methods). Researchers developed the various gas cleaning systems for the post treatment of the tar like regenerative sand bed filter, wet packed bed scrubber-based, the monolith catalyst test reactor, fluid catalytic cracking system, etc. Tar is a major unsolved constituent of gasification technology. It can be eliminated with in-situ thermal cracking. Hence there is a need to explore the feasibility of loose biomass in downdraft gasifier along with the tar cracking.

Present work is an attempt to study the feasibility of spherical shape saw dust briquette and cylindrical pellet in a 5 kW_e down draft gasifier and evaluate performance of gasifier along with the gas quality and tar yield.

2.9 SCOPE OF RESERACH

As discussed in the previous subsection an attempt has been made to investigate the performance of downdraft gasifier which is designed for woodchip along with reduction in tar and development of tar cracking unit.

The scope of the work is given as

- Performance evaluation of biomass gasifier in terms of feedstock properties, zone temperatures, equivalence ratio, producer gas composition, Producer gas production rate. Comparison of gas yield quality in terms of different feed materials such as wood chips, biomass briquettes, pellets and biomass-dolomite pellet
- Improvement in gas composition through in-situ treatment by biomass-dolomite pellet.

- Thermal cracking of the tar gained from biomass gasification. Experimentation with various blends of tar with dolomite as catalyst.

2.10 SUMMARY

A detailed literature review was conducted and discussed in the present chapter. Limitations of performance of downdraft gasifier are presented. Based on these findings present works are identified and formulated. Subsequently Chapter 3 presents the characterization of the feedstock used for the current experiential investigation in the downdraft gasifier. This study gives scope for the selection of optimum feedstock for gasification to acquire good composition producer gas.

CHAPTER 3

CHARACTERIZATION OF BIOMASS

3.1 INTRODUCTION

As discussed in the previous Chapter, utilization of biomass for power generation has gained popularity to substitute the use of fossil fuel for last few decades. Biomass gasification is considered to be superior to direct combustion due to environmental compatibility. However, technology related to gasification is influenced by physical, chemical as well as thermal properties of biomass feed in gas production. Moreover, most of the biomass used in fixed bed gasifier is reported to be solid biomass sized to a particular dimension. Feasibility of use of loose biomass in a conventional wood chip fed gasifier is hardly known. In the present Chapter an extensive study is carried out to characterize different type of biomass to find the potential application in conventional fixed bed gasifier.

3.2 SAMPLE PREPARATION FOR CHARACTERIZATION

Locally available loose biomass such as saw dust, rice husk and mustard husk are considered for the characterization. These biomasses are considered as the same are available abundantly in most of the country sides of tropical countries. As present work is aimed at to use loose biomass to substitute solid wood chips, briquettes and pellets are made with the aforementioned biomasses. Waste newspapers are used as a binder. Details of methods of preparation of briquettes and pellets are explained in the subsequent Chapter. The composition and notation used in the Table 3.1 indicates the briquette composition in terms of percentage by weight of binder material (waste newspaper) used.

Table 3.1 Briquette composition with notations

Material	B_{05}	B_{10}	B_{15}	B_{20}	B_{25}
Biomass (%)	95	90	85	80	75
Waste newspaper as binder (%)	05	10	15	20	25

Another series of characterization is done with biomass added with dolomite powder in the form of pellets. Table-3.2 presents the list of various pellets under study. The notation used in the Table 3.2 indicates the pellet composition in terms of percentage by weight of dolomite used. For example, P_{05} stands for the pellet with 5% dolomite by weight. Thus P_{10} represents pellet with 90% of biomass and 10% of dolomite by weight.

Table 3.2 Pellet composition with notations

Material	P_{00}	P_{10}	P_{20}	P_{30}	P_{40}
Biomass (%)	100	90	80	70	60
Dolomite as catalyst (%)	00	10	20	30	40

3.3 TYPE OF CHARACTERIZATION

The characterization of biomass briquettes, pellets and loose biomass is carried out in the present investigation. The analysis includes the following:

1. Proximate analysis
2. Ultimate analysis
3. Calorific value
4. Feedstock Handling Characteristics
5. Thermogravimetric analysis
6. Fibre analysis

3.4 PROXIMATE ANALYSIS

3.4.1 METHODOLOGY

The proximate analysis of biomass material is carried out in muffle furnace (Fig.3.1)

Fig.3.1. Muffle furnace

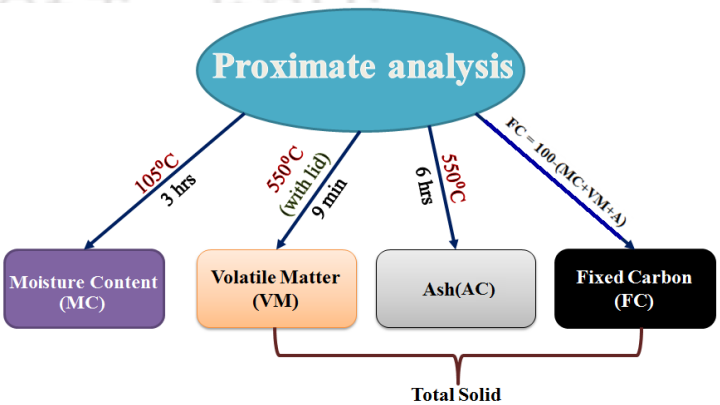

Fig. 3.2 Proximate analysis layout

Characterization of the biomass samples is carried out by using ASTM Method D5373-02 (2003). A schematic diagram of the process adapted for proximate analysis is given in Fig. 3.2.The analysis is carried out for (a) moisture content, (b) volatile matter content, (c) ash content and (d) fixed carbon content. The entities are calculated in weight percentage.

a. Moisture content (%)

The percentage of moisture content on dry basis [MC_{db} (%)] in biomass briquettes is determined with Eq.3.1. One gm sample of feedstock is taken in a crucible. It is dried in Muffle furnace at 105°C for 3hrs. Then weight change is measured after 3hrs.

$$MC_{db}(\%) = \frac{A - B}{A} \times 100 \tag{3.1}$$

where

A=Sample weight before drying

B=Sample weight after drying

b. Volatile matter (%)

The percentage of volatile matter [VM (%)] is calculated for 1gm sample of feedstock. It is pulverized in a crucible and placed in a muffle furnace at a temperature of 550°C for 9 min. Then it is cooled in desiccators. The weight is measured after cooling the sample and volatile matter (%) is determined by Eq.3.2.

$$VM(\%) = \frac{B - C}{B} \times 100 \tag{3.2}$$

Where,

B =Sample weight after drying

C = Sample weight after drying in desiccators

c. Ash content (%)

The percentage ash content [AC (%)] is determined by heating 1 gm of the feedstock sample in the furnace at a temperature of 550°C for 6 h and weighed after cooling in desiccators to obtain the weight of ash. The ash content (%) is determined by using Eq.3.3.

$$AC\ (\%) = \frac{D}{B} \times 100 \qquad (3.3)$$

Where,

B =Sample weight after drying

D = weight of sample after heating the sample at 550°C for 4 hours.

d. Fixed carbon

The percentage of fixed carbon [FC (%)] is calculated by subtracting the sum of percentage moisture content [MC (%)], percentage volatile matter [VM (%)] and percentage ash content [AC (%)] from 100 as given in Eq. 3.4.

$$FC\ (\%) = 100 - [MC\ (\%) + VM(\%) + AC(\%)] \qquad (3.4)$$

3.4.2 PROXIMATE ANALYSIS OF BIOMASS BRIQUETTE

The proximate analysis for biomass briquette for the various compositions of biomass and binder is given in Table-3.3.

Table 3.3 Proximate analysis of biomass briquettes (Shelke and Mahanta, 2014)

Briquette	Proximate analysis	B_5	B_{10}	B_{15}	B_{20}	B_{25}
Saw dust briquette	Moisture [%]	12.40	12.59	12.39	12.5	11.67
	Volatile matter [%]	72.65	73.41	73.87	73.88	74.29
	Ash content [%]	2.96	3.32	3.36	4.23	4.68
	Fixed Carbon [%]	11.99	10.68	10.38	9.39	9.36
Rice husk powder briquette	Moisture [%]	12.18	11.99	11.95	11.69	11.36
	Volatile matter [%]	61.96	61.87	63.08	63.39	63.81
	Ash content [%]	15.57	15.55	15.55	15.11	15.34
	Fixed Carbon [%]	10.29	10.59	9.42	9.81	09.49
Mustard husk powder briquette	Moisture [%]	10.16	10.09	9.87	10.42	10.28
	Volatile matter [%]	64.38	63.93	63.12	61.82	61.18
	Ash content [%]	4.14	4.32	4.67	4.84	5.12
	Fixed Carbon [%]	21.32	21.66	22.34	22.92	23.42

Figure 3.3 shows the variation of moisture content with binder composition. It is observed that the MC (%) for the saw dust is higher than the rice husk briquette and mustard husk briquette while mustard husk briquettes had lowest moisture content (%).

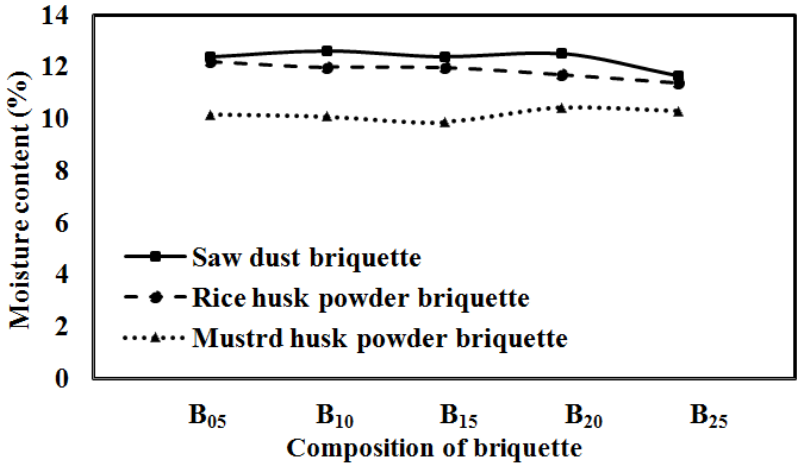

Fig.3.3. Moisture content (%) for various biomass briquette

Variation of volatile matter (%) with binder composition is shown in Fig. 3.4. It is noticed that volatile matter released in case of sawdust briquettes is more as compare to rice-husk briquettes and mustard husk briquette. The mustard husk briquettes had higher VM release than rice husk powder briquette up to 15% binder content afterword it decreases slightly.

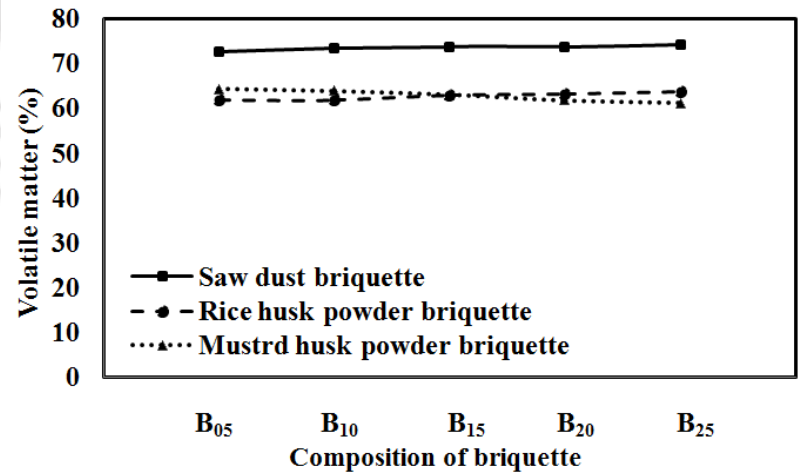

Fig.3.4. Volatile matter (%) for various biomass briquette

The ash content (%) for various briquette compositions for different materials are shown in Fig. 3.5. It is observed that saw dust briquette has lowest ash content than the rice husk powder briquette and mustard husk powder briquette. While the rice husk powder briquette has highest ash content (%).

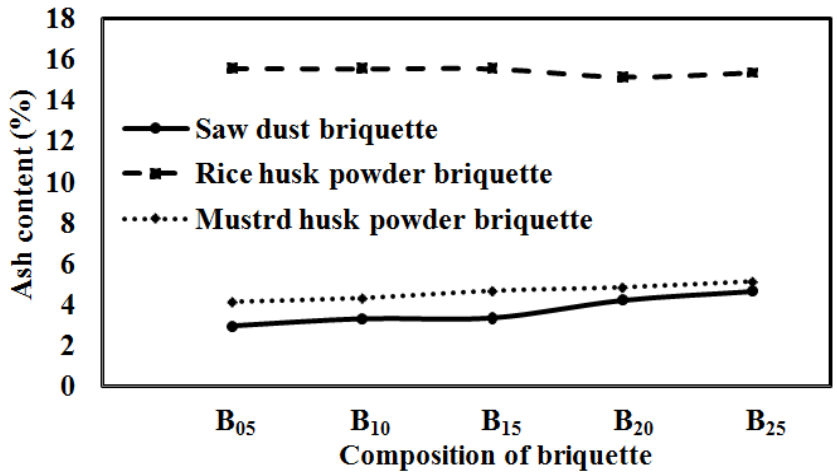

Fig.3.5. Ash content (%) for various biomass briquette

The variation of fixed carbon (%) with respect to briquette composition is shown in Fig. 3.6. The saw dust briquette has higher FC (%) than rice husk briquette up to 20% binder then it decrease. As the binder percentage increased fixed carbon content decreased in sawdust briquettes and becomes nearly equal to rice-husk.

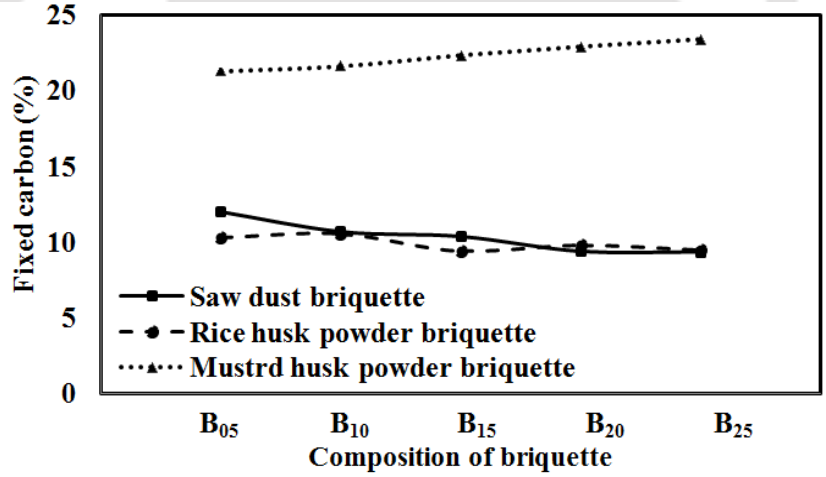

Fig.3.6. Fixed carbon (%) for various biomass briquette

3.4.3 PROXIMATE ANALYSIS OF BIOMASS-DOLOMITE PELLET

The proximate analysis for biomass-dolomite pellets is carried out as per the methodology explained in subsection 3.4.1. It is carried out for the various proportions of the biomass and dolomite. The moisture content percentage, volatile matter percentage, ash content percentage and fixed carbon percentage for biomass-dolomite pellet of saw dust and mustard husk powder are calculated and tabulated in Table-3.4.

Table 3.4 Proximate analysis of biomass-dolomite pellets

Biomass-	Proximate analysis	P_{00}	P_{10}	P_{20}	P_{30}	P_{40}
Saw dust-dolomite pellet	Moisture [%]	9.79	11.18	12.59	12.94	13.57
	Volatile matter [%]	74.18	73.87	73.41	72.65	71.83
	Ash content [%]	2.76	2.96	3.32	3.96	4.71
	Fixed Carbon [%]	13.27	11.99	10.68	10.45	9.89
Mustard husk powder-dolomite pellet	Moisture [%]	9.46	10.16	11.09	11.62	12.12
	Volatile matter [%]	65.92	64.38	63.93	62.89	62.11
	Ash content [%]	3.7	5.67	6.32	7.17	7.84
	Fixed Carbon [%]	20.92	19.79	18.66	18.32	17.93

Figure 3.7 shows the moisture content percentage for various compositions of biomass and dolomite. It is observed that the percentage of moisture content for the saw dust-dolomite pellet is higher than mustard husk briquette. Initially the difference is less but afterward as the percentage of dolomite increase the difference is also increased. The percentage of moisture content is increasing with increase in dolomite percentage.

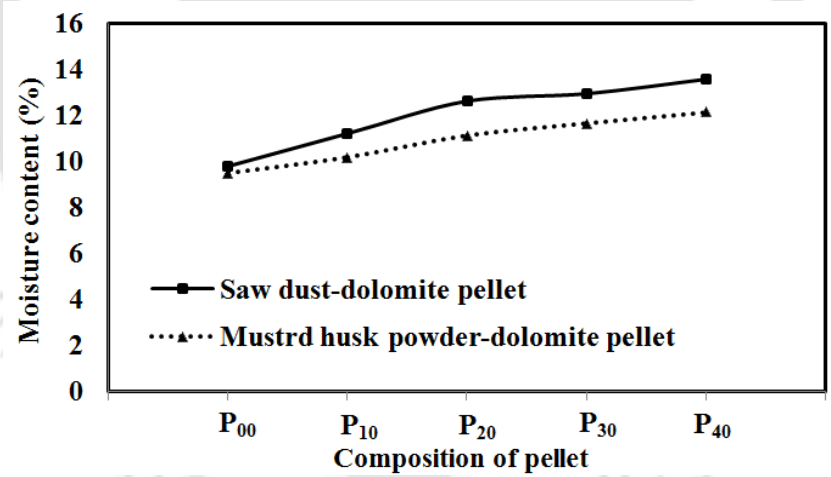

Fig.3.7. Moisture Content (%) for biomass-dolomite pellet

The variation in percentage of Volatile matter with respect to various compositions of biomass-dolomite pellets is shown in Fig.3.8. It is noted that the percentage of volatile matter decreases with the increase in the dolomite for both the biomass. It is observed that the volatile matter release is higher for the sawdust-dolomite pellet than the mustard husk-dolomite pellet.

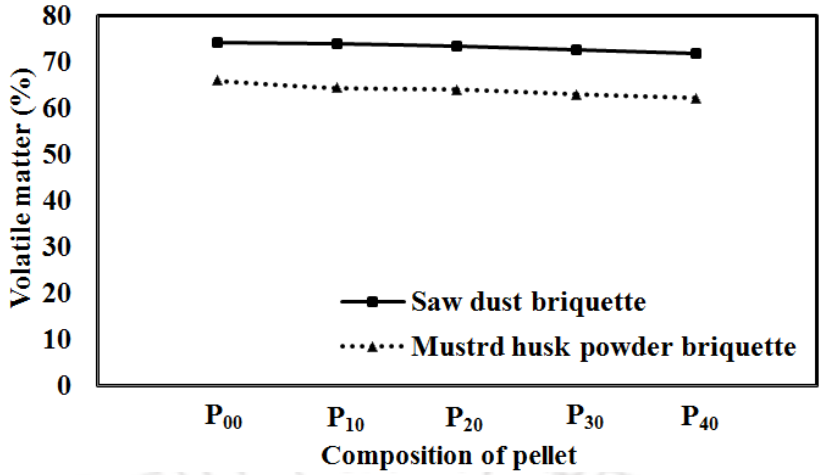

Fig.3.8. Volatile matter (%) for biomass-dolomite pellet

The Figure 3.9 show percentage of ash content versus the biomass-dolomite pellet composition. It is observed that the Ash content increase with increase in the dolomite percentage for both the biomass. The percentage of ash content is found comparatively more in amount for the mustard husk-dolomite pellets. Initially the difference is less but as the dolomite percentage increased the difference also increases.

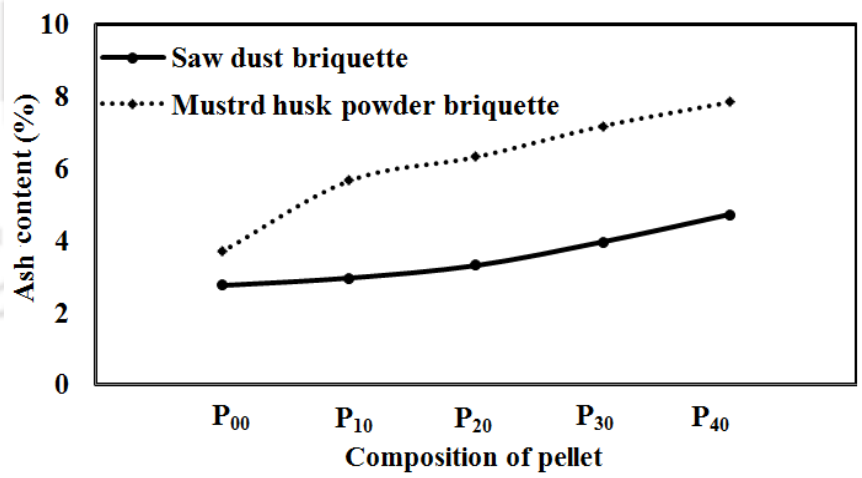

Fig.3.9 Ash content (%) for biomass-dolomite pellet

The percentage of fixed carbon content for the biomass is decreased with respect to increase in percentage of dolomite as shown in Fig.3.10. It is seen that the mustard husk dolomite-pellet has comparatively higher percentage of fixed carbon content than the sawdust-dolomite pellet.

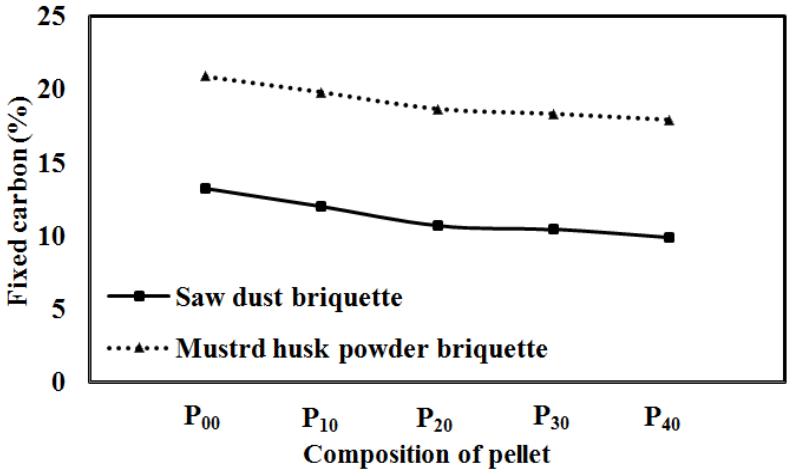

Fig. 3.10 Fixed carbon percentage for biomass-dolomite pellet

3.5 ULTIMATE ANALYSIS

The chemical constituent of the biomass are quantified with ultimate analysis. It is presented with the formula $C_xH_yO_z$ where x, y, and z are the elemental fractions carbon (C), hydrogen (H), nitrogen (N) and sulphur (S), respectively. Ultimate analysis is carried out using Euro EA Elemental Analyzer, a facility available in the Guwahati Biotech Park at IIT Guwahati. The ultimate analysis of various dried and grained samples is given in Table-3.5. Biomass formulation is given in Appendix-I.

Table 3.5 Ultimate analysis of biomass (Wt. %)

Material	C%	H%	N %	S%	Ash%	O%
Saw dust	44.547	8.872	4.462	-----	1	41.119
Rice husk powder	37.51	5.72	0.62	-----	16.59	39.56
Mustard husk powder	42.305	7.205	0.6	0.17	6.335	43.385

3.6 DETERMINATION OF CALORIFIC VALUE

The calorific value or heating value of the fuel is defined as the energy liberated by the complete oxidation of a unit mass of a fuel. It is determined by using bomb calorimeter (Fig. 3.11) by ASTM Method E 711-87 (2004). The stainless steel container (Bomb) is surrounded by a large temperature bath. The fuel is burnt in the bomb in presence of oxygen at about 600 atm. The change in temperature of water bath due to burning of a known quantity of fuel is measured using high precision thermometer. Heating value is given by the equation 3.5.

$$HV = \frac{WE \times \Delta T}{\text{Weight of the sample taken}} \quad (3.5)$$

Where,

HV = Heating value of the fuel to be determine

WE = Weight equivalent of the bomb calorimeter = 2568.293 calories / °C

$\Delta T = T_f - T_i$ (Final value – Initial value)

Fig.3.11 Bomb calorimeter

3.6.1 CALORIFIC VALUE OF THE BIOMASS BRIQUETTE

The calorific value for briquettes of various biomass materials for the different composition of the binder is calculated as given in Table-3.6. Present experiment is carried out with 0.5 gm weight of the sample of biomass.

Table 3.6 Heating value of various biomass briquette samples

Composition	Saw dust briquette	Rice husk powder briquette	Mustard husk powder briquette
	Heating value [MJ/kg]	Heating value [MJ/kg]	Heating value [MJ/kg]
B_{05}	18.28	15.05	15.50
B_{10}	17.42	13.96	14.60
B_{15}	17.20	13.55	14.15
B_{20}	16.56	13.33	13.68
B_{25}	15.91	13.12	13.29

The comparative analysis of calorific value for the various biomass materials for different composition of binder is shown in Fig. 3.12. It is observed that the calorific value of the saw dust briquette for all the variants is higher than the rice husk powder briquette and mustard husk powder briquette. While the calorific value of the mustard husk powder briquette is lower than the rice husk briquette powder and sawdust briquette.

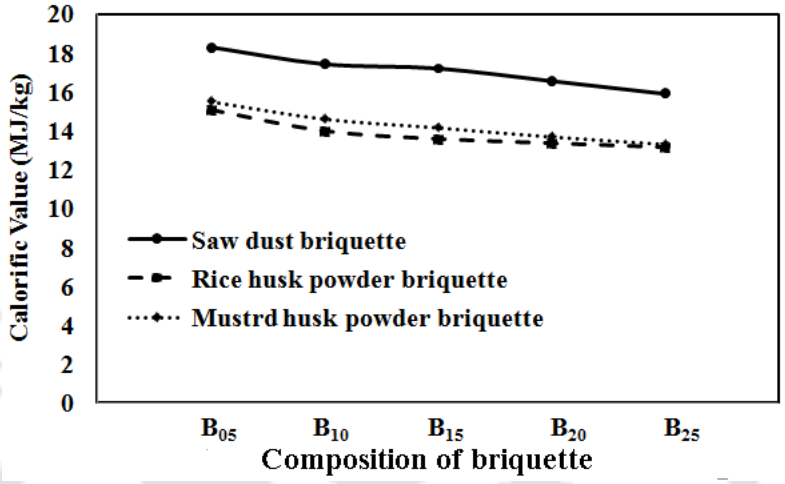

Fig.3.12 Calorific value of biomass briquette for various briquette composition

3.6.2 CALORIFIC VALUE OF THE BIOMASS-DOLOMITE PELLET

The calorific value for various biomass-dolomite pellets for different combination of the dolomite is calculated and tabulated in table 3.7.

Table 3.7 Heating value of various biomass-dolomite pellet samples

Composition	Saw dust-dolomite pellet	Mustard husk powder-dolomite pellet
	Heating value [MJ/kg]	Heating value [MJ/kg]
P_{00}	18.11	15.83
P_{10}	15.78	13.43
P_{20}	14.29	12.21
P_{30}	12.76	11.13
P_{40}	11.83	10.36

The comparative analysis of sawdust-dolomite pellet and Mustard husk dolomite pellet is presented in Fig.3.13. It is observed that the calorific value presented for the sawdust-dolomite pellet for all the composition is higher than the rice husk powder-dolomite pellet.

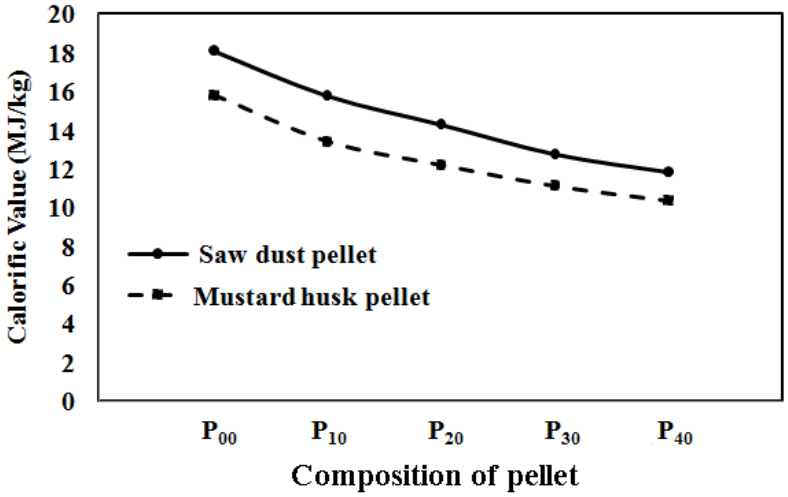

Fig.3.13 Calorific value of biomass-dolomite pellet for various compositions

3.7 FEEDSTOCK HANDLING CHARACTERISTICS

3.7.1 METHODOLOGY

a) Compressive resistance

Compressive resistance (or crushing resistance or hardness) is the maximum crushing load a pellet/briquette can withstand before cracking or breaking. Compressive resistance of the densified products is determined by diametrical compression test. A single pellet/briquette is placed between two flat, parallel platens which have facial areas greater than the projected area of the pellet/briquette. The load at fracture point, i.e. the maximum load, is converted into stress using the Eq. 3.6.

$$\sigma = \frac{F}{A} \tag{3.6}$$

Where,

σ = Compressive stress

F = Load at fracture

A = Cross sectional area of plane of fracture

An increasing load is applied at a constant rate, until the test specimen fails by cracking or braking. The load at fracture is read off a recorded stress-strain curve, which is the compressive strength and reported as force or stress (Kaliyan and Morey, 2009; Richard, 1990). In present work the stress value is calculated with the INSTRON machineby ASTM 1037-93(1995). The INSTRON machine with briquette is as shown in Fig.3.14.

Fig.3.14 Instron Machine

Figure 3.15 shows diametrical compression test of the biomass briquette. The briquette is placed between the two platens. Similarly the diametrical compression test for biomass-dolomite pellet is carried out as shown in Fig. 3.16.

Fig.3.15 Compression test of briquette

Fig.3.16 Compression test of pellet

b) Impact resistance index

The impact resistance index (IRI) is calculated by ASTM D440-86 (Drop Shatter for Coal) method. It is a durability test. A practical performance target for impact resistance of a biomass feedstock would be to sustain a number of falls from a stationary start and a

height of 2 meters onto a concrete floor. This test usually involves averaging the results of 3 to 6 single drop tests. Each briquette/pellet is repeatedly dropped until it fractures. The number of drops and the number of pieces the briquette breaks into are recorded. These data are used to calculate the IRI. The acceptable lowest and maximum values of IRI are 50 and 200, respectively [Richard (1990)]. The IRI value is calculated by Eq. 3.7.

$$IRI = \frac{n}{N} \times 100 \tag{3.7}$$

Where,

IRI = Impact resistance index

N = Average number of pieces

n = Average number of drops

c) Density

i) Density of briquette

The density of the briquette is measured with the ASAE (1998) Standard, ASAE S269.4 (DEC 1996). The weight of the briquette is measured in an analytical balance. Water is taken in the flask. The briquette is immersed in the water. The briquette should be immersed in the container until it is 50 mm below the water surface. The initial and final volume of water with the briquette immersed is recorded. The density of the briquette is calculated with the Eq.3.8.

$$\rho = \frac{m}{(V_f - V_i)} \tag{3.8}$$

Where,

ρ = Density

m = Mass

V_i = Initial volume of water, in mL

V_f = Final volume of water, in mL

ii) Density of pellet

The density of the pellet is calculated by using the Eq. 3.9. The weight of pellet is measured in an analytical balance. The diameter and length is measured and accordingly the volume is calculated.

$$\rho = \frac{m}{V} \quad (3.9)$$

Where,

ρ = Density

m = Mass

V= Volume

3.7.2 BRIQUETTE HANDLING CHARACTERISTICS

Table 3.8 presents the handling characteristics for the various biomass briquettes with different percentage of binder.

Table 3.8 Handling Characteristics of biomass briquette

Composi-tion	Saw dust briquette			Rice husk powder briquette			Mustard husk powder briquette		
	Stress [MPa]	IRI	Density [kg/m^3]	Stress [MPa]	IRI	Density [kg/m^3]	Stress [MPa]	IRI	Density [kg/m^3]
B_{05}	0.024	800	574.59	0.031	180	615.97	0.013	529	498.17
B_{10}	0.046	650	570.01	0.056	425	597.68	0.014	648	356.33
B_{15}	0.059	900	563.24	0.057	150	595.66	0.017	610	354.19
B_{20}	0.072	950	559.4	0.075	100	569.02	0.021	750	352.08
B_{25}	0.118	100	534.42	0.129	900	553.87	0.023	123	248.45

Figure3.17 shows stress analysis for the various composition of the briquette. It is observed that the stress values for the rice husk powder briquettes are comparatively higher than the sawdust briquette and mustard husk powder briquette.

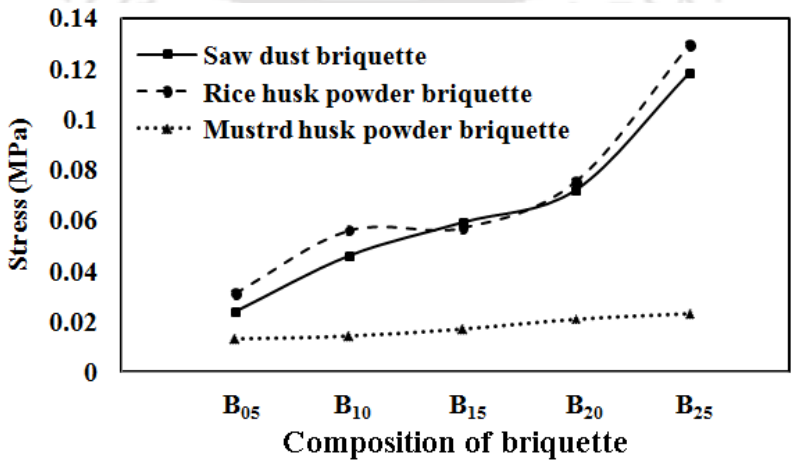

Fig.3.17 Stress analysis of biomass briquettes

While the mustard husk powder briquette has lesser values of the stress comparative to rice husk powder briquette and saw dust powder briquette.

The impact resistance index analysis for the three variants of briquette for the various compositions is shown in Fig.3.18. It is observed that the IRI value for all the briquette compositions is satisfactory.

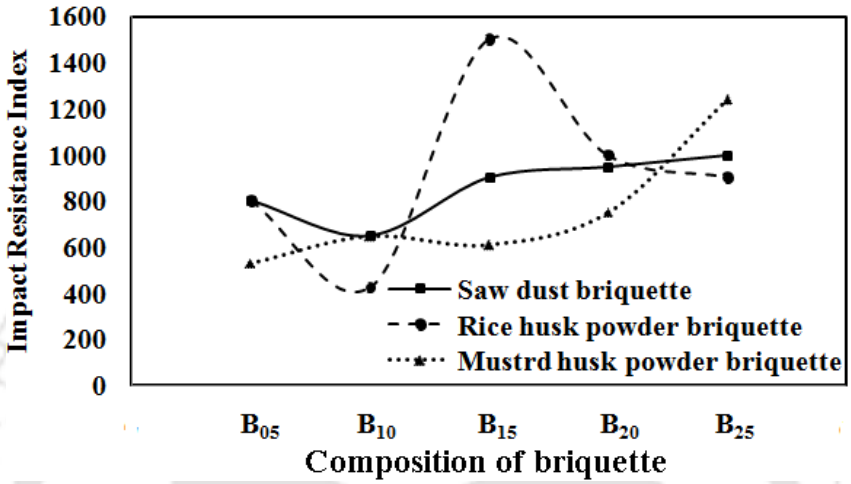

Fig.3.18 IRI analysis of biomass briquettes

The density analysis for the various compositions of the briquette is shown in Fig. 3.19. It is observed that the density of the rice husk briquette is higher than the saw dust briquettes. While the density of the mustard husk briquette is less than the sawdust briquette.

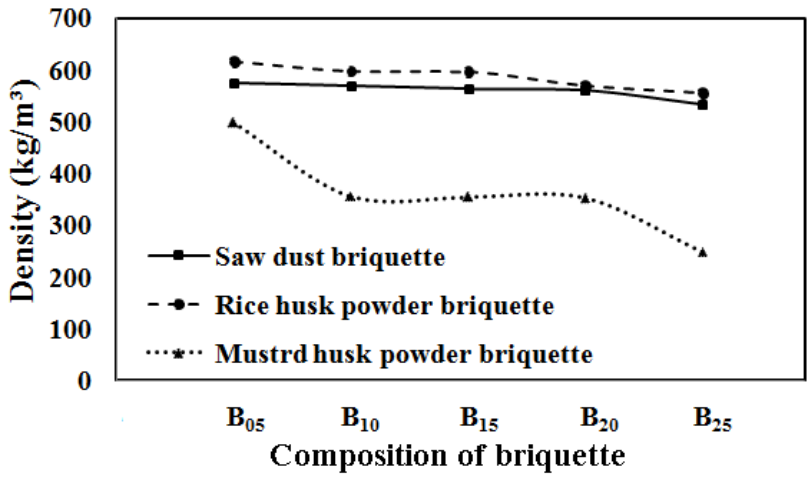

Fig.3.19 Density analysis of biomass briquettes

3.7.3 PELLET HANDLING CHARACTERISTICS

Table 3.9 presents the calculated values of the handling characteristics as stress, IRI and density of the various biomass-dolomite pellets are enumerated in Table-3.9.

Table-3.9 Handling characteristic of biomass-dolomite pellet

Composition	Saw dust-dolomite pellet			Mustard husk powder-dolomite pellet		
	Stress [MPa]	IRI	Density [kg/m^3]	Stress [MPa]	IRI	Density [kg/m^3]
P_{00}	3.34	6874	598	1.09	2800	480
P_{10}	1.75	4218	720	0.51	1350	650
P_{20}	1.55	2725	767	0.43	1025	684
P_{30}	1.13	1650	807	0.04	825	691
P_{40}	1.02	435	829	0.02	320	712

The stress analysis characteristic for the sawdust-dolomite pellets and mustard-husk dolomite pellets are platted in Fig. 3.20. It is observed that the stress withstand by the saw-dust dolomite pellet is higher than the mustard-husk dolomite pellet. The value of the stress found higher for the less composition of dolomite.

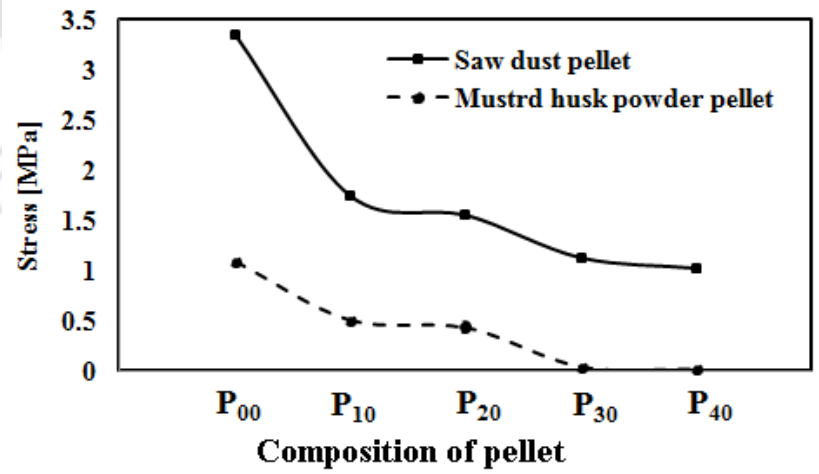

Fig.3.20 Stress analysis of biomass-dolomite pellets

Figure 3.21 shows the comparative analysis of impact resistance index of the saw-dust dolomite pellet and mustard-husk dolomite pellet. It is seen that the IRI index for the sawdust-dolomite pellet is higher than the mustard husk dolomite pellet. When the dolomite percentage is less the difference between these two variants is higher but as the dolomite percentage is increased the difference between these two variants decreases.

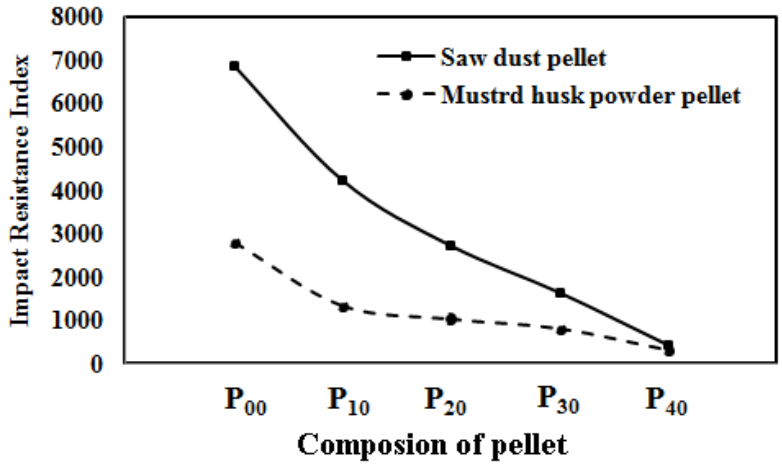

Fig.3.21 IRI analysis of biomass-dolomite pellets

The comparative analysis of density for the various compositions of the sawdust-dolomite pellet and mustard-husk dolomite pellet is shown in Fig.3.22. It is noted that the density is increases with the percentage of dolomite for both cases. It is noticed that the density of the saw dust pellet is higher than mustard husk pellet.

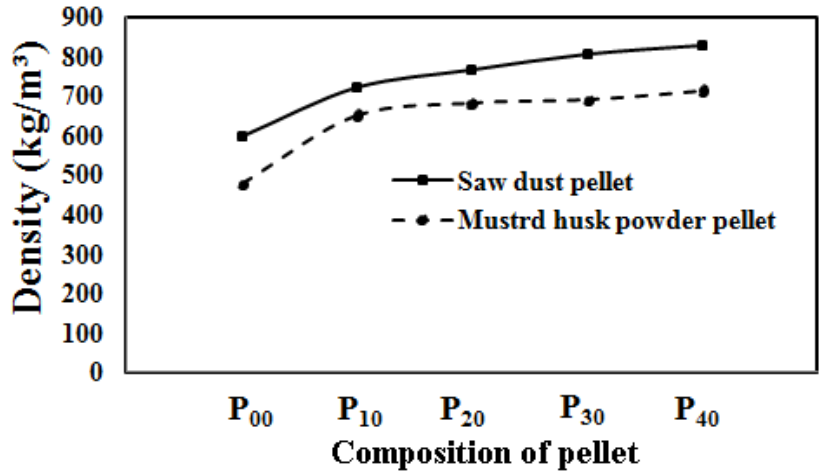

Fig.3.22 Density analysis of biomass-dolomite pellets

3.8 THERMOGRAVIMETRIC ANALYSIS

Thermogravimetric analysis (TGA) is a technique which measures the change in mass of a sample as it is heated, cooled or held at a constant temperature in a controlled atmosphere. Thermogravimetric analysis is carried out with dynamic thermogravimetric technique. In this technique a continuous recording of weight change of the sample in a flowing or static gas atmosphere is made as a function of time or temperature at a fixed heating rate, and plotted against temperature. The heating rate can be varied over a wide range and it can hold at various temperatures for specified times [Gaur and Reed (1995)].

Pyrolysis of biomass is significantly dependent on the main components of cellulose, hemicelluloses and lignin (Yang, et al., 2007). Hemicellulose and lignin started to decompose at lower temperatures compared with cellulose during TGA analysis; however, lignin is found to be decomposed over the whole investigated temperature (from ambient to 900^0C) and produced the highest residue after the TGA experiment (Yang et al., 2005;Yang, et al., 2007). The various researchers have carried out pyrolysis of cellulose, hemicellulose and lignin using thermogravimetric analysis (TGA) (Yang et al., 2007; Biagini, et al., 2006) Lignin decomposes slower, over a broader temperature range (200-500°C) than cellulose and the hemicellulose components of biomass (Mihai, et al., 2010).

In the present study the TG and DTG analysis of biomass briquettes and pellets is carried out with Simultaneous Thermal Analyzer (STA) 8000 offered by PerkinElmer Incorporation. A TGA consists of a sample pan of alumina which is supported by a precision balance. That pan resides in a furnace and is heated during the experiment. The mass of the sample is monitored during the experiment. A sample purge gas controls the sample environment. This gas is an inert gas that flows over the sample and exits through an exhaust. A small sample of the briquette/pellet species is heated in alumina sample pan in an inert gas atmosphere in non isothermal condition. Nitrogen gas is used as inert gas for present experimentation. The flow rate of Nitrogen is maintained at 20 ml/min. The scanning rate (β) is maintained 10°C/minute in the range of 40-900^{o}C. The wall temperature into reactor is monitored with R (PT-PT/Rh) type thermocouples. The STA 8000 analyzer is controlled by PerkinElmer's proprietary Pyris™ software platform, which provides intuitive, user-friendly options for high-sensitivity analysis of thermal data. The data is automatically recorded through this softwrae. This gives the weight change of the biomass species with an electronic microbalance. DTG curve give information about rate of change in weight of fuel sample with respect to the temperature. In this study influence of heating rate on degradation of briquette and pellet are investigated by STA 8000.This method gives thermo chemical conversion of a fuel. The schematic of the experimental setup is shown in Fig. 3.23.

Fig. 3.23.PerkinElmerSimultaneous Thermal Analyzer (STA) 8000

In the present experimentation as reported by various researchers (Zheng and Kozinski 2000;Vamvuka et.al 2003; Seo et.al 2010) the three zones hemicelluloses, cellulose and lignin are observed in temporal weight loss and DTG curve. It is considered that the hemicelluloses decomposed between 200-300^{o}C (Phase-2), celluloses decomposed between 300-400^{o}C (Phase-3) and lignin decomposed between 400^{0}C to 900^{0}C (Phase-4) and moisture is released from 40-200^{o}C (Phase-1).

3.8.1 THERMOGRAVEMETRIC ANALYSIS OF BIOMASS BRIQUETTE

TGA is carried out for five varieties of biomass briquettes of three types of biomasses saw dust, rice husk powder and mustard husk powder. The temporal weight losses curve and DTG curve for biomass briquette samples are shown in Fig. 3.24 to 3.69**.**

A) TGA analysis of saw dust briquette

TGA analysis of saw dust briquette is shown in Fig. 3.24 to Fig 3.60 for the binder composition 5% to 25%. Figure 3.24 shows the temporal and DTG curve for the saw dust B_{00}. It is seen that 4.24 % moisture, 11.59 % hemicelluloses, 50.52 % cellulose and 20.06 % lignin is released. The maximum dip of the DTG curve is observed at temperature 369°C.

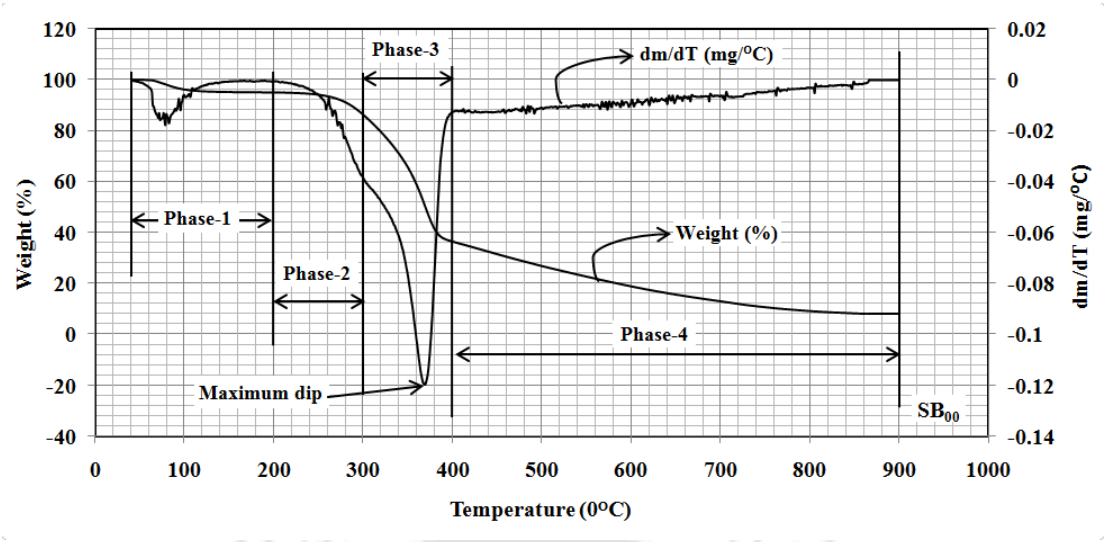

Fig.3.24. TGA analysis of saw dust

The graph of weight loss vs. Temperature and DTG curve is shown in Fig. 3.25 for saw dust briquette B_{05} with 5% binder. It is seen that water loss of 4.25%, release of hemicelluloses 11.59%, cellulose 50.52% and lignin 20.06% takes place. The DTG curve shows that the maximum dip takes place at temperature 356°C.

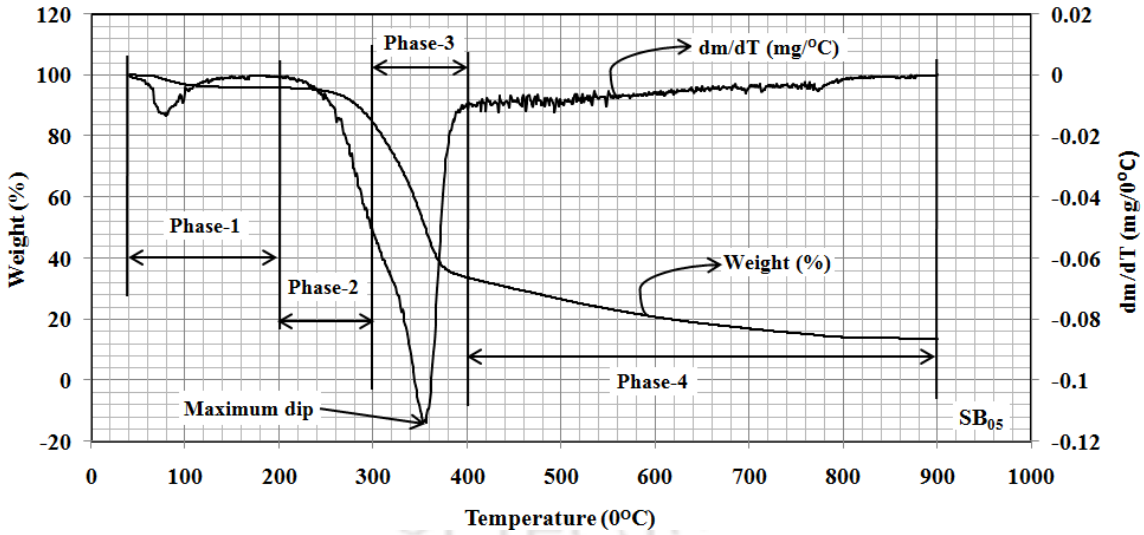

Fig.3.25 TGA analysis of saw dust briquette B_{05}

The Figure 3.26 shows the temporal and DTG curve for the saw dust briquette B_{10}. It is observed that the 4.68 % moisture, 11.27 % hemicelluloses, 50-65 % cellulose and in 23.72 % lignin is released. The maximum dip of 355°C is observed on DTG curve.

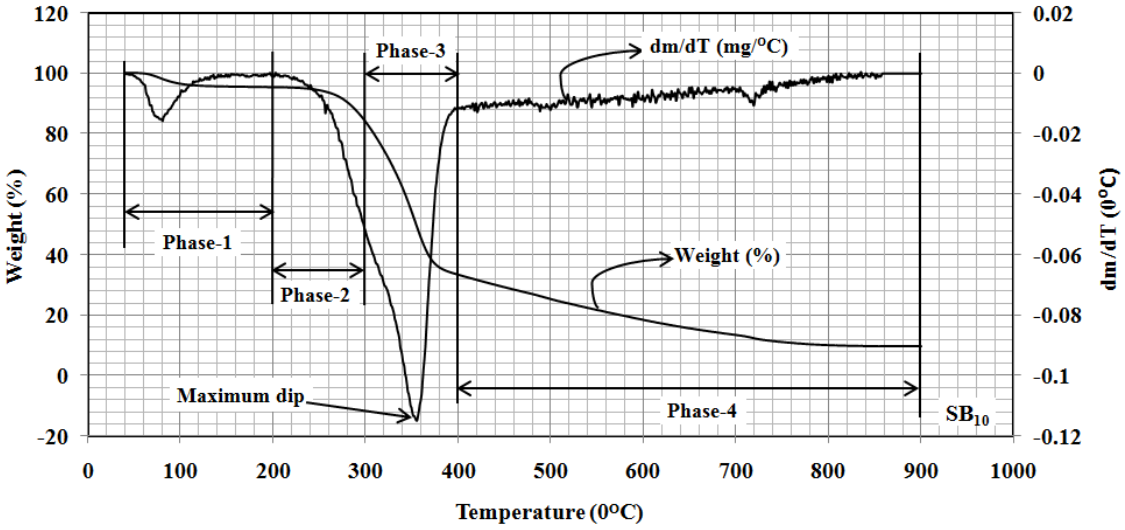

Fig. 3.26 TGA analysis of saw dust briquette B_{10}

The weight loss and DTG Graph for the sawdust briquette B_{15} is shown in Fig.3.27 with 15% binder. It is seen that the 2.82 % moisture, 9.87 % hemicelluloses, 53.97 % cellulose and 16.25 % lignin is released. The maximum dip on DTG curve is observed at 361°C.

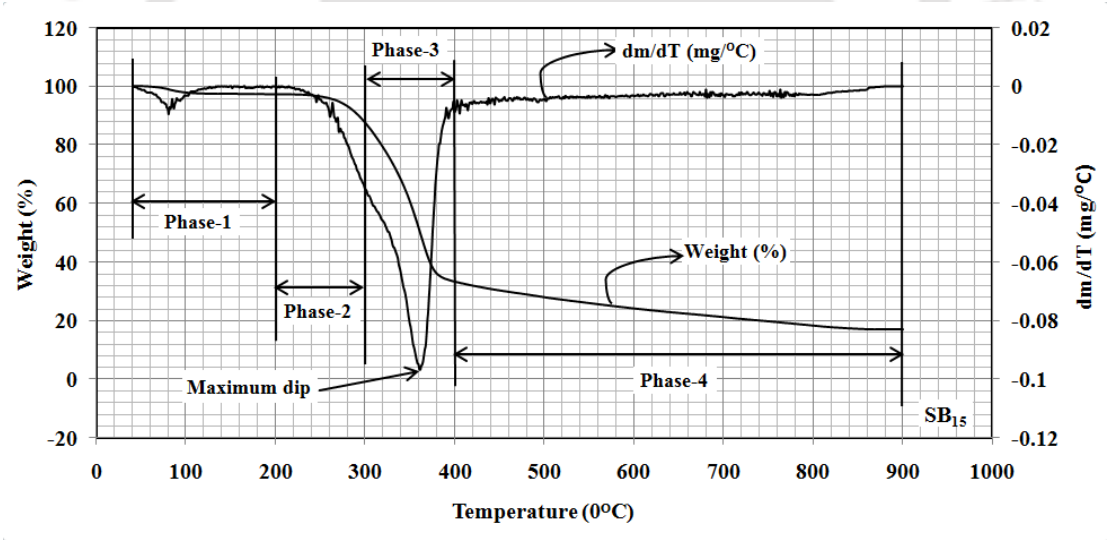

Fig.3.27 TGA analysis of saw dust briquette B_{15}

The Figure 3.28 shows the weight loss with respect to temperature curve and DTG curve for the saw dust briquette B_{20}. It is studied that 2.61 % moisture, 10.01 % hemicelluloses, 55.07 % cellulose and in 14.39 % lignin is released during TGA. Maximum dip at 364°C is observed on DTG curve.

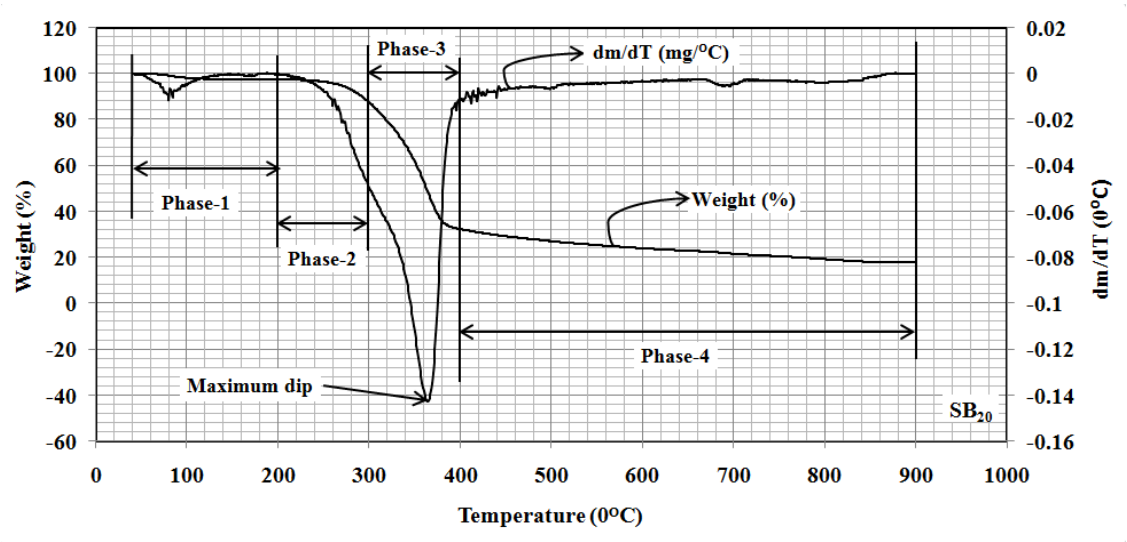

Fig.3.28. TGA analysis of saw dust briquette B_{20}

Figure 3.29 shows the temporal and DTG curve for the saw dust briquette B_{25}. It is observed that 2.27 % moisture, 9.04 % hemicelluloses, 56.91 % cellulose and 15.12 % lignin is released. It is seen that DTG curve has maximum dip at 370°C.

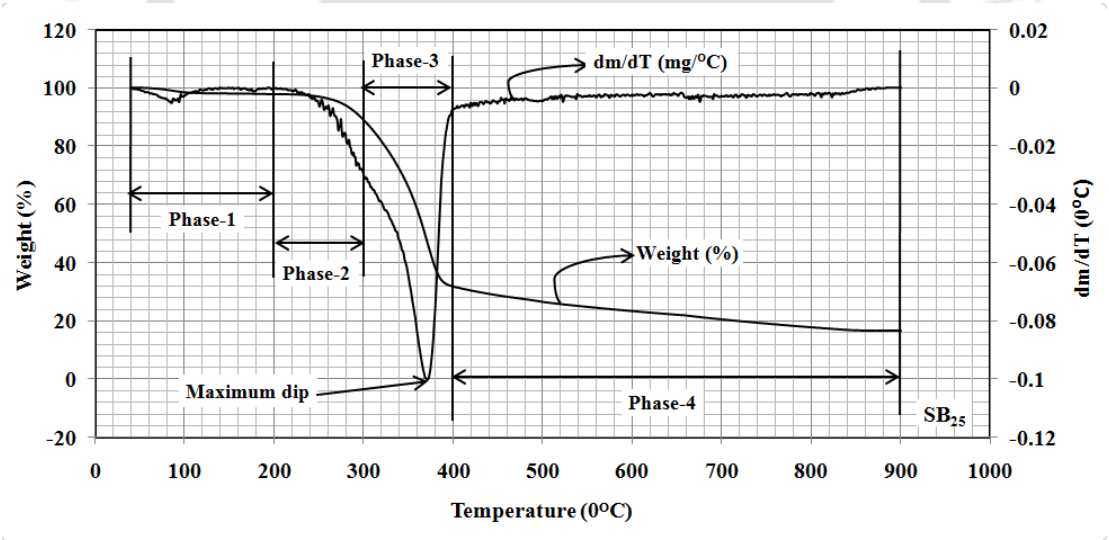

Fig.3.29. TGA analysis of saw dust briquette B_{25}

Table-3.10 shows comparative percentage analysis of moisture, hemicelluloses, cellulose and lignin in phase-1 (40-200°C), phase-2 (200-300°C), phase-3 (300-400°C) and phase-4 (400-900°C) respectively. It is observed that the percentage of cellulose is increased and percentage of lignin is decreased with increase in the percentage of binder.

Table-3.10. Saw dust briquette Percentage weight in various phases during TGA

Sawdust Briquette	Phase-1 (Moisture)	Phase-2 (Hemi cellulose)	Phase-3 (Cellulose)	Phase-4 (Lignin)	Ash
	Temperature (^{O}C)				
	40-200	200-300	300-400	400-900	900
B_{00}	5.03	9.16	49.54	28.25	8.02
B_{05}	4.24	11.59	50.52	20.06	13.60
B_{10}	4.68	11.27	50.65	23.72	9.68
B_{15}	2.82	9.87	53.97	16.25	17.09
B_{20}	2.61	10.01	55.07	14.39	17.92
B_{25}	2.27	9.04	56.91	15.12	16.66

B) TGA analysis of rice husk powder briquettes

Thermogravimetric analysis of rice husk briquette is carried out with variation of binder from 5% to 25% and it is shown in Fig. 3.30 to 3.65. TGA analysis of rice husk powder is shown in Fig 3.45. The weight loss with respect to temperature and DTG curve are platted. It is observed that the moisture, cellulose, hemicelluloses and lignin released are 7.64%, 12.26%, 36.25% and 20.59% respectively. The maximum dip of DTG curve located at 319^{o}C.

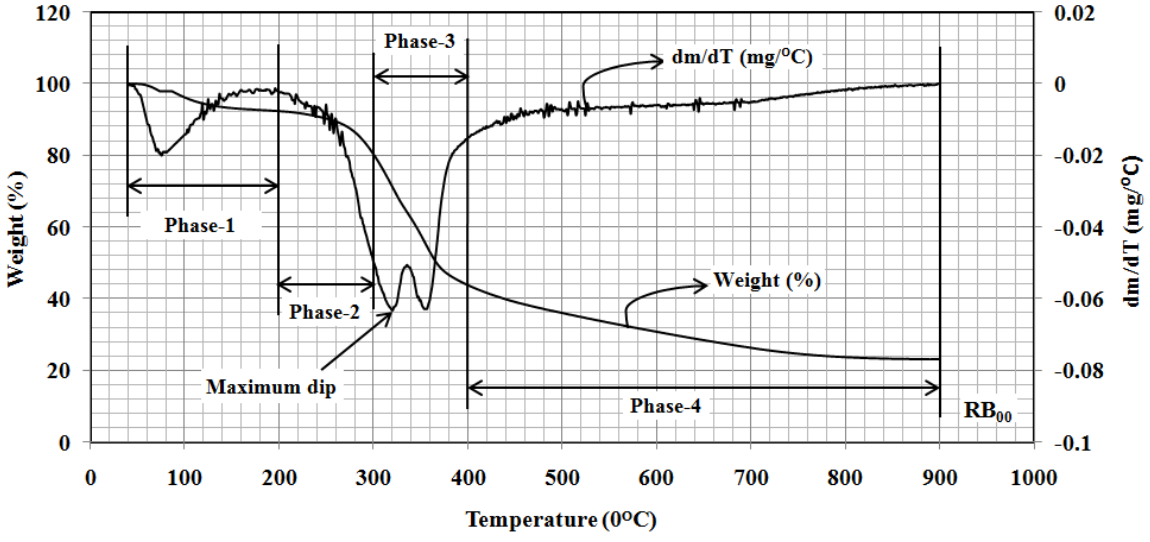

Fig. 3.30. TGA analysis of rice husk powder

Figure 3.31 shows TGA analysis of rice husk powder briquette B_{05}. It is observed that with increase in temperature moisture, cellulose, hemicelluloses and lignin are released in

5.52%, 11.28%, 36.05% and 16.77% respectively. DTG curve shows maximum dip at 356°C.

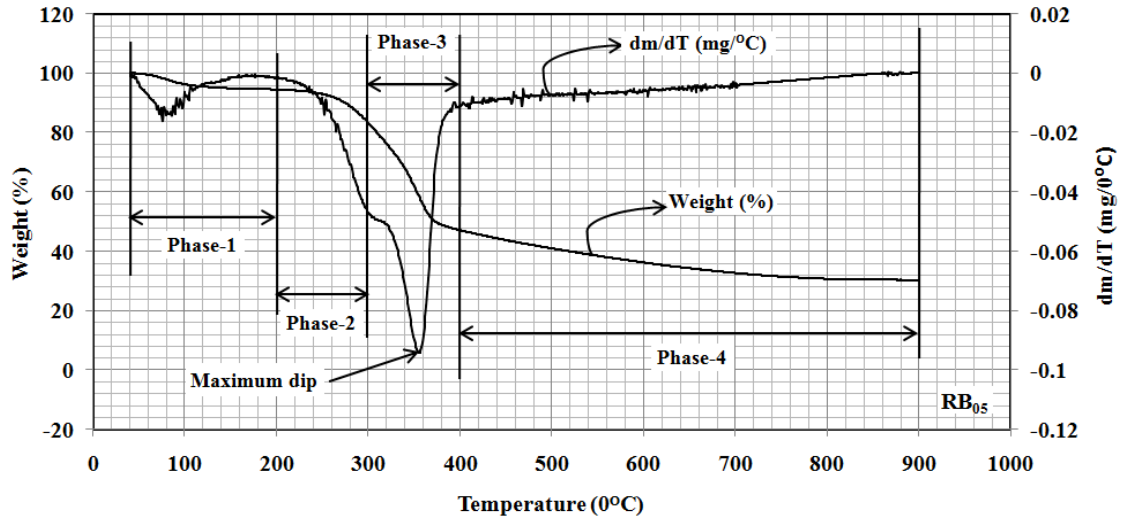

Fig. 3.31 TGA analysis of rice husk powder briquette B_{05}

Figure 3.32 shows TGA analysis of rice husk powder briquette B_{10}. It is seen that the moisture, hemicellulsoe, cellulose and lignin are released in 4.52%, 10.43%, 46.20% and 12.52% respectively in phase 1-4. The maximum dip on DTG curve takes place at 320°C.

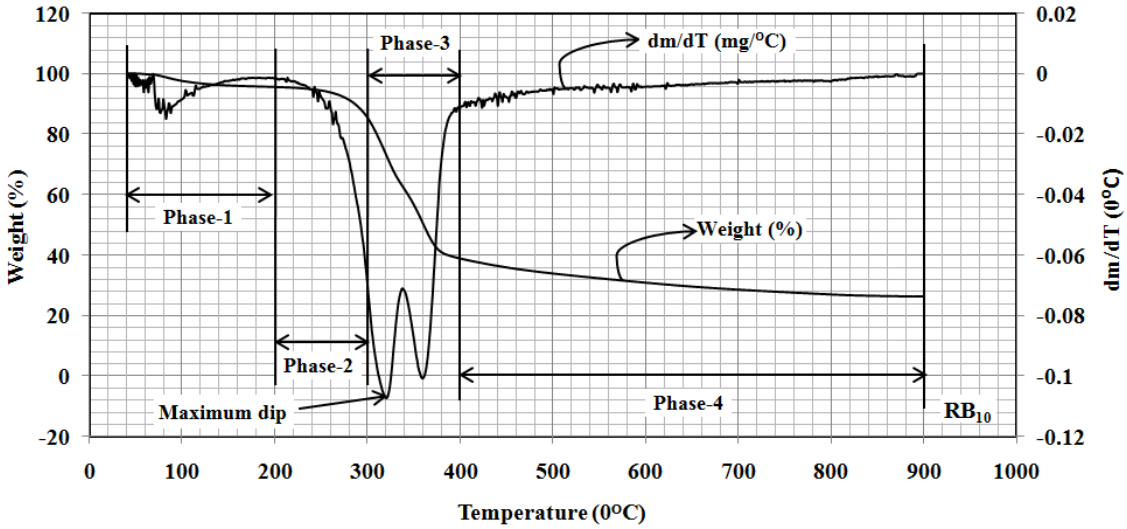

Fig. 3.32 TGA analysis of rice husk powder briquette B_{10}

The TGA analysis of rice husk powder briquette B_{15} with weight loss and DTG curve is shown in Fig. 3.33. It is observed that moisture, hemicelluloses, cellulose and lignin are released 4.52%, 23.30%, 24.32%, and 13.18% respectively. DTG curve maximum dip takes place at 317°C.

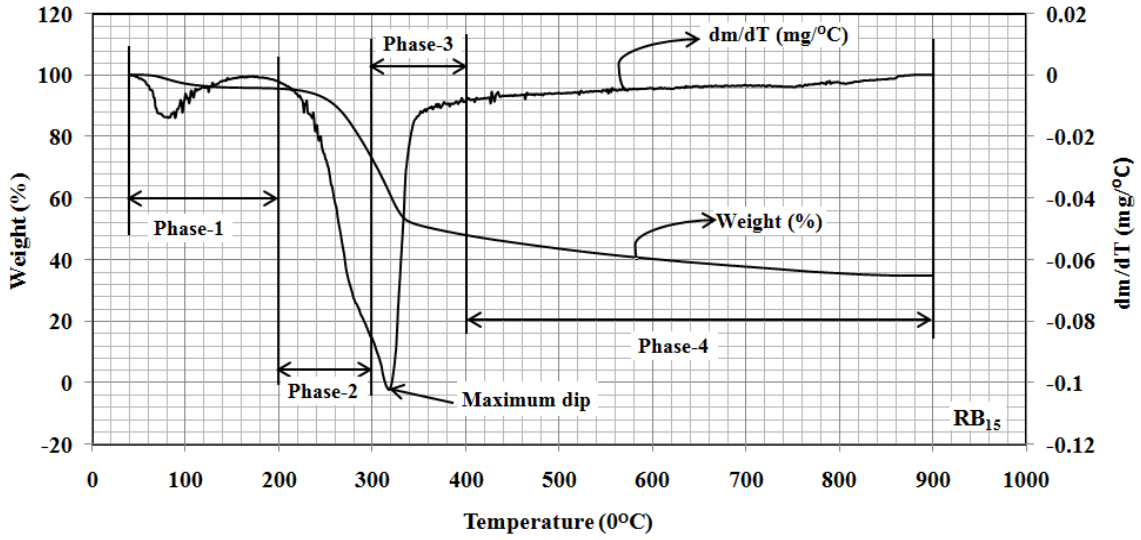

Fig. 3.33 TGA analysis of rice husk powder briquette B_{15}

Figure3.34 shows TGA analysis of rice husk powder briquette B_{20}.It is noticed that moisture, hemicellulose, cellulose and lignin are released 6.10 %, 11.62 %, 38.58 %, and 29.46 % respectively. The maximum dip on DTG curve is observed at temperature 350°C.

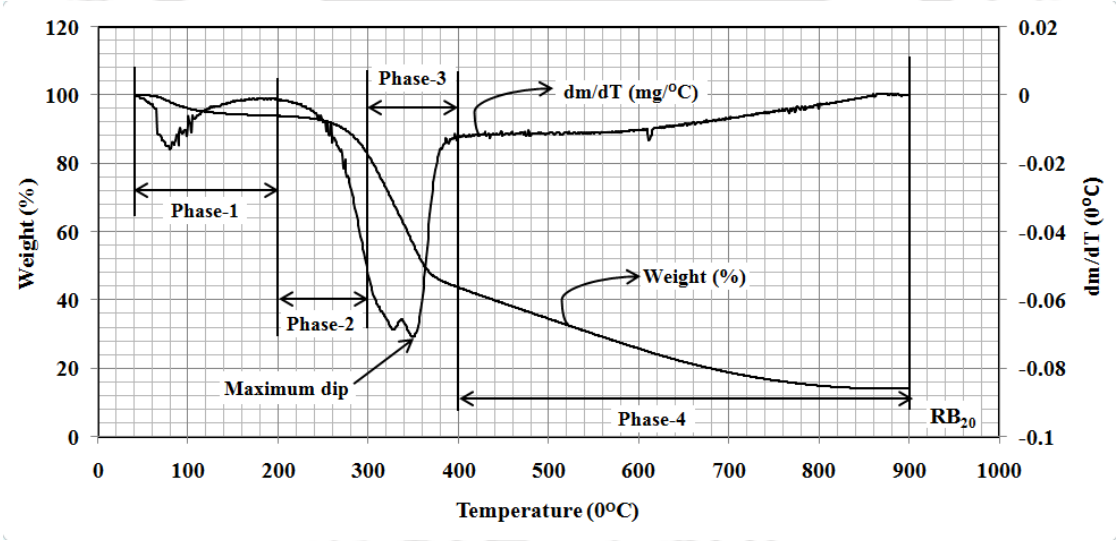

Fig. 3.34 TGA analysis of rice husk powder briquette B_{20}

TGA analysis of rice husk powder briquette B_{25} is shown in Fig.3.35. It is seen that moisture, hemicellulsoe, cellulose and lignin are released 2.44 %, 10.40 %, 46.85 %, and 12.83 % respectively. The maximum dip on DTG curve is observed at temperature 355°C.

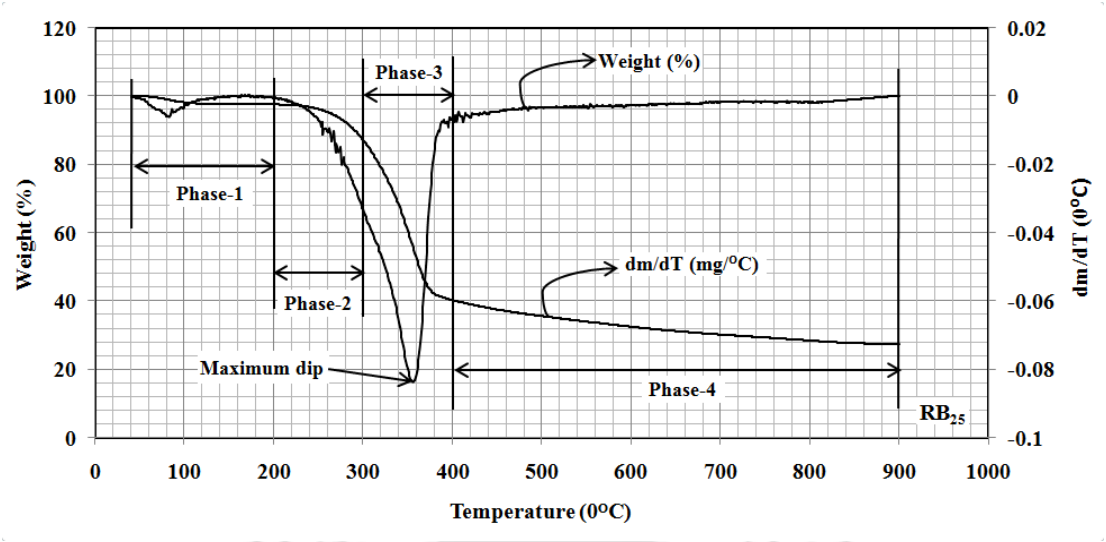

Fig. 3.35 TGA analysis of rice husk powder briquette B_{25}

Table 3.11 gives the comparative information about the variation in release of different constituents during TGA for rice husk powder briquette. The percentage weight loss in various phases differs with binder briquette composition and temperature variation from 40-900°C.

Table-3.11.Rice husk powder briquette percentage weight loss in various phases

Rice-husk powder Briquette	Phase-1 (Moisture)	Phase-2 (Hemi cellulose)	Phase-3 (Cellulose)	Phase-4 (Lignin)	Ash
	Temperature (°C)				
	40-200	200-300	300-400	400-900	900
B_{00}	7.64	12.26	36.25	20.59	23.26
B_{05}	5.52	11.28	36.05	16.77	30.36
B_{10}	4.52	10.43	46.20	12.52	26.33
B_{15}	4.52	23.30	24.32	13.18	34.66
B_{20}	6.10	11.62	38.58	29.46	14.23
B_{25}	2.44	10.40	46.85	12.83	27.47

C) TGA analysis of mustard husk powder briquettes

Lab experiments are performed for TGA analysis of mustard husk powder briquette with variation of binder from 5% to 25%. Weight loss and DTG curves are shown in Fig. 3.36 to 3.61. TGA analysis of mustard husk powder is shown in Fig 3.36. It is observed that weight loss for release of moisture, cellulose, hemicelluloses and lignin are 6.05%, 18.12%, 32.40% and 22.81% respectively. DTG curve has maximum dip at 321°C.

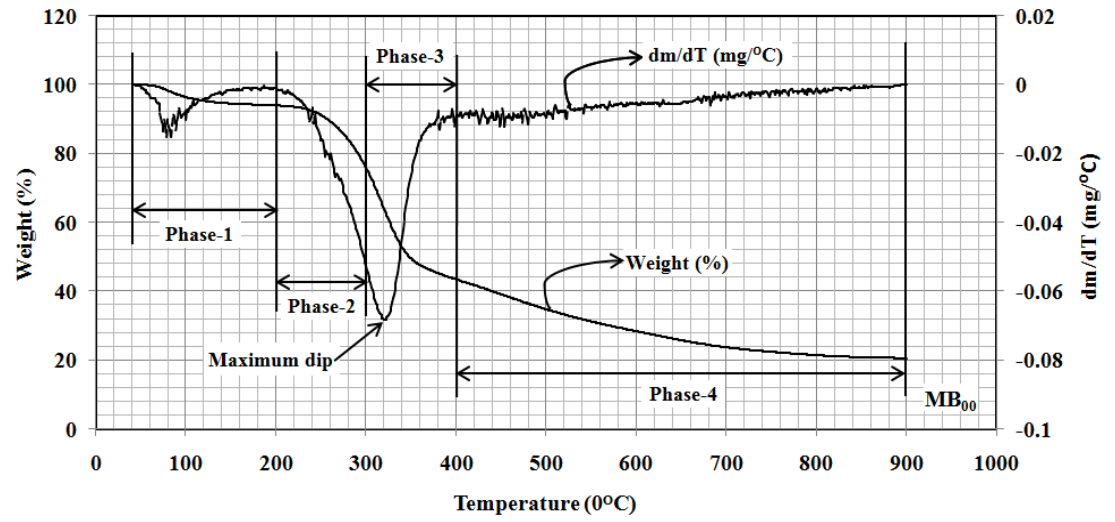

Fig. 3.36. TGA analysis of mustard husk powder

TGA analysis of mustard husk powder briquette B_{05} is shown in Fig.3.37.It is seen that moisture, hemicellulsoe, cellulose and lignin are released 9.20%, 17.04%, 28.18% and 28.77% respectively. The maximum dip on DTG curve is observed at temperature 312°C.

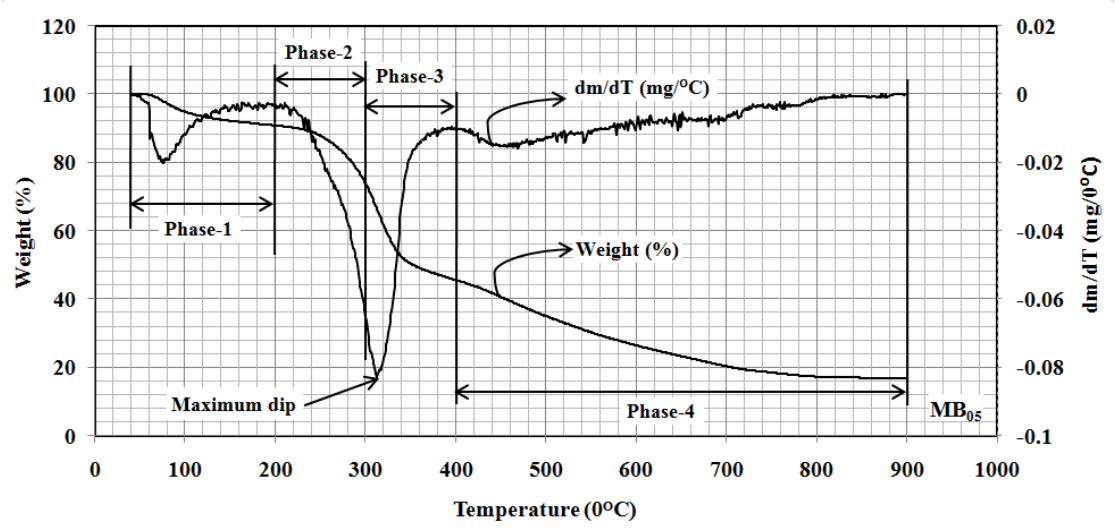

Fig. 3.37. TGA analysis of mustard husk powder briquette B_{05}

Figure 3.38 shows the TGA analysis of mustard husk powder briquette B_{10}. It is observed that the release of moisture, hemicelluloses, cellulose and lignin is in 6.50 %, 16.45 %, 30.90 %, and 24.05 % respectively. The maximum dip on DTG curve is seen at temperature 322°C.

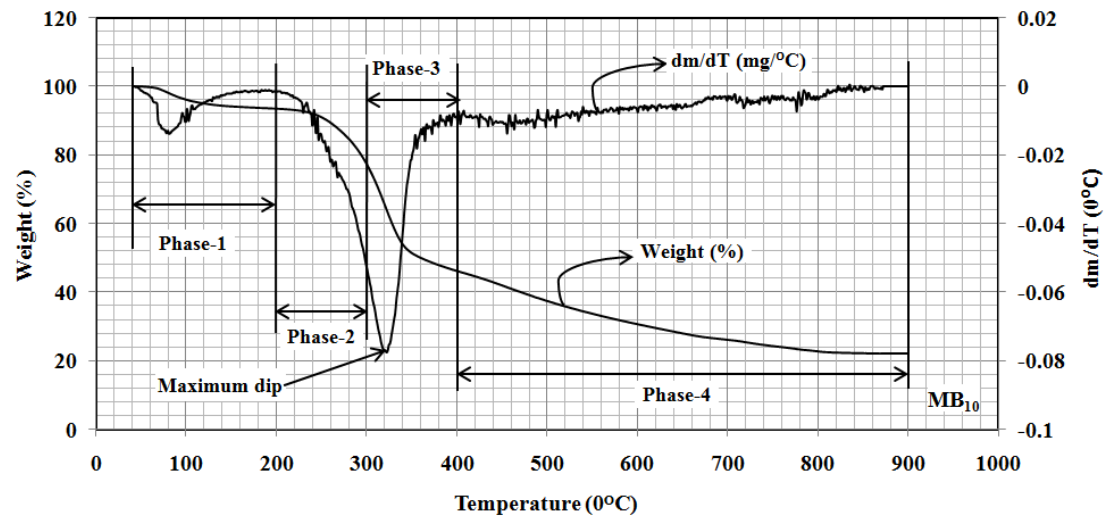

Fig. 3.38. TGA analysis of mustard husk powder briquette B_{10}

TGA analysis of mustard husk powder briquette B_{15} is shown in Fig. 3.39. The release of moisture, hemicelluloses, cellulose and lignin is 3.92 %, 12.85 %, 42.11 %, and 13.77 %, respectively. It is observed that DTG curve has a maximum dip at temperature 336°C.

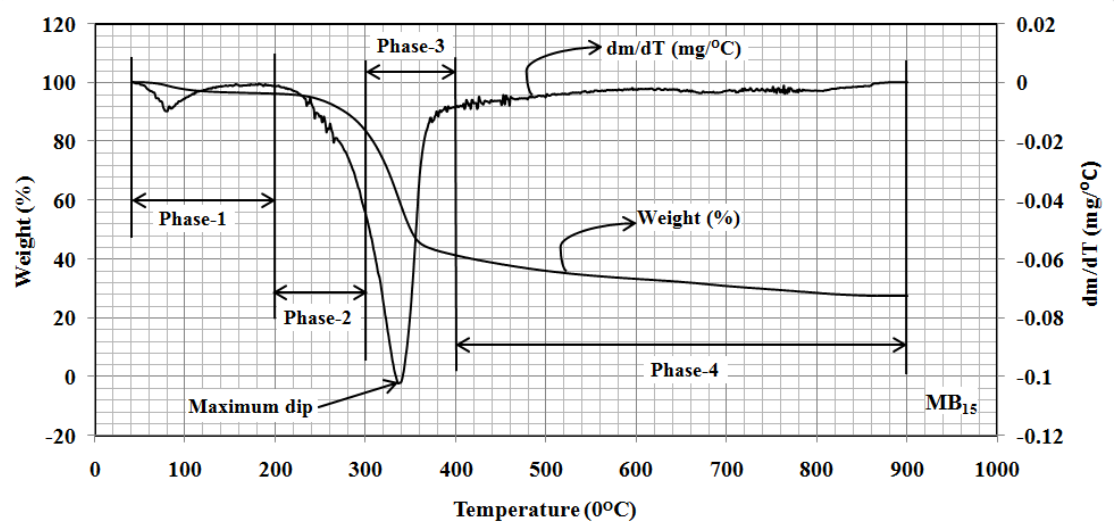

Fig. 3.39 TGA analysis of mustard husk powder briquette B_{15}

Weight loss and DTG Graph for mustard husk powder briquette B_{20} is shown in Fig.3.40 with 15% binder. It is seen that the 5.88 % moisture, 15.15 % hemicelluloses, 35.28 % cellulose and 29.04 % lignin is released. The maximum dip on DTG curve is observed at 321°C.

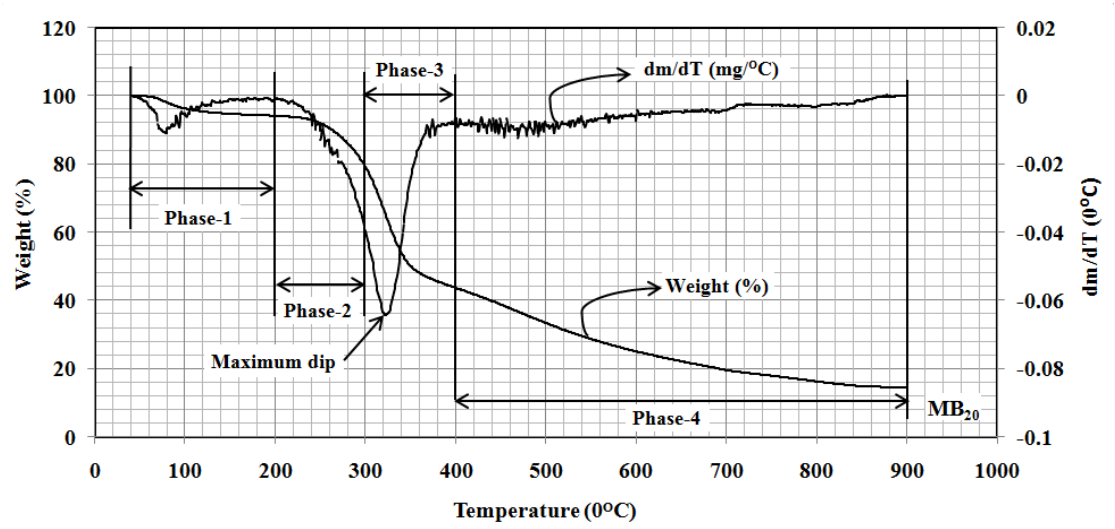

Fig. 3.40 TGA analysis of mustard husk powder briquette B_{20}

The graph of weight loss vs. Temperature and DTG curve is shown in Fig. 3.41 for mustard husk briquette B_{25} with 5% binder. It is seen that moisture, hemicelluloses, cellulose and lignin are released in amount 3.77 %, 13.19 %, 35.38 % and 15.22 % respectively. The DTG curve shows that the maximum dip takes place at temperature 332°C.

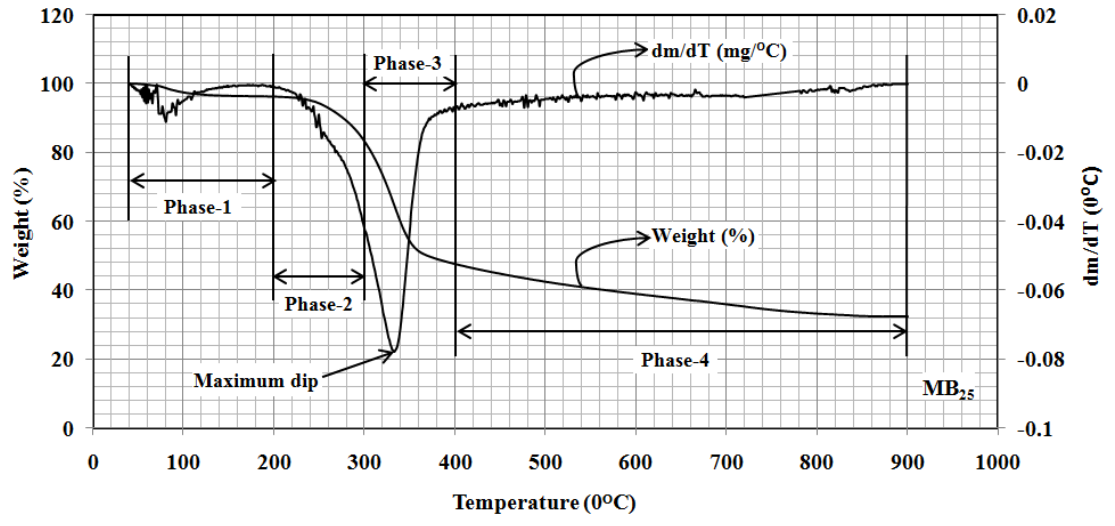

Fig. 3.41 TGA analysis of mustard husk powder briquette B_{25}

The relative analysis of mustard husk powder briquette is done for the various percentage of binder varying from 5% to 25%. In this weight percentage of released moisture, hemicellulose, cellulose and lignin with respect to temperature is analysed with TGA. The biomass is heated from temperature 40-900°C.The data is tabulated in Table-3.12.

Table-3.12. Mustard husk powder briquettes percentage weight in various phases

Mustard-husk powder Briquette composition	Phase-1 (Moisture)	Phase-2 (Hemi cellulose)	Phase-3 (Cellulose)	Phase-4 (Lignin)	Ash
	Temperature (^{O}C)				
	40-200	200-300	300-400	400-900	900
	Weight (%)				
B_{00}	6.05	18.12	32.40	22.81	20.62
B_{05}	9.20	17.04	28.18	28.77	16.79
B_{10}	6.50	16.45	30.90	24.05	22.09
B_{15}	3.92	12.85	42.11	13.77	27.35
B_{20}	5.88	15.15	35.28	29.04	14.66
B_{25}	3.77	13.19	35.38	15.22	32.44

The maximum dip temperature is noted as tabulated in Table-3.13 from Fig. 3.39–3.41 for TGA of sawdust briquette, rice husk briquette and mustard husk briquette. The maximum dip point indicates the maximum pyrolysis of biomass briquette. The maximum dip temperature observed for the saw dust is from 355-370^{o}C, for rice husk briquette is 319-356^{o}C and for mustard husk powder briquette 312-336^{o}C. This indicates that pyrolysis temperature range of mustard husk briquette is less than sawdust briquette and rice husk briquette. While pyrolysis temperature range for saw dust briquettes is higher than remainder.

Table-3.13. DTG curve maximum dip temperature (^{0}C) for the various biomass briquette

Biomass briquette	**B_{00}**	**B_{05}**	**B_{10}**	**B_{15}**	**B_{20}**	**B_{25}**
Sawdust briquette	**369**	**356**	**355**	**361**	**364**	**370**
Rice-husk powder briquette	**319**	**356**	**320**	**317**	**350**	**355**
Mustard husk powder briquette	**321**	**312**	**322**	**336**	**321**	**332**

The comparative TGA analysis of sawdust, rice husk powder and mustard husk powder is shown in Fig. 3.42. It is observed from the DTG graph is shifted to left side for rice husk powder than mustard husk powder and then saw dust powder. This indicates that pyrolysis of rice husk powder is earlier than for mustard husk powder and then saw dust. The amount of pyrolysis is increases in order rice husk powder- mustard husk powder and sawdust powder.

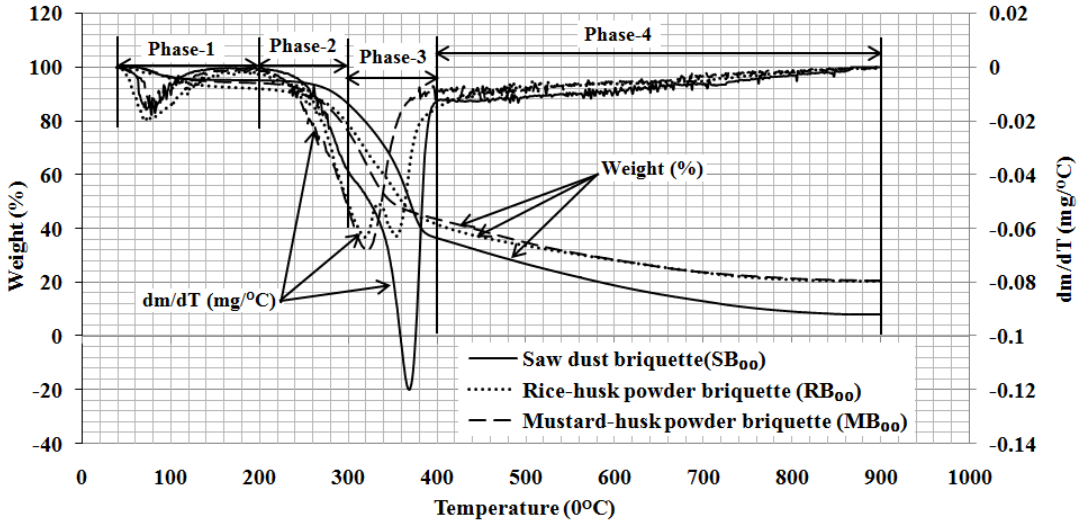

Fig. 3.42 Comparative analysis of TGA for various biomass material

The comparative analysis of sawdust briquette, rice husk powder briquette and mustard husk powder briquette for a composition of B_{15} is shown in Fig. 3.43.

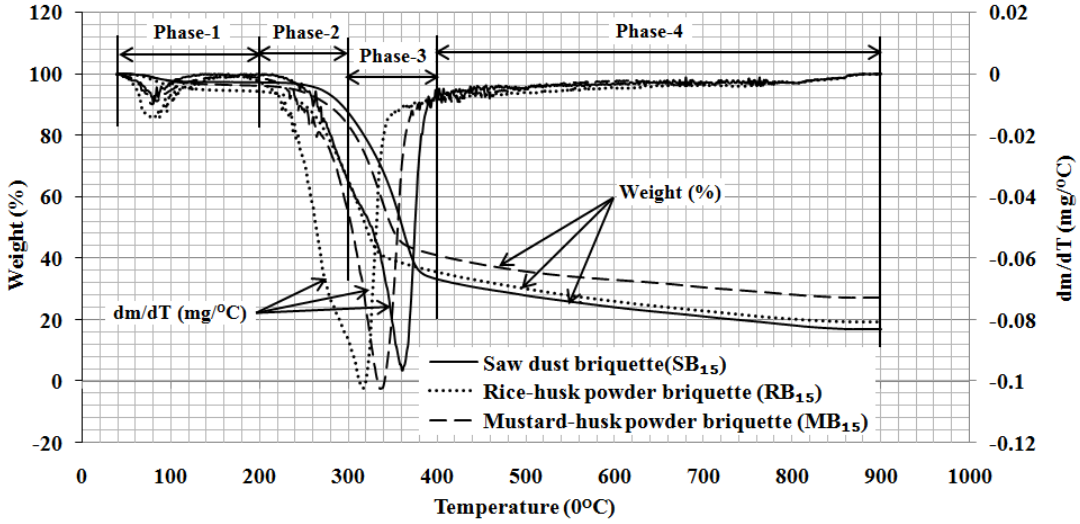

Fig. 3.43. Comparative analysis of TGA of briquette$B_{15}$for various material

Figure 3.42 follows the same pattern of pyrolysis as in Fig. 3.43 for 15% dolomite. The pyrolysis is shifted towards left side in order of rice husk powder briquette – mustard husk powder briquette - saw dust powder briquette. This indicates that pyrolysis of rice husk briquette is earlier than for mustard husk briquette and saw dust briquette. Amount of pyrolysis is less in order mustard husk– briquette rice husk briquette –saw dust briquette.

3.8.2 TGA OF BIOMASS-DOLOMITE PELLET

The saw dust-dolomite and mustard husk powder-dolomite pellet are used for the present investigation. The percentage of dolomite in pellet is varied from 0-40 % in step of 10 %. Sample is heated from temperature 40-900^{o}C with rate of 10^{o}C per minute.The graph is platted for weight loss versus temperature and DTG as shown in Fig. 3.44 to Fig.3.51**.** It is considered that the moisture is released from 40^{0}C to 200^{0}C (Phase-1), hemicelluloses decomposed between 200^{0}C to 300^{0}C (Phase-2), celluloses decomposed between 300-400^{o}C (Phase-3), pre lignin decomposed between 400-680^{o}C (Phase-4), tar is cracked between 680-800^{o}C (phase-5) and post lignin is decomposed between 800-900^{o}C (phase-6).

A) TGA analysis of saw dust-dolomite pellet

Figure 3.44 shows the TGA for sawdust-dolomite pellet P_{10}. It is noticed that moisture is released 5.02%, hemicelluloses decomposed 8.98 %, cellulose decomposed 41.39 %, pre lignin decomposed 9.70%, tar is cracked 14.33 % and post lignin cracked 0.43 %. DTG curve has two dips. The first dip is at temperature 364^{o}C and second dip is at temperature 733^{o}C where tar is cracked.

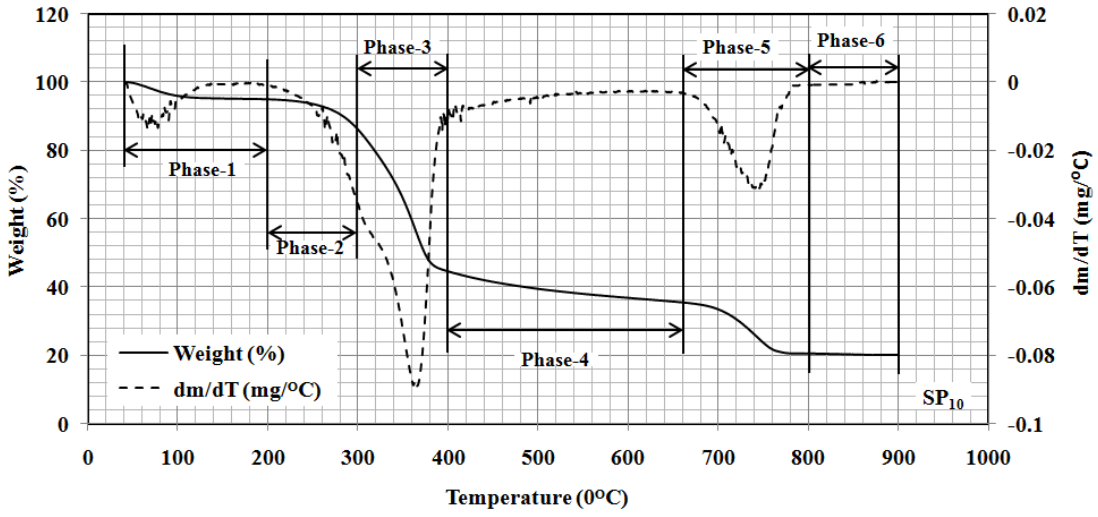

Fig.3.44 TGA analysis of saw dust-dolomite pellet P_{10}

Figure 3.45 shows TGA for sawdust-dolomite pellet P_{20}.. It is seen that the moisture, hemicelluloses, cellulose and lignin are released in 5.61 %, 5.74 %, 30.9 %, and 14.65 % respectively. Tar is cracked 20.10% and post lignin released 0.14 %. DTG curve has two dips. The first dip is at temperature 366^{o}C and second dip is at temperature759^{o}C.

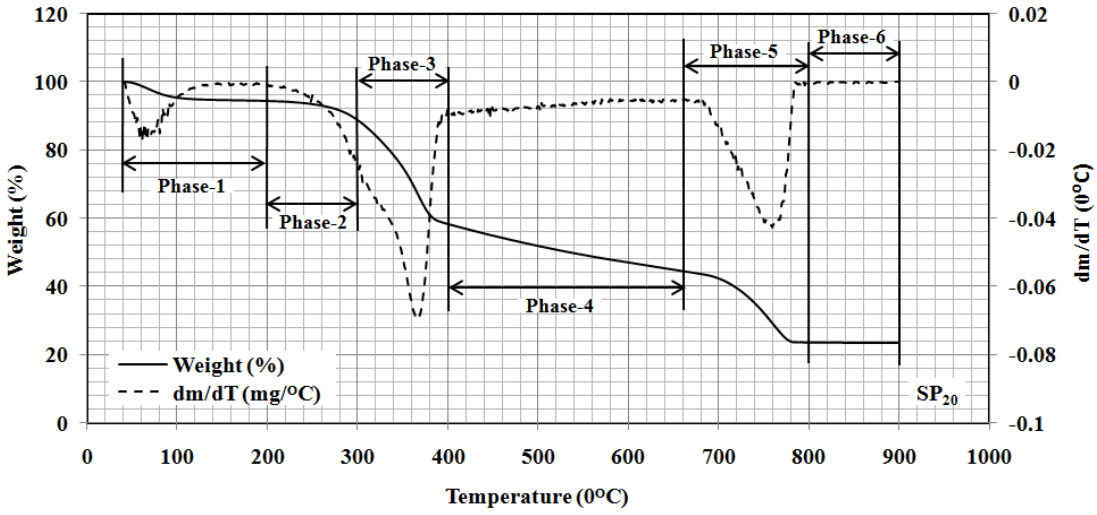

Fig.3.45 TGA analysis of saw dust-dolomite pellet P_{20}

Thermogravimetric analysis of sawdust-dolomite pellet P_{30} is carried out as shown in Fig.3.46. It is seen that moisture released 7.60 %, hemicelluloses decomposed 11.94 %, cellulose decomposed 19.49 %, pre lignin decomposed 12.73 %, tar is cracked 19.73 % and post lignin cracked 1.72 %. DTG curve has two dips first is at temperature 320^{o}C and second dip is at temperature 760^{o}C.

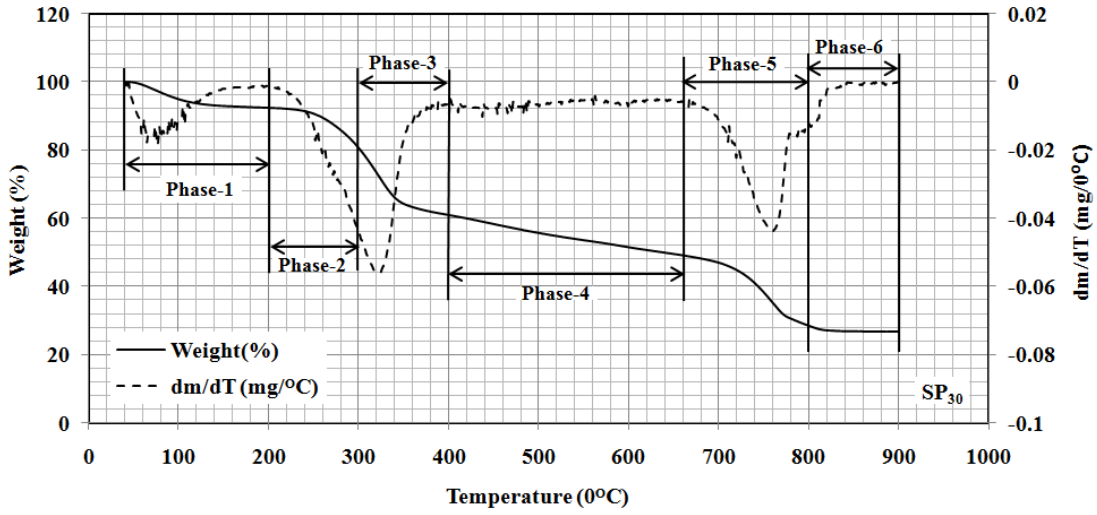

Fig.3.46 TGA analysis of saw dust-dolomite pellet P_{30}

Figure 3.47 shows the thermogravimetric analysis of sawdust-dolomite pellet P_{40}. It is noticed that moisture, hemicelluloses, cellulose and lignin are released in 6.26 %, 7.66 %, 22.46 % and 12.72 %, respectively. Tar is cracked 18.60 % and post lignin decomposed 2.71 %. DTG curve has two dips first is at temperature 321^{o}C and second dip is at temperature 758^{o}C.

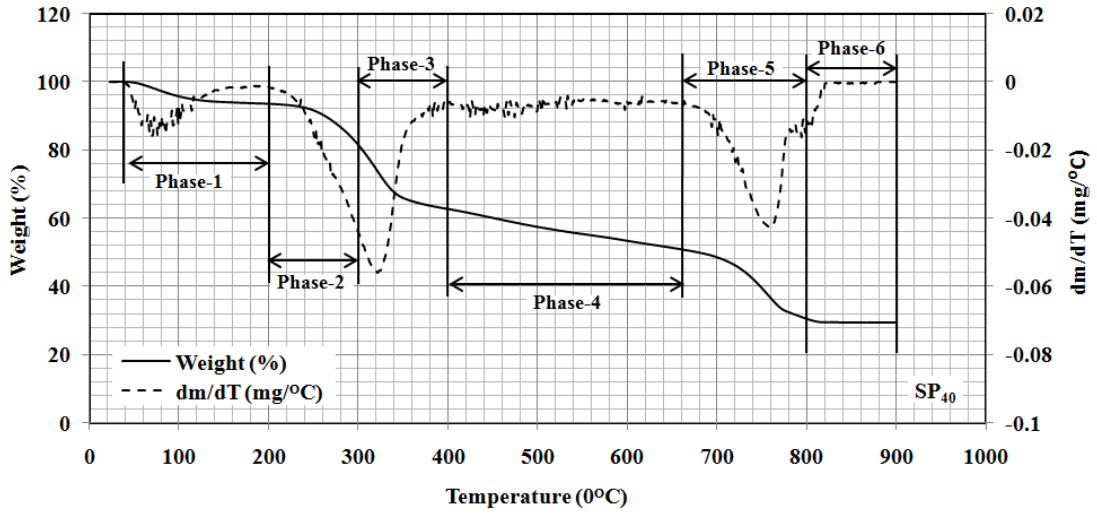

Fig.3.47 TGA analysis of saw dust-dolomite pellet P_{40}

The comparative percentage weight loss of sawdust-dolomite in different phases for various composition of dolomite during TGA is shown in Table-3.14.

Table-3.14 Sawdust-dolomite pellet weight (%) loss in various phases during TGA.

Sawdust - dolomite pellet	Phase-1 (Moisture)	Phase-2 (Hemi cellulose)	Phase-3 (Cellulose)	Phase-4 (Lignin)	Phase-5 (Tar cracking)	Phase-6 (Lignin)	Ash
	Temperature (^{O}C)						
	40-200	**200-300**	**300-400**	**400-680**	**680-800**	**800-900**	**900**
	Weight (%)						
P_{00}	5.03	9.16	49.54	28.25			8.02
P_{10}	5.02	8.98	41.39	9.70	14.33	0.43	20.14
P_{20}	5.61	5.74	30.39	14.65	20.10	0.14	23.37
P_{30}	7.60	11.94	19.49	12.73	19.73	1.72	26.79
P_{40}	6.26	7.66	22.46	12.72	18.60	2.71	29.57

It is observed that the percentage of cellulose decomposed is decrease with the increase in percentage of dolomite. Lignin decomposition is observed higher for the pellet composition P_{20}. The tar cracking is also observed higher for composition P_{20}.

B) TGA analysis of mustard husk powder-dolomite pellet

TGA for mustard husk powder-dolomite pellet is studied for various composition of dolomite. Figure 3.48 shows the thermo-gravimetric analysis of mustard husk powder -

dolomite pellet P_{10}. It is observed that moisture is released 5.54 %, hemicelluloses decomposed 7.00 %, cellulose decomposed 38.56 %, pre lignin decomposed 12.82 %, tar is cracked 12.46 % and post lignin cracked 0.74 %. It is observed that DTG curve has two dips. The first dip is at temperature 370^{o}C and second dip is at temperature 733^{o}C where tar is cracked.

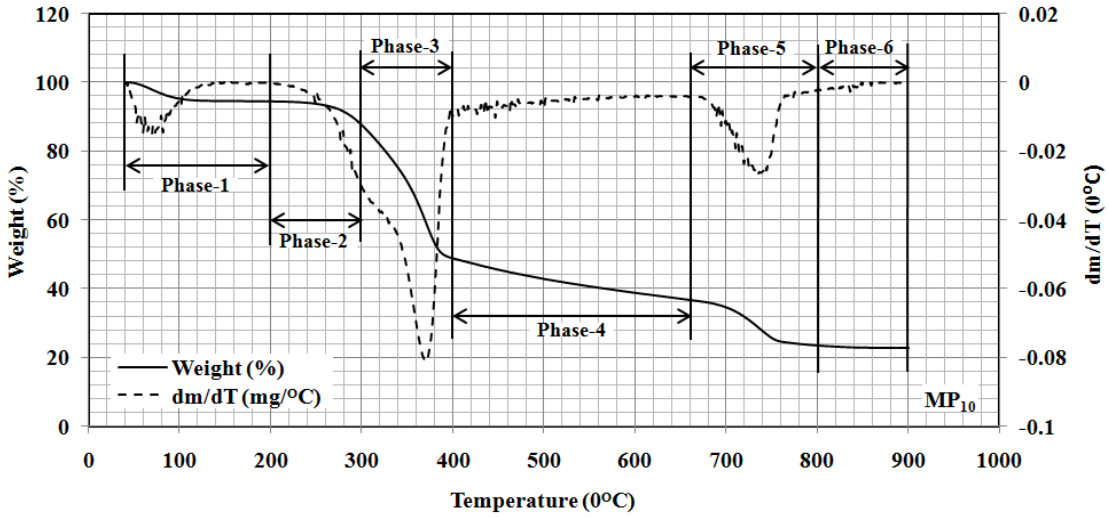

Fig.3.48 TGA analysis of mustard husk powder-dolomite pelletP_{10}

Figure 3.49 shows the thermogravimetric analysis of mustard husk powder-dolomite pellet P_{20}. It is noticed that moisture, hemicelluloses, cellulose and lignin are released in 4.04 %, 6.63 %, 36.21 % and 10.20 % respectively. Tar is cracked 17.10 % and post lignin decomposed 0.27 %. DTG curve has two dips first dip is at temperature 370^{o}C and second dip is at temperature 752^{o}C.

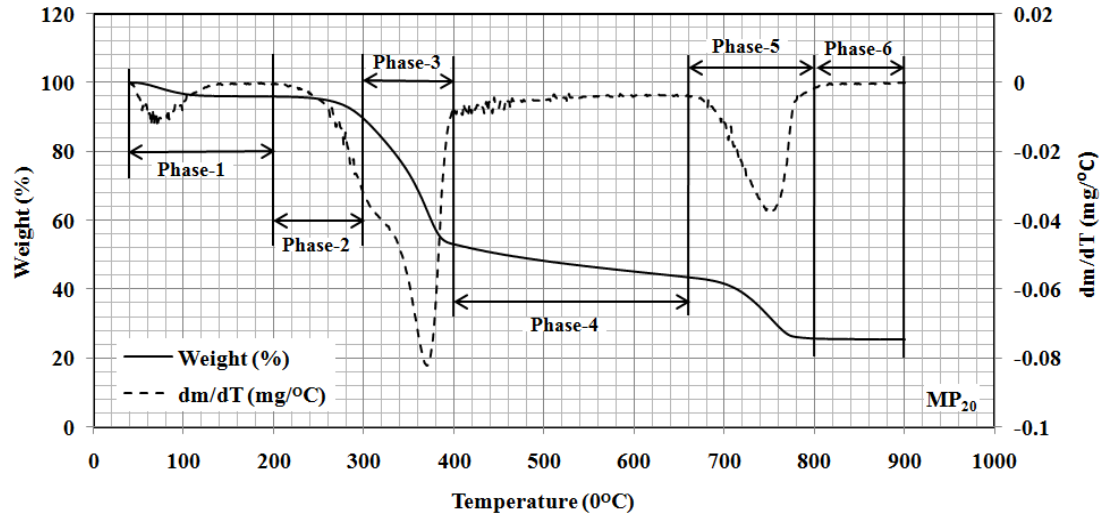

Fig.3.49 TGA analysis of mustard husk powder-dolomite pellet P_{20}

Figure 3.50 presents TGA of mustard husk powder-dolomite pellet P_{30}. The moisture, hemicelluloses, cellulose and lignin are released in 4.33 %, 6.10 %, 40.37 % and 8.87 %, respectively. Tar is cracked 12.42 % and post lignin liberated 0.34 %. DTG curve has two dips first dip at temperature 375^{o}C and second dip is at temperature 737^{o}C.

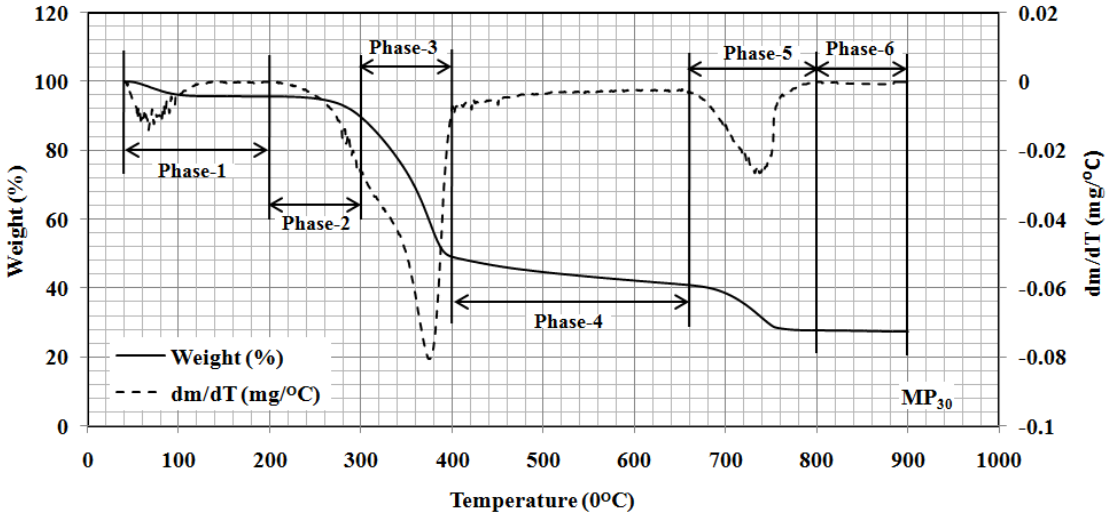

Fig.3.50 TGA analysis of mustard husk powder-dolomite pellet P_{30}

Fig.3.51 presents TGA of sawdust-dolomite pellet P_{20} moisture, hemicelluloses, cellulose and lignin are released in 7.40 %, 13.59 %, 20.49 % and 19.00 % respectively, Tar is cracked 9.53 % and post lignin liberated 0.16 %. DTG curve has two dips first dip is at temperature 316^{o}C and second dip is at temperature 736^{o}C.

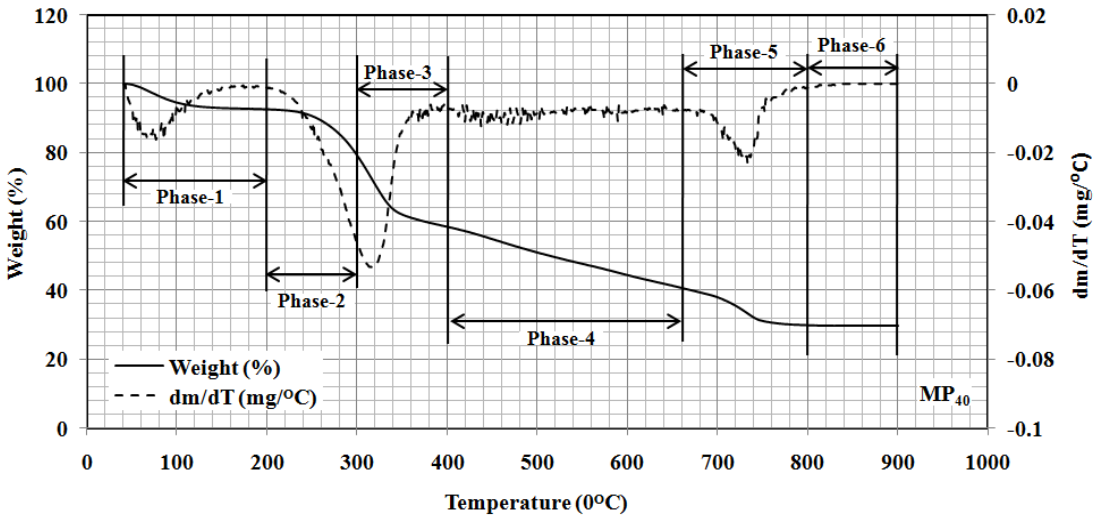

Fig.3.51. TGA analysis of mustard husk powder-dolomite pellet P_{40}

The comparative TGA of mustard husk powder-dolomite pellet varying with dolomite content is carried out and tabulated in Table-3.15. It is observed that tar is cracked in higher amount for the mustard husk powder-dolomite pellet composition P_{20}.

Table-3.15. Mustard husk powder-dolomite pellet weight loss (%) in various phases during TGA

Mustard husk - dolomite pellet	Phase-1 (Moisture)	Phase-2 (Hemi cellulose)	Phase-3 (Cellulose)	Phase-4 (Pre-Lignin)	Phase-5 (Tar cracking)	Phase-6 (Post-Lignin)	Ash
	Temperature (^{O}C)						
	40-200	**200-300**	**300-400**	**400-680**	**680-800**	**800-900**	**900**
	Weight (%)						
P_{00}	6.05	18.12	32.40	22.81			20.6
P_{10}	5.54	7.00	38.56	12.82	12.46	0.74	22.8
P_{20}	4.05	6.63	36.21	10.20	17.10	0.27	25.5
P_{30}	4.33	6.10	40.37	8.87	12.42	0.34	27.5
P_{40}	7.40	13.59	20.49	19.00	9.53	0.16	29.8

The relative analysis of dip temperature of DTG curve for sawdust-dolomite pellet and mustard husk powder-dolomite pellet is carried out and tabulated in Table-3.16. The first dip temperature for saw dust-dolomite pellet varies from 321-369^{o}C and for mustard husk-dolomite pellet 321-375^{o}C. The second dip temperature for saw dust-dolomite pellet varies from 744-760^{o}C and for mustard husk-dolomite pellet 733-752^{o}C.

Table-3.16. Relative analysis of dip temperature (^{o}C) of DTG curve for biomass-dolomite pellet

Biomass-dolomite pellet	Dip	P_{00}	P_{10}	P_{20}	P_{30}	P_{40}
Sawdust-dolomite pellet	First	369	364	366	320	321
	Second	NA	744	759	760	758
Mustard husk powder-dolomite pellet	First	321	370	370	375	316
	Second	NA	733	752	737	736

3.9 FIBRE ANALYSIS

Fibre is a starch free and fibrous part of plant materials. It constitutes cellulose, hemicellulose and lignin. In the present work, fibre analysis of wood chips, biomass briquette and pellet is carried out with the Vansoet method of analysis for the extraction of neutral detergent fibre (NDF), acid detergent fibre (ADF) and acid detergent lignin (ADL). Experiment is performed with Pelican make Fibreplus FES 02 R analyzer as shown in Fig.3.52.

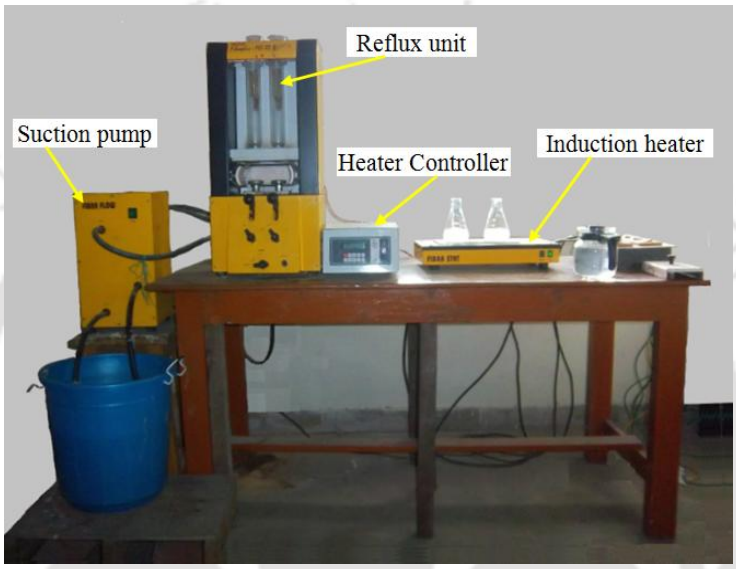

Fig.3.52 Vansoet method Pelican makeFibreplus FES 02 R analyzer

It consists of reflux unit, suction pump, heater controller and induction heater as shown in Fig. 3.53. The sample is refluxed in the reflux unit.

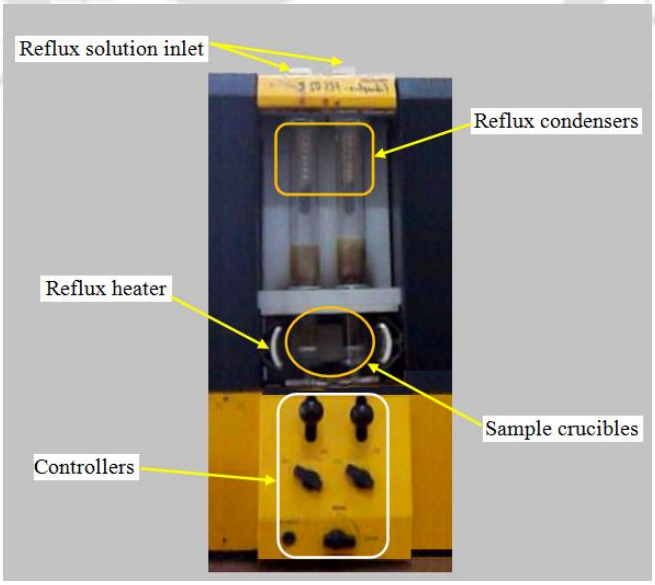

Fig.3.53 Reflux unit

The cell contents which are soluble in neutral detergents solution (NDS) include Lipids, sugars, organic acids, starch, soluble proteins, non protein nitrogenous compounds and other water soluble matter. While the insoluble material known as Neutral detergent Fibre (NDF) comprises cell wall constitutes which include Hemicellulose, Cellulose, Lignin, Keratins and silica. When cell contents treated with the acid detergent solution (ADS), Hemicellulose, some cell wall Nitrogenous compounds and acid soluble ash pass into solution leaving all insoluble fraction consisting of Cellulose, Lignin and acid insoluble ash, which is named as acid detergent fibre (ADF) or Lignin cellulose. Afterward, when ADF treated with 72 % H_2SO_4, cellulose is dissolved in the acid leaving behind the lignin and acid insoluble ash from which Lignin can be determined by loss of ignition.The preparation methodology of ADS, NDS And reagent 72 % H_2SO_4 is mentioned in the Appendix-II. Experimental procedure for determination of NDF, ADF and ADL is as given in Table-3.17

Table-3.17. Procedure for determination of NDF, ADF and ADL

Determination of NDF	Determination of ADF	Determination of ADL
Procedure 1) Weigh 0.5-1 gm dried sample in the crucible 2) Add 100 ml Neutral detergent solution, 2 ml decahydronaphthalene and 0.5 gm sodium sulphite. 3) Heat to boiling, reflux for 60 minutes. 4) Filter and rinse the sample with hot water. Repeat washing. 5) Wash twice with acetone. 6) Dry the crucible in hot air oven at 100 ^{0}c for 8 hr and weight the crucible.	Procedure 1) Weigh 1 gm of sample. 2) Add 100ml acid detergent solution and 2ml decahyronapthalene 3) Heat to boiling, reflux for 60 min 4) Filter and rinse the sample with hot water 5) Wash with acetone 6) Wash with hexane, if required 7) Dry at 100 ^{0}c for 8 hrs in the muffle furnace and weight the crucible.	Procedure 1) Prepare the ADF 2) Add 72% H_2SO_4 to ADF. Filters for three times 3) After 3 hours filter off as much as acid possible. Wash the content with hot water until it is free from acid. 4) Dry at 100 ^{0}c for 8 hrs in muffle furnace and weight the crucible. 5) Ash the residue in the muffle furnace and weight the crucible.

The Experimental layout of Fibre analysis is shown in Fig. 3.54

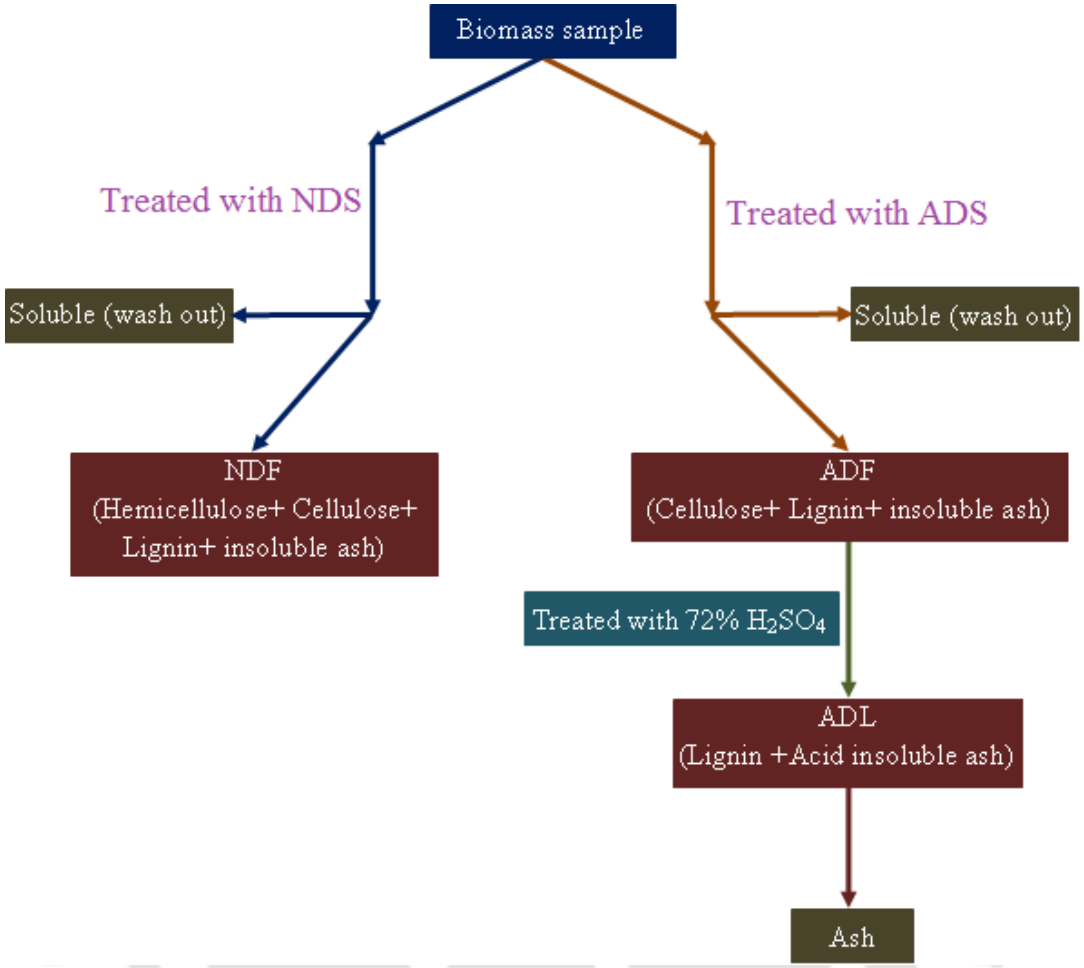

Fig. 3.54. Experimental layout of Fibre analysis

The NDF is calculated by using the Eq.3.10.

$$\text{NDF}=\frac{\left(\text{Weight of crucible + cell wall constituents}\right)-\text{ weight of crucible}}{\text{Weight of sample}}\times 100 \qquad (3.10)$$

The ADF is calculated by using the Eq.3.11.

$$\text{ADF}=\frac{\left(\text{Weight of crucible + Fibre}\right)-\text{ weight of crucible}}{\text{Weight of sample}}\times 100 \qquad (3.11)$$

The ADL is calculated by using the Eq.3.12.

$$\text{ADL}=\frac{\left(\text{Weight of crucible + Lignin}\right)-\text{ (Weight of crucible + Ash)}}{\text{Weight of sample}}\times 100 \qquad (3.12)$$

Hemiellulose is calculated by using Eq.3.13.

$$\text{Hemicellulose (H) (\%)} = \text{NDF-ADF} \tag{3.13}$$

Cellulose is calculated by using Eq.3.14.

$$\text{Cellulose (C) (\%)} = \frac{\text{(Weight of crucible + Fibre) - (Weight of crucible + Lignin)}}{\text{Weight of sample}} \times 100 \tag{3.14}$$

Lignin is calculated by using Eq.3.15.

$$\text{Lignin (L) (\%)} = \text{ADL} \tag{3.15}$$

3.9.1 FIBRE ANALYSIS (FA) OF BIOMASS BRIQUETTE

The percentage of hemicelluloses (H), cellulose (C) and lignin (L) are calculated by Fibraplus Van soest method for various compositions of saw dust briquette, rice husk briquette and mustard husk briquettes and reported in Table-3.18.

Table-3.18 Lignocellulostic analysis of biomass briquette by Fibraplus Van soest method

Briquette Composition	Saw dust briquette			Rice husk powder briquette			Mustard husk powder briquette		
	H%	C%	L%	H%	C%	L%	H%	C%	L%
B_{05}	18.36	50.09	15.71	19.32	40.66	28.54	21.32	48.41	16.62
B_{10}	14.26	53.68	13.89	18.57	42.65	25.99	16.95	50.64	16.33
B_{15}	14.04	53.96	12.26	17.97	46.03	22.32	16.45	51.03	15.96
B_{20}	13.66	54.64	10.65	15.36	46.89	19.45	15.04	56.08	15.32
B_{25}	13.23	56.41	10.06	14.33	48.98	16.41	14.95	57.22	11.61

It is observed that with increase in binder percentage, the percentage of hemicellulose decreases, percentage of cellulose increases and percentage of lignin decreases for all the variants of saw dust briquette, rice husk briquette and mustard husk briquettes. It is noticed that saw dust briquettes had hemicelluloses 13.26 % -18.36 %, cellulose 50.09 %-56.41 % and lignin 10.06 %-15.71 %.Rice husk powder briquettes had hemicelluloses

14.33% -19.32%, cellulose 40.66 %-48.98 % and lignin 16.41 % -28.54 %. Mustard husk powder briquettes had hemicelluloses 14.95 % -21.32 %, cellulose 48.21 %-57.22 % and lignin 11.61 % -16.62 %. It is studied that the percentage of hemicelluloses for saw dust briquette < rice husk briquette < mustard husk briquette. The percentage of cellulose for rice husk briquette<saw dust briquette< mustard husk briquette. The percentage of lignin for saw dust briquette<mustard husk briquette< rice husk briquette.

3.9.2 FIBRE ANALYSIS (FA) OF BIOMASS-DOLOMITE PELLET

The lignocellulostic analysis of biomass-dolomite pellet is carried out by FA methodology. The percentage of hemicelluloses, cellulose and lignin are calculated by Fibraplus Van soest apparatus for various compositions of saw dust briquette, rice husk briquette and mustard husk briquettes and reported in Table-3.19.

Table-3.19 Lignocellulostic analysis of biomass-dolomite pellet by Fibre analysis methodology

Composition	Saw dust-dolomitepellet			Mustard husk powder-dolomite pellet		
	H%	C%	L%	H%	C%	L%
P_{00}	28.95	45.61	16.65	33.19	39.32	7.99
P_{10}	26.29	38.79	13.57	32.16	34.38	6.6
P_{20}	25.26	32.32	13.3	31.27	30.37	5.66
P_{30}	19.04	21.39	12.85	24.2	20.61	3.82
P_{40}	13.07	19.99	11.37	23.56	12.17	3.57

It is observed that with increase in binder percentage, the percentage of hemicellulose decreases, percentage of cellulose increases and percentage of lignin decreases for saw dust-dolomite pellet and mustard husk-dolomite pellet. It is seen that saw dust-dolomite pellet had hemicelluloses 13.07 % -28.95 %, cellulose 19.99 %-45.61% and lignin 11.37 % -16.65%. Mustard husk powder-dolomite pellet had hemicelluloses 23.56 %-33.19 %, cellulose 12.17 %-39.32 % and lignin 3.57 % -7.99 %. It is studied that the percentage of hemicellulose for saw dust-dolomite pellet < mustard husk-dolomite pellet. The percentage of cellulose for saw dust-dolomite pellet > mustard husk-dolomite pellet. The percentage of lignin for saw dust-dolomite pellet >mustard husk-dolomite pellet.

3.9.3 LIGNOCELLULOSTIC ANALYSIS OF BIOMASS BRIQUETTE BY TGA METHOD.

The percentage of hemicelluloses, cellulose and lignin are calculated by TGA technique. In that case it is considered that the hemicellucose released between 200-300^{o}C, the cellulose released 300-400^{o}C and lignin decomposed in 400-900^{o}C. The values for various compositions of saw dust briquette, rice husk briquette and mustard husk briquettes are reported in Table-3.20. It is noticed that saw dust briquettes had hemicelluloses 9.04 %-11.59 %, cellulose 49.54%-56.91% and lignin 14.39%-28.25%. Rice husk powder briquettes had hemicelluloses 10.40%-23.30%, cellulose 24.32%-46.85% and lignin 12.83% -29.46%. Mustard husk powder briquettes had hemicelluloses 12.85% -18.12%, cellulose 28.11%-42.11% and lignin 13.77% -29.04%.

Table-3.20 Lignocellulostic analysis of biomass briquettes by TGA technique

Briquette Composition	Saw dust briquette			Rice husk powder briquette			Mustard husk powder briquette		
	H%	C%	L%	H%	C%	L%	H%	C%	L%
B_{00}	9.16	49.54	28.25	12.26	36.25	20.59	18.12	32.40	22.81
B_{05}	11.59	50.52	20.06	11.28	36.05	16.77	17.04	28.18	28.77
B_{10}	11.27	50.65	23.72	10.43	46.20	12.52	16.45	30.90	24.05
B_{15}	9.87	53.97	16.25	23.30	24.32	13.18	12.85	42.11	13.77
B_{20}	10.01	55.07	14.39	11.62	38.58	29.46	15.15	35.28	29.04
B_{25}	9.04	56.91	15.12	10.40	46.85	12.83	13.19	35.38	15.22

It is observed that the obtain values of HCL are not relative in regular. This is because for the simplicity, values of HCL released are considered within the fixed range of temperature. Actually the release of HCL starts from the initial temperature rise itself. It is studied that the percentage of hemicellulose for rice husk briquette > mustard husk briquette >saw dust briquette. The percentage of cellulose for saw dust briquette > rice husk briquette > mustard husk briquette. The percentage of lignin for mustard husk briquette >saw dust briquette >rice husk briquette.

3.9.4 LIGNOCELLULOSTIC ANALYSIS OF BIOMASS-DOLOMITE PELLET BY TGA METHOD

The lignocellulostic analysis of biomass-dolomite pellet is carried out by TGA method. The percentage of hemicelluloses, cellulose and lignin are evaluated. It is observed that saw dust-dolomite pellet had hemicelluloses 7.66% -11.94%, cellulose 19.49%-49.54% and lignin 28.25%-34.89%. Mustard husk powder-dolomite pellet had hemicelluloses 6.1% -18.12%, cellulose 20.49%-40.37% and lignin 21.63% -28.69%.The values of HCL for various compositions of saw dust-dolomite pellet and mustard husk-dolomite pellet are reported in Table-3.21.

Table-3.21 Lignocellulostic analysis of biomass pellets by TGA technique

Composition	Saw dust-dolomitepellet			Mustard husk powder-dolomite pellet		
	H%	C%	L%	H%	C%	L%
P_{00}	9.16	49.54	28.25	18.12	32.4	22.81
P_{10}	8.98	41.39	24.46	7	38.56	26.02
P_{20}	5.74	30.39	34.89	6.63	36.21	27.57
P_{30}	11.94	19.49	34.18	6.1	40.37	21.63
P_{40}	7.66	22.46	34.03	13.59	20.49	28.69

It is studied that percentage of hemicellulose for saw dust-dolomite pellet < mustard husk-dolomite pellet, percentage of cellulose for saw dust-dolomite pellet > mustard husk-dolomite pellet and percentage of lignin for saw dust-dolomite pellet >mustard husk-dolomite pellet.

3.10 DOLOMITE POWDER X- RAY DIFFRACTION (XRD) ANALYSIS.

Dolomite is one of the constituent of biomass-dolomite pellets. The dolomite powder [$CaMg(CO_3)2$] is used in preparation of the biomass-dolomite pellet which works as catalyst during the gasification process. It is purchased from market with the size 200 mesh. XRD analysis of this dolomite is carried out with the X-ray diffraction analysis instruments facilitate by department of mechanical engineering IIT Guwahati and sponsored by Ministry of Steel. Figure 3.55 depicts dolomite powder X- ray diffraction pattern.

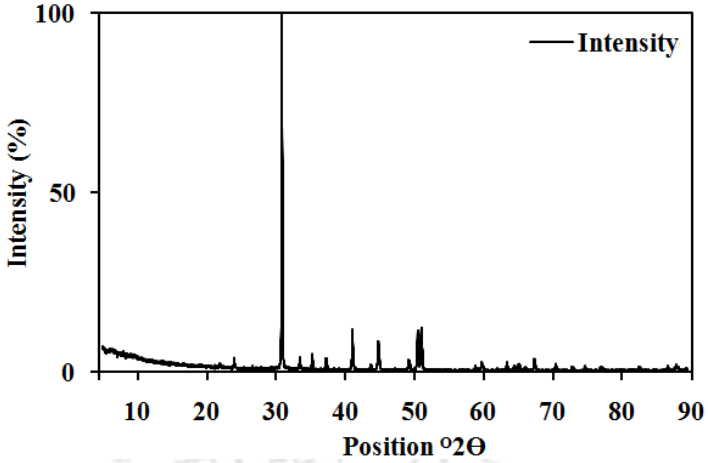

Fig.3.55. X-ray diffraction pattern of dolomite powder

The analysis software is supplied with the XRD instrument. The data produced for the present sample is matched with the Crystallography open database (COD). It is observed that the present data base pattern is best fit with the reference pattern code COD 96-900-3509.

3.11 SUMMARY

The characterization of all the samples is carried out by performing proximate analysis, ultimate analysis, and feedstock handling characteristics, determining the calorific value, thermogravimetric analysis and fibre analysis. All the feedstock has good amount of volatile matter and carbon content. The handling characteristic of biomass briquette and biomass- dolomite pellet is nearly matching with the woodchips.

The weight loss and the rate of weight loss are determined with the thermogravimetric analysis. It is observed that the biomass briquette undergoes devoltalzation for temperature between 200-400^{o}C. The biomass-dolomite pellet undergoes devoltalization in two stages. The first stage is from 200^{0}C-400^{0}C and the second stage is from 700-800^{o}C which is responsible for cracking of the tar. The dolomite enhances the characterization of the pellets. Lignocellulosic characteristics are carried out by the Van soest fibre analysis method. The values calculated are compared with the estimated values by TGA analysis. In all the respect the biomass briquette and biomass dolomite pellets are compatible with the woodchip. This study is helpful for the selection of appropriate composition of briquettes and pellets for the gasification. Forthcoming experiments are planned with briquette B_{15} and all variant of biomass dolomite pellet.

Chapter 4 presents the experimental setup and procedure for performing the experiments with woodchips, saw dust briquette and biomass-dolomite pellet in 5kW downdraft gasifier. It includes experimental setup, procedure, and instrumentation. It also describes the measurement techniques for thermal behavior of the gasifier, tar content analysis and gas yield and quality analysis of the producer gas. At the last it gives information about the material and methodology for the feedstock preparation.

CHAPTER 4

EXPERIMENTAL SETUP AND PROCEDURE FOR BIOMASS GASIFICATION

4.1 INTRODUCTION

This chapter describes the experimental setup and procedure for the gasification of biomass in a downdraft gasifier. An existing downdraft gasifier is instrumented and experiments were conducted with biomass briquette B_{15} containing saw dust. The operational procedure of the downdraft gasification, positioning of various zones inside downdraft gasifier, thermocouple casing development and fixation of thermocouples inside gasifier at various location are discussed in detail. The instrumentation of downdraft gasifier for the temperature measurement, pressure measurement, air flow rate, and producer gas flow rate is explained. The scrubbing and gas filtration system along with tar collection and measurements is also described. Methods for production of biomass briquettes and pellets are described at the last part of the chapter.

4.2 EXPERIMENTAL SETUP

The downdraft gasifier system used for the present experiment is shown in Fig 4.1. It consists of four parts:

1. Gasification unit
2. Gas scrubbing unit
3. Gas filtration unit
4. Utilities containing a 5 kW dual fuel diesel engine coupled to a d. c generator.

The heart of experimental set-up is the gasifier which consists of three parts as shown in Fig. 4.1.

1. Inverted cone frustum shape hopper
2. Cylindrical shape reaction chamber
3. Conical shape ash chamber

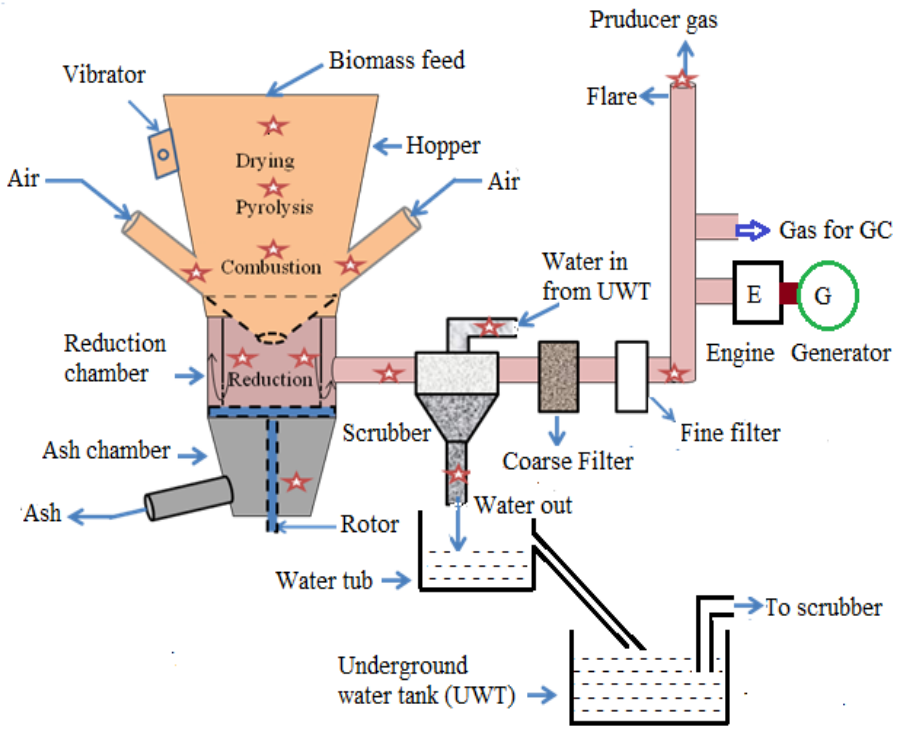

Fig. 4.1 Simplified layout of downdraft biomass gasifier

The downdraft gasifier is apparently divided into seven zones based on the thermo chemical conversion of phenomenon. These zones starting from the top are

1. Drying zone
2. Pre-pyrolysis zone
3. Pyrolysis zone
4. Pre-combustion
5. Combustion zone
6. Reaction zone
7. Ash chamber

The height of the gasifier is 1620 mm. The diameter at the pyrolysis zone is 440 mm and the diameter at the reduction zone is 346 mm. The depth and diameter of the reduction zone are 330 mm and 256 mm, respectively. The ash produced during gasification is removed by rotating the rotor inside the reaction chamber. The arrangement is provided to prevent clogging of the biomass at the throat. Specifications of downdraft gasifier are given in Annexure-III and ancillaries attached to the same are given in Appendix-IV. A pictorial view of the experimental set up is presented in Fig. 4.2.The producer gas exit at bottom (from the reduction zone) is connected with the various downstream systems e.g. venturi scrubber, cyclone separator, coarse filter, fine filter and a flare with valve. Gas

produced in the reaction chamber is scrubbed and cooled in scrubber. Water is recirculated from water tank to the scrubber with the help of scrubber pump. Gas is separated from water in a cyclone separator connected to the scrubber and same goes to the filtration units (coarse and fine filters connected in series). Cool and clean producer gas is then available at the flare for utilization. Components of the downdraft gasifier are described as follows.

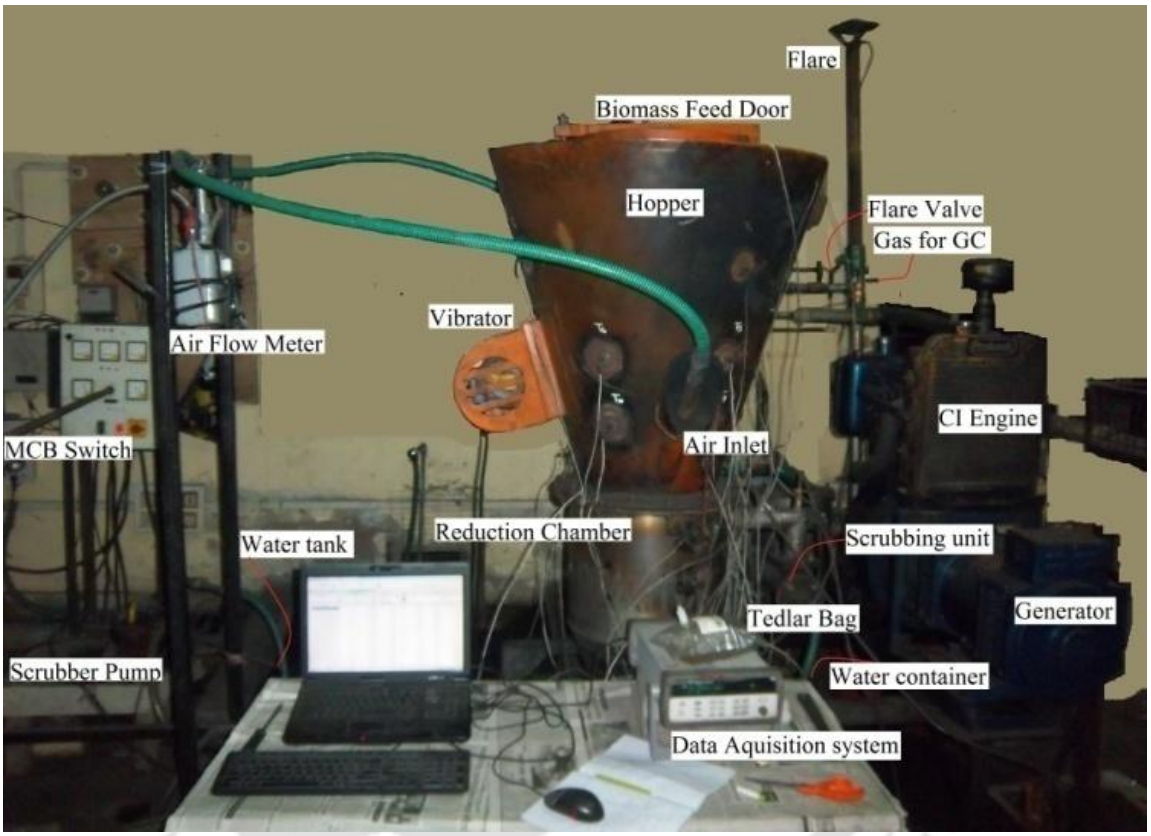

Fig.4.2 Picture of the Experimental Set-up

4.2.1 HOPPER

The hopper is located above the reaction chamber. Various biomasses are feed into the hopper through the lid attached at the top as shown in Fig. 4.2. A vibrator consists of an electric motor with an unbalanced weights attached to its shaft is erected on the slanting face of the hopper as shown in Fig. 4.2. It is fitted on the surface of hopper at a distance of 930 mm from the top. The vibrator requires power 0.9 kW_e and rotates with the speed 1370 mm. It assists in the flow of biomass feedstock to the downward direction inside the gasifier avoiding the clogging of feedstock at the venture throat.

4.2.2 REACTION CHAMBER

The reaction chamber is located just above the support structure grouted to the foundation. It is filled with charcoal pieces with average size 15-20 mm up to a height of 210 mm from flange as shown in Fig.4.3 (a). At the bottom of reaction chamber grate is provided for ash removal and rotor blade are provided for the stirring of the charcoal pieces as shown in Fig. 4.3 (b).

Fig.4.3(a) Reaction chamber with charcoal

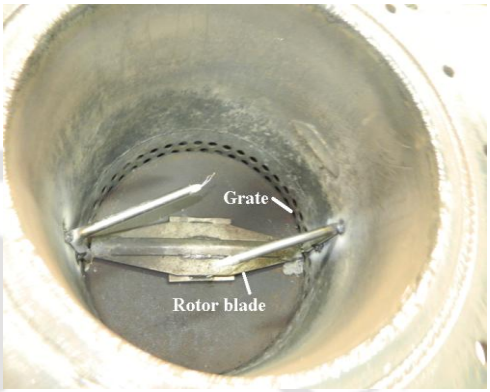

Fig. 4.3(b) Grate inside reaction chamber

4.2.3 ASH CHAMBER

The ash chamber is located below the reaction chamber as shown in Fig. 4.4(a). The ash is collected from reaction chamber through grate (perforated sheet of reaction chamber) in the ash cone. The ash is removed from the ash cleaning door. A combo rotor as shown in Fig. 4.4 (b) is used at the base of the gasifier. It rotates the rotor blade located inside the reaction chamber with the torque 30 kg-cm to facilitate the removal of ash from the system.

Fig.4.4(a) Ash collection cone

Fig.4.4(b) Combo rotor

4.2.4 SCRUBBER AND CYCLONE SEPARATOR

The hot producer gas coming out from the reaction chamber goes through a scrubbing unit so as to clean and cool the gas (Fig. 4.5(a)). Hot gas while passing through the venturi tube of the scrubber is injected with water at the venturi throat so as to bring down the temperature of the same thus leading to the condensation of a large portion of tar. In order to achieve high purity of producer gas the same is next passed through a cyclone separator as shown in Fig. 4.5(b). Condensed tar remaining with the cooled gas undergoes separation in this device. The tar thus separated is collected in a water tub. Fairly good quality producer gas is led to the filtration unit after the gas goes out from the cyclone separator.

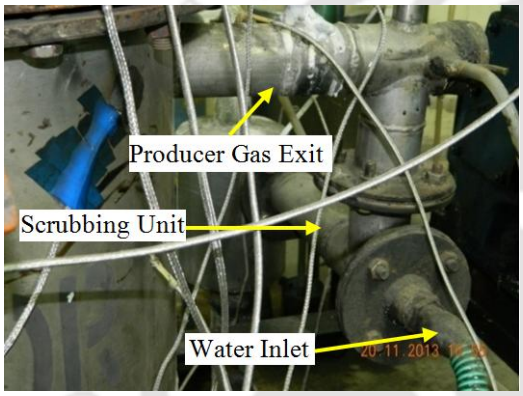

Fig. 4.5(a) Scrubbing unit

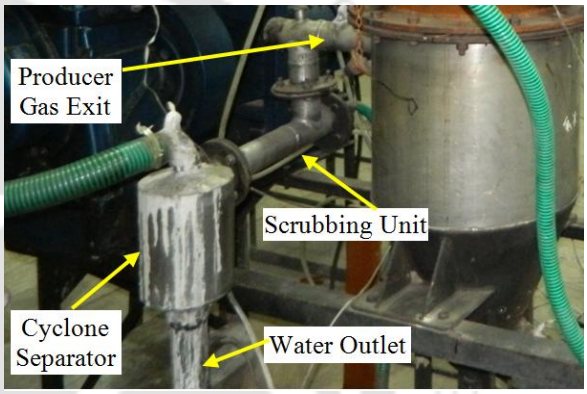

Fig. 4.5(b) Cyclone separator

4.2.5 WATER TANK AND WATER TUB

The scrubbing of the producer gas is carried out with the fresh and clean water taken from the water tank as shown in Fig. 4.6(a).

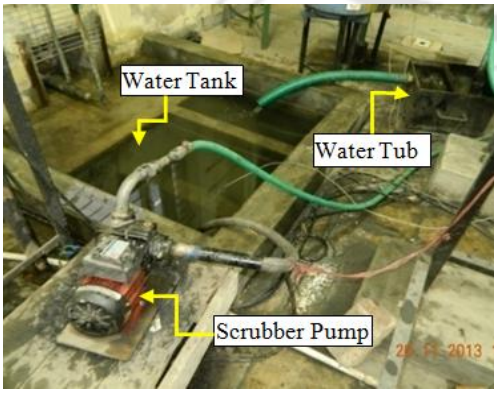

Fig.4.6(a) Water tank with scrubber pump

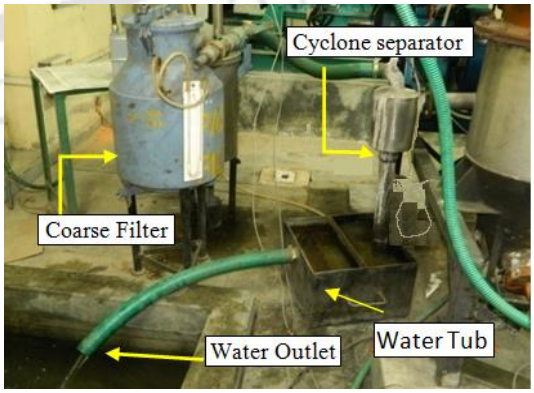

Fig. 4.6(b) Water tub below cyclone separator

A 0.6 kW_e scrubber pump is used for circulation of water from water tank to the scrubber and cyclone separator. Water containing condensed tar coming out from the cyclone separator is rejected to the water tank again through a water tub (Fig. 4.6(b)). Condensed tar is separated from water and collected from the water tub.

4.2.6 COARSE AND FINE FILTER

Treated producer gas in scrubber and cyclone separator is then passed through a coarse and fine filter for removal of moisture and particulate matter. The coarse filter is shown in Fig.4.7 (a). Saw dust is used as the filter media for the course filter whereas fabric with fine pores is used in the fine filter (Fig. 4.7(b)). Thus good quality gas is obtained after filtration.

Fig.4.7 (a) Coarse filter with saw dust as filter material.

Fig. 4.7(b) Fine filter with fabric material bag as filter.

The producer gas obtained after filtration can be used in the dual fuel engine coupled to a d. c. generator to produce electricity. The quality of the gas can be judged by flaring the same at the exit of flare pipe. In case of use of the gas in the engine, the valve at the bottom of the flare pipe is turned on to pass the gas to the suction pipe of the engine.

4.3 SENSORS AND INSTRUMENTATION

4.3.1 DETAILS OF THERMOCOUPLES USED

The gasifier is instrumented with thermocouples, manometers and air/gas flow meters to measure the temperature profile, pressure drop and flow rate of air as well as gas produced in the system. Two types of the thermocouples are used for the thermal analysis of the gasification process. Both the K and T type of thermocouples are used based on the expected temperature profile inside the gasifier. Measuring range of K-type thermocouple

is reported to be 0-1350^{o}C whereas it is in the range of 0-800^{o}C for the T-type thermocouples. K-type thermocouples are used to observe the inside performance of gasifier. T-type thermocouples are used to measure the temperature along the outer surface of the gasifier.

K-type thermocouple consists of two wires Chromel (90% Nickel and 10% Chromium) and Alumel (95% Nickel, 2% Manganese, 2% Aluminum and 1% Silicon). T-type thermocouple consists of Copper and constantan (55% copper and 45% nickel). Calibration of thermocouple is given in Appendix-V

The thermocouple are of wire type so could not remain straight inside the hopper. Moreover, as the gasifier is conical with varied cross-section, lengths of the thermocouples are different at different locations. Further, feedstock being hard, bare thermocouples cannot be used inside the gasifier. So to satisfy this, stainless steel casings are specially made and the same are placed inside these casings with proper sealing.

The hopper of the downdraft gasifier was drilled for welding and positioning nuts for tightening and placing the thermocouple casing. The casings are tightened to these nuts inside the surface of gasifier. The provision of SS casing also increases the retention time of the biomass progressive movement inside the hopper. This improves the gasification process. The outside and inside drill surface of the hopper for the provision of thermocouple casing is shown in Fig 4.8 (a) and Fig.4.8 (b).

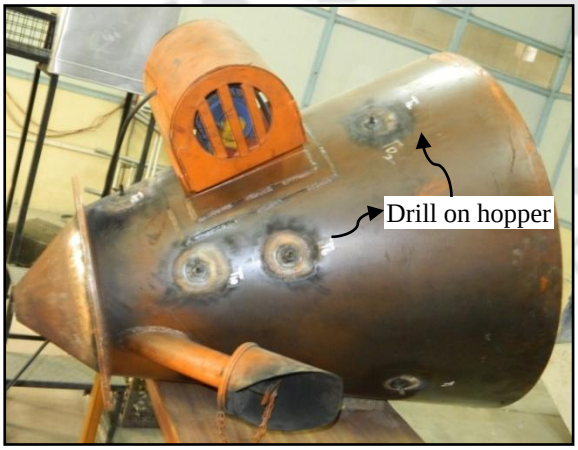

Fig 4.8(a) External view of drills on hopepr

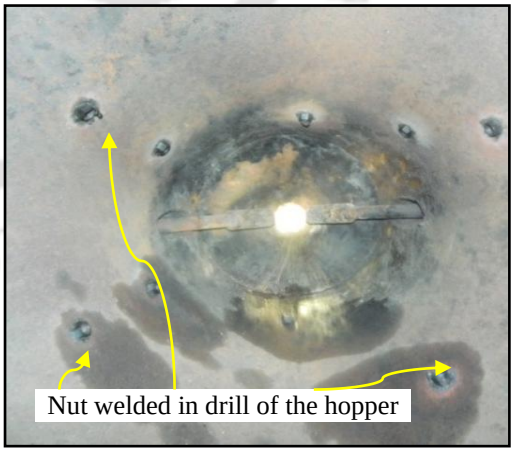

Fig. 4.8(b) Internal drills indside hopper

The thermal analysis of gasifier is carried out by measuring temperature with 36 thermocouples out of which 18 are used in radial as well as axial locations inside the

gasifier, 11 thermocouples were used along the outer surface of gasifier. Remaining 7 thermocouples are used along the producer gas flow pipe line. The location of thermocouples inside the gasifier and along the outer surface is as shown in Fig. 4.9.

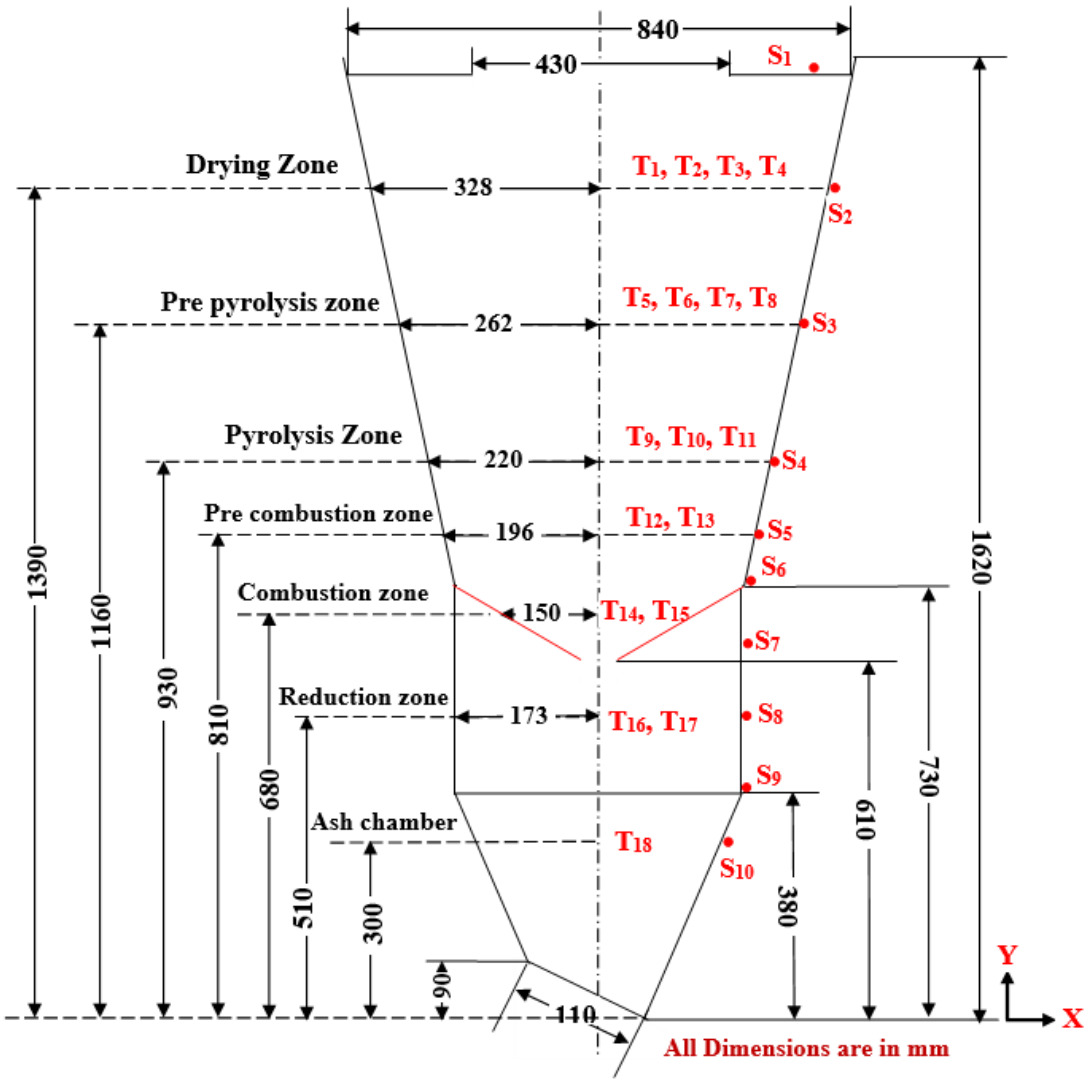

Fig. 4.9 Location of thermocouple in various zone

The thermocouples S_1, S_2, S_3, S_4, S_5 and S_6 are placed along the surface of the hopper at each zone. The thermocouples S_7, S_8 and S_9 are placed along the surface of reaction chamber. The thermocouple S_{10} is placed along the surface of ash collection cone.

Table-4.1 shows the location of the thermocouple at various locations inside the downdraft gasifier. It elucidates the various zones diameter, distance of the each zone from the base of the ash collection cone and number of thermocouple used in each zone.

Table 4.1 Thermocouple at various locations inside the downdraft gasifier

Location	Number of thermocouples	Number of thermocouples on surface of gasifier	Distance from the base of the gasifier (mm)	Diameter of the zone (mm)
Drying zone	4	1	1390	656
Pre-pyrolysis zone	4	1	1160	524
Pyrolysis zone	3	1	930	440
Pre-combustion zone	2	1	810	392
Combustion zone	2	1	680	300
Reduction zone	2	3	510	346
Ash Collection cone	1	1	300	260

Figures 4.10 (a)-(c) presents the pictorial view of thermocouples with casing and position of their sensing beads inside the gasifier.

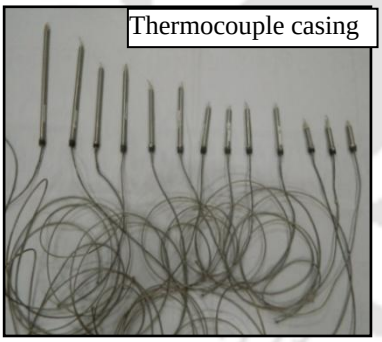

Fig. 4.10(a) SS thermocouple casing

Fig. 4.10(b) Hopper with thermocouple casing

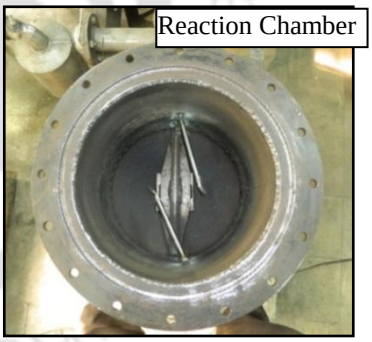

Fig. 4.10(c) Reaction chamber with thermocouple casings

Figures 4.11(a)-(b) gives information about location of thermocouple beads radically positioned inside the gasifier at drying zone and pre-pyrolysis zone, respectively. The diameters of the hopper at the drying zone and pre-pyrolysis zones are 656 mm and 524 mm, respectively. The four thermocouples $T_{1,}$ $T_{2,}$ $T_{3,}$ and T_4 are placed at a distance of 44mm, 122mm, 158mm and 262mm, respectively from the vertical axis of the hopper in the drying zone. Same are placed in pre-pyrolysis zone (T_5, $T_{6,}$ T_7 and T_8) at a radial distance of 30 mm, 112 mm, 152 mm, and 210 mm, respectively.

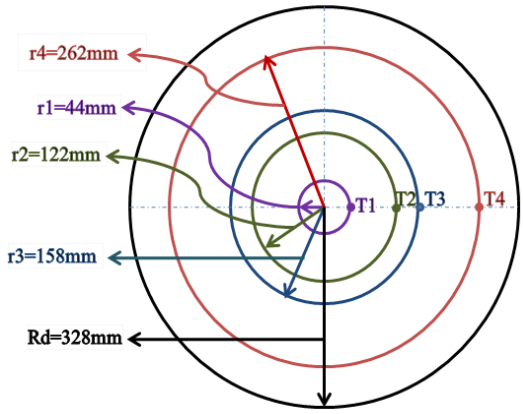

Fig. 4.11(a) Radial position of thermocouple location in drying zone

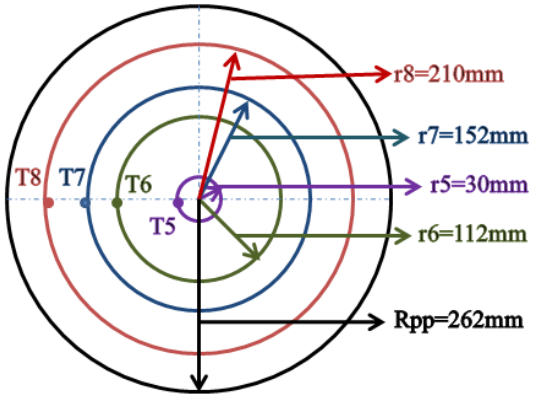

Fig. 4.11(b) Radial position of thermocouple location in prepyrolysis zone

Similarly, the radical location of thermocouples inside the pyrolysis and pre-combustion zone is shown in Fig.4.12 (a) and Fig.4.12 (b), respectively. The diameter of the gasifier at the pyrolysis and pre-combustion zone are measured to be 440 mm and 392 mm, respectively. The thermocouple T_9, T_{10} and T_{11} in pyrolysis zone are placed at a distance of 100 mm, 110 mm and 152 mm, respectively from the vertical axis of the hopper while the thermocouple T_{12}, and T_{13} in pre combustion zone are placed at 82 mm and 110 mm, respectively.

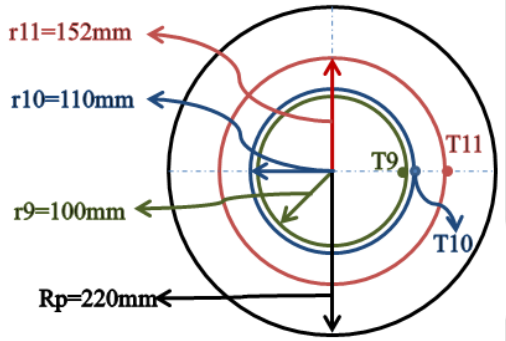

Fig. 4.12a. Radial position of thermocouple location in pyrolysis zone

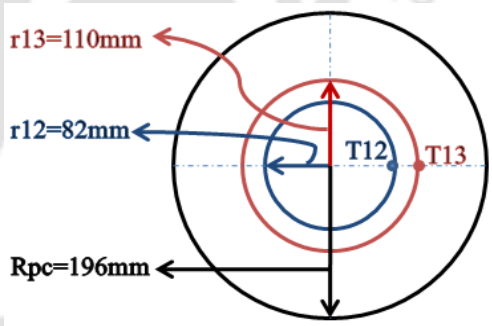

Fig. 4.12b. Radial position of thermocouple location in pre-combustion zone

Similarly, the radical location of thermocouple in the combustion zone, reduction zone and ash collection cone is shown in Fig.4.13 (a)-(c), respectively.

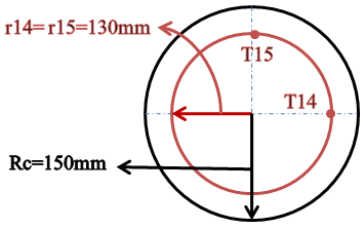

Fig. 4.13(a) Radial position of thermocouple location in combustion zone

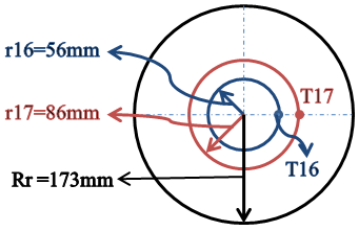

Fig. 4.13(b) Radial position of thermocouple location in reduction zone

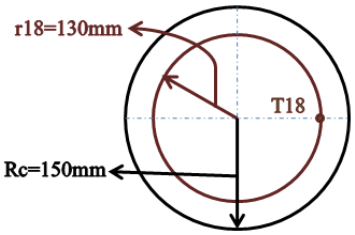

Fig. 4.13(c) Radial position of thermocouple location in manual ash collection cone

Thermal behavior of the producer gas coming out of the gasifier is measured by placing the thermocouples inside producer gas line at various places like exit of the reaction chamber, entry and exit to the filters and the gas flare. Temperature of water at inlet and outlet to the scrubber are also measured. Table 4.2 presents the locations of thermocouple in the system.

Table 4.2 Thermocouple at various locations along producer gas line

Particulars of data collection	Notation of Thermocouples	Number of thermocouples
Measurement of producer gas temperature at the exit of reaction chamber	T_{19}	1
Surface temperature measurement of producer gas pipe line at the exit of reduction chamber	S_{11}	1
Measurement of producer gas temperature at the entry to the filters	T_{20}	1
Measurement of producer gas temperature at the exit to the filters	T_{21}	1
Measurement of flame temperature at the flare	T_{22}	1
Measurement of water temperature at the inlet to the scrubber	T_{23}	1
Measurement of water temperature at the outlet to the scrubber	T_{24}	1
Measurement of room temperature	T_{25}	1

The thermocouples were connected to the multiplexers. These multiplexers were engrossed inside the data acquisition system (Make: Agilent). The data acquisition system is connected to the computer device and readings are noted by using Agilent software (Fig. 4.14).

Fig. 4.14 Data acquisition for temperature recording

4.3.2 INSTALLATION OF PRESSURE GAUGE

Three manometers are used to measure the pressure drop in the gasification system. One manometer is used across the gasifier (above the reduction zone) and the exit of producer gas pipeline. Draught produced for air suction can be observed from this manometer reading. The second manometer is placed across the coarse filter chamber and the third manometer is placed across the producer gas inlet to fine filter and gas accumulation chamber after filtration inside fine filter as shown in Figs. 4.15 (a)-(b).

Fig. 4.15(a) Coarse filter Manometer

Fig. 4.15(b) Fine Filter Manometer

4.3.3 INSTALLATION OF FLOW METER

Two flow meters are used in the experiment to measure the flow of gas and air. The first flow meter measures the flow of air intake to the gasifier as shown in Fig 4.16 (a). The air intake took place through inlet of the flow meter and delivered to the two air intake ports of the downdraft gasifier. Figure 4.16 (b) shows the connection of the flow meter with the

producer gas flow line. The second flow meter measures the gas flow rate coming out after the complete filtration as shown in Fig 4.16 (c).

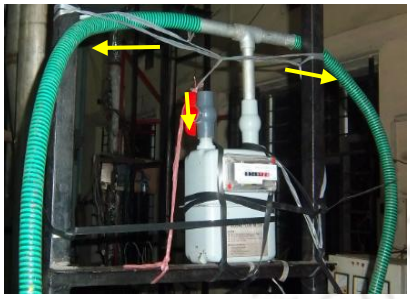

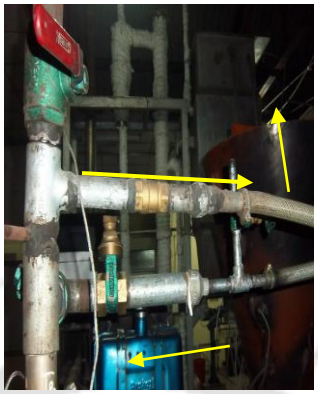

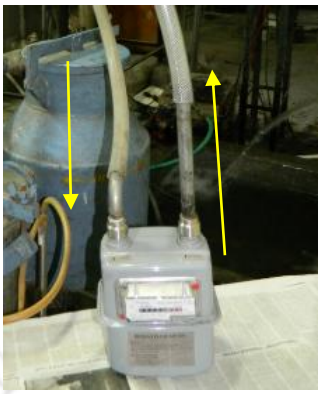

Fig. 4.16(a) Air flow meter **Fig. 4.16(b) Gas flow line** **Fig. 4.16(c) Gas flow meter**

4.3.4 PRODUCER GAS SAMPLE COLLECTION

The producer gas has the various constituents like H_2, CO, CH_4, etc. The sample of producer gas obtained in the gasification process is collected from the gas line. It is collected after successive filtration from the coarse filter and fine filter. The location of gas sample collection point is shown in Fig. 4.17(a). The sample is collected in a Tedlar bag as shown in Fig. 4.17(b). The further investigation to measure the percentage of various constituents of collected gas is carried out with gas chromatography (GC) analysis.

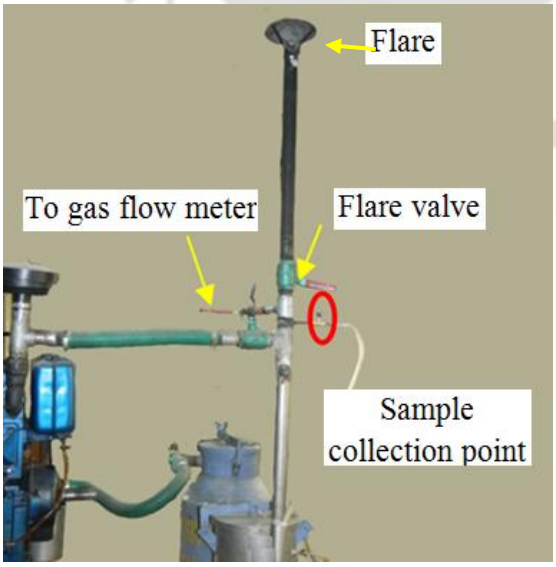

Fig.4.17(a) Sample collection point **Fig.4.17(b) Tedlar bag**

4.3.5 TAR MEASUREMENT

Tar produced in the gasification process is collected and measured from various locations as given in Appendix-VI. In gasification tar is collected from water tub, water tank, and measured by weight difference of material in coarse filter and bag in fine filter. The detail of tar measurement, properties and cracking techniques are illustrated in Chapter 6.

4.4 EXPERIMENTAL PROCEDURE

The gasifier is installed with the thermocouples, airflow meter, gas flow meter and manometers. Manometer and airflow readings are taken by manual measurements while temperature records are collected through a data acquisition system (Agilent make) connected to a computer and thermocouples. Before starting the experiments, the reaction chamber is filled with 5kg of charcoal. Subsequently the hopper is mounted over the reaction chamber. The asbestos rope of 19mm diameter is put between the reaction chamber and the hopper. This avoids the leakage of the gases. The feedstock is feed in the gasifier through the feed door located at the top (Fig.4.18).

Fig. 4.18 Feeding of gasifier

The experiment is carried out for the three feedstock (a) wood chip, (b) saw dust briquette and (c) biomass pellet. The first test is carried out by feeding hopper with 80-85 kg of woodchips of cylindrical shape with approximate size 25mm × 25mm, second test is carried out by feeding 70-80 kg of sawdust briquette of spherical shape with approximate diameter of 25mm and third test is carried out with saw dust pellet/ saw-dust dolomite pellet of cylindrical shape with approximate size 17mm × 25mm. The care is taken that the hopper is filled with the biomass completely. The feed door is closed after loading the solid biomass. Saw dust is added to the coarse filter. The filtering bag in the fine filter cleaned and again mounted inside the filter. The scrubber pump is started which creates

suction inside the gasifier and the flare valve is slightly opened. Controlled amount of air is allowed to enter into the reaction chamber through air nozzles. The gasifier is ignited by bringing diesel/oil dipped lighted torch onto the two air nozzles one after another, so that flame is sucked into combustion chamber as shown in Fig. 4.19

Fig 4.19 Firing of the gasifier

Gas production is detected at the flare by burning with a kindler. It is observed that medium heating value gas is generated within 5-10 minutes from the start of the gasification process. The gas is checked by lightening at flare with kindler. When it catches the fire, it is supplied to the dual fuelled CI Engine for power generation with coupled generator. The gasification process undergoes as per the combustion and reduction reactions. Heat is generated in the combustion zone. That heat propagates to the pyrolys is and drying zone and biomasses starts to release volatiles and convert to char which drops down to the reduction chamber. Heat generated into combustion zone also propagates into reduction zone. Special ash handling mechanism is provided at the bottom of the reduction zone so that no clinkers can form. Ash from the reduction chamber is transferred to the ash chamber which can be removed easily.

The experiment is carried out by setting various equivalence ratios. The equivalence ratio is obtained by controlling the flow rate of air which is passing through the air nozzle. Eequivalence ratio (ER) is defined as ratio of (measured air flow rate to biomass flow rate) to the (stoichiometric air flow rate to biomass flow rate).The equivalence ratio is calculated by the Eq.4.1 (Ravindranath et al., 2004). Calculation of stoichiometric ratio is given in Appendix-VII.

$$ER = \frac{(A/F)_{actual}}{(A/F)_{Stoichiometric}} \qquad (4.1)$$

The calorific value of producer gas (MJ/Nm^3) is calculated by equation 4.3 (Rajvanshi, 1986)

$$Q_{CVg} = \frac{\left(x_1 \times CV\right)_{H_2} + \left(x_2 \times CV\right)_{CO} + \left(x_3 \times CV\right)_{CH_4}}{100} \quad (4.2)$$

x_1, x_2, x_3, x_4 and x_5 are the volumetric percentage of H_2, CO, CH_4, CO_2, N_2 in producer gas. The required calorific value of the each compound is given in Table-4.3

Table-4.3 Calorific value of the various compounds

Compound	H_2	CO	CH_4	CO_2	N_2
	x_1				
Calorific value (MJ/m^3)	12.78	12.71	39.76	0	0

The average conversion efficiency (η_{Gas}) (cold gas efficiency) of the gasifier is calculated by the equation 4.3 (Rajvanshi, 1986).

$$\eta_{Gas} = \frac{\left(\text{Calorific value of the gas/kg of fuel}\right)}{\text{Average Calorific value of 1 kg of fuel}} = \frac{\left(CV_{Gas}\left(MJ/m^3\right) \times Pg\left(m^3/kg\right)\right)}{CV_{Feedstock}\left(MJ/kg\right)} \quad (4.3)$$

Where,

CV_{Gas}= Calorific value of the gas (MJ/Nm^3)

$CV_{Feedstock}$= Calorific value of the feedstock (MJ/kg)

P_g= Producer gas generated (Nm^3/kg)

The carbon conversion efficiency (η_c) of the gasifier is calculated from the gas composition by equation 4.4 [Gungul et al. (2014)

$$\eta_c = \frac{Pg\left(m^3/kg\right) \times \left(CO\% + CO_2\% + CH_4\%\right) \times 12}{22.4 \times C\%} \quad (4.2)$$

4.5 FEEDSTOCK PREPARATION

The experiments are carried out with wood chips of pongamapinnata, biomass briquette and biomass-dolomite pellet. In the present work the biomass characterization is carried out for all the feedstock which is used for the experimentation. The biomass briquettes are made with the material sawdust of pongamia pinnata, rice husk powder, mustard husk powder. The pellets are manufactured using the raw material saw dust of pongammia pinnata and mustard husk. The wood chips of the size approximately 25 mm length and 25 mm diameter cut by the woodcutter, briquettes of spherical size approximately 25 mm in diameter were prepared by hand and pellets of in 20 mm in diameter and 25 mm-35 mm in length were manufactured in pelletizing machine.

4.5.1 PREPARATION OF WOOD CHIPS

The present experimental set up is designed for the gasification of wood chips. The basic experiments are carried out by using this wood chips as a feedstock. The wood chips of pongamapinnata are used for the present experimentation. The branches of the wood are collected and kept for the sun drying. The continuous monitoring on the moisture content of the wood is done. When the moisture is reaches 13-15% wood is cut in chips in shape of approximately 25 mm diameter and 25 mm length with the help of woodcutter as shown in Fig. 4.20. The Figure 4.21 shows the wood chips cut with this wood cutter.

Fig.4.20 Wood cutter

Fig.4.21 Wood chips

4.5.2 PREPARTION OF BIOMASS BRIQUETTE

The biomass briquettes are prepared by using the materials (1) biomass, (2) Waste newspapers as binder and (3) Water. Three types of briquette are prepared using the various compositions of biomass material and waste newspaper. The saw dust briquettes, rice husk briquettes and mustard husk briquettes are prepared by using the biomass

materials saw dust of pongamapinnata, rice husk powder and mustard husk powder respectively. The five samples were prepared for each biomass with different compositions of biomass and binder. The five compositions of the briquette are prepared for each biomass material. Briquette compositions with notations are given in Table-4.4.

Table 4.4. Briquette composition with notations

Briquette composition	B_{05}	B_{10}	B_{15}	B_{20}	B_{25}
Biomass (%)	95	90	85	80	75
Waste newspaper as binder (%)	05	10	15	20	25

Biomass briquettes are prepared using various proportion of biomass: waste newspaper: water. The mixture (biomass + binder): water is in proportion of 1:2 used for the preparation of briquette. Figure 4.22 shows the constituent of the briquette. The biomass briquettes are prepared manually in spherical shape of average diameter 25 mm as shown in Fig. 4.23.

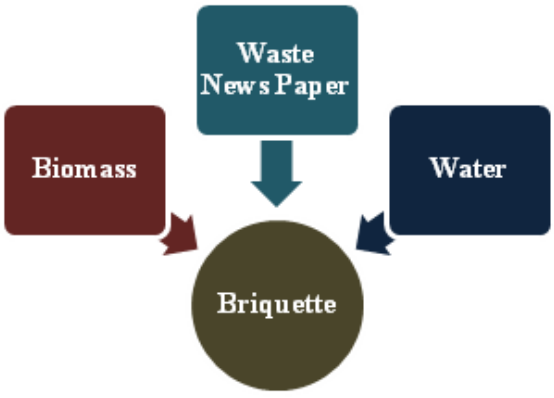

Fig.4.22 Briquette constituent

Fig.4.23 Handmade Briquettes

At first a fixed quantity of binder as shown in Table-4.3 is mixed with water which forms sticky solution. After that, biomass material is added to it in stated quantity and mixed thoroughly to obtain homogeneous slurry. The spherical briquettes are prepared by hand with squeezing out the excess water. The briquettes are prepared of approximate size 25 mm in diameter. The briquette preparation mechanism is elaborated in the Fig 4.24.

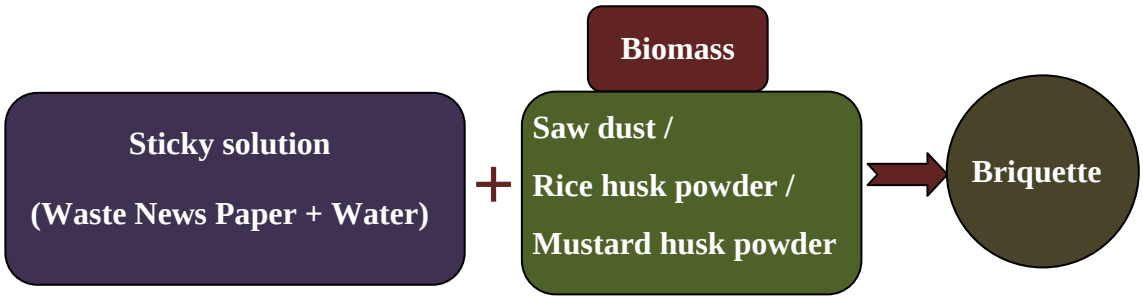

Fig.4.24 Briquette preparation mechanism

These briquettes are prone to deformation due to high moisture content. Conventional sun drying for a period of 2 weeks is done to prevent the deformation. Moisture content of the final briquettes is maintained at 15% (approx.) (Shelke and Mahanta, 2014 b).

4.5.3 MANUFACTURING OF BIOMASS-DOLOMITE PELLETS

Biomass-dolomite (BD) pellets are manufactured with the pelletizer machine. The materials used for preparation of pellets are (1) Biomass, (2) Dolomite as catalyst for tar cracking and (3) Water. Two biomasses used for pellet manufacturing are (a) pongammia pinnata dust (Fig.4.25) and (b) mustard husk powder (Fig.4.26). The mustard husk powder is obtained by grinding the mustard husk (Fig.4.27) in grinding mill.

Fig. 4.25 Pongamiapinnata powder

Fig. 4.26 Mustard husk powder

Fig.4.27 Mustard husk

Five samples are prepared for each biomass with different compositions of biomass and dolomite as shown in Table 4.5.

Table 4.5. Composition of biomass and catalyst for manufacturing BD pellet

Type of material	Composition of biomass and catalyst with notations				
	P_{00}	**P_{10}**	**P_{20}**	**P_{30}**	**P_{40}**
Biomass (%)	100	90	80	70	60
Dolomite as catalyst (%)	00	10	20	30	40

Biomass-dolomite pellets are manufactured with the Pellet Press Model 250 as shown in Fig 4.28. This pellet press is made by Hi Tech Agro Projects Pvt. Ltd. The specification of machine is given in Appendix-VIII. The machine consists of hopper, compressing chamber, pellet receiver, electric motor, and gear box. The compressing chamber consists of a vertical shaft (aligned with gear box), rotor block and dies plate. At first electrical motor is started. Its linear rotating motion is transformed into vertical rotating motion with the help of gear box. The gear box reduced the speed of the motor in a gear ratio of 5:1. The rotor block is mounted on the vertical shaft with aligned key. Figure 4.29 shows rotor block with roller, roller shaft and dies plate.

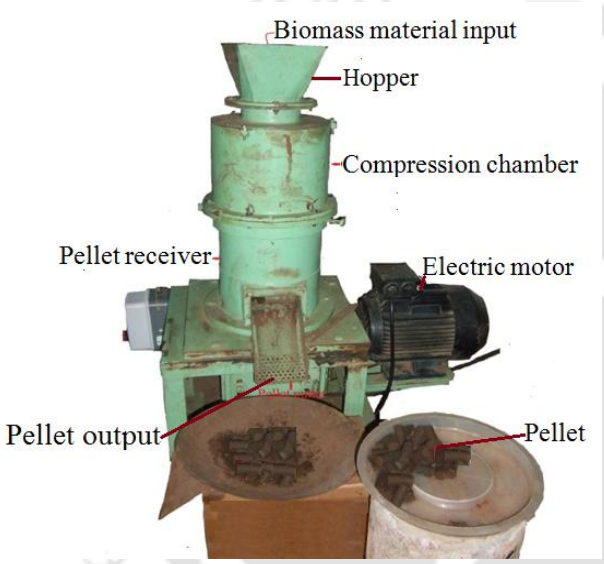

Fig 4.28 Pellet press

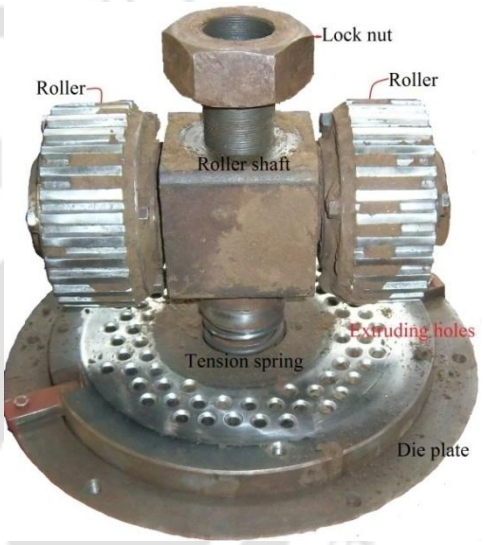

Fig. 4.29 Rotor block with die plate

Rotor block consists of two rollers as shown in Fig 4.30. The roller has slots on its peripheral surface. It has rotational as well as spinning motion.

Fig. 4.30 Rollers of the Pellet press.

Fig. 4.31 Die plate of the Pellet press

Roller rotates on the die plate. The die plate is as shown in Fig.4.31. It consists of a 45 number of holes. The diameter of each hole is 17mm.The pellets are prepared from the

mixture of biomass, dolomite and water (Fig. 4.32). The composition of the biomass and dolomite is selected from table 3.2. The dolomite powder is mixed with biomass powder thoroughly and then this mixture is mixed with water. The mixture (biomass + dolomite catalyst): water is prepared in proportion of 1:1.Afterword this mixture is feed through the hopper to the pellet press. The electric Motor is started, which rotates the rotor shaft. Rotor shaft rotates rotor block on the die plate. The rollers are rotating as well as spinning on the die plate. The material is pressed between the rollers and dies plate. There is a friction between the rollers, biomass material, casing of the compressing chamber and die plate. Due to friction heat is generated. This heat results in release of volatile matter from biomass which works as binding agent. The pellet material trapped between roller and dies plate squeezed through dies due to impact force of roller and extruded in the form of pellets through the dies plate. Five kinds of pellets for each biomass are manufactured with various compositions of biomass and dolomite with the pellet press. The time required for preparation of pellet with pure biomass is comparatively higher than the biomass-dolomite pellets. This implies that the dolomite works as catalyst as well as binding agent. The pellets are as shown in Fig. 4.33.

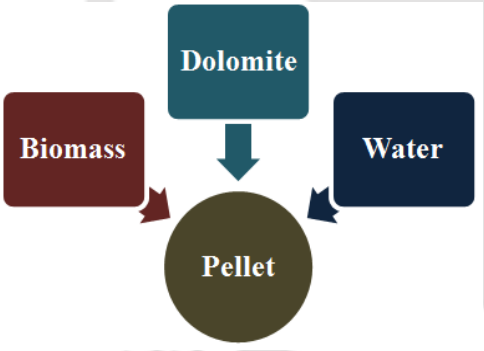

Fig. 4.32 Pellet constitution

Fig. 4.33 Biomass-dolomite pellets

4.6 SUMMARY

In this Chapter, Experimental set up and procedure for the downdraft gasification is studied. The downdraft gasifier is instrumented with K type and T type thermocouples, manometers, air flow meter, gas flow meter and producer gas sample collection mechanism for GC analysis. The experimental procedure is described in the subsections 4.3.1, 4.3.2 and 4.3.3. The material and methodology of the feedstock preparation is presented. Three types of feedstock are prepared in the required shape and size. These feedstock are wood chips, biomass briquettes and biomass- dolomite pellets. In Chapter 5

performance analysis of downdraft gasifier is studied with the various feedstock viz. wood chips, biomass briquettes, biomass pellets, and biomass-dolomite pellets. The experiments are carried out to check the feasibility of loose biomass in the downdraft gasifier in the form of briquette and pellet. The innovative attempts are made for the in-situ treatment of the tar using the biomass-dolomite pellet.

CHAPTER 5

RESULTS AND DISCUSSION ON FIXED BED GASIFICATION

5.1 INTRODUCTION

The experimental studies on biomass gasification are carried out in a 5kW$_e$ downdraft gasifier. Various types of the biomass feedstock, as described in the chapter 4, are used for the present experiments. A detail study is conducted to evaluate the thermal behaviour of the gasifier. Estimation of producer gas flow rate and composition with different feedstock are also presented in the subsequent sections. Estimation of tar produced during gasification is also presented in this Chapter.

5.2 ZONE WISE DESCRIPTION OF THE DOWNDRAFT GASIFIER

Based on the preliminary investigations the downdraft gasifier is divided into seven zones starting from the top as (a) drying zone, (b) pre-pyrolysis zone (c) pyrolysis zone, (d) pre-combustion zone, (e) combustion zone, (f) reduction zone and (g) ash chamber. When the biomass is feed into gasifier, it is not distributed uniformly inside the hopper at uppermost level. Thus 120 mm space from the top of the hopper is not considered in the present study. The remaining space is distributed in various zones as given in the Table-5.1.

Table 5.1 Hypothetical height (mm) of various zone from bottom of ash chamber

Zone	Height of thermocouple along the axis of gasifier	Range of zone	Thickness of zone
Drying	1390	1500-1270	230
Pre-pyrolysis	1160	1270-1040	230
Pyrolysis	930	1040-870	170
Pre-combustion	810	870-730	140
Combustion	680	730-610	120
Reduction	510	610-380	230
Ash chamber	300	380-Base level	380

The vertical section of the downdraft gasifier discussed in chapter 4 (section 4.2.2) is reproduced for clarity as shown in Fig.5.1. The figure represents the location of the thermocouples along with the zones mentioned in Table 5.1.

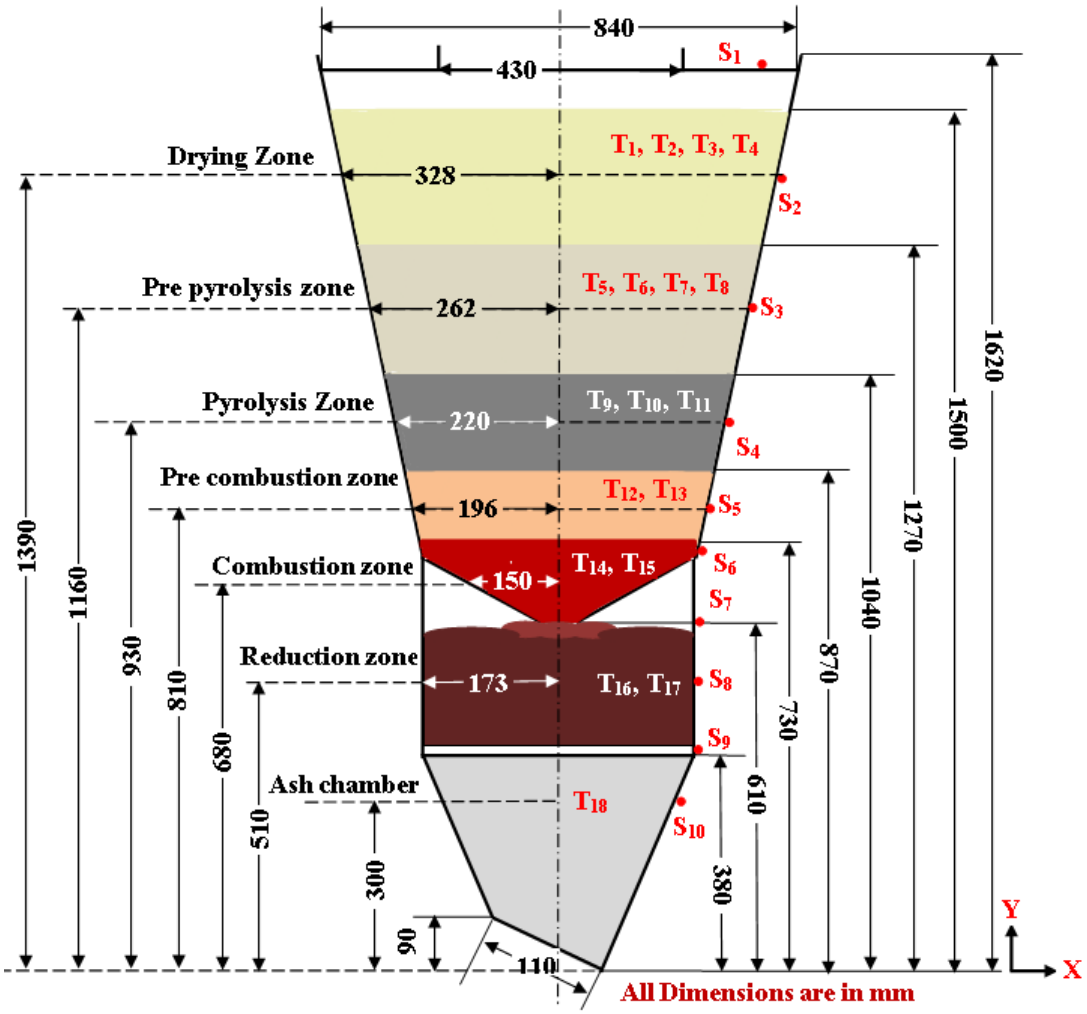

Fig.5.1 Location of various zones inside downdraft gasifier

5.3 GASIFICATION WITH WOOD CHIPS AS FEEDSTOCK

The experiments are performed with cylindrical wood chips of average size 25mm × 25 mm and equivalence ratios (ER) in the range of 0.19–0.43. The ERs are obtained by varying intake air flow rate. Moisture content of woodchip is controlled in the range of 12–15 %. Each set of experiment is carried out for duration of 8 hours with input feedstock of 85-90 kg. Experiments are repeated 3 to 4 times for reproducibility of results. Measured data are considered as an average of repeated experiments.

5.4 VARAIATION OF TEMPERATURE ALONG AXIAL DIRECTION

Figures 5.2 present the thermal behavior of the gasifier for wood chips. In these figures the variation of temperature with time for different zones at various equivalence ratio are presented (Fig.5.1). Long duration of temporal variation of temperature is observed with wood chips. It is observed that temperature in combustion zone, pre-combustion zone, pyrolysis zone and reduction zone are varies from 700 –1150 °C, 180 –320 °C, 60–150 °C and 300–480 °C respectively. Large fluctuations in temperature with wood chips are due to the erratic flow of woodchip from drying zone to combustion zone. Major problem being observed is due to the stickiness of wood chips with tar. Errors in all plots are well within $\pm 5-8$ % [Shelke and Mahanta 2014 a]. **Temperature (°C)**

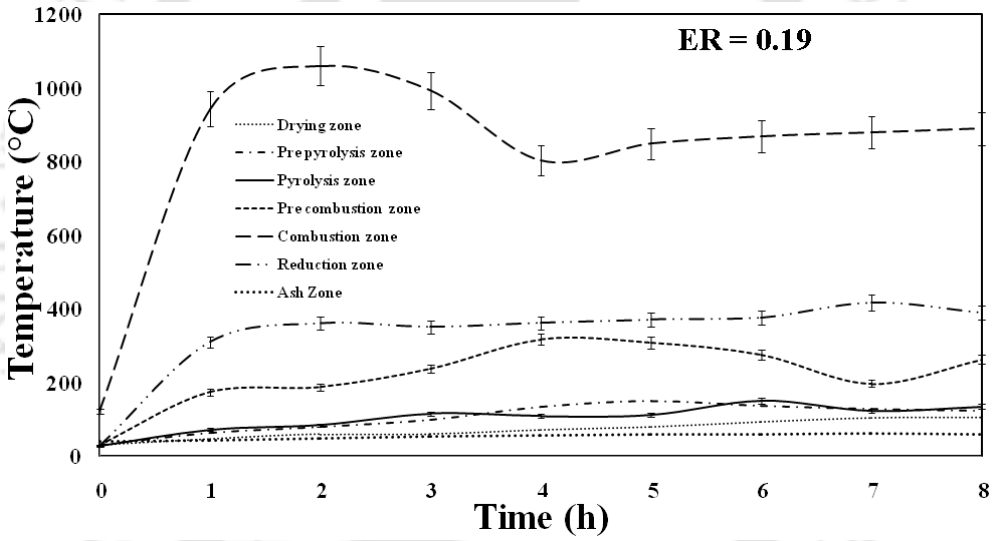

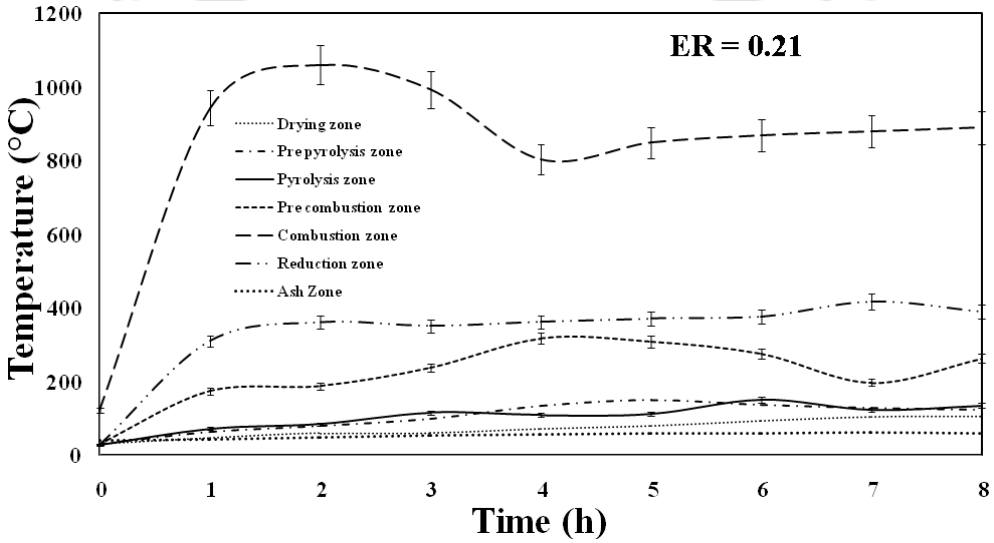

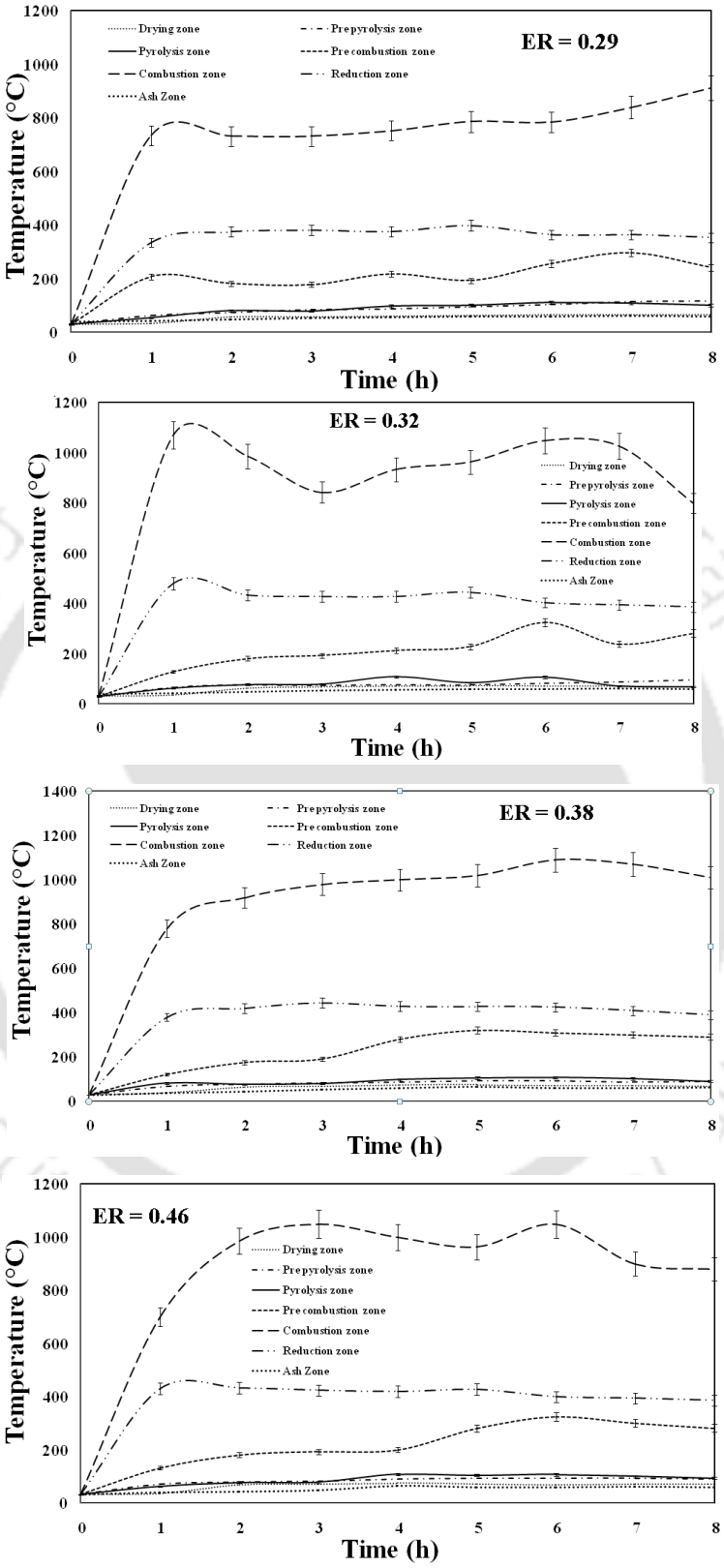

Fig.5.2. Thermal behavior of gasifier along axial direction for woodchip at various ER.

Figure 5.3 presents the behavior of the gasifier along the vertical axis after 4 h (τ =4 h) with different ER. It is observed that the temperature in the various zones will affect the gasification reaction. As the ER increases the temperature in the combustion zone increases. The temperature at ER 0.32, 0.38 and 0.43 is observed comparative higher. The increase in ER increases the temperature which results into the reduction in the tar.

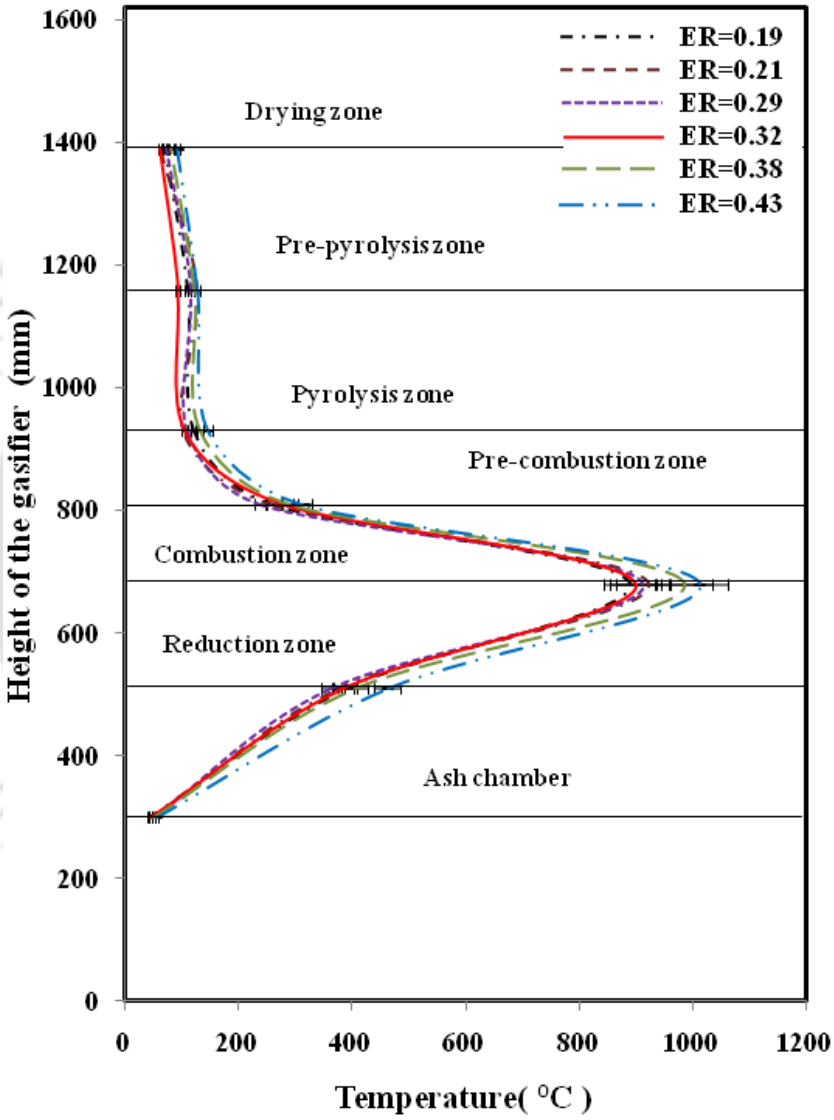

Fig.5.3 Thermal behavior of gasifier along vertical axis at various ER at τ =4 h

In all the cases temperature in combustion is observed higher and decreases along the upward as well as downward axial direction. The heat generated in combustion zone transmitted towards pyrolysis zone followed by drying zone and towards bottom side to reduction zone.

Meanwhile feedstock is moving continuously downward by gravitational force and light vibration caused by the vibrator. During this passage of time feedstock undergoes various conditions. This study reveals state of feedstock inside the gasifier.

5.5 VARIATION OF TEMPERATURE ALONG THE RADIAL DIRECTION

The variation of temperature along the radial direction obtained from thermocouples placed at various distance from the axis of the gasifier (Fig.5.1). The thermal behavior of gasifier is observed for the 8 h with respect to the distance from vertical axis and various ER.

5.5.1 THERMAL BEHAVIOUR OF GASIFIER IN DRYING ZONE

Figure 5.4 presents Variation of temperature with respect to time and ER in drying zone.

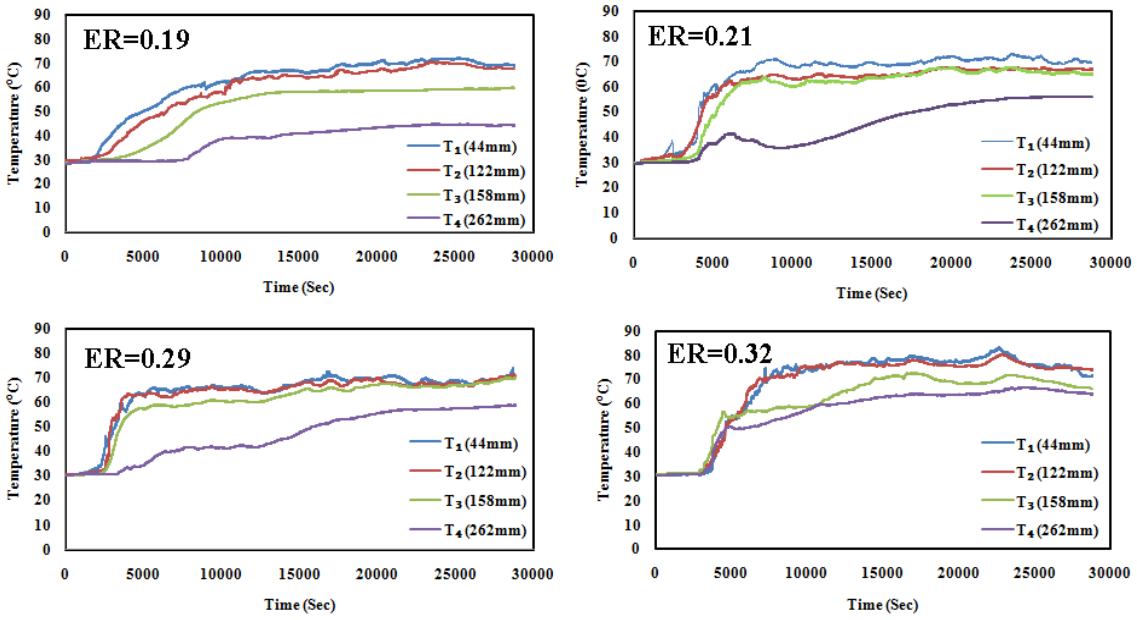

Fig. 5.4 Thermal behavior of gasifier in drying zone at various ER

It is observed that the temperature decreases with increase in radial direction and ER. The comparative analysis of data obtained for maximum temperature from the trend of temperature of feedstock versus time at various ER is given in Table-5.2. The maximum temperature in the drying zone is observed to be 83.18 °C for an ER of 0.32. The lowest temperature is observed at ER=0.19 and determined with the help of a thermocouple located at a distance of 262 mm from the central axis.

Table 5.2 Maximum temperature obtain in drying zone at various ER

Thermocouple	ER=0.19	ER=0.21	ER=0.29	ER=0.32
T_1 (44mm)	72.24	73.39	74.13	83.18
T_2 (122mm)	70.81	67.80	71.24	80.41
T_3 (158mm)	59.99	67.90	70.10	72.63
T_4 (262mm)	44.86	56.14	58.83	66.77

5.5.2 THERMAL BEHAVIOUR OF GASIFIER IN PRE-PYROLYSIS ZONE

Figure 5.5 presents the temperature in pre-pyrolysis zone with respect to the radial distance and ER from the axis of the gasifier.

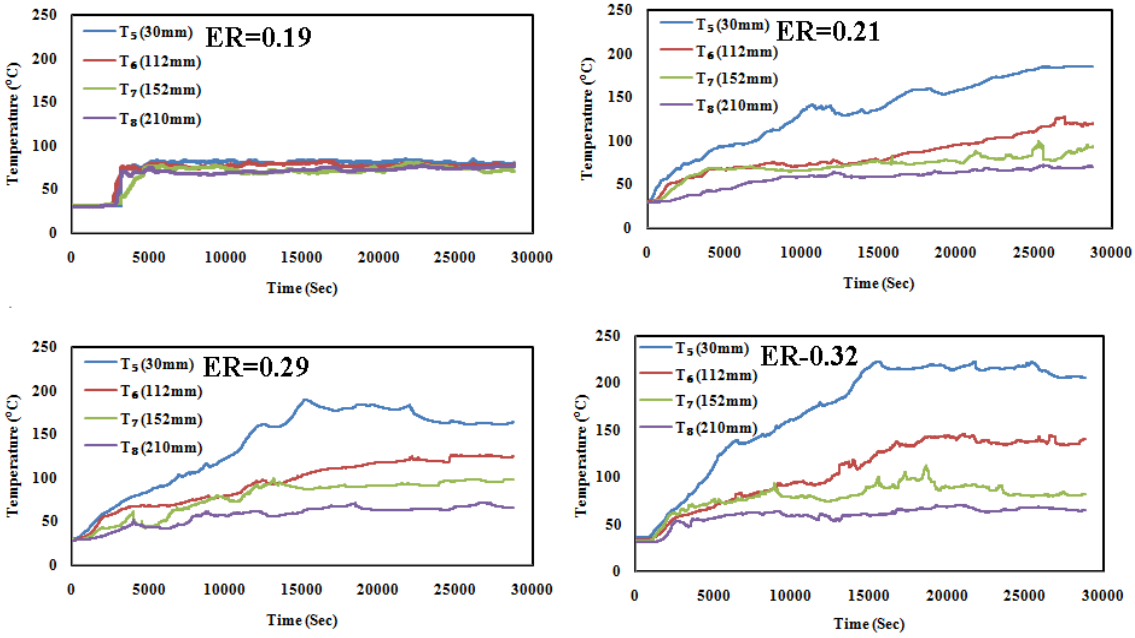

Fig. 5.5 Thermal behavior of gasifier in pre pyrolysis zone at various ER

It is observed that the temperature at ER= 0.19 is less up to 80^{o}C compared to other ER. The temperature in pre pyrolysis zone is increased with increase in ER. At the same time it is decreased with increase in radial distance of thermocouple from vertical axis. The maximum temperature noticed in the pre pyrolysis zone is 222.78^{o}C at ER= 0.32. Table-5.3 gives information about maximum temperature observed during the experimentation with various ER.

Table 5.3 Maximum temperature obtain pre pyrolysis zone at various ER

Thermocouple	ER=0.19	ER=0.21	ER=0.29	ER=0.32
T_5 (30mm)	84.599	186.508	190.1765	222.977
T_6 (112mm)	82.328	127.686	126.129	145.674
T_7 (152mm)	80.829	99.553	99.262	112.713
T_8 (210mm)	77.623	72.479	71.854	70.949

5.5.3 THERMAL BEHAVIOUR OF GASIFIER IN PYROLYSIS ZONE

Figure 5.6 presents the temperature measured by the thermocouple in the radial direction for various ER. In all cases temperature measured near the axis is higher and it is decreasing as the distance of thermocouple is increasing from axis towards the hopper.

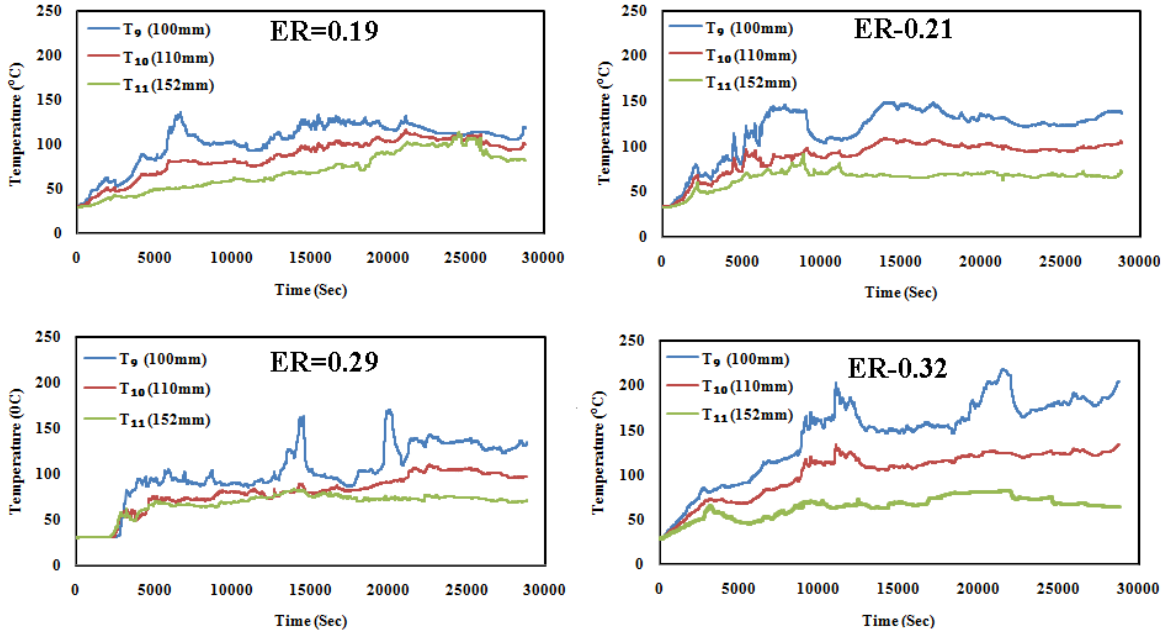

Fig. 5.6 Thermal behavior of gasifier in pyrolysis zone for wood chip at various ER

It is observed that temperature in pyrolysis zone increases with the increase in ER. However thermocouple at a radial distance 100 mm and 152 mm from the vertical axis shows the increasing value with increase in ER. But, thermocouple at a radial distance 110 mm showed the arbitrary values of temperature with increase in ER.This is may be caused due to retention of high as well as low temperature feedstock near that thermocouple for more time which results into the measurement of high and low temperature. The maximum temperature

measured by thermocouple in pyrolysis zone at various equivalence ratios is tabulated in Table-5.4.

Table 5.4 Maximum temperature obtain pyrolysis zone at various ER

Thermocouple	ER=0.19	ER=0.21	ER=0.29	ER=0.32
T_9 (100mm)	135.55	149.359	170.185	218.748
T_{10} (110mm)	116.75	109.02	110.311	134.489
T_{11} (152mm)	114.836	91.153	83.186	82.302

5.5.4 THERMAL BEHAVIOUR IN PRE-COMBUSTION ZONE

Figure 5.7 presents temperature measured in pre-combustion zone at various distance and ER.

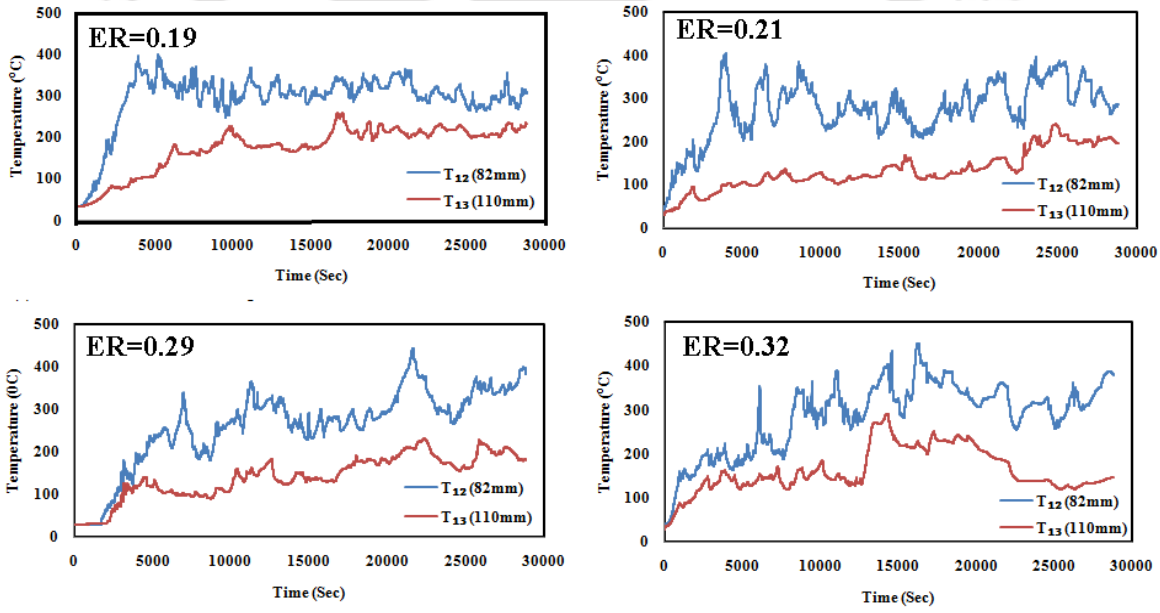

Fig.5.7 Thermal behavior of gasifier in pre combustion zone at various ER

Similar observation of increasing temperature with decrease in radial distance is observed. The temperature at thermocouple 82 mm away from vertical axis is increasing with increase in the ER. But for the thermocouple at 110 mm from the vertical axis shows the unsystematic values. This is may be due to continuous motion or stuck of the wood chips. The maximum temperatures obtain at various thermocouples and equivalence ratio is given in Table-5.5.

Table 5.5 Maximum temperatures obtain in pre-combustion zone at various ER

Thermocouple	ER=0.19	ER=0.21	ER=0.29	ER=0.32
T_{12} (82mm)	400.452	405.755	444.34	451.58
T_{13} (110mm)	260.063	240.316	230.71	290.65

5.5.5 THERMAL BEHAVIOUR IN COMBUSTION AND REDUCTION ZONE

Trend of temperature versus time for 8 hrs in combustion zone and reduction zone is shown in Fig 5.8.

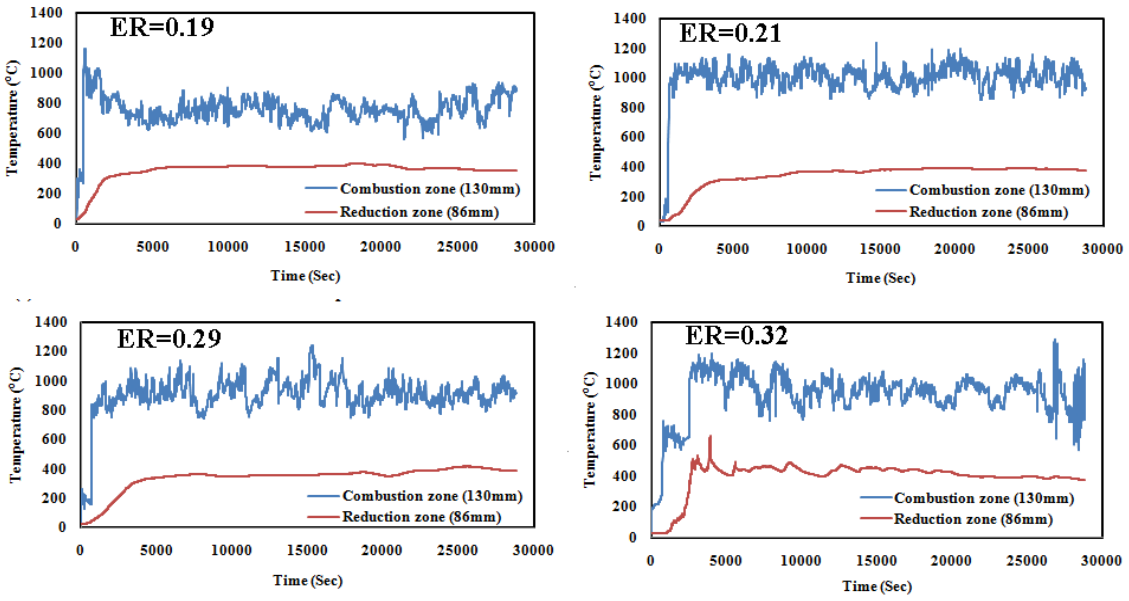

Fig. 5.8 Thermal behavior of gasifier in combustion and reduction zone at various ER

Table-5.6 gives the maximum temperature during the 8 hrs of operation. The temperature in combustion zone increased with increase in ER. The minimum temperature observed is 1161.75 ^{o}C for ER equal to 0.19 and maximum temperature 1201.01 ^{o}C is at ER equal to 0.32. The combustion is a unsteady process. So lots of fluctuations are observed in the combustion temperature. The maximum reduction zone temperature for ER equal to 0.19 is seen 403 ^{o}C and maximum temperature observed for ER equal to 0.32 is noticed 660 ^{o}C. It is seen that the reduction zone temperature also increases with increase in ER. This study reveals that heat produced in combustion zone propagates along central line and disbursed in surrounding mass.

Table 5.6 Maximum temperature obtain in combustion and reduction zone at various ER

Thermocouple	ER=0.19	ER=0.21	ER=0.29	ER=0.32
Combustion zone T_{14} and T_{25} (130 mm)	1161.75	1239.43	1240.80	1291.01
Reduction zone T_{16} and T_{17}(86 mm)	402.99	394.54	417.88	660.07

5.5.6 THERMAL PROFILE IN THE ASH CHAMBER

Figure 5.9 presents the temperature inside the ash chamber. It is observed that ash chamber temperature increases with increase in the ER. It reaches maximum up to 80 ^{o}C for ER 0.32.

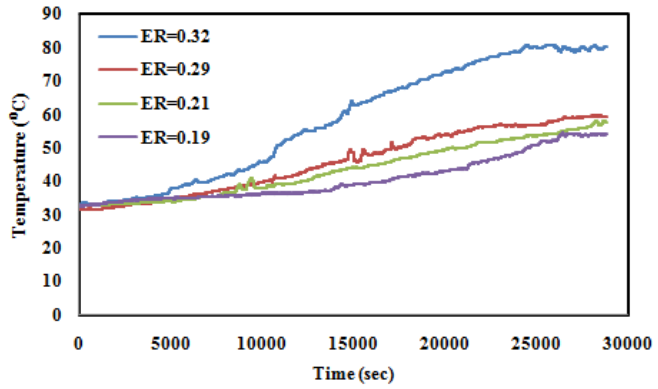

Fig 5.9 Temperature inside ash chamber (T_{18}) at various ER

5.5.7 TEMPERATURE PROFILE OF RAW PRODUCER GAS

Figure 5.10 shows temperature of raw producer gas at just exit of the reduction chamber. It is observed in range of 130–190 ^{o}C for the ER equal to 0.32.Temperature of gas increases with increase in the ER.

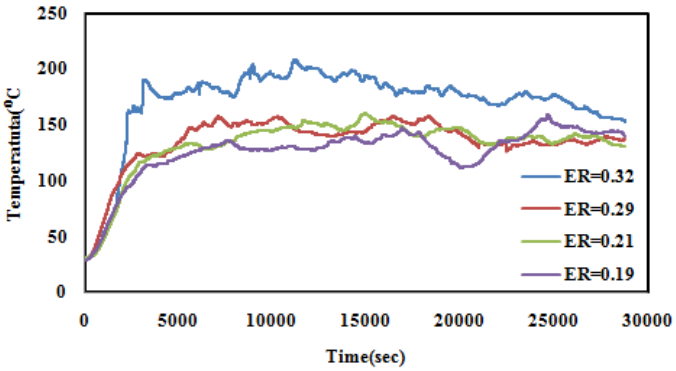

Fig. 5.10 Temperature of raw producer gas (T_{19}) at various ER

5.5.8 VARIATION OF TEMPERATURE ALONG OUTER SURFACE OF GASIFIER

The variation of temperature along surface of the gasifier is observed with the 10 number of thermocouples placed outside along the gasifier surface is shown in Fig.5.11.

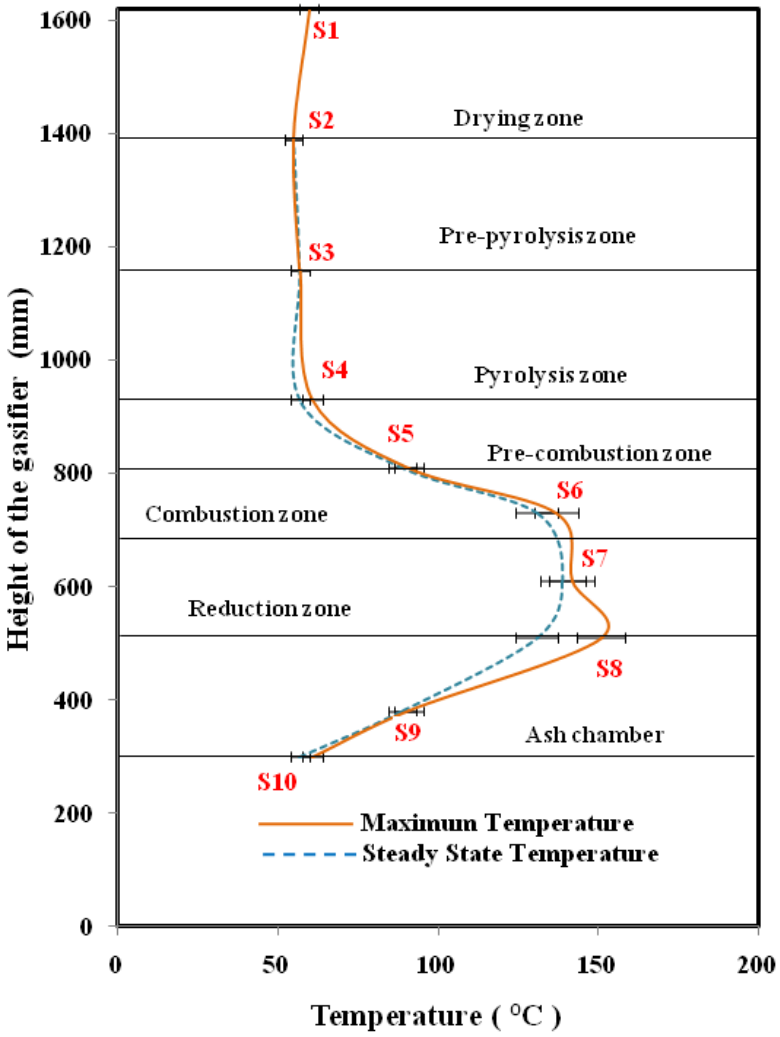

Fig. 5.11 Surface temperature of the gasifier

Less variation in surface temperature is observed up to 50–60^{o}C from top of gasifier to pyrolysis zone afterward there is increase in the surface temperature. Particularly temperature is higher near to the combustion and reduction zone up to 180^{o}C. Afterward temperature towards the surface of ash chamber is decreased and reaches to 57^{o}C. Thus there is a need of relatively more thickness of insulation on the outer surface of both the combustion and

reduction zones improving the performance of the gasifier. Thickness of insulation on the surface of other zones is less significant. Alternatively, there is a scope for recovery low quality waste heat from the outer surface of both the combustion and reduction zones.

5.6 VARIATION OF TEMPERATURE ALONG THE GAS LINE

The temperatures along the gas line at various places such as venturi scrubber, cyclone separator, before and after filter are measured. Along the scrubbing line the temperature of water inlet and outlet is observed up to 2–4^{o}C. This temperature difference is very small due the higher mass flow rate of water compare to the producer gas flow rate. Whereas variation in the temperature of producer gas before and after scrubbing is observed up to 130–150 ^{o}C. The temperature of the gas before and after filtration has also a very small difference of 2–3 ^{o}C because the gas is already cooled at atmospheric temperature in the scrubber by water. The 2–3 ^{o}C change in surrounding temperature is also noticed.

5.7 GASIFICATION OF BIOMASS BRIQUETTE

Experiments are performed with saw dust briquette with spherical shape of average diameter 25mm and ERs in range of 0.0.27– 0.46. The ERs are obtained by varying intake air flow rate. The saw dust briquettes (B_{15}) are prepared manually using 15% newspaper as binder. Moisture content of B_{15} is controlled in the range of 12–15 %. Each set of experiment is carried out for 8 hour duration with initial feedstock of 75–80 kg similar to the experiments carried out with wood chips. The variation of temperatures for saw dust briquette along the axial direction is shown in Fig. 5.12 for ER = 0.27, 0.32, 0.37, and 0.46, respectively. The graph represents temperature change in various zones with respect to time. The temperature is observed for duration of 8 hours and graph is plotted for time for every one hour duration. It is observed that the temperature in combustion zone is more than 800 ^{o}C in all the cases. Temperature in the reduction zone is observed in the range of 200 –500 ^{o}C. Temperature in the pre-combustion zone is also observed in the range of 200–400 ^{o}C. Moreover, temperature in each zone increases with increase in ER.

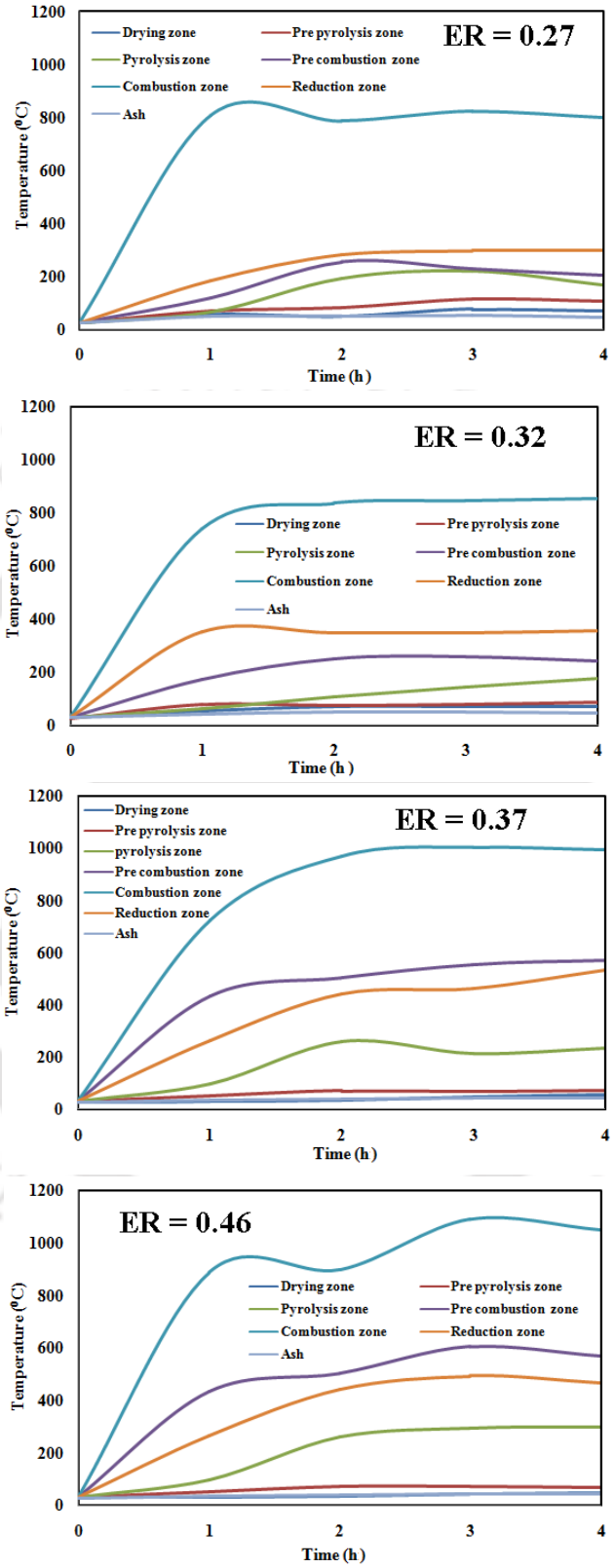

Fig. 5.12 Thermal behavior of downdraft gasifier for biomass briquette

Figure 5.13 presents variation of temperature along vertical axis of gasifier after 4 h (τ =4h) for various ERs.

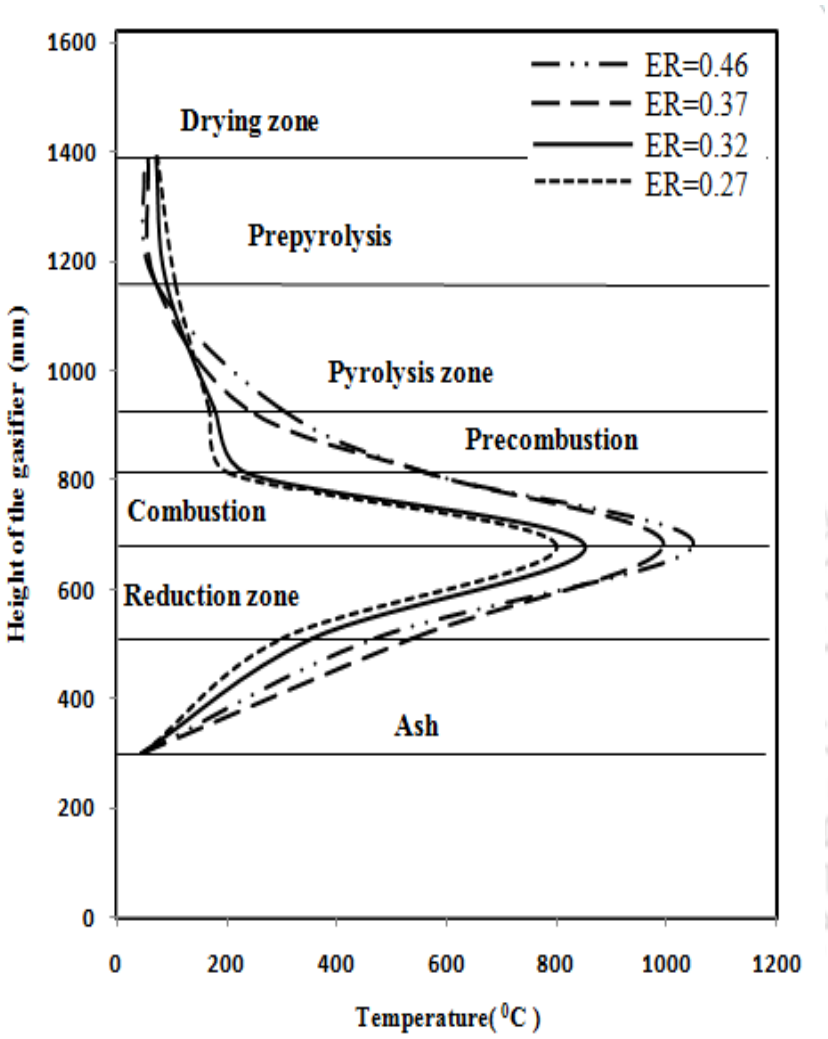

Fig.5.13 Thermal behavior of gasifier for saw dust briquette along the vertical axis for various ER at τ =4 h.

It is observed that the temperature in the various zones will affect the gasification reaction. As the ER increases the temperature in the combustion zone increases. Temperature in combustion zone and reduction zone at ER= 0.46 is higher than ER= 0.27, ER=0.32 and ER=0.37, respectively. However temperature in pre-combustion zone for ER = 0.46 and for ER= 0.37 is almost same. Similar observation is made for the temperature profile for ER = 0.32 and ER = 0.27.

5.8 GASIFICATION OF BIOMASS PELLETS

Experiments are performed with cylindrical shape saw dust and mustard husk powder pellets of average size 17 mm ×25 mm and ERs in range of 0.0.24–0.43. The pellets are manufactured using a pelletizer. Moisture content of P_{00} is controlled in the range of 12–15%. Similarly moisture content of other samples is also controlled in the same range. Each set of experiment is carried out for 8 hour duration with initial feedstock of 80-85 kg.

Figure 5.14 presents variation of temperature at different zones for gasification of biomass pellets. The variation is presented at the end of four hours of operation of the gasifier (τ = 4h). It is observed from the figure that temperature increases with the ER from 750–1100 ^{o}C in the combustion zone. However, variation of temperature is less pronounced in other zones for different ERs.

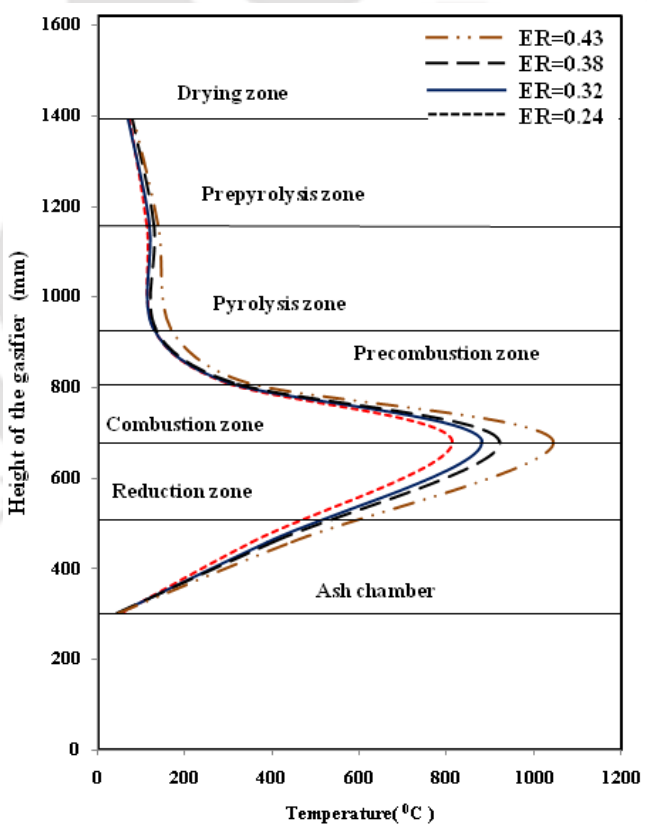

Fig.5.14 Thermal behavior of gasifier for saw dust pellet at various ER at τ =4 h.

It is observed from the figure that the temperature in the various zones increases with ERs. The measurable change in temperature is noticed in combustion zone. However, temperature in pre-combustion zone is nearly same for all cases. As the ER increases the temperature in the combustion zone increases significantly. The temperature in reduction zone also increases with increase in ER but the change in temperature is relatively lower than that of combustion zone.

5.9 COMPARISON OF GAS COMPOSITION FOR VARIOUS FEEDSTOCKS

Gas obtained from the gasification of woodchips (WC), sawdust briquettes (B_{15}) and saw dust pellets (P_{00}) for various ERs are analyzed and its constituents are presented in Table 5.7. Experiments are repeated 3 to 4 times for reproducibility of results. Measured data are considered as an average of repeated experiments. Errors are well within $\pm 2-3\ \%$.

It is observed from this table that quality of gas decreases with increase in ER. Compared to woodchips, B_{15} and P_{00} give relatively low amount of hydrogen and methane which indicates reduction in calorific value of the gas. Increase in percentage of hydrogen gas is observed for B_{15} for ER = 0.37. Overall it is observed from the table that relatively good quality gas is obtained from the feedstock under study for ER=0.32.

It is observed that H_2 obtained with gasification of briquettes B_{15} and sawdust pellets P_{00} compared to gasification of woodchips decrease by 25.25% and 56.29%, respectively for the ER in the operating range of 0.24–0.29. Similarly, Methane percentage also decreases with gasification of B_{15} and P_{00} by 17.89% and 34.40%, respectively. Decrease of CO for both the briquettes and pellets are also observed to be hardly 2.58 % and 1.64 %, respectively. Similarly, reduction in percentage of H_2, and CH_4 by 5.64% and 49.82%, respectively for briquette and 58.73% and 23.49%, respectively for pellets is observed. Whereas, percentage of CO increased by 11.4% and 34% for gasification in comparison to woodchips for ER =0.32. However, for ER range 0.37–0.38, percentage of H_2, CO and CH_4 is increased by 9.56%, 29.58% and 12.38%, respectively for briquette and in case of pellets H_2 is decreased by 62.74 % and CO and CH_4 increased by 26.19 % and 103.54 %, respectively compare to woodchips.

Table 5.7 Gas composition obtained from the gasification of various feedstock with different ER

Compositions	WC	B_{15}	P_{00}	WC	B_{15}	P_{00}	WC	B_{15}	P_{00}	WC	B_{15}	P_{00}
	Equivalence ratio (ER)											
	0.24-0.29			0.32			0.37-0.38			0.41-0.46		
	0.29	0.27	0.24				0.38	0.37	0.38	0.43	0.46	0.41
H_2	16.87	12.61	7.71	18.27	17.24	7.54	18.2	19.94	6.78	13.56	7.11	6.66
CO	17.04	16.6	16.76	15.26	17	20.45	14.2	18.4	17.92	13.78	16.8	18.41
CH_4	2.18	1.79	1.43	2.81	1.41	2.15	1.13	1.27	2.3	0.79	1.43	2.79
CO_2	14.12	18.78	15.36	14.42	12.46	11.01	16.23	11.17	14.12	17.94	17.36	12.69
N_2	49.35	50.13	57.92	49.17	51.39	57.98	50.02	48.36	58.79	51.76	53.96	58.37

5.10 QUALITATIVE TEST FOR PRODUCER GAS

The qualitative test for producer gas obtained from various feedstocks is conducted by flaring the gas produced at the gas outlet by using a kindler. The gas produced is noticed within 5-10 minutes from the start of gasification process. Blue flame is observed for woodchips and pellets. While yellowish flame is observed for briquettes. It may be due to the moisture content in the gas. The photographs of flame produced for various feedstocks are given in Fig. 5.15.

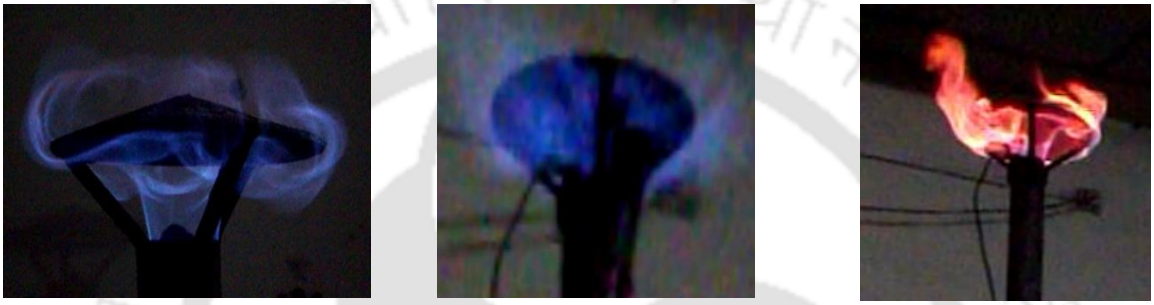

Woodchip **Sawdust pellet** **Saw dust briquette**

Fig.5.15 Flame for producer gas obtained from various feedstock

5.11 IN-SITU GASIFICATION OF BIOMASS-DOLOMITE PELLET

In gasification process the biomass is converted into producer gas along with the tar. Tar is a major hurdle in generation of power. As it is sticky in nature and create problem in movement of the piston in the cylinder of internal combustion engine. Here an attempt is made to reduce tar by using dolomite as a catalyst mixed with feed material. In-situ removal of the tar is reported by (Rapagna, et al. 2000; Sutton, et al. 2001) using fluidized bed gasifier. The inline tar treatment in downdraft gasifier is hardly observed. In the present work biomass-dolomite pellets are used for the gasification which cracks the tar inside the gasifier. Dolomite plays an important role in the tar cracking process as a catalyst (Dayton et al.,2002; Simell, et al., 1995). They reported that dolomite can assist in cracking of tar at temperature in the range of 700 $^{\circ}$C – 800 $^{\circ}$C. The biomass pellets are manufactured with the pelletizer from saw dust and mustard husk powder by mixing with various proportions of dolomite by weight.

As discussed in the subsection 5.9, gasification of sawdust-dolomite pellet is carried out with the ER = 0.32 as the same is favorable for better gas production. Figure 5.16 presents the thermal behavior of the downdraft gasifier along the vertical axis for the various compositions of saw dust-dolomite pellets. It is observed from this figure that combustion zone temperature is in the range of 850–900 ^{o}C indicating usability of dolomite as a catalyst. Temperature of the reduction zone and pre-combustion zone are observed to be in the range of 330–550 ^{o}C and 110–300 ^{o}C, respectively. Further, it is also observed that the temperature in combustion zone decreases with the increase in the weight percentage of dolomite.

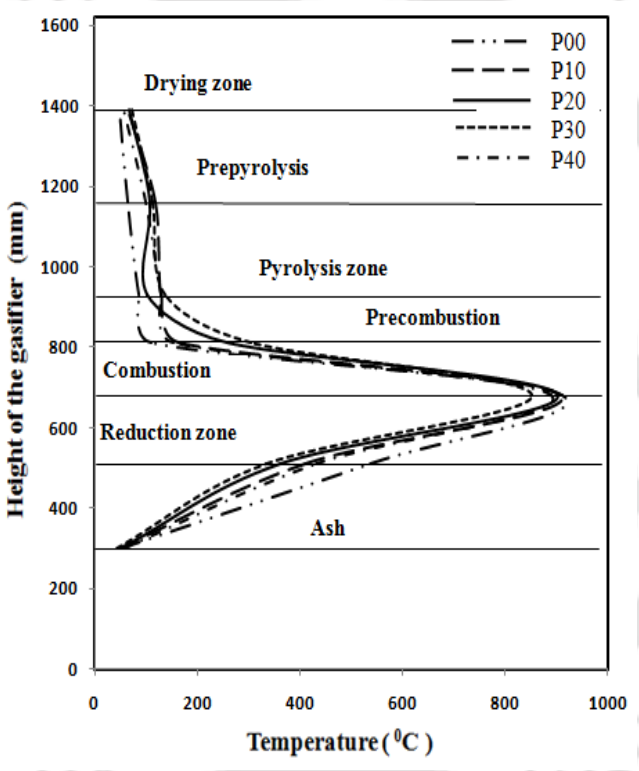

Fig.5.16 Zone-wise variation of temperature with sawdust-dolomite pallets for various ER

The comparative zone-wise variation of temperature for WC, B_{15}, P00 and P_{20} are presented in Fig. 5.17. It is observed that temperature resulted due to gasification is higher for the WC followed by P_{20}, B_{15} and P_{00}. Similar kind of profile is also observed in the reduction zone. However, temperatures for all the feedstock in pre-combustion zone are observed to be similar.

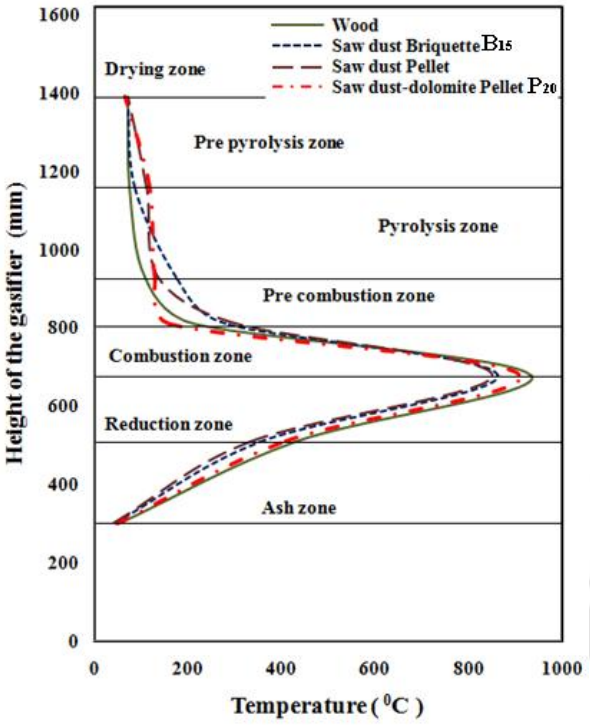

Fig 5.17 Thermal behavior of the gasifier for various feedstock at ER 0.32

Gas composition obtained from gasification of sawdust-dolomite pellets is presented in Table-5.8. It is observed from this table that the pellets without dolomite (P_{00}) yield low quality gas with low percentage of hydrogen. It is also observed that up to P_{20} the quality of the gas improves. However, with further increase of dolomite in pellets deteriorates the quality of the gas. Thus it is inferred from this Table that pellet with 20% dolomite by weight gives the best quality gas with an ER = 0.32.

Table-5.8 Gas composition obtained for gasification of saw dust-dolomite pellet

Saw dust Pellet Composition	H_2	CO	CH_4	CO_2	N_2	Gas flow rate (Nm^3/kg)
P_{00}	7.54	20.45	2.15	11.01	58.78	2.40
P_{10}	15.05	22.06	2.99	15.31	44.39	2.23
P_{20}	17.9	22.8	2.67	16.39	40.11	2.41
P_{30}	6.43	17.22	1.29	23.7	51.01	2.33
P_{40}	2.49	6.22	-----	24.97	66.11	2.34

Table-5.9 presents producer gas flow rate obtained for the sawdust-dolomite pellet at ER=0.32. Less variation in gas flow rate are observed. However, gas flow rate for P_{20} is slightly higher than the other four compositions.

Table 5.9 Gas flow rate (Nm^3/hr) in gasification of saw dust dolomite pellet

Pellet composition	P_{00}	P_{10}	P_{20}	P_{30}	P_{10}
Producer gas flow rate	2.40	2.41	2.43	2.42	2.41

Similar experiments are conducted with mustard husk and gas composition results are given in Table 5.10 with ER = 0.32. It is observed from the table that quality of gas yield is inferior in nature. This is may be due to the early pyrolysis of gas due to volatile oil content in mustard powder. Compositions of gas obtained from for $P_{20}$is superior to all other compositions of mustard husk pellets. Hence mustard husk pellets are not considered for further experimentation.

Table-5.10 Gas composition for mustard husk-dolomite pellet

Mustard husk powder Pellet Composition	H_2	CO	CH_4	CO_2	N_2
P_{00}	0.8	2.0	-----	10.5	86.7
P_{10}	1.3	2.5	-----	12.4	83.8
P_{20}	2.6	5.38	4.8	26.0	56.6
P_{30}	0.5	-----	-----	0.7	98.8
P_{40}	--	--	--	--	--

5.12 TAR COLLECTED IN GASIFICATION OF VARIOUS FEEDSTOCK

Table 5.11 presents the amount of tar collected in water tub, water tank, coarse filter and fine filter of the experimental setup. Tar obtained after gasification of woodchips (WC), biomass briquette (B_{15}) and pellets (P_{00}, P_{20}) with different ERs are presented in this table. The tar collected is considered as an average of repeated experiments. Errors are well within $\pm 5-7\ \%$. It is observed from this table that tar formation is lowest with P_{20}. This indicates cracking of tar inside the gasifier with 20% by weight of dolomite is higher compared to all.

Table-5.11 Tar collected in (gm/Nm^3) for gasification of various feedstock

Location of Tar	WC	B_{15}	P_{00}	WC	B_{15}	P_{00}	P_{20}	WC	B_{15}	P_{00}	WC	B_{15}	P_{00}
	Equivalence ratio (ER)												
	0.24-0.29			0.32				0.37-0.38			0.41-0.46		
	0.29	0.27	0.24					0.38	0.37	0.38	0.43	0.46	0.41
Water Tub	0.998	0.901	0.925	0.766	0.694	0.757	0.435	0.628	0.616	0.643	0.522	0.642	0.568
Water Tank	2.467	2.680	2.533	2.102	2.208	2.136	1.146	1.761	1.895	1.961	1.434	1.958	1.815
Coarse Filter	0.888	0.885	0.735	0.540	0.659	0.604	0.499	0.451	0.556	0.554	0.389	0.553	0.501
Fine Filter	0.001	0.001	0.001	0.001	0.001	0.001	0.001	0.001	0.001	0.001	0.001	0.001	0.001
Total	4.354	4.467	4.194	3.408	3.563	3.498	2.080	2.841	3.068	3.158	2.345	3.155	2.884

5.13 PERFORMANCE PARAMETERS FOR THE GASIFICATION OF VARIOUS FEEDSTOCKS AT VARIOUS ERs

The performance parameters of the producer gas obtained from the gasification experiment of woodchip (WC), sawdust briquette (B_{15}), saw dust pellet (P_{00}) with various ERs cracking are calculated and presented in the Table 5.12. The performance parameters presented are the producer gas flow rate, calorific value, gasifier conversion efficiency and carbon conversion efficiency of the feedstock.

The flow rate of the producer gas obtained from the WC, B_{15}, and P_{00} are in the range of 2.26–2.47 Nm^3/h, 2.20–2.54 Nm^3/h and 2.22–2.43 Nm^3/h, respectively. The saw dust briquette has the highest flow rate 2.54 Nm^3/h at ER = 0.37 and lowest gas flow rate of 2.20 Nm^3/hr at ER = 0.27 compared to others.

The calorific value of the producer gas obtained from the WC, B_{15}, and P_{00} are in the range 3.80–4.58 MJ/Nm^3, 3.61–5.39 MJ/Nm^3, and 3.680–4.42 MJ/Nm^3, respectively. The highest calorific value (5.39 MJ/Nm^3) is observed at ER = 0.32 and ER = 0.37 for woodchips and saw dust briquettes, respectively. Similar results are reported by Guangul et al.,(2014) and Patel et al. (2014). However, sawdust briquette has the lowest calorific value at ER=0.46.

The gas conversion efficiency is found to be in the range of 52–65%, 58–79% and 45–59% for WC, B_{15}, and P_{00}, respectively. The gas conversion efficiency is found to be maximum with 79% for saw dust briquettes and found to be minimum (45%) for saw dust pellet at ER= 0.24.

The carbon conversion efficiency is observed to be 90–97%, 90–98%, 90–99% for gasification of WC, B_{15}, and P_{00}, respectively. The highest carbon conversion efficiency of 99% is obtained for pellets at ER = 0.38 and ER = 0.41. Experimental uncertainties are given in Appendix- IX.

Table-5.12 Parameters of gasification for various feedstock

Parameter	WC	B_{15}	P_{00}	WC	B_{15}	P_{00}	WC	B_{15}	P_{00}	WC	B_{15}	P_{00}
	Equivalence ratio (ER)											
	0.24-0.29			0.32			0.37-0.38			0.41-0.46		
	0.29	0.27	0.24				0.38	0.37	0.38	0.43	0.46	0.41
Producer gas flow rate (Nm^3/kg)	2.26	2.20	2.22	2.33	2.41	2.40	2.39	2.54	2.40	2.47	2.30	2.43
Calorific value of the producer gas (MJ/Nm^3)	5.19	4.43	3.68	5.39	4.92	4.42	4.58	5.39	4.06	3.80	3.61	4.30
Gas conversion efficiency (%)	65	57	45	69	69	59	61	79	54	52	48	58
Carbon conversion efficiency (%)	90	98	90	91	90	97	91	94	99	97	98	99

5.14 SUMMARY

A detailed experimental investigation was conducted in an existing biomass downdraft gasifier unit with woodchips as feed material. Thermal behavior of the gasifier, yield and composition of the gas and quantity of tar obtained for various ERs is presented and discussed. Feasibility study of using different biomass briquettes and pellets for gasification in the same gasifier was conducted. Thermal behavior, gas yield and composition with all the stated feed materials are compared. In-situ gasification with biomass-dolomite mixture was also conducted and optimum proportion of dolomite for in-situ tar cracking was established. A novel tar cracking set up developed for post gasification process is presented in the next Chapter along with results and discussion.

CHAPTER 6

THERMAL CRACKING OF TAR

6.1 INTRODUCTION

One of the major disadvantages of gasification is the formation of tar along with the producer gas. Tar condenses at low temperature blocking and fouling the process equipment such as engines and turbines. In-situ tar cracking has been reported for the fluidized bed gasification whereas majority of the researchers have indicated post treatment of tar for fixed bed gasifier. Thermo-chemical cracking of tar is reported by Devi et al. (2003). Both the in-situ as well as thermal cracking of tar is attempted in the present investigation. A liquid-gas bubbling fluidized bed is developed in the present work to crack tar with dolomite as catalyst. Parametric studies are conducted to evaluate the performance of the equipment developed.

6.2 CHARACTERIZATION OF TAR

Various properties of the tar such as density, specific gravity and viscosity are calculated as given below:

DENSITY

The density of the tar is calculated by using the Eq. 6.1.

$$\text{Density} = \frac{(m_1 - m_2)}{V} \tag{6.1}$$

Where, m_1 = Weight of flask filled with tar, in kg

m_2 = Weight of empty flask, in kg

V = Volume of the tar in flask

SPECIFIC GRAVITY

The specific gravity of tar is calculated by using the Eq.6.2. It is defined as the ratio of density of substance to the density of the reference substance (water).

$$\text{Specific Gravity} = \frac{\text{Density of tar}}{\text{Density of water}} \tag{6.2}$$

VISCOSITY

Viscosity of tar is calculated with a Rheometer (Make: Anton Paar, Model-Phsica MCR101). The flow Curve (shear stress v/s shear rate) is plotted as shown in Fig. 6.1. It is observed that the shear stress is not varying linearly with the shear rate. So biomass tar can be treated as a Non-Newtonian fluid. The viscosity curve (velocity v/s shear rate) is plotted and shown in Fig. 6.2. It is seen that there is a rapid decrease in viscosity with increase in shear rate. This behavior is similar to the behavior of pseudo plastic material. Viscosity of the tar at 27^{o}C and shear rate 1 per sec is found to be 10.4 Pa-s.

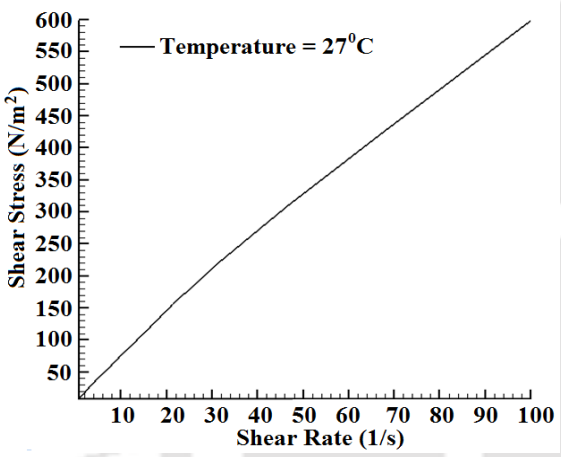

Fig.6.1 Flow curve

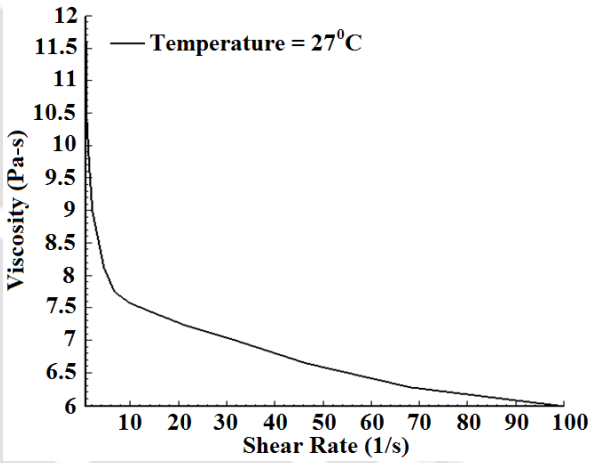

Fig.6.2 Viscosity curve

Properties of tar obtained after biomass gasification are given in Table 6.1.

Table-6.1 Various properties of the biomass tar

Density(Kg/m^3)	Specific Gravity	Viscosity (Pa-s)
1057	1.057	10.4

6.3 EXPERIMENTAL SETUP FOR TAR CRACKING

A bubbling gas-liquid fluidized bed setup is developed to investigate tar cracking as shown in Fig. 6.3. The thermal cracking unit consists of a tar cracking chamber (TCC) made of GI pipe of length 900mm and inner diameter 101.4 mm. The TCC is assembled with an electric heater and an aeration pipe at the bottom. The set-up is developed based on the properties of tar and principle of gas-liquid fluidization. Specification of tar cracking unit is given in Appendix-X

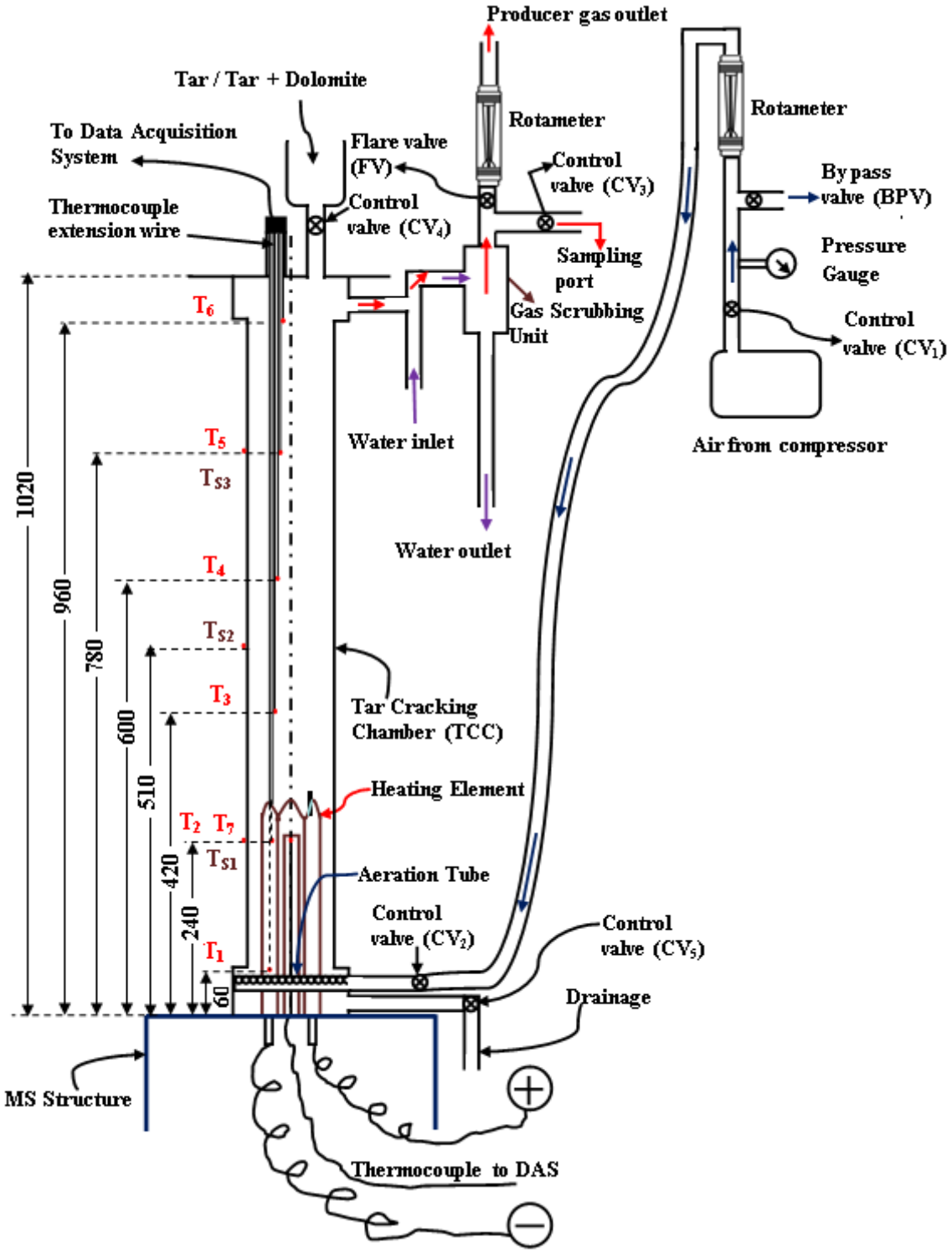

Fig. 6.3. Schematic diagram of experimental setup.

Various components of the experimental set up are (1) Air inlet manifold, (2) Aeration pipe, (3) Electric heater, (4) Tar cracking chamber, (5) Tar inlet,(6) Gas outlet, and (7) Gas scrubbing system.

6.3.1 AIR INLET MANIFOLD

Air inlet manifold is used to provide the air to the aeration pipe for fluidization. It is located at the bottom of TCC. A 5 kW_e reciprocating compressor is connected to the air inlet manifold. A control valve (CV_1) followed by a rotameter is installed in the outlet of compressor to vary and measure the air flow rate. Precaution is taken to maintain sufficient pressure head of the inlet air for facilitating fluidization and to prevent the back flow of tar. Thus air manifold is attached at a higher location compared to the TCC as shown in Fig. 6.3. A by-pass valve (BPV) is installed along the air flow line ahead of the rotameter to avoid excess air control. Another control valve (CV_2) is installed at the air inlet manifold before entry of air to the aeration pipe. This valve is used to prevent the backflow of liquid tar mixture from TCC to the air inlet manifold. A pictorial view of the air before entering to the aeration pipe is shown in Fig. 6.4. The drainage port as shown in the figure is used to drain out the tar residues after each set of experiment through the valve CV_5.

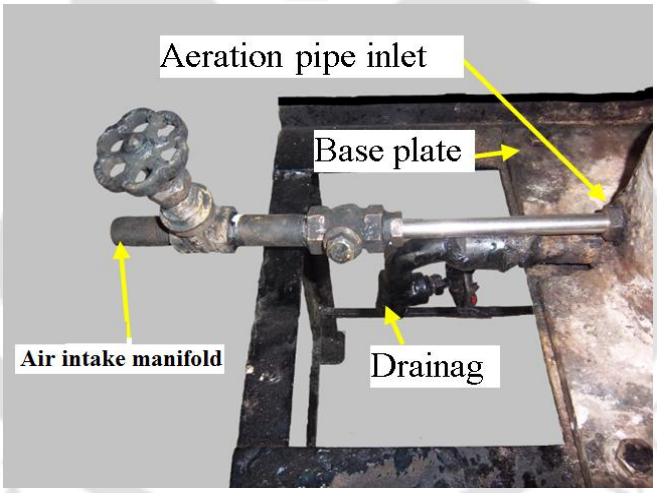

Fig.6.4. Air inlet.

6.3.2 AERATION PIPE

The aeration pipe is used to fluidize the liquid tar in the TCC. This pipe is specially made with stainless steel 304 (SS 304) with 210 number of holes on upper side of its surface. The aeration pipe of internal diameter 12.7 mm is made in the shape of English letter “C” closed at both ends (Fig. 6.5). The air inlet manifold is connected to the aeration pipe at the bottom of TCC. Both the diameter and pitch of the holes are maintained with dimension of 2 mm, respectively.

Fig.6.5. Aeration pipe.

6.3.3 ELECTRIC HEATER

The electric heater is used to supply heat to tar inside TCC. Elemental heater of 4 kWe is used to generate heat inside present setup. It is tightened with base plate of TCC coupling as shown in Fig.6.6. The elemental heater is mounted in such a way that it is passed through C shape aeration pipe as is shown in Fig.6.7. The single phase 230VAC power is supplied to elemental heater through a variac which in turn is connected with an ammeter and voltmeter. The required amount of power is supplied by varying the variac to generate the desired amount of heat inside the TCC.

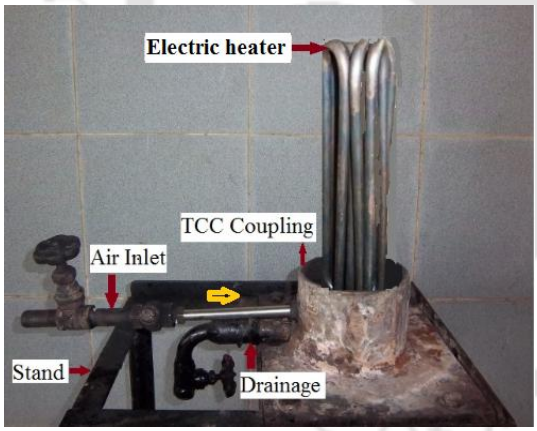

Fig 6.6 Electric heater.

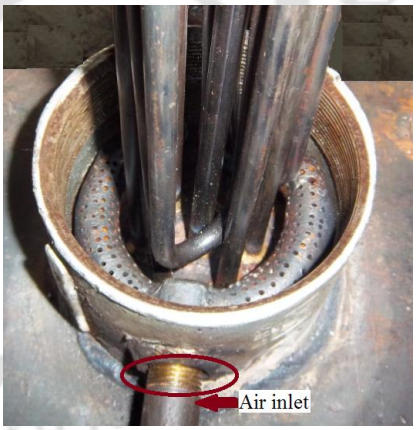

Fig. 6.7 Aeration pipe with electric heater

6.3.4 TAR CRACKING CHAMBER (TCC)

The heart of the unit is tar cracking chamber (TCC) in which air and liquid tar undergoes bubbling fluidization at high temperature resulting in cracking of tar. This unit is made of GI pipe of 3 mm thickness having inner diameter of 101.6 mm and height of 900 mm. The bottom of the TCC is closed by welding with a SS plate of 5 mm thickness. Precaution is taken to make the entire TCC leak proof. The unit is mounted on a frame

made of mild steel. The outer surface of TCC is insulated with glass wool to prevent the heat loss.

6.3.5 TAR INLET

Tar inlet is used to provide tar into TCC. It is a cylindrical shaped small hopper. A control valve is placed between TCC and tar inlet hopper. Inlet is situated at the top of the TCC as shown in Fig. 6.8.

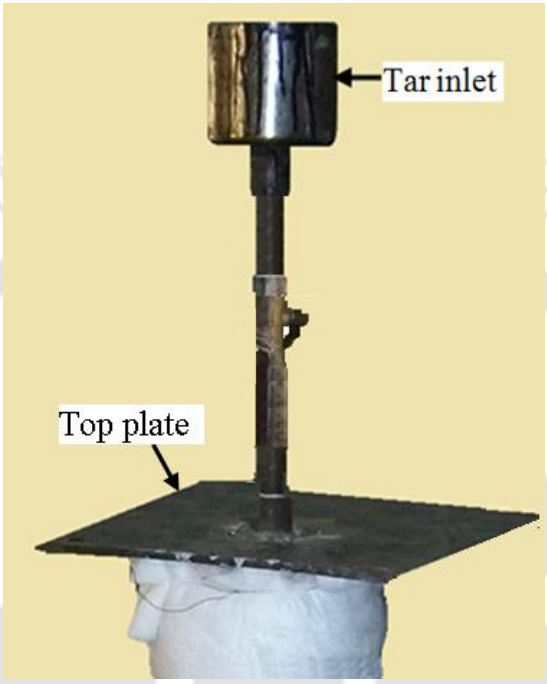

Fig. 6.8 Tar inlet

6.3.6 CRACKED GAS OUTLET

The cracked tar gas is coming out through the exit of the TCC at the upper side of the TCC and subsequently enters into the scrubbing unit. Afterward it passes through a rotameter and then to the outside atmosphere as shown in Fig. 6.3.

6.3.7 CRACKED GAS SCRUBBING UNIT

Figure 6.9 presents the components of the scrubbing unit and assembly in the workshop. It is a direct contact type heat exchanger which scrubs and cools cracked-gas. Scrubbing unit has a gas inlet and water inlet aligned with each other. Cracked-gas is mixed with water and condenses the un-cracked tar. Cracked-gas is separated in cyclone separator. It came out from top exit of the separator and can be used as a fuel for running the utilities. Condensed un-cracked tar residue comes out from the downward exit along with water. The gas scrubbing unit is attached with pressure gauge and rotameter as shown in Fig.6.10. Gas sample is collected through the sampling port for testing its constituents.

Tedlar bag is used to collect the gas from the sampling port for analysis in gas chromotograph (Make: Chemito, model: CERES-800 plus).

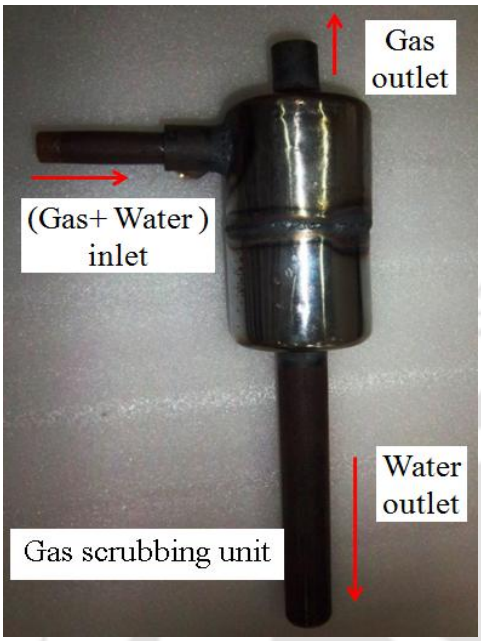

Fig. 6.9 Assembled gas scrubbing unit

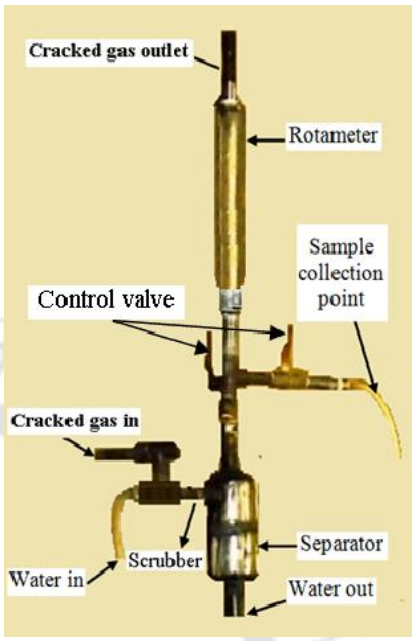

Fig. 6.10 Gas scrubbing unit with instrumentation

6.4 SENSORS AND INSTRUMENTATION

The experimental setup for tar cracking is instrumented with various sensors and instruments. Details are given as follows:

6.4.1 DETAILS OF THERMOCOUPLES USED

Thermal behavior of bubbling fluidized bed tar cracking unit is analyzed by using 10 number of K type thermocouples [Chromel (90% Nickel and 10% Chromium) and alumel (95% Nickel, 2% Manganese, 2% Aluminum and 1% Silicon)] as shown in Fig. 6.3. Thermocouples are placed at various positions along the height of the TCC with respect to the base plate. These are located inside and along the outer surface of TCC. Six numbers of thermocouples are placed inside TCC for measuring temperature of tar. Three thermocouples are placed along the outer surface of the TCC. One thermocouple is inserted in the middle of the hollow tube embedded inside the electric heater to measure the temperature generated due to heating (Fig. 6.11). Extension wires of all the thermocouples are passed through a mild steel tube placed eccentric to the tar inlet which in turn, is connected to a data acquisition system through a multiplexer. Signal from the data acquisition system are registered in a laptop (Fig. 6.12).

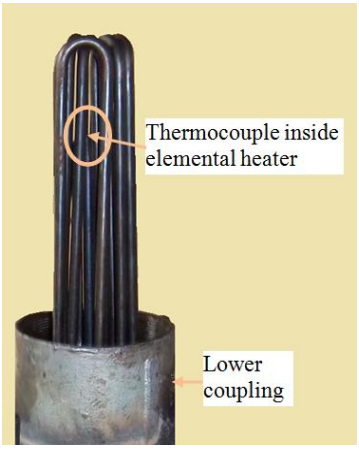

Fig. 6.11 Thermocouple inside heater

Fig. 6.12 Data acquisition system (DAS)

Table-6.2 shows location and number of thermocouples used in the experimental set up.

Table-6.2 Thermocouples at various locations of TCC

Location	Distance from base plate of TCC (mm)	No. of
Inside TCC	60	1
	240	1
	420	1
	600	1
	780	1
	960	1
Inside Electric Heater	240	1
Along the outer surface of TCC	240	1
	510	1
	780	1

6.4.2 INSTALLATION OF PRESSURE GAUGE

The pressure of the supplied air is measured with the help of a Bourdon type pressure gauge. The air pressure gauge is mounted on the air inlet manifold after delivery from the compressor. Variation of bed pressure is conducted along the surface of the TCC by installing 5 (Five) Bourdon tube pressure gauges P_1, P_2, P_3, P_4 and P_5 as shown in Fig. 6.13.

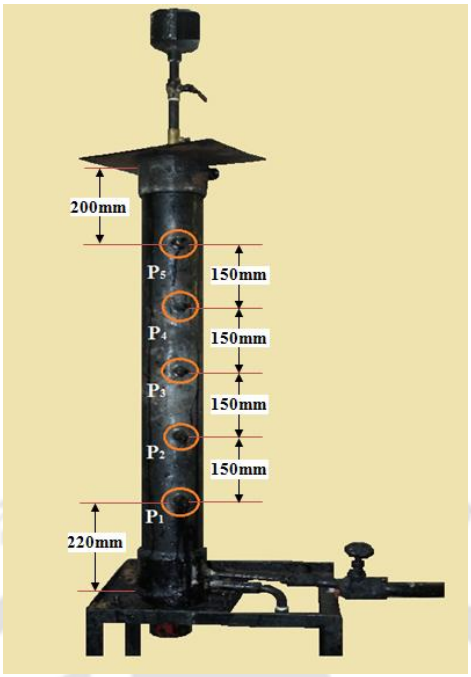

Fig. 6.13 Pressure gauge locations on TCC

6.4.3 INSTALLATION OF ROTAMETER

Rotameters are used to measure the flow rate of air as well as cracked-gas as shown in Fig. 6.3. One rotameter is placed between compressor and TCC entrance. Another is mounted at exit of TCC after separator which measures the flow rate of cracked-gas going out from scrubbing unit.

6.4.4 POWER INPUT

The electric heater inside the TCC is energized with 230 V, single phase electric supply line. The input is controlled using a variac and input power is measured using a voltmeter and an ammeter. The power supply to the experimental set up is shown in Fig. 6.14.

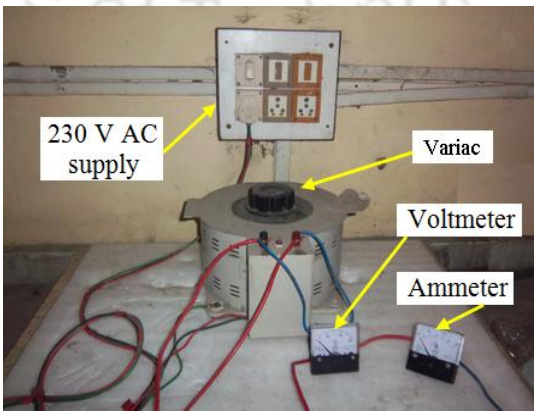

Fig. 6.14 Variac with ammeter and voltmeter

6.5 EXPERIMENTAL PROCEDURE

The tar is fed through the tar inlet located at the top of the TCC through the control valve (CV_4). Measured amount of air is supplied from the compressor to the aeration pipe through the air inlet manifold. The velocity of the air entering to the TCC is maintained slightly above the minimum fluidization velocity to facilitate bubbling fluidization. The air above the minimum fluidization velocity is blown through the holes in the aeration pipe directed towards the upward side inside the TCC in the form of bubbles. Bubbles starts rising, increasing its size and coalesces. Heat generated in the electric heater propagates along the riser (TCC) with the gas-liquid phases. Series of experiments are conducted with air and tar followed by tar and dolomite mixtures in presence of air as fluidizing medium. Temperature achieved in this process is in the range of 198- 837^0 C. The raw cracked-gas comes out through the tar outlet located at the upper side of the TCC as shown in the schematic diagram (Fig.6.3). Raw cracked gas is then passed through the cyclone separator in which cold water is injected resulting in condensation of un-cracked tar particles which is drained out with water.

At the beginning the TCC is filled with 6 kg of liquid tar fed through the tar inlet. Meanwhile water is started to circulate inside the scrubber. The flare valve is opened. The air is supplied with volumetric air flow rate in the range of 0.0005-0.0015m^3/sec to TCC through aeration system. Electrical supply is given to the elemental heater through the variac. The Gas production is detected at the flare by burning the same with a kindler. The unused or left over tar is then drained out through the drain valve connected at the bottom of TCC unit.

Manometer and airflow readings are taken by manual measurements while temperature reading from the thermocouples are collected through a data acquisition system (Make: Agilent) connected to a laptop. The experiment is carried out for various volumetric air flow rate, weight of the sample and heat inputs. Investigation is carried out for the various percentage of dolomite in the tar. The care is taken to close the tar inlet valve completely once 6 kg of liquid tar is fed to TCC. Care is taken for proper electrical connections so as to avoid short-circuiting of the heating element and TCC unit. The TCC unit is properly sealed so as to avoid leakage of gas from unit.

After completion of each set of experiment the electric heater is switched off, followed by closure of the air valve (CV_2) and full opening of the flare valve (FV). Then scrubber tab is switched off after 5-10 minutes.

Experiments are conducted in batches. First set of experiments are conducted with liquid tar. Similar experiments are conducted later on with tar and dolomite blends. For performance study of the unit, heat input, air flow rate and percentage of dolomite are varied for each set of experiments.

6.6 PREPARATION OF FEEDSTOCK

The present experiments are carried out with the tar produced during biomass gasification process. Various proportions of dolomite mixed with tar are shown in Table 6.3. Tar-dolomite (TD) in table stands for tar-dolomite mixture and subscript indicates percentage of dolomite by weight in the mixture.

Table-6.3 Tar-dolomite mixture used for the experiments

Sample Name	TD_{00}	TD_{05}	TD_{10}	TD_{15}	TD_{20}
Dolomite (weight %)	00	05	10	15	20
Tar weight percentage	100	95	90	85	80

6.7 RESULTS AND DISCUSSION

Variation of bed height due to fluidization with amount of tar for different flow rate of air is presented in Fig. 6.15.

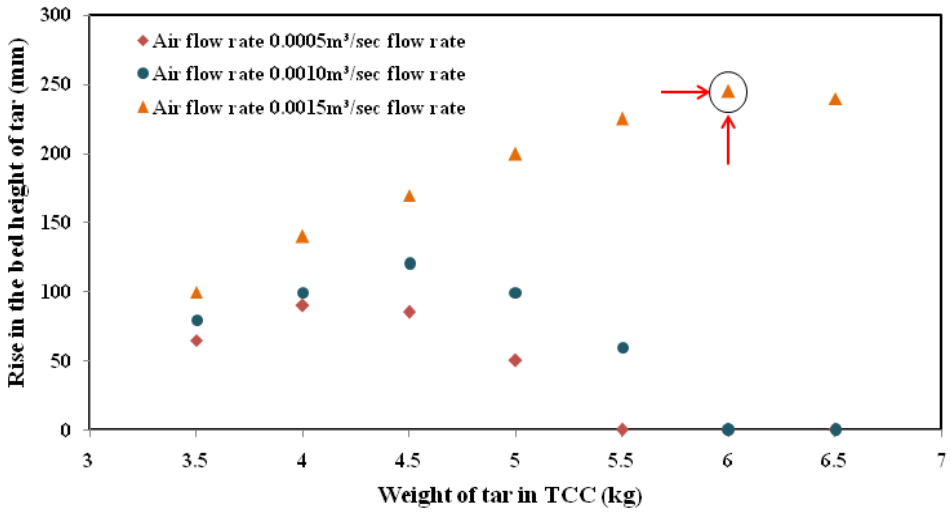

Fig.6.15 Rise in the bed height of the tar for various air flow rate

Air flow rate in the range of 0.005-0015 m^3/sec is considered for the study. Liquid tar weighing 3.5 kg to 7 kg in a step of 0.5 kg was considered for each flow rate of air. The expansion of bed for each air flow rate is plotted and compared to the other flow rates. It is observed that the rise in the bed for the air flow rate 0.0015m^3/sec to be highest for the 6 kg of tar which is most favorable for carrying out the tar-cracking inside the TCC. Based on the behavior of bed expansion as indicated in Fig. 6.15, series of experiments are conducted with air flow rate of 0.0015m^3/sec and 6 kg of tar/tar and dolomite as inventory for cracking. Figure 6.16 presents the variation of pressure along the height of the TCC. It is observed from the figure that pressure decreases with increase in height of TCC. This figure shows a smooth variation of pressure due to the fluidization of gas and liquid.

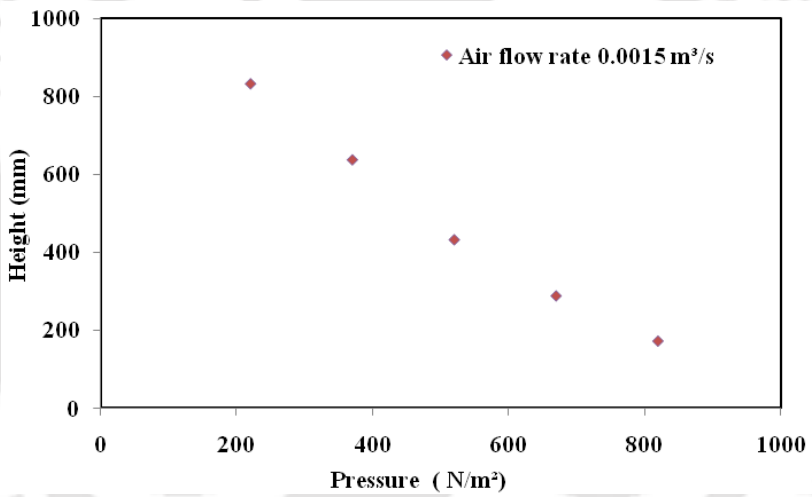

Fig. 6.16 Pressure inside TCC at various pressure points

Operating matrix for experiment for thermal cracking of tar is given in Table-6.4.

Table-6.4 Operating matrix for experimentation

Name	Heat input (kWe)	Air flow rate (m^3)	Quantity of tar (kg)
TD_{00} (Pure Tar)	3.5	0.0015	6
	3.0		
	2.5		
TD_{05} (Dolomite 5 %)	3.5	0.0015	6
TD_{10} (Dolomite 10)	3.5	0.0015	6
TD_{15} (dolomite 15)	3.5	0.0015	6
TD_{20} (dolomite 20)	3.5	0.0015	6

6.7.1 PERFORMANCE EVALUATION OF TCC WITH LIQUID TAR

Variation temperature along the centre line of TCC is presented in Fig. 6.17. Experiments are conducted with 6 kg of liquid tar with 0.0015 m^3/secair flow rate. Comparison of temperature is shown with three different heat inputs, namely, 2.5 kW_e, 3.0 $kW_e$and 3.5 kW_e, respectively. It is observed from this figure that temperature shows an initial increase up to thermocouple T_2 and afterward decrease along the height of the bed. The temperature variation is highest for the heat input of 3.5 kW_e along the TCC. The higher temperature is recorded with thermocouple T_2 in lower part of TCC for all the three cases. It is observed to be 837°C, 589°C and 525°C for the heat input 3.5, 3.0 and 2.5 kW_e, respectively. However, variation of temperature for the heat input of 3.0 kW_e and 2.5 kW_e are marginal. The minimum temperature is measured with thermocouple T_6 located at a distance 960 mm from the base. Temperature at this location is 201, 201 and 258°C for the heat input 2.5, 3.0 and 3.5 kW_e, respectively.

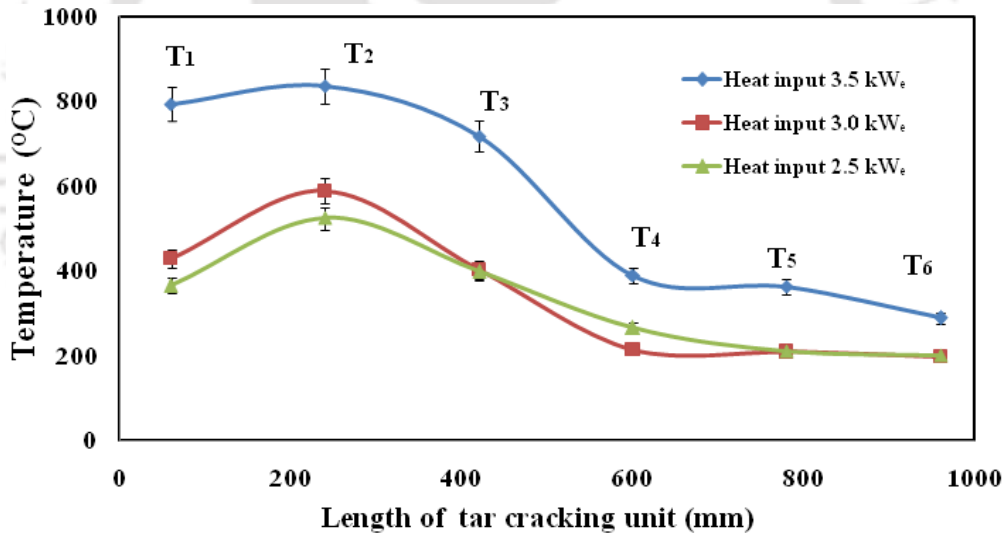

Fig.6.17 Axial thermal behavior of TCC

Figure 6.18 shows thermal behavior of TCC for heat input 3 kW_e and 2.5 kW_e with respect to time. These plots are presented for all the seven thermocouples placed along the centre of the TCC. Figure 6.19 presents similar results for heat input of 3.5 kW_e. It is noticed that temperature in TCC is decreased with decrease in heat input. Further time taken to achieve the highest temperature (location T_2) is minimum (1270 s) for the heat input of 3.5 kWe.

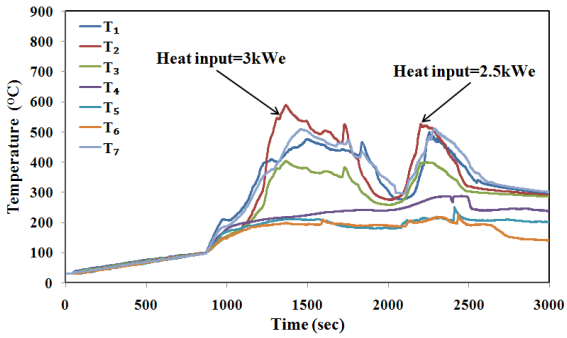

Fig.6.18 Thermal behavior of TCC at 2.5 and 3.0 kW_e

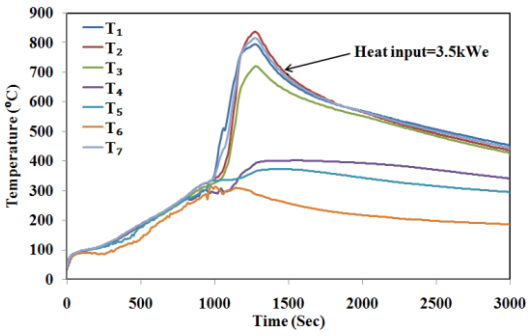

Fig.6.19 Thermal behavior of TCC at 3.5 kW_e

6.7.2 QUALITATIVE TEST OF CRACKED GAS

Qualitative test is conducted by flaring the gas produced at the gas outlet by using a kindler. Initially white smoke releases for first 10 minutes followed by progressive combustion till 45 minutes which gives an evidence of formation of medium to high quality cracked gas. The photographs of progressive flame of cracked-gas obtained from tar cracking with heat input of 3.5 kW_e are given in the Fig.6.20.

Fig 6.20 Progressive flame of the gas obtained from the tar

6.7.3 GAS COMPOSITION OF CRACKED-GAS

Gas obtained by cracking of liquid tar (TD_{00}) with heat input of 2.5-3.5 kWe is collected at the sampling port with tedlar bags and tested in gas chromotograph. Table-6.5 presents the composition of gas tested in gas chromatograph. It is observed from the table that the cracked-gas composition for heat input 3.5 kW_e is better than other two heat inputs. It is noticed that the volume percentage of H_2 for the heat input of 3.5 kW_e is 15.66 % and 23.07% higher than the 3.0 kWe and 2.5 kW_e, respectively.

Table-6.5 Composition of cracked-gas obtained from liquid tar with various heat input

Heat input (kW_e)	Volumetric air flow rate (m^3/sec)	Gas Composition				
		H_2	CO	CO_2	N_2	CH_4
2.5	0.0015	7.8	13.3	39.2	36.3	3.4
3.0		8.3	13.9	39.7	34.5	3.6
3.5		9.6	18.6	22.6	46.7	2.5

Similarly, the volume percentage of CO for 3.5 kW_e heat input is 33.81 % and 39.84 % higher than the 3.0 kWe and 2.5 kW_e heat input, respectively. However, the volume percentage of CH_4 is 30.55 % and 26.47 % less than heat input of 3.0 kW_e and 2.5 kW_e, respectively. Reduction in CH_4 is due to the accelerated cracking of tar into H_2 and CO.

6.7.4 VOLUMETRIC CRACKED-GAS FLOW RATE AND TAR RESIDUE

Table-6.6 presents the volumetric flow rate of the cracked gas and residue of tar for the heat inputs in the range of 2.5-3.5 kWe. It is observed from this table that the volumetric flow rate of cracked-gas increases with heat input. However, residue collected decreases with heat input. It is clear from this table that cracking of liquid tar is enhanced with increase in heat input to the heater.

Table-6.6 Volumetric cracked-gas flow rate residue for various heat input

Heat input (kW_e)	Volumetric air flow rate (m^3/sec)	Volumetric cracked-gas flow rate (m^3/sec)	Weight of tar (kg)	Weight of residual (kg)
2.5	0.0015	0.0022	6.0	0.682
3.0		0.0028		0.612
3.5		0.0034		0.528

6.7.5 PERFORMANCE EVALUATION OF TCC WITH TAR-DOLOMITE MIXTURE

Based on the experiments conducted with liquid tar cracking, series of similar experiments are conducted for various mixtures of tar and dolomite. Experiments are conducted with 5-20% dolomite by weight in each set of experiments with heat input of 3.5 kWe. Total mixture is maintained at 6 kg. Air flow rate is controlled at 0.0015 m^3/sec. Subsequent experiments are carried out on tar cracking for the selection of tar-dolomite blend.

6.7.6 THERMAL BEHAVIOR WITH TAR-DOLOMITE MIXTURES

Figure 6.12 presents the comparison of temperature profile along the height of the TCC for liquid tar (TD_{00}) and tar-dolomite mixtures (TD_{05}, TD_{10}, TD_{15} and TD_{20}).Variation of temperature along the centre line of TCC is presented in Fig. 6.21.

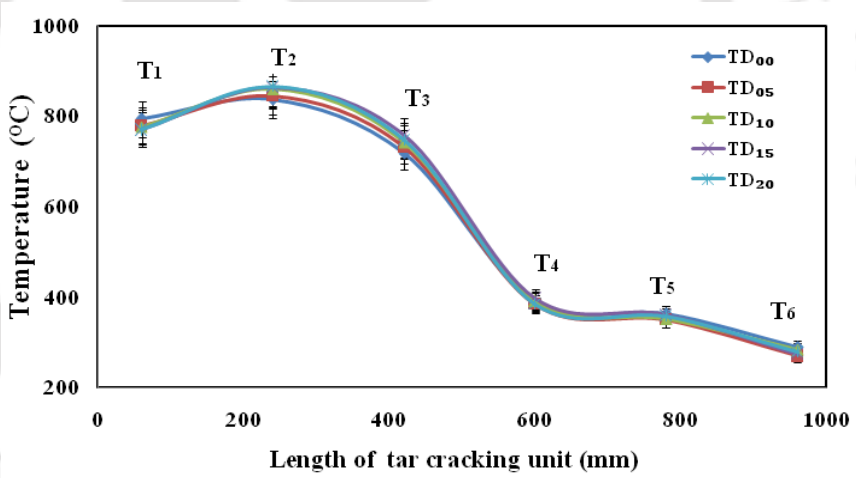

Fig. 6.21 Thermal profile of the TCC for the various TD blends

Experiments are conducted with 6 kg of inventory with air flow rate of 0.0015 m^3/s and heat input 3.5 kW_e. Comparison of temperature is shown with five various inventory of liquid tar-dolomite mixtures. It is observed from this figure that temperature shows an initial increase up to thermocouple T_2 and afterward decreasing trend along the height of the bed. The temperature variation is small for all five liquid-tar dolomite mixture along the TCC. The higher temperature is recorded with thermocouple T_2 in lower part of TCC for all the three cases. It is observed to be 866°C, for the TD_{20}. Though there is small change in the temperature but it is increasing with respect to the increase in the quantity of the tar. However, variations of temperature for other thermocouples are marginal. The

minimum temperature of 268°C is measured with thermocouple T_6 located at a distance 960 mm from the base.

6.7.7 GAS COMPOSITION OF CRACKED-GAS

Gas obtained by cracking of liquid tar (TD_{00}) and liquid tar-dolomite mixtures are collected at the sampling port with tedlar bags and tested in gas chromotograph. Table-6.7 presents the composition of gas tested in gas chromatograph. It is observed that the percentage of H_2 is increasing with increase in dolomite percentage up to 15% afterward it decreases. The percentage of CO is increased with the increase in dolomite percentage up to 10% then it decreases with increase in the percentage of dolomite.

Table-6.7 Gas Chromatography of cracked-gas for various tar-dolomite mixture

Tar-dolomite blend	Heat input (kWe)	Volumetric air flow rate (m^3/sec)	Gas Composition				
			H_2	CO_2	N_2	CH_4	CO
TD_{00}	3.5kWe	0.0015	9.6	22.6	46.7	2.5	18.6
TD_{05}			13.7	38.8	15.8	4.4	27.4
TD_{10}			13.7	16.0	28.9	1.4	40.0
TD_{15}			16.0	17.0	28.5	1.2	37.3
TD_{20}			10.3	24.67	49.32	0.72	13.7

The percentage of H_2 in cracked-gas is higher for TD_{05}, TD_{10}, TD_{15} and TD_{20} than TD_{00} (liquid tar) by 42.7%, 42.7%, 66.7% and 7.3%, respectively. The percentage of CO in cracked-gas is higher for TD_{05}, TD_{10}, and TD_{15} than TD_{00} by 47.3%, 115.1% and 100.5%, respectively. However, CO percentage is less for TD_{20} by 73.9% with respect to TD_{00}.The percentage of CH_4 in cracked-gas is higher for TD_{05} than TD_{00} (tar) by 76%, and lower for TD_{10}, TD_{15} and TD_{20} by 56%, 48% and 28.8%, respectively.

6.7.8 VOLUMETRIC CRACKED-GAS FLOW RATE AND WEIGHT RESIDUE

Table 6.8 presents the volumetric flow rate of the cracked gas and residue of liquid tar (TD_{00}) and tar-dolomite mixtures (TD_{05}, TD_{10}, TD_{15} and TD_{20}). It is observed from this table that the volumetric flow rate of cracked-gas increases with increase in percentage of dolomite. The tar-dolomite mixture TD_{05}, TD_{10}, TD_{15}, and TD_{20} has higher cracked-gas flow rate than TD_{00} by 5%, 9.1%, 10.3% and 10.9%, respectively. However, residue

collected decreases with percentage of dolomite. It is clear from this table that cracking of liquid tar is enhanced with increase in dolomite percentage. The weight of total residue increases with increase in the weight of the dolomite. This is happened due to the presence of extra weight of dolomite which is not taking part in thermal cracking.

Table-6.8 Cracked-gas flow rate and weight of total and actual tar residual for various TD blend

Tar-dolomite blend	Vol. air flow rate (m^3/sec)	Vol. cracked-gas flow rate (m^3/sec)	Wt. of TD blend (kg)	Wt. of Total residual (kg)	Wt. of actual residual
TD_{00}	0.0015	0.00340	6.0	0.528	0.528
TD_{05}		0.00353		0.722	0.422
TD_{10}		0.00371		0.938	0.338
TD_{15}		0.00375		1.135	0.235
TD_{20}		0.00377		1.314	0.114

6.8 SAMPLE ANALYSIS FOR PRE AND POST TAR CRACKING

The gas composition of cracked-gas obtained from the liquid tar-dolomite mixture with 10% and 15% dolomite (TD_{10}, TD_{15}) are superior to the other three mixtures. As TD_{10} shows better performance in terms of gas yield, further investigation for pre and post cracking is carried out with TD_{10} samples. The various measuring instrument is given in Appendix-XI.

6.8.1 C-H-N-S ANALYSIS OF PRE AND POST TD_{10} SAMPLE

The CHNS analysis of pre and post TD_{10} sample is carried out using EuroEA Elemental Analyzer. Ultimate analysis gives the information about the percentage of C, H, N, and S present in sample. Table-6.9 gives comparative data of CHNS analysis of pre and post tar.

Table-6.9 Ultimate analysis of pre and post TD_{10} sample (Wt. %)

TD_{10} sample	C%	H%	N %	S%
Pre (before thermal cracking)	77.582	6.079	1.665	1.967
Post (after thermal cracking)	78.919	1.928	1.329	-----

It is observed that percentage of carbon is less in case of pre TD_{10} by 1.017% than post TD_{10}. The percentage of hydrogen is 31.715% higher in case of pre TD_{10}. The percentage of nitrogen is 20.18% higher in case of pre TD_{10}. No sulfur was detected in post TD_{10} sample.

6.8.2 THERMOGRAVIMETRIC ANALYSIS OF PRE AND POST TD_{10} SAMPLE

Figure 6.22 presents TGA for pre and post TD_{10} sample. The weight loss of 80% and 23.60% is observed for pre and post cracking TD_{10} sample, respectively. The maximum amount of pre tar is cracked and converted into the cracked-gas and very less amount of heavy hydrocarbon remained un-cracked.

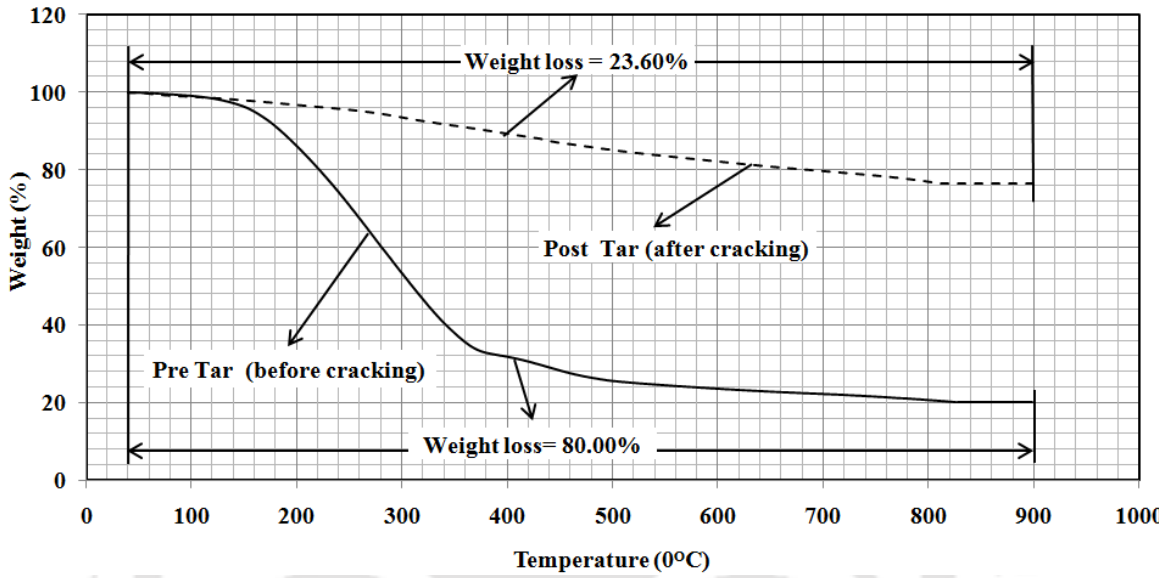

Fig.6.22 Comparative TGA analysis of Pre Tar and Post

6.8.3 COMPOSITION ANALYSIS OF PRE AND POST TD_{10} SAMPLE USING FESEM AND EDS

Chemical composition analysis of pre and post TD_{10} sample is carried out using Field Emission Scanning Electron Microscope (make-Zeiss and model- Sigma) and Energy Dispersive Spectroscopy (EDS). The morphology of pre TD_{10} is given in Table-6.10. It gives concentration of Carbon, and minor amounts of Oxygen and Sulfur.

Table-6.10 EDS of various spots on the surface of Pre TD_{10} sample

Element	Spectrum 1	Spectrum 2	Spectrum 3	Spectrum 4
C	60.1	61.1	62.4	63.7
N	28.8	25.71	24.8	23.8
O	12.5	12.7	12.2	11.8
S	0.5	0.5	0.6	0.7

Figure 6.23 shows the FESEM of pre TD_{10} test material (before thermal cracking) and its EDS for spectrum 1, spectrum 2, Spectrum 3 and spectrum 4 corresponds to various spots is shown Fig. 6.24 (a–d).

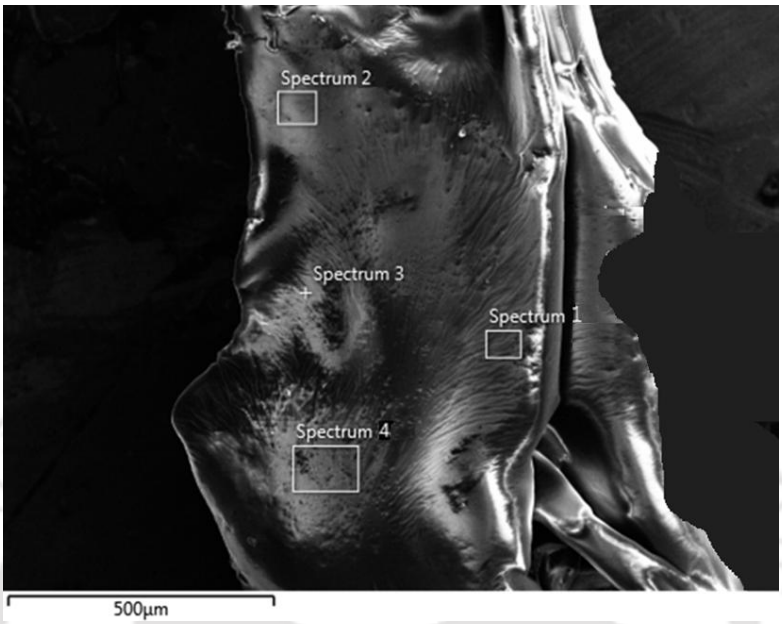

Fig. 6.23. FESEM of Pre TD10

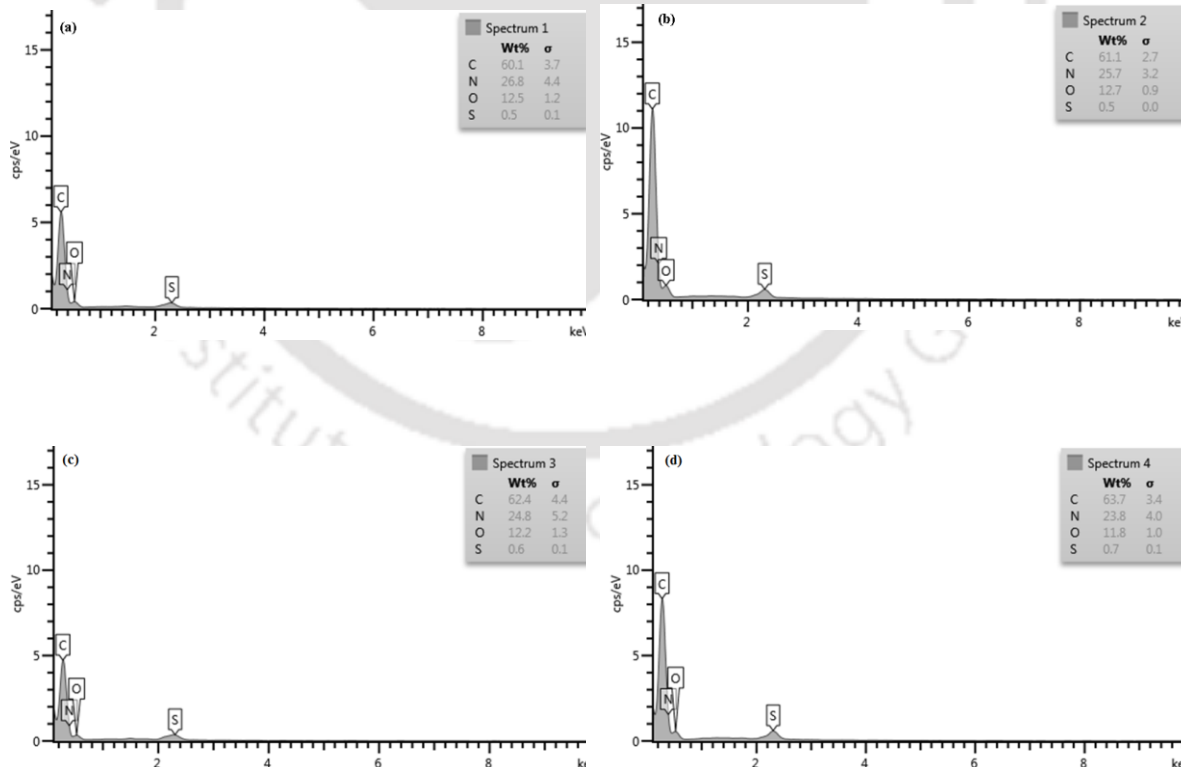

Fig. 6.24a EDS of spectrum 1: Pre TD_{10}, Fig. 6.24b EDS of spectrum 2: Pre TD_{10}, Fig. 6.24c EDS of spectrum3: Pre TD_{10}, Fig. 6.24d EDS of spectrum 4:Pre TD_{10}

Figure 6.25 presents FESEM of post TD_{10} sample. The spectrum 1, spectrum 2, spectrum 3 and spectrum 4 correspondto various spots on the surface of TD_{10} are as shown in Fig.6.26 (a-d).

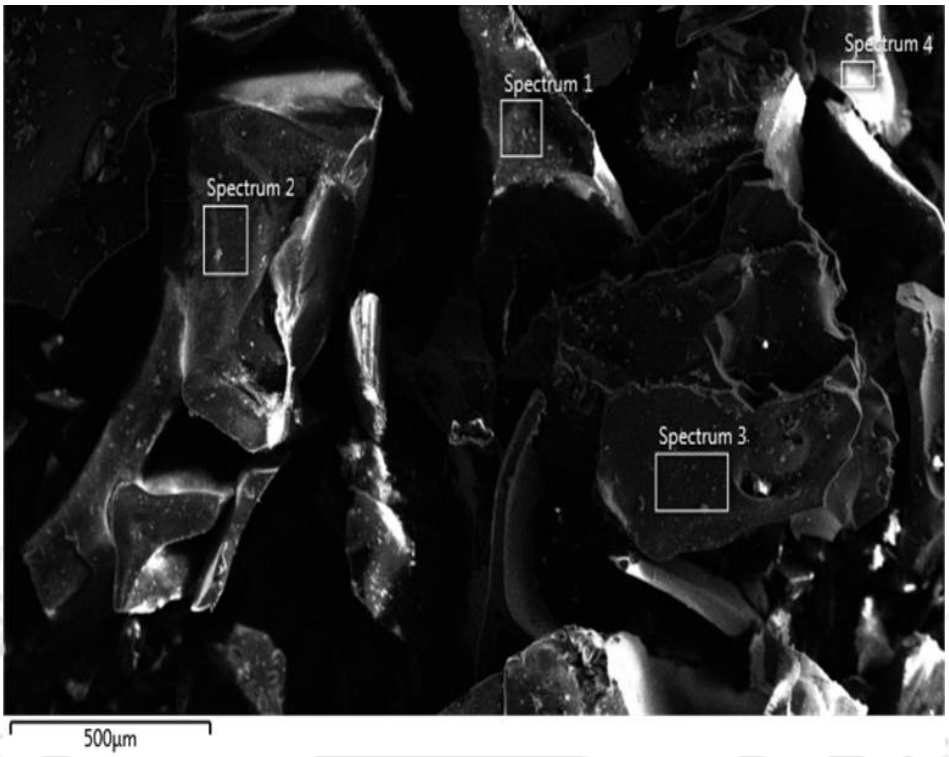

Fig. 6.25 FESEM of Post TD_{10}

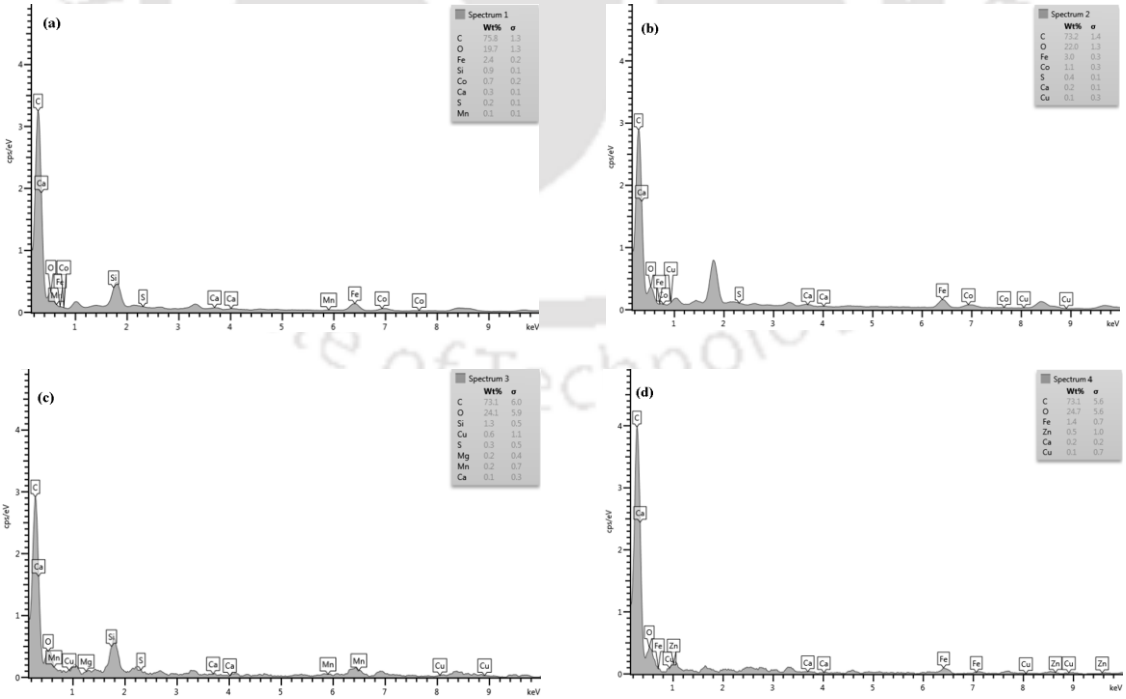

Fig. 6.26 a. EDS of spectrum 1: Post TD_{10}, Fig. 6.26b. EDS of spectrum 2: Post TD_{10}, Fig. 6.26c. EDS of spectrum 3: Post TD_{10}, Fig. 6.26d. EDS of spectrum 4: Post TD_{10}

Table-6.11 gives the composition of various elements present in the EDS (Fig. 26 a-d) of post TD_{10}.In the morphology of post TD_{10} sample absence of nitrogen is observed. It also shows the presence of oxygen and in addition some minor element Fe, Si, CO, Ca, S, Mg, Mn, Cu and Zn. The presence of these minor elements is may be due to wearing of TCC and electric heater. The presence of dolomite in TD_{10} also shows occurrences of some elements.

Table-6.11 EDS of various spots on the surface of Post TD_{10} sample

Element	Spectrum 1	Spectrum 2	Spectrum 3	Spectrum 4
C	75.8	73.2	73.1	73.1
O	19.7	22.0	24.1	24.1
Fe	2.4	3.0	-	1.4
Si	0.9	-	1.3	-
CO	0.7	0.2	-	-
Ca	0.3	-	-	0.2
S	0.2	0.4	0.3	-
Mg	-	-	0.2	-
Mn	0.1	-	0.2	-
Cu	-	0.1	0.6	0.1
Zn	-	-	-	0.5

The four spectrums (Fig. 26a-d) of the post TD_{10} sample gives higher composition of carbon compare to the four spectrums (Fig. 24 a-d) of post TD_{10} sample. This shows that the heavy hydrocarbon in tar which is not cracked contains the higher amount of carbon.

6.8.4 FOURIER TRANSFORM INFRARED SPECTROSCOPY (FTIR) ANALYSIS OF PRE AND POST TD_{10} SAMPLE

The spectroscopy of the pre and post TD_{10} sample is carried out with FTIR instrument (Model: IR Affinity Make: SHIMADZU). FTIR spectrometer simultaneously collects high spectral resolution data over a wide spectral range. Figure 6.27 presents a pattern in the two spectra for two samples.

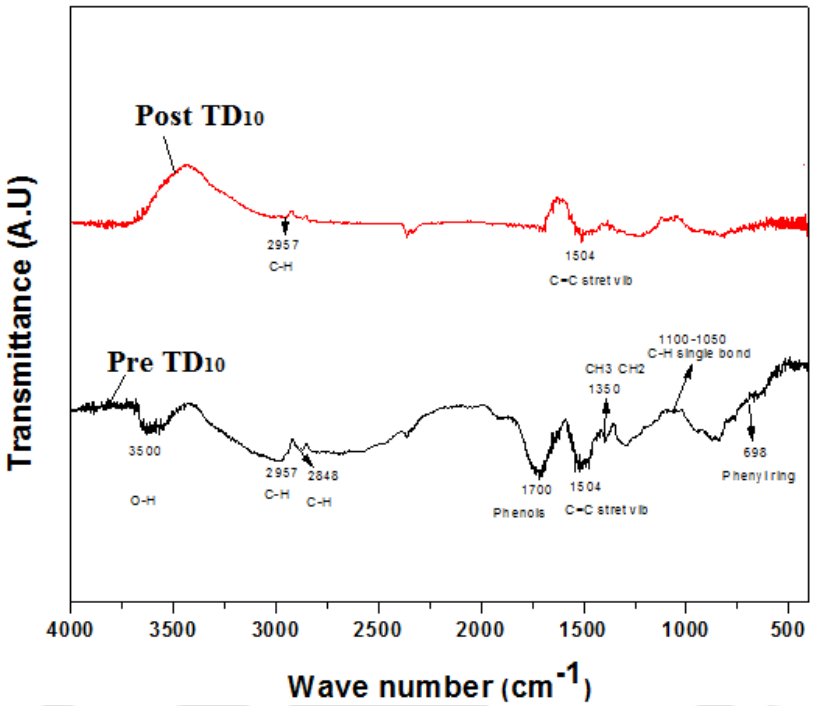

Fig. 6.27. Comparative analysis of FTIR spectra for pre and post TD_{10} sample

The various groups are observed for pre TD_{10} sample. (1) The peaks observed between 3000and 2850 cm−1 correspond to C−H stretching vibrations and (2) those between 1450 and 1350 cm−1 represent C−Hde formation vibrations that verify the presence of $-CH_3$, CH_2,and C−H groups. (3) Signal around 1700 cm−1 probably corresponds to some oxygen-containing compounds such as phenol, ketone and carboxylic acid. (4) Absorption peaks detected from 1625 and 1575 cm^{-1}aswell as those between 950 and 800 cm−1 indicate the presenceof mono- and polycyclic aromatic compounds. Peak between 1675 and 1352 cm^{-1} represents double bonds(C= C) from alkenes functional group. (6) Spectra observed around 1100 and 1050 cm^{-1} show single bonds (C−H) and long linear aromatic hydrocarbons. (7) Absorption is observed at 3200–3600 cm^{-1}, recognized to free phenolic OH and COOH groups. (8) The ether and phenolic OH at 1100– 1200 cm^{-1}. (9) Peaks at 1400–1600 cm^{-1} are certainly ascribed to aromatic structures. Biomass tar contains more oxygen groups, namely phenol-group fraction.

It is observed that the maximum functional groups are disappeared in Post TD_{10} sample. C-H stretching vibrations are seen at 2967 cm^{-1} and at 1504 C=C stretching id observed. The groups are identified by comparing FTIR spectra given by Krishna and Pugazhenthi (2011) and Balanco (2012) as given in Appendix-IX.

6.8.5 COMPARATIVE ANALYSIS OF PRE AND POST TD_{10} SAMPLE BY GC-MS

The composition of tar-dolomite pre and post samples is determined by GC-MS using a Mass Spectrometer (Make-Varian 450-GC &Varian 240). Figure 6.28 presents GC–MS spectrum Chromatograph for the Pre TD_{10} sample.

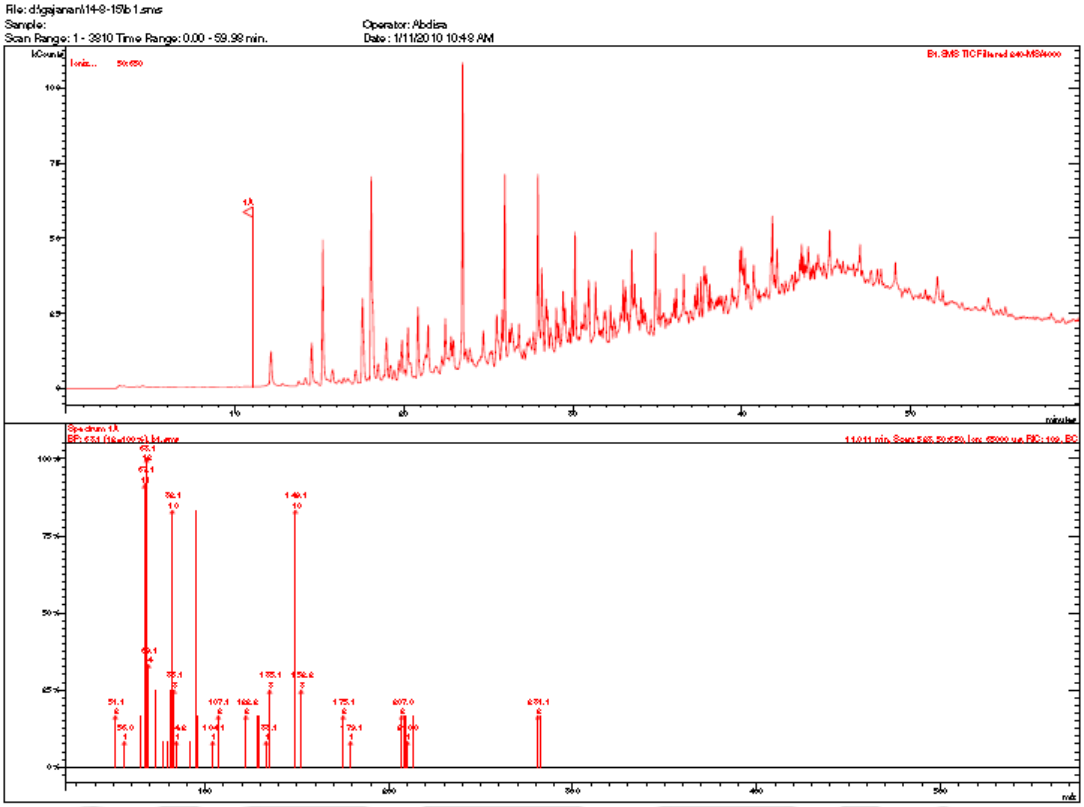

Fig. 6.28 GC–MS spectrum Chromatograph for the Pre TD_{10}

The results of the GCMS are evaluated with the Search NIST Libraries for Spectrum Hit List as given in Table-6.12

Table-6.12 GCMS Compound analysis of Pre TD_{10} sample

S.N.	RT (min)	Compound	M W	Formula	Probability(%)
1	12.126	3-Aminopyridine	94	$C_5H_6N_2$	41.33
2	12.126	2-Aminopyridine	94	$C_5H_6N_2$	25.87
3	12.126	4-Aminopyridine	94	$C_5H_6N_2$	22.86
4	12.126	Carbonic acid, ethyl phenyl ester	166	$C_9H_{10}O_3$	3.11

5	12.126	Pyrimidine, 4-methyl	94	$C_5H_6N_2$	1.79
6	14.185	2-Cyclopenten-1-one, 2,3-dimethyl	110	$C_7H_{10}O$	61.94
7	14.185	1,3-Phenylenediamine	108	$C_6H_8N_2$	34.46
8	14.185	1,2-Benzenediamine	108	$C_6H_8N_2$	34.46
9	16.439	Phenol, 2,3-dimethyl	122	$C_8H_{10}O$	39.30
10	16.439	Phenol, 2,5-dimethyl	122	$C_8H_{10}O$	11.56
11	16.439	Phenol, 2,6-dimethyl	122	$C_8H_{10}O$	9.76
12	16.439	Phenol, 3,5-dimethyl	122	$C_8H_{10}O$	9.38
13	16.439	Phenol,3,5-dimethyl, methylcarbonate	179	$C_{10}H_{13}NO_2$	7.93
14	16.439	Phenol, 2,4-dimethyl	122	$C_8H_{10}O$	7.93
15	16.439	Phenol, 3,4-dimethyl	122	$C_8H_{10}O$	6.23
16	16.439	Phenol, 2-ethyl	122	$C_8H_{10}O$	1.51
17	16.439	Phenol, 3-ethyl	122	$C_8H_{10}O$	1.16
18	16.439	1,3,5-Cycloheptatriene, 1-methoxy	122	$C_8H_{10}O$	0.75
19	16.439	Phenol, 2,5-dimethyl-, acetate	164	$C_{10}H_{12}O_2$	0.75
20	16.439	Benzenemethanol, 4-methyl	122	$C_8H_{10}O$	0.69
21	16.439	Benzene, 1-methoxy-4-methyl	122	$C_8H_{10}O$	0.58
22	16.439	3-Methylbenzyl alcohol	122	$C_8H_{10}O$	0.47
23	16.439	Phenol, 3,4-dimethyl-, acetate	164	$C_{10}H_{12}O_2$	0.41
24	16.439	Phenol, 2,5-dimethyl-, acetate	164	$C_{10}H_{12}O_2$	0.75
25	16.439	Phenol, 4-ethyl	122	$C_8H_{10}O$	0.17
26	16.439	Benzenemethanol, .alpha.-methyl	122	$C_8H_{10}O$	0.13
27	16.439	Phenol, 3-ethyl-, acetate	164	$C_{10}H_{12}O_2$	0.10
28	16.439	Benzeneethanol,2-methoxy-	166	$C_{10}H_{14}O_2$	0.09
29	16.439	Benzene, 1-methoxy-3-methyl	122	$C_8H_{10}O$	0.04
30	16.837	Benzene, 1,2,4,5-tetramethyl	134	$C_{10}H_{14}$	22.64
31	16.837	Benzene,2-ethyl-1,3-dimethyl	134	$C_{10}H_{14}$	7.43
32	16.837	Benzene,2-ethyl-1,4-dimethyl	134	$C_{10}H_{14}$	7.43
33	16.837	Benzene,1-ethyl-2,4-dimethyl	134	$C_{10}H_{14}$	7.14
34	16.837	Benzene,4-ethyl-1,2-dimethyl	134	$C_{10}H_{14}$	5.61

35	16.837	o-Cymene	134	$C_{10}H_{14}$	5.61
36	16.837	Benzene,1-ethyl-3,5-dimethyl	134	$C_{10}H_{14}$	5.39
37	16.837	Benzene,1-methyl-3-(1methylethyl)	134	$C_{10}H_{14}$	4.76
38	16.837	p-Cymene	134	$C_{10}H_{14}$	3.84
39	16.837	Benzene,1-ethyl-2,3-dimethyl	134	$C_{10}H_{14}$	3.84
40	16.837	1,3,8-p-Menthatriene	134	$C_{10}H_{14}$	1.02
41	16.837	6,7-Dimethyl-3,5,8,8a-tetrahydro-1H-2-benzopyran	164	$C_{11}H_{16}O$	0.72
42	16.837	1,3,5-Cycloheptatriene,3,7,7 trimethyl	134	$C_{10}H_{14}$	0.21
43	16.837	Benzene, 1,3-diethyl	134	$C_{10}H_{14}$	0.11
44	16.837	Benzene, 1,4-diethyl	134	$C_{10}H_{14}$	0.11
45	16.837	Benzene, tert-butyl	134	$C_{10}H_{14}$	0.07
46	16.837	Benzene, 1,2-diethyl	134	$C_{10}H_{14}$	0.06
47	16.837	2,6-Dimethyl-1,3,5,7-octatetraene, E,ER	134	$C_{10}H_{14}$	0.06
48	17.141	Phenol, 2-ethyl	122	$C_8H_{10}O$	70.24
49	18.062	Phenol, 2-ethyl	122	$C_8H_{10}O$	53.33
50	18.131	Memantine	179	$C_{12}H_{21}N$	95.36
51	22.444	Tributylamine	185	$C_{12}H_{27}N$	38.01
52	22.927	Tributylamine	185	$C_{12}H_{27}N$	39.64
53	22.937	Sarcosine anhydride	142	$C_6H_{10}N_2O_2$	24.02
54	23.289	Pyridine, 2,6-diethyl	135	$C_9H_{13}N$	75.41
55	23.422	2-Coumaranone	134	$C_8H_6O_2$	64
56	23.422	Ethanol,2-(ethylphenylamino)	165	$C_{10}H_{15}N_O$	17.44
57	23.422	Pyridine, 2,6-diethyl	135	$C_9H_{13}N$	7.94
58	23.408	Pyridine, 2,6-diethyl	135	$C_9H_{13}N$	63.83
59	23.408	Ethanol,2-(ethylphenylamino)	165	$C_{10}H_{15}NO$	14.32
60	23.408	2-Coumaranone	134	$C_8H_6O_2$	10.97
61	28.160	1,8-Naphthyridin-2-amine,5,7-dimethyl	173	$C_{10}H_{11}N3$	64
62	28.501	Naphthalene, 1-isocyanato	169	$C_{11}H_7NO$	46.91

63	29.959	1-Hydroxyphenazine	196	$C_{12}H_8N_2O$	85.86
64	35.137	Acridine	179	$C_{13}H_9N$	64.53
65	35.137	Benzo[f]quinolone	179	$C_{13}H_9N$	18.29
66	35.137	Phenanthridine	179	$C_{13}H_9N$	12.91
67	37.237	9-Vinylcarbazole	193	$C_{14}H_{11}N$	52.49
68	37.237	Acridine, 9-methyl	193	$C_{14}H_{11}N$	20.75
69	37.237	2-Phenylindolizine	193	$C_{14}H_{11}N$	14.65
70	37.237	Iminostilbene	193	$C_{14}H_{11}N$	9.17
71	37.366	2-Phenylindolizine	193	$C_{14}H_{11}N$	65.02
72	37.587	2-Phenylindolizine	193	$C_{14}H_{11}N$	80.08
73	37.587	1H-Indole, 2-phenyl	193	$C_{14}H_{11}N$	7.13
74	37.587	3-Phenylindole	193	$C_{14}H_{11}N$	6.30
75	37.587	Acridine, 9-methyl	193	$C_{14}H_{11}N$	2.11
76	37.587	[1,1'-Biphenyl]-4-acetonitrile	193	$C_{14}H_{11}N$	1.49
77	37.587	Carbamazepine, TMS derivative	308	$C_{18}H_{20}N_2OS$	1.43
78	37.587	2'-Hydroxyacetophenone,TMS derivative	208	$C_{11}H_{16}O_2Si$	0.56
79	48.033	Benzo(a) acridine	229	$C_{17}H_{11}N$	81.69

The results of Pre TD_{10} sample states that tar-dolomite sample contains of many organic species varying from molecular weight 94 to 229 and compounds 3-Aminopyridineto Benzo (a) acridine.

Figure 6.29 presents GC–MS spectrum Chromatograph for the Post TD_{10} sample .

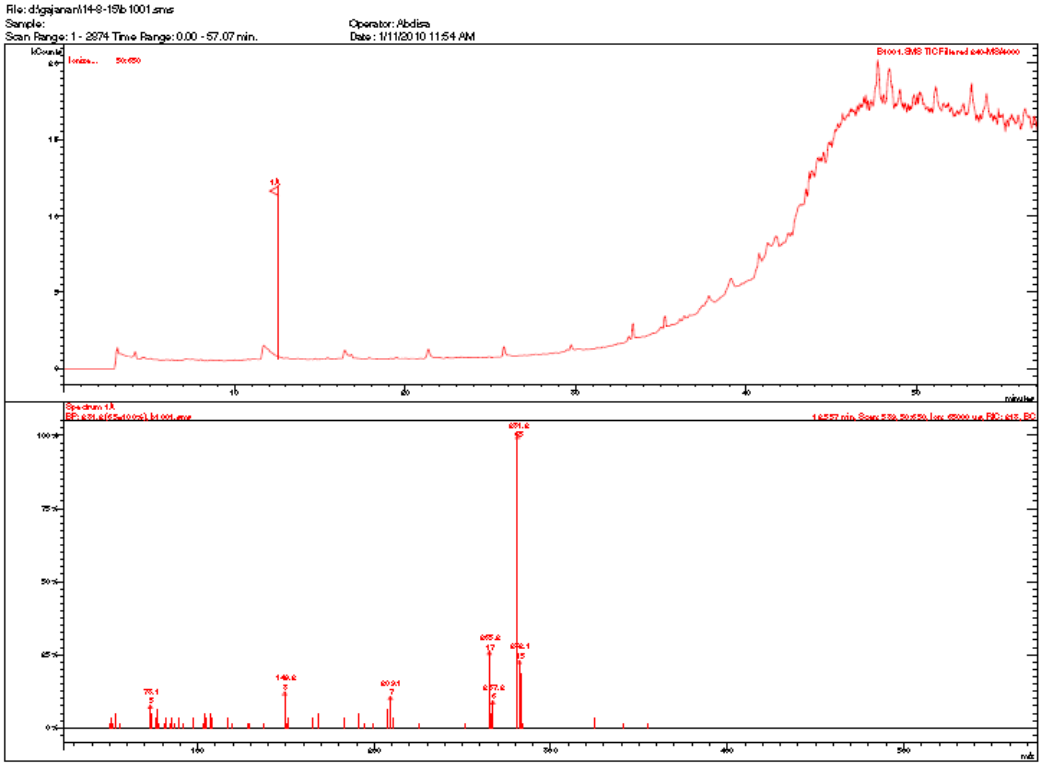

Fig.6.29 GC–MS spectrum Chromatograph for the Post TD_{10}

The results obtain from the GCMS Post TD_{10} sample is evaluated with the data base of NIST Libraries for Spectrum Hit List. The compounds found are listed in the Table-6.13.

Table-6.13 GCMS Compound analysis of Post TD_{10} sample

S.N.	RT (min)	Compound	MW	Formula	Probability (%)
1	4.418	Silane, dimethoxydimethyl	120	$C_4H_{12}O_2Si$	
2	11.690	Cyclotetrasiloxane, octamethyl	296	$C_8H_{24}O_4Si_4$	79.21
3	11.690	Benzoic acid, 4-methyl-2-	296	$C_{14}H_{24}O_3Si_2$	15.51
4	11.877	Cyclotetrasiloxane, octamethyl	296	$C_{14}H_{24}O_3Si_2$	97.51
5	12.229	Cyclotetrasiloxane, octamethyl	296	$C_{14}H_{24}O_3Si_2$	93.17
6	16.445	Cyclotetrasiloxane, octamethyl	296	$C_{14}H_{24}O_3Si_2$	81.66
7	16.843	Benzene, 1,2,4,5-tetramethyl	134	$C_{10}H_{14}$	38.05
8	16.843	Benzene, 1-ethyl-2,3-dimethyl	134	$C_{10}H_{14}$	9.20
9	16.843	Benzene, 1-ethyl-3,5-dimethyl	134	$C_{10}H_{14}$	3.36
10	16.843	o-Cymene	134	$C_{10}H_{14}$	3.10

11	16.843	Benzene, 1-ethyl-2,4-dimethyl	134	$C_{10}H_{14}$	2.61
12	21.364	Cyclohexasiloxane, dodecamethyl	444	$C_{12}H_{36}O_6Si_6$	98.59
13	25.791	Cycloheptasiloxane, tetradecamethyl	518	$C_{14}H_{42}O_7Si_7$	97.48
14	29.749	Cyclooctasiloxane, hexadecamethy	592	$C_{16}H_{48}O_8Si_8$	95.02
15	33.122	Cyclononasiloxane, octadecamethyl	666	$C_{18}H_{54}O_9Si_9$	96.87

The results of GCMS of post TD_{10} sample shows that the compounds with molecular weight. 120-666 are present. This indicates that the heavy tar is not cracked completely but it presents in small amount. The compounds found are Silane, dimethoxydimethyl, Cyclotetrasiloxane, octamethyl to Cyclononasiloxane, Octadecamethyl.

6.9 SUMMARY

Development of an experimental set up and procedure for the thermal cracking of the tar is presented in this chapter. Based on hydrodynamic study and principle of liquid-gas fluidization the tar cracking unit is developed. Experiments were conducted with liquid tar as well as tar and dolomite mixtures with various proportions. It was observed that thermal cracking of tar is successful in terms of gas yield, gas compositions and residue formation. Thermal profile along the tar cracking chamber shows favorable temperature for catalytic cracking of tar with dolomite. 10-15 % dolomite by weight is found to crack tar producing good quality gas. Conclusions and scope for future work is presented in the next chapter.

CHAPTER 7

CONCLUSIONS AND SCOPE FOR FUTURE WORK

7.1 CONCLUSIONS

Fix bed gasifier has the good potential for the thermo-chemical conversion of the biomass into the producer gas which is utilized for the power generation and heat appliances. However, most of the fixed bed gasifiers are designed for the gasification of solid feedstock limiting to the use of loose biomass in the same. A detail study is therefore required to see the functionality of fixed bed gasifier with loose biomass. Thermal performance, gas constituents and quality are some of the major aspects regarding workability of an existing gasifier with other kind of biomass (loose biomass). Formation of tar is another problem associated with such systems as the tar formed can clog and damage the piston-cylinder and the engine block. Experimental studies on downdraft gasifier are elaborated on utilization of loose biomass in densified form and more emphasis is given on the in-situ cracking of the tar. The in-situ cracking of the tar is predicted on cracking of tar inside the gasifier using the biomass-dolomite pellets and developing a novel tar cracking device which may be retrofitted to gasifier.

The feedstock is prepared by densification of loose biomass in the form of briquettes and pellets. The briquettes are handmade and prepared with waste newspaper as binder in spherical shape of 25 mm (approx.) diameter. Pellets are manufactured with pelletizer in cylindrical shape with 18 mm diameter and 25 mm length. Thermal behavior, gas quality and constituents of gas generated by gasification of biomass briquettes and pellets are compared with that of woodchips in an existing downdraft gasifier.

Before proceeding for the gasification, few locally available biomasses are identified and characterized. Samples with saw dust, rice husk powder and mustard husk powder are prepared in the form of briquettes and pellets to check for the feasibility to use as a feedstock in the fixed bed gasifier. The characterization involves ultimate analysis, proximate analysis, estimation of heating value, density, and impact resistance index and stress analysis. In addition to this the characterization is also done for thermo gravimetric

and fibre analysis. It was found that briquettes and pellets are having desirable properties to use as a feedstock in the gasifier.

The parametric study of downdraft gasifier is performed in four range of equivalence ratio as 0.19- 29, 0.32, 0.36-0.37 and 0.41-0.46.

The conclusions drawn from the present investigations are summarized below.

- The temperature inside the gasifier increase with increase in the equivalence ratio for all the briquettes pellets as well as woodchips. However, temperature was reducing for the sawdust-dolomite pellets.
- The temperature in combustion zone was observed to be varying from 700^0C to 1250^oC. Heat generated during combustion is transferred to pre combustion followed by pyrolysis, pre-pyrolysis and drying zone and to reduction zone. The temperature measured in pre-combustion, pyrolysis, pre-pyrolysis and drying zone are 230–451^oC,135–230^oC,85–225^o C respectively. The temperatures in reduction zone and ash chamber are400–450^oC and 40–70^oC, respectively.
- It is noticed that heat is generated in the combustion zone is propagated to the pyrolysis followed by drying zone and biomasses released volatiles and converted to char which dropped down to the reduction chamber. Heat also propagated into reduction zone. This results in reduction reaction and generation of producer gas.
- Composition of the producer gas obtained with woodchip mainly consists of 18.27% H2, 15.26% CO and 2.81% CH4. The flow rate of gas and calorific value are found to be 2.33 Nm^3/kg and 5.39 MJ/m^3, respectively. The gasifier conversion efficiency of 69% and carbon conversion efficiency 91% is obtained with gasification of woodchips.
- The producer gas composition for briquette B_{15} is found good at ER 0.37 in terms of gas quality. The gas composition of the producer gas obtained from saw dust briquettes contents 19.94% H_2, 18.4% CO and 1.27% CH_4. The gas yield with the flow rate 2.41 Nm^3/kg, calorific value 4.92 MJ/m^3, gasifier conversion efficiency 69% and carbon conversion efficiency 90%.
- The producer gas composition for pellets without dolomite is found to be better than other pellets for ER= 0.32 in terms of gas quality. The gas composition of the

producer gas obtained from saw dust pellet contents 7.54% H_2, 20.45% CO and 2.15% CH_4.The gas yield with the flow rate 2.4 Nm^3/kg, calorific value 4.42 MJ/m^3, gasifier conversion efficiency 59% and carbon conversion efficiency 97% were obtained.

- It is observed that H_2 obtained with gasification of briquettes B_{15} and sawdust pellets P_{00} compared to gasification of woodchips decrease by 25.25% and 56.29%, respectively for the ER in the operating range of 0.24–0.29. Similarly, Methane percentage also decreases with gasification of B_{15} and P_{00} by 17.89% and 34.40%, respectively. Decrease of CO for both the briquettes and pellets are also observed to be hardly 2.58 % and 1.64 %, respectively. Similarly, reduction in percentage of H_2, and CH_4 by 5.64% and 49.82%, respectively for briquette and 58.73% and 23.49%, respectively for pellets is observed. Whereas, percentage of CO increased by 11.4% and 34% for gasification in comparison to woodchips for ER =0.32. However, for ER range 0.37–0.38, percentage of H_2, CO and CH_4 is increased by 9.56%, 29.58% and 12.38%, respectively for briquette and in case of pellets H_2 is decreased by 62.74 % and CO and CH_4 increased by 26.19 % and 103.54 % respectively compare to woodchips.

- Increase in equivalence ratio reduces the tar in producer gas. The decrease in quantity of tar obtained is observed for all the cases.

- It is observed from TGA analysis that the biomass pellet without dolomite undergoes devoltalization in one stage from 200-400^oC. However, biomass-dolomite pellet undergoes devoltalization in two stages. The first stage is from 200-400$^oC$and the second stage is from 700-800^oC which assists for the reduction of tar in gasification process.

- The experiments on in-situ tar cracking are performed with five compositions saw dust-dolomite pellet and mustard husk dolomite pellet. The saw dust pellet P_{20} has good gas composition compare to other four as 17.89% H_2, 22.80% CO and 2.66% CH_4. However, inadequate gasification is observed with the mustard husk pellet and furthermore mustard husk is not suggested for the gasification.

- The drastic tar reduction is observed with the in-situ tar cracking methodology. The comparative study for all the feedstock at equivalence ratio 0.32 is carried

out. Accordingly tar is reduced by 36.1 %, 28.7%, 31.8% for wood chips, sawdust briquettes (B_{15}) and pellets, respectively.

- Dolomite is mixed with tar in the proportion 5-20% by weight for thermal cracking in the developed tar cracking set up. It is found that the tar-dolomite mixture with 10% dolomite by weight is most preferable in the terms of gas quality and cracked-gas flow rate. The gas composition for the tar with 10% dolomite is found to be superior to all other samples tested. The gas chromatography of the cracked -gas obtained with TD_{10} has composition of 13.7% H_2, 40% CO and 1.4% CH_4 which is satisfactory for thermal applications.

7.2 SCOPE FOR FUTURE WORK

The scopes and suggestions for further studies are enlisted below

- There is scope for the comparative study on thermal cracking of tar using different catalysts like zeolite, alkali metals, nickel and etc. for good quality crack-gas and maximum conversion of tar into crack-gas.
- The coal-biomass pellet with various proportion of catalyst will be also a good study in sector of power production.
- Energy and exergy studies may be conducted for the entire gasification system.
- Experiment may be conducted on utilization of waste heat from the gasifier surface.
- The performance of present liquid-gas bubbling fluidized bed set up has limitation with heating by electrical heater. It may be replaced with concentrated solar radiative heating with stem injection.
- Numerical simulations can be used for scaling of gasifier.
- The simulations and scale up of tar cracking unit can be conducted.

REFERENCES

Abu, El-R. Z., Bramer, E. A., and Brem, G., (2004). "Review of catalysts for tar elimination in biomass gasification processes," Ind. Eng. Chem. Res., 43, pp. 6911-6919.

Adeyemi, I., Janajreh I., Arink T., Ghenai C., (2017). "Gasification behavior of coal and woody biomass: Validation and parametrical study," Applied Energy 185, 1007–1018.

Agarwal, A. K., (2007). "Bio-fuels (alcohols and biodiesel) applications as fuels for internal combustion engines," Progress in Energy and Combustion Science, Vol. 33, pp. 233–271.

Ahmed, I. and Gupta, A. K., (2009). "Characteristics of cardboard and paper gasification with CO_2," Applied Energy, Vol. 86, pp. 2626-2634.

Ahrenfeldt, J., Thomsen, T. P., Henriksen, U., Clausen, L. R., (2012). "Biomass gasification cogeneration - A review of state of the art technology and near future perspective," Applied Thermal Engineering, pp. 1-11.

Antonopoulos, I. S., Karagiannidis, A., Elefsiniotis, L., Perkoulidis, G., Gkouletsos, A., (2012). "Development of an innovative 3-stage steady-bed gasifier for municipal solid waste and biomass," Fuel, Vol. 93, pp. 589–600.

Asadullah, M., (2014). "Barriers of commercial power generation using biomass gasification gas: A review," Renewable and sustainable energy reviews, Vol. 29, pp. 201-215.

Babu, S. P., (2005). "Observation on the current status of biomass gasification" IEA Bioenergy Report.

Balat, M., Mehmet, B., Elif, K., Havva, B., (2009). "Main routes for the thermo-conversion of biomass into fuels and chemicals Part 2 gasification systems" Energy Conversion and Management, Vol. 50, pp. 3158–68.

Basu, P., (2010). "Biomass gasification and pyrolysis practical Design," Academic Press, Elsevier, USA.

Berrueco, C., Lorente, E., Van Niekerk, D., Millan, M., (2014). "Evolution of tar in coal pyrolysis in conditions relevant to moving bed gasification," Energy & Fuels, Vol. 28(8), pp. 4870-4876.

Bhave, A. G., Vyas, D. K., Patel, J.B., (2008). "A wet packed bed scrubber-based producer gas cooling–cleaning system," Renewable Energy, Vol. 33, pp. 1716–20.

Biagini, E., Barontini, F., and Tognotti, L. (2006). "Devolatilization of biomass fuels and biomass components studied by TG/FTIR technique," Industrial and Engineering Chemical Reaserch, Vol. 45, pp. 4486–93.

Blanco, P. H., Wu, C., Onwudili, J. A., Williams, P. T., (2012). "Characterization of tar from the pyrolysis/gasification of refuse derived fuel: Influence of process parameters and catalysis," Energy Fuels, 26, 2107−2115.

Bridgwater, A. V., (1995). "The technical and economic feasibility of biomass gasification for power generation," Fuel, Vol. 14(5), pp. 631-653.

Buragohain, B., Mahanta, P., Moholkar, V. S. (2010). "Biomass gasification for decentralized power generation: The Indian perspective," Renewable and Sustainable Energy Reviews, Vol. 14, pp.73–92.

Cardozo, E. Erlich, C. Alejo, L. Fransson, T. H., (2014). "Combustion of agricultural residues: An experimental study for small-scale applications," Fuel, (115) 778–787.

Catharina, E., Torsten, H., and Fransson,, (2011). "Downdraft gasification of pellets made of wood, palm-oil residues respective bagasse: Experimental study," Applied Energy, Vol.88, pp. 899–908.

Chiemchaisri, C., Charnnok, B., Visvanathan, C., (2010). "Recovery of plastic wastes from dumpsite as refuse-derived fuel and its utilization in small gasification system," Bioresource Technology, Vol.101, pp. 1522–1527.

Corella, J., Toledo, J. M., Padilla, R., (2004). "Olivine or dolomite as in-bed additive in biomass gasification with air in a fluidized bed: which is better?" Energy & Fuels, Vol.18, pp. 713-720.

Dassapa, S., Sridhar, G., Sridhar, H. V., Rajan, N.K.S., Paul, P. J., Upasani, A., (2010). "Producer gas engines-proponent of clean energy technology." Energy Conversion and Management, Vol. 51, pp. 452–458.

Dayton, D., (2002). "A review of the literature on catalytic biomass tar destruction-milestone completion report." NREL/TP-510-32815, National Renewable Energy Laboratory, DOI:www.osti.gov/bridge .

Delgado, J., Aznar, M. P., Corella, J., (1996). “Calcined dolomite, magnesite, and calcite for cleaning hot gas from a fluidized bed biomass gasifier with steam: Life and usefulness,” Industrial and Engineering Chemistry Research Vol. 35 (10), pp. 3637–3643.

Devi, L., Ptasinski, K. J., Janssen F.J.J.G., (2003). “A review of primary measures for tar elimination in biomass gasification process,” Biomass and Bioenergy, Vol.24. pp.125-140.

Devi, L., Ptasinski, K.J., Janssen, F.J.J.G., (2005). “Pretreated olivine as tar removal catalyst for biomass gasifiers: Investigation using naphthalene as model biomass tar,” Fuel Processing Technology, Vol. 86, pp. 707– 730.

Dogru, M., Howarth, C. R., Akay, G., Keskinler, B., Malik, A., (2002). “Gasification of hazelnut shells in a downdraft gasifier,” Energy, Vol. 27, pp. 415-427.

Dou, B., Gao, J., Sha, X., Baeka, S.W., (2003). “Catalytic cracking of tar component from high-temperature fuel gas,” Applied Thermal Engineering, Vol.23, pp. 2229–2239.

El-Rub, Z. A., Bramer E. A., Brem G. (2004). “Review of catalysts for tar elimination in biomass gasification processes,” Ind. Eng. Chem. Res., Vol.43, pp. 6911-6919.

Erlich, C, Ohman M, Bjornbom E and Fransson T.H.. (2005). "Thermochemical characteristics of sugar cane bagasse pellets," Fuel,Vol. 84, pp 569-575

Erlich, C., Fransson T. H., (2011), “Downdraft gasification of pellets made of wood, palm-oil residues respective bagasse: Experimental study,” Applied Energy, Vol. 88, pp. 899-908

Gai, C., Dong, Y., (2012), “Experimental study on non-woody biomass gasification in a downdraft gasifier.” International journal of hydrogen energy, Vol. 37, pp. 4935 - 4944.

Grieco, E. M., Gervasio, C., Baldi, G., (2013). “Lanthanum–chromium–nickel perovskites for the catalytic cracking of tar model compounds.” Fuel, Vol. 103, pp. 393–397.

Guangul, F. M., Sulaiman S. A., Ramli, A., (2014). “Gasifier Study of the effects of operating factors on the resulting producer gas of oil palm fronds gasification with a single throat downdraft gasifier,” Renewable Energy,Vol.72, pp. 271-283.

Hasler, P., & Nussbaumer, T., (1999). “Gas cleaning for IC engine applications from fixed bed biomass gasification,” Biomass and Bioenergy, Vol.16, pp.385-395.

Jankeset, G. G., Trninic, M. R., Stamenic, M. S., Simonovic, T. S., Tanasic, N. D., And Labus, J. M., (2012). "Biomass gasification with CHP production a review of the state-of-the-art technology and near future perspectives," Thermal Science, Vol.16 (1), pp. 115-130.

Jeya Singh V. C., Sekhar S. J., (2016). "Performance studies on a downdraft biomass gasifier with blends of coconut shell and rubber seed shell as feedstock," Applied Thermal Engineering 97 (2016) 22–27.

Jorapur, R., & Rajvanshi, A. K., (1997). "Sugercane leaf- bagasse gasifier for industrial heating application." Biomass and Bioenergy, Vol. 13 (3), pp. 141-146.

Jordan, A. C., Akay, G., (2013). "Effect of CaO on tar production and dew point depression during gasification of fuel cane bagasse in a novel downdraft gasifier." Fuel Processing Technology, Vol.106, pp. 654–660.

Kaliyan, N., and Morey, R. V., (2009). "Factors affecting strength and durability of densified biomass products." Biormass and Bioenergy, Vol.33 (3), pp. 337-359.

Kannaiyan, S., Madhavan, V. R., Rajagopal, S., Jayabalan, A., (2016). "An experimental analysis on tar cracking using nano structured Ni-Co/Si-P catalyst in a biomass gasifier-based power generating system," Applied Thermal Engineering 97 (2016) 13–21.

Khater, E. M. H., Ibiary, N. N. E., Khattab, I. A., Hamad, M. A., (1992). "Gasification of rice hulls" Biormass and Bioenergy Vol. 3(5), pp. 329-333.

Kirkels, A. F., Geert, P. J. V., (2011). "Biomass gasification: Still promising? A 30-year global overview" Renewable and Sustainable Energy Reviews, Vol. 15, pp. 471–481.

Kjellstrom, B., A., Forslund A., H. and Martinac, I., (2005). "Renewable energy technologies for decentralised rural electricity services," SEI Climate and Energy Programme, Swedish Environment Institute (SEI) Stockholm, Sweden.

Kline, S. J., and McClintock F. A., (1953). "Describing uncertainties in single-sample experiments," Mechanical Engineering, Vol. 75, No. pp 3-8.

Krishna, S. V. and Pugazhenthi, G. (2012). "Structural and thermal properties of polystyrene/CoAl-layered double hydroxide nanocomposites prepared via solvent blending: effect of LDH loading" Journal of Experimental Nanoscience, 8:1, 19-31

Laksmono, N., Paraschiv, M., Loubar, K.T.M., (2013). "Biodiesel production from biomass gasification tar via thermal/catalytic cracking." Fuel Processing Technology, Vol.106, pp.776–783.

Li, X, Grace JR, Watkinson, AP, Lim, CJ, Ergudenler, A. (2001). "Equilibrium modeling of gasification: a free energy minimization approach and its application to a circulating fluidized bed coal gasifier," Fuel, 80 (2):195–207.

Long, I., and Wang, T., (2011). "Case studies for biomass/coal co-gasification in IGCC applications." Proceedings of ASME Turbo Expo, June 6-10, Vancouver, Canada.

Maniatis, K., (2001). "Progress in biomass gasification: an overview." Progress in Thermo chemical Conversion of Biomass (Ed. Bridgwater AV), Blackwell Science Ltd. Oxford (UK), pp.1-31.

Mastellone, M. L., Arena, U., (2008). "Olivine as a tar removal catalyst during fluidized bed gasification of plastic waste." AIChE Journal, Vol.54 (6), pp.1656–1667.

Mihai, B., and Bornelia, V., (2010). "Thermal degradation of lignin – a review." Cellulose Chemistry and Technology, Vol.44 (9), pp.353-363.

Milne, T. A., Evans, R. J., Abatzoglou, N., (1998). "Biomass gasifier tars: Their nature, formation, and conversion," NREL/TP-570-25357.

Moffat, R. J., 1982, "Contributions to the theory of single-sample uncertainty analysis," ASME Journal of Fluids Engineering, Vol. 104, pp. 250-260.

Myren, C., Hornell, C., Bjornbom, E., Sjostrom, K., (2002). "Catalytic tar decomposition of biomass pyrolysis gas with a combination of dolomite and silica." Biomass and Bioenergy, Vol. 23, pp.217 – 227.

Orío, J Corella, I Narváez, (1997). "Performance of different dolomites on hot raw gas cleaning from biomass gasification with air," Industrial & engineering chemistry, Vol.36 (9), pp 3800–3808

Panwara, N. L., Kothari, R., Tyagi, V. V., (2012). "Thermo chemical conversion of biomass – Eco friendly energy routes." Renewable and Sustainable Energy Reviews, Vol. 16, pp. 1801– 1816.

Patel, V. R., Upadhyay D. S., Patel R. N (2014). "Gasification of lignite in a fixed bed reactor: Influence of particle size on performance of downdraft gasifier," Energy, Vol. 78, pp. 323-332.

Patel, V.R, Patel D. Varia N. S., Patel R. N., (2016). "Co-gasification of lignite and waste wood in a pilot-scale (10 kWe) downdraft gasifier," Energy xxx 1-11.

Pathak, B. S., Kapatel D. V., Bhoi P. R., Sharma A M and Vyas D. K., (2007). "Design and development of sand bed filter for upgrading producer gas to IC engine quality fuel," International Energy Journal, Vol. 8, pp.15-20.

Pathak, B. S., Patel, S. R., Bhave, A. G., Bhoi, P. R., Sharma, A. M., Shah, N. P., (2008). "Performance evaluation of an agricultural residue-based modular throat-type down-draft gasifier for thermal application." Biomass And Bioenergy, Vol. 32, pp.72 – 77.

Patil, K., Bhoi, P., Huhnke, R., Bellmer, D., (2011). "Biomass downdraft gasifier with internal cyclonic combustion chamber: Design, construction, and experimental results." Bioresource Technology, Vol. 102, pp.6286–6290.

Powell, J. J., Aquino, F., Capareda, S., (2007). "Performance of a portable downdraft gasifier." Beltwide Cotton Conferences, New Orleans, Louisiana, January 9-12.

Prasad, L., Subbarao P. M. V., and Subrahmanyam, J. P., (2014). "Pyrolysis and gasification characteristics of Pongamia residue (de-oiled cake) using thermogravimetry and downdraft gasifier," Applied Thermal Engineering, Vol.63: pp.379-386

Prasad, L., Subbarao, P. M. V., Subrahmanyam, J. P., (2015). "Experimental investigation on gasification characteristic of high lignin biomass (Pongamia shells),"Renewable Energy, Vol.80, pp.415-423.

Qin, K., Lin, W., Jensen, P.A., Jensen, A.D., (2012). "High temperature entrained flow gasification of biomass." Fuel, Vol.93, pp.589–600.

Rajvanshi, A.K., (1986). "Biomass gasification," Chapter (No.4) in book Alternative Energy in Agriculture, Vol. II, Ed. D. Yogi Goswami, CRC Press, pp. 83-102.

Raman, P., Ram, N.K., Gupta, R., (2013). "A dual fired downdraft gasifier system to produce cleaner gas for power generation: Design, development and performance analysis," Energy, Vol. 54, pp. 302-314.

Rapagna, S., Jand, N., Kiennemann, A., Foscolo, P., (2000). "Steam-gasification of biomass in a fluidised-bed of olivine particle," Biomass and Bioenergy, Vol.19, pp. 187-197.

Rathore, N. S., Panwar, N. L., Chiplunkar, Y. V., (2009). "Design and techno economic evaluation of biomass gasifier for industrial thermal application," African Journal of Environmental Science and Technology, Vol. 3(1), pp. 006-012.

Ravindranath, N. H., Somashekar H. I., Dasappa S., and Reddy, J. C. N. (2004). "Sustainable biomass power for rural India: Case study of biomass gasifier for village electrification," Current Science, Vol.87 (7), pp. 932-941.

Reed, T. B., Walt, R., Ellis, S., Das, A., Deutch, S., (1999). "Superficial velocity - the key to downdraft gasification." Presented at 4th Biomass Conference of the Americas; Oakland, CA.

Richards, S.R., (1990). "Physical testing of fuel briquettes." Fuel Process Tech, Vol.25, pp. 89-100.

Roche, E., Andrés, J. M. D., Narros, A., Rodríguez, M. E., (2014). "Air and air-steam gasification of sewage sludge. The influence of dolomite and throughput in tar production and composition." Fuel, Vol. 115, pp.54–61.

Sadka, S. S, Ghaly,A. E., Sabbah, M. A, (1998). "Development of an air-steam fludized bed gasifier," Journal of agricultural engineering, Vol.15 (1), pp. 47-52.

Sang, J. Y., Yung, S., Yong-Ku, K., Jae-Goo, L., (2012). "Gasification and power generation characteristics of rice husk and rice husk pellet using a downdraft fixed-bed gasifier.," Renewable Energy, Vol.42, pp.163-167.

Seo, D. K., Park, S. S., Hwang, J. and Yu, T., (2010). "Study of the pyrolysis of biomass using thermo-gravimetric analysis (TGA) and concentration measurements of the evolved species," Journal of Analytical and Applied Pyrolysis, Vol. 89, pp.66–73

Shabbar, S Janajreh, I., (2013), "Thermodynamic equilibrium analysis of coal gasification using Gibbs energy minimization method," Energy Converse Manage 6665:755–63.

Sharma, A. K., (2011). "Experimental investigations on a 20 kWe, solid biomass gasification system," Biomass and Bioenergy, Vol. 35, pp.421-428.

Shelke, G. N., Mahanta, P. and Patil, R. S., (2014a), "Experimental studies on thermal behavior of downdraft gasifier," Proceedings of the World Congress on Engineering , London, U.K., 2 - 4, July, WCE, Vol II: pp 1356-1359.

Shelke, G. N. and Mahanta, P. (2014b). "Biomass briquette characterization for downdraft gasification," Applied Mechanics and Materials. Vols. 592-594: pp 2442-2446.

Shelke, G. N. and Mahanta, P. (2016). "Feasibility study on utilization of biomass briquette in a conventional downdraft gasifier," International Energy Journal 16 (2016) 157-166.

Sheth, P.N. and Babu, B.V., (2009). "Experimental studies on producer gas generation from wood waste in a downdraft biomass gasifier." Bio-resource Technology, Vol. 100, pp. 3127–3133.

Simell, P. A., Leppalahti, J. K., Kurkela, E. A., (1995). "Tar-decomposing activity of carbonate rocks under high CO_2 partial pressure," Fuel, Vol.74 (6), pp. 938-945.

Simone, M., Barontini, F., Cristiano, N., Leonardo, T., (2012). "Gasification of pelletized biomass in a pilot scale downdraft gasifier," Bio-resource Technology, Vol.116, pp. 403–412.

Sivakumar, K., and Mohan, N. K., (2010). "Performance analysis of downdraft gasifier for agriwaste biomass materials," Indian Journal of Science and Technology, Vol. 3 (1), pp. 58-60.

Sivakumar, K., Mohan, N. K., and Sivaraman, B., (2012). "Performance analysis on briquetting bio mass with different size in 10 Kw_e down draft gasifier," Procedia Engineering, Vol.38, pp. 3824 – 3832.

Sridhar, H. V., Sridhar, G., Dasappa, S., Rajan N. K. S. and Paul P. J., (2005). "Experience of using various biomass briquettes in IBG (IISc Bioresidue Gasifier)," Proceedings of 14th European Biomass Conference & Exhibition Biomass for Energy, Industry and Climate Protection. 749-752.

Striugas, N., K. Zakarauskas, G. Stravinskas, and V. Grigaitiene. (2012). "Comparison of steam reforming and partial oxidation of biomass pyrolysis tars over activated carbon derived from waste tire," Catalyst Today, 196/67.

Sun, Y., Jiang, J., Efthymios, K., Junming, X., Linna, Li., Shuheng, Z., Weihong, Y., (2012). "Development of a bimetallic dolomite based tar cracking catalys," Catalysis Communications, Vol.20, pp. 36–40.

Sutton, D., Kelleher, B., Ross, Julian, R. H., (2001). "Review of literature on catalysts for biomass gasification," Fuel Processing Technology, Vol. 73, pp.155–173.

Thomas, N., Truls, L., Krister, S., (2006). "Metallic iron as a tar breakdown catalyst related to atmospheric fluidised bed gasification of biomass," Fuel, Vol. 85, pp. 689–694.

Turare, C., (2002), "Biomass gasification-technology and utilization," Humanity development library: document text.

Vamvukaa, D., Kakarasb, E., Kastanakia, E., Grammelisb, P., (2003). "Pyrolysis characterastics and kinetics of biomass residuals mixture and lignite," Fuel, Vol. 82, pp. 1949-1960.

Varshney, R., Bhagolia, J. L., Mehta, C. R., (2010). "Small biomass gasification technology in india – an overview," Journal of Engineering, Science and Management Education, Vol. 3, pp.33-40.

Velegol, D., Gautam, M., Shamsi, A., (1997). "Catalytic cracking of a coal tar in a fluid bed reactor," Powder Technology, Vol.93, pp. 93- 100.

Vyarawalla, F., Parikh, P. P., Dak H. C. Jain B. C.; (1984). "Utilisation of biomass for Motive power generation gasifier engine system," Biomass 5 (1984) 227-242.

Wei, L., Pordesimo, L. O., Haryanto, A., Wooten, J., (2011), "Co-gasification of hardwood chips and crude glycerol in a pilot scale downdraft gasifier," Bio-resource Technology, Vol.102, pp. 6266–6272.

Xiwei, X., Jiang, E., Mingfeng, W., Bosong, L., (2012). "Rich hydrogen production from crude gas secondary catalytic cracking over Fe/g-Al_2O_3," Renewable Energy, Vol. 39, pp. 126-131.

Yang, H., Yan, R., Chen, H., Lee, D. H., and Zheng, C., (2007). "Characteristics of hemicellulose, cellulose and lignin pyrolysis," Fuel, Vol. 86, pp. 1781–1788.

Yang, H., Yan, R., Chen, H., Zheng, C., Lee, D. H., and Liang, D.T., (2005). "In-depth investigation of biomass pyrolysis based on three major components: hemicellulose, cellulose and lignin," Energy Fuels, Vol.20, pp. 388–93.

Zainal, Z. A., Rifau, A., Quadir, G. A., Seetharamu, K. N., (2002). "Experimental investigation of a downdraft biomass gasifier," Biomass and Bioenergy, Vol. 23, pp. 283–289.

Zheng, G., and Kozinski, J. A., (2000). "Thermal events occurring during the combustion of biomass residue," Fuel, Vol.79, pp. 181–92.

APPENDICES

APPENDIX – I

BIOMASS FORMULATION

Formulation of Pongamia pinnata

The pieces of the Pongamia pinnata wood are used for the gasification purpose in the downdraft gasifier. The ultimate analysis of the biomass used in the downdraft, for the composition of carbon (C), hydrogen (H), nitrogen (N) and sulphur (S), will be carried out using EuroEA Elemental Analyzer given as follows.

Name	N %	C%	H%	S%	Ash%	O%
Saw dust	4.462	44.547	8.872	-----	1	41.119

% of O = 100 - (% of C + % H + % N + % of Ash)

% of O = 100 – (44.547+8.872+4.462 + 1)

% of O = 41.119

(a) The following chemical equations are used for the calculation.

$$C + O_2 \rightarrow CO_2 \quad (1)$$

Using the molecular weight of the element 12 kg of carbon combines with 32 kg of oxygen and form 44 kg of CO_2.

$$1 \text{ kg of } C + \frac{8}{3} \text{ kg of } O_2 \rightarrow \frac{11}{3} \text{ kg of } CO_2 \quad (2)$$

(b)

$$2H_2 + O_2 \rightarrow 2H_2O \quad (3)$$

4kg of H_2 combines with the 32kg of O_2 and form 36kg of water.

$$4\text{kg of } H_2 + 32\text{kg of } O_2 \rightarrow 36\text{kg of } H_2O \quad (4)$$

$$1\text{kg of } H_2 + \ 8\text{kg of } O_2 \rightarrow \ 9\text{kg of } H_2O \tag{5}$$

Combustion process is highly irreversible with a large increase in entropy. It takes place at rapid rate.

Convert the mass concentration to number of kmol per 99kg biomass

$$C : n = \frac{44.547}{12.01} = 3.709 \tag{7}$$

$$H : n = \frac{8.872}{1.008} = 8.8 \tag{8}$$

$$O : n = \frac{41.119}{16} = 2.569 \tag{9}$$

$$N : n = \frac{4.462}{14.08} = 0.317 \tag{10}$$

Biomass formula obtained

3.709 C 8.8 H 2.560 O 0.317N $\Longrightarrow$ $\mathbf{C_{3.709}H_{8.8}O_{2.560}N_{0.317}}$ $\Longrightarrow$ $\mathbf{CH_{2.37}O_{0.69}}$

References	Biomass formula
Present work (Pongamia pinnata)	$\mathbf{CH_{2.37}O_{0.69}}$
Hand book of downdraft gasifier engine system SERI U.S. Department of energy	$\mathbf{CH_{1.4}O_{0.27}}$
Biomass gasification and pyrolysis by (Basu, 2010)	$\mathbf{CH_{1.35}O_{0.617}}$

APPENDIX – II

SOLUTION PREPARATION FOR FIBRE ANALYSIS

1) Neutral detergent solution (NDS)

a) Sodium lauryl sulphate - 30 gm
b) Di sodium ethylene diamine tetra acetate (EDTA) dehydrate crystals - 18.61 gm
c) Sodium borate decahydrate - 6.81gm
d) Disodium hydrogen phosphate anhydrous- 4.56gm
e) 2-Ethoxy ethanol (ethylene glycol mono ethyl ether) - 10 ml

Preparation

Take EDTA and sodium borate decahydrate in a beaker. Add some of the distilled water, shake and heat until these are dissolved. Add sodium lauryl sulphate and 1-ethoxy ethanol. Put disodium hydrogen phosphate in a separate beaker and add some of the distilled water and heat until it is dissolved. Mix both the solution properly and check PH to range between 6.9 and 7.1. If it is made properly then PH adjustment will be requiredrarely.

i) Decahydronaphthalene
ii) Acetone
iii) Sodium sulphate

2) Acid detergent solution (ADS).

a) 1N H_2SO_4- 49.04 gm/lit
b) Cetyltrimethyl ammonium bromide (CATB) – 20 gm

Add 20gm of (CTAB) to 1N H_2SO_4

i) Decahydronaphthalene
ii) Acetone
iii) N-Hexane

3) Reagent : H_2SO_4 72% by weight

It is prepared with 583 ml H_2SO_4 in 417 ml H_2O

APPENDIX – III

SPECIFICATION OF DOWNDRAFT BIOMASS GASIFIER

In the present experimentation on biomass gasification and feasibility of loose biomass in terms on biomass briquette and pellet is studied with the specification of Ankur make downdraft gasifier. The specification of downdraft gasifier is given as below.

GASIFIER	
Model	WBG-5 in scrubbed, clean gas mode
Related capacity (Elect.) in dual fuel mode	Gross output- 5 Kw Net output - 4kWe
Gasifier type	Downdraft
Average gas calorific value	1000 kcal/Nm^3
Gasification temperature	1050-1100^{0}C
Fuel storage capacity	85kg
Ash removal	Manual, Dry ash discharge
Start-up	Through scrubber pump
Fuel type and size	Wood/woody waste with maximum dimension not exceeding 25mm
Permissible moisture content in	Less than 20% (wet basis)
Biomass charging	On-line batch mode, by topping up once every 4
Rated hourly consumption	4-5kg/hr
Rated hourly ash discharge	0.250 - 0.380
Typical conversion efficiency	>75%
Typical gas composition reported by manual.	CO: 19 ± 3% H_2: 18 ± 2% CO_2:10 ± 3% CH_4- 13 ± 3% N_2- 50
Average diesel replacement	60 -75%
Biomass drying system	Based on hot exhaust engine output ≈ 4.0 kg/hr of wood pieces approx, 25 mm × 25 mm size

APPENDIX – IV
SPECIFICATION OF AUXILIARIES OF DOWNDRAFT BIOMASS GASIFIER

The downdraft gasifier consists of various auxiliaries as

A) Vibrator Motor
B) Comb Rotor motor
C) Gear Box for Comb Rotor
D) Scrubber Pump
E) Motor for Wood Cutter
F) Blade for Wood Cutter
G) Engine Generating Set

ENGINE SYSTEM	
Description	Single Cylinder, 1500 RPM, 7.36 kW, 10 BHP, water cooled, engine handle start.
ELECTRIC GENERATOR	
Description	Directly coupled to engine, 1500 rpm, 415 V, 3-Phase,
VIBRATOR MOTOR	**"ELCEN" MAKE**
HP	0.12
Voltage	415
RPM	1370
Phase	Three
MOTOR (COMBO ROTOR)	**"STEP SYN" AC SYNCRONOUS MOTOR**
Torque	30 kg.cm
Voltage	230
Full Load current	0.45 amp
Phase	single
GEAR BOX (COMBO ROTOR)	**"BONFIGLIOLI MAKE"**
Reduction ratio	60:1
Type	VF44
SCRUBBER PUMP	**AC, SINGLE PHASE TULLU PUMP**
kW	0.06

RPM	2800
Voltage	230V
MOTOR (WOOD CUTTER)	
HP	0.5
RPM	2800
Voltage	415
CUTTER BLADE	**TUNGSTEN CARBIDE CIRCULAR SAW**
Outer diameter	6” 150 cm
Number of teeth	40
Arbor diameter	25.4 mm

APPENDIX – V

CALIBRATION OF THERMOCOUPLE

The calibration of thermocouple is carried out by keeping one junction of the two dissimilar metals at constant temperature (at 0°C) and other junction is maintained at variable temperatures. The water circulating bath is used to maintain variable temperature. A high precision multi-meter is connected in the circuit to see the emf generation. The emf (millivolt) is recorded for every 5 °C temperature increase of water bath. The calibration curve for K type thermocouple is presented in the Fig.1. T type thermocouple is shown in Fig.2. Calibration charts were used for high temperature measurement.

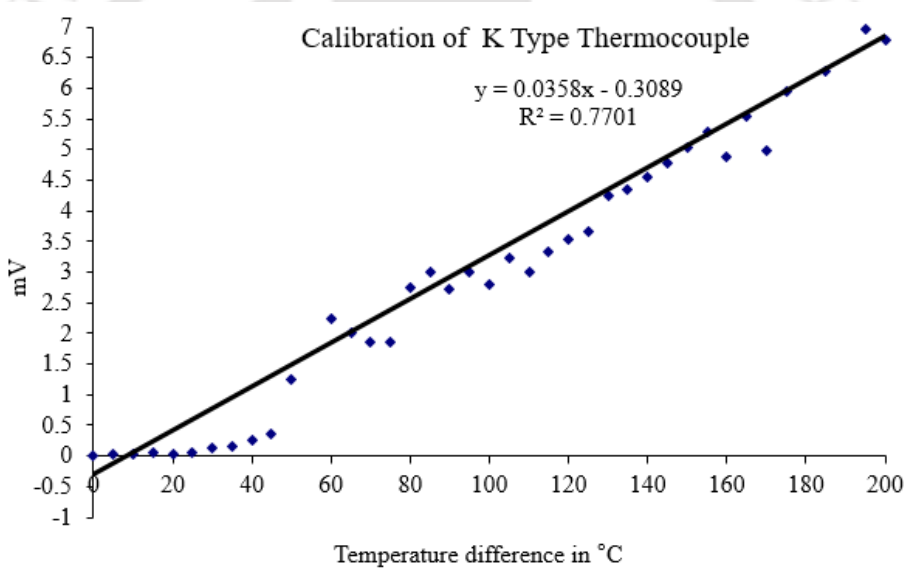

Fig. 1 Calibration of T type thermocouple

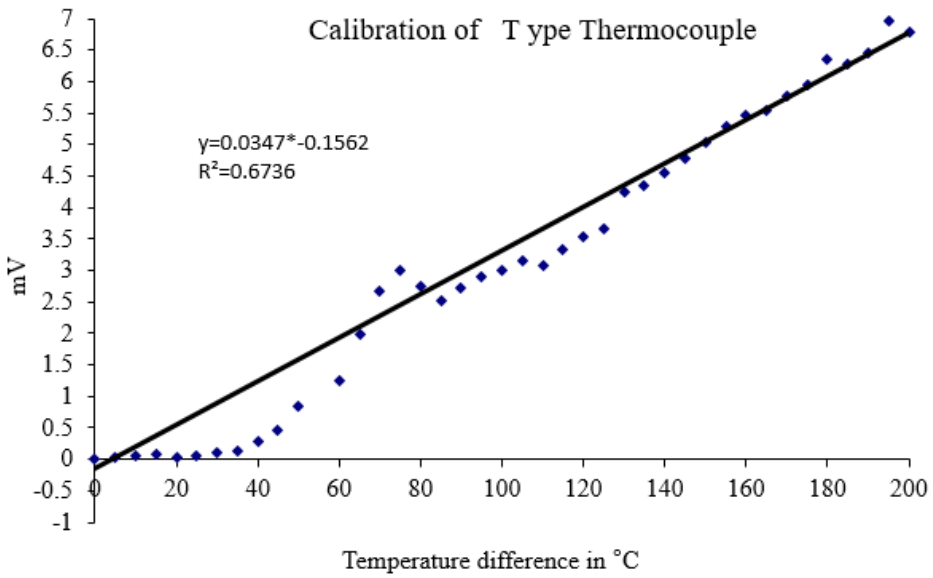

Fig. 2 Calibration of thermocouple

APPENDIX – VI

LOCATION OF TAR COLLECTION

Fig. 1 Tar collected in water tub

Fig. 2 Tar collected in water tank

Fig. 3 Tar deposited in coarse filter

Fig. 4 Tar deposited in fine filter

APPENDIX – VII

CALCULATION OF STOICHIOMETRIC A/F RATIO

The equation for the complete combustion of biomass can be written as Eq. 11

$$(3.709C + 8.8H + 2.569O + 0.317N) + a(O_2 + 3.76N_2) \rightarrow xCO_{2+y}H_2O + (0.317 + 7.52a)N \quad (1)$$

C Balance: x= 3.709

H_2 Balance: y= 4.4

O_2 Balance: 2.569+2a=2x+ y

a =x+0.05y- 1.285

a =3.709 + (0.05×4.4)-1.285

a = 4.624

$$(3.709C + 8.8H + 2.569O + 0.317N) + a(O_2 + 3.76N_2) \rightarrow 3.790CO_{2+}4.4H_2O + 17.54N_2 \quad (2)$$

$$\left(\frac{A}{F}\right)stoic = \frac{m_{air}}{m_{fuel}} = \frac{a(O_2 + 3.76N_2)}{99} = \frac{4.624 \times (32 + (3.76 \times 28.016))}{99} = \frac{4.624 \times 137.34}{99} = 6.41 \quad (3)$$

Hence

$$\left(\frac{A}{F}\right)stoic = 6.41 \quad (4)$$

The stoichiometric A/F ratio 6.41 is assumed same and used for calculation of equivalence ratio of all the biomass i.e. wood chip, biomass briquette, biomass pellet and biomass-dolomite pellet in the present experimentations.

APPENDIX – VIII

SPECIFICATION OF PELLET PRESS

The Pellet press is used to manufacture the biomass pellets. The pongamiapinnata dust pellet, Mustard husk pellet and pongamiapinnata-doliomite dust pellet, Mustard husk-dolomite pellets are prepared with this machine. The specification of Pellet Press is as given below.

PELLET PRESS MACHINE (HYTECH MAKE)	
Die plate diameter	250 mm
Die diameter	17 mm
Roller diameter	130 mm
Roller width	46 mm
No. of rollers	2
MOTOR	**"HAVELLS-LAFERT" MAKE THREE PHASE INDUCTION MOTOR**
HP (kW)	7.5 (5.5)
RPM	1139
Voltage	415 V
GEAR BOX	**"ELECON" Make**
Gear reduction ratio	5:1
Type	SNUSM
Size	3.5 inch

APPENDIX – IX
EXPERIMENTAL UNCERTAINTIES

The experimental uncertainties are calculated using theory of sequential perturbation technique by Kline and McClintok, 1953 and Moffat, 1982. This method describes the degree of accuracy with which the measurements has been made. The resolution or uncertainty of each measuring instrument is expressed with the same odds. These measurements are used to calculate some desired results of the experiments. These results show their uncertainty with respect to actual results.

Let us assume the dependent parameter N, which is a function of variables $x_1, x_2, x_3, ...x_n$ (Eq-1) such as

$$N = f(x_1, x_2, x_3, ..., x_n) \quad 1$$

The uncertainty ΔN due to the individual uncertainties of the independent parameters termed as $\Delta N_1, \Delta N_2, \Delta N_3, \Delta N_4, ..., \Delta N_n$ can be written as Eq-2

$$\pm N = \left[\left(\frac{dN}{dx_1} \Delta N_1 \right)^2 + \left(\frac{dN}{dx_2} \Delta N_2 \right)^2 + ... + \left(\frac{dN}{dx_n} \Delta N_n \right)^2 \right]^{1/2} \quad 2$$

1. Uncertainty in calculation of gas flow rate

The gas flow rate calculated as

$$P_g = \frac{m_g}{m_f}$$

Where, P_g is the mass flow rate of producer gas, m^3/kg

m_g is the mass flow rate gas, m^3/h, $\Delta N_1 = \pm 0.02\%$

m_f is the feedstock flow rate, kg/h, $\Delta N_2 = \pm 0.02\%$

Differentiating the above equation with respect to m_g and m_f

$$\frac{dP_g}{dm_g} = \frac{1}{m_f}$$

$$\frac{dP_g}{dm_g} = m_g$$

The overall uncertainty is

$$\pm N = \left[\left(\frac{dP_g}{dm_g} \Delta N_1 \right)^2 + \left(\frac{dN}{dx_2} \Delta N_2 \right)^2 \right]^{1/2}$$

$$= \left[\left(\frac{1}{m_f} \times 0.02 \right)^2 + \left(m_g \times 0.02 \right)^2 \right]^{1/2}$$

$$= \left[\left(\frac{1}{2.23} \times 0.02 \right)^2 + \left(4.28 \times 0.02 \right)^2 \right]^{1/2}$$

$$= \pm 0.086$$

2. Uncertainty calculation of calorific value of producer gas

The calorific value of producer gas can be calculated as

$$Q_{cv} = \frac{\left(x_1 \times CV \right)_{H_2} + \left(x_2 \times CV \right)_{CO} + \left(x_3 \times CV \right)_{CH_4}}{100}$$

Where, Q_{cv} is the calorific value of producer gas

The independent parameters are

x_1 - Percent hydrogen gas, (% vol.), $\Delta N_1 = \pm 0.02\%$

x_2 - Percent carbon monoxide gas, (% vol.), $\Delta N_2 = \pm 0.03\%$

x_3 - Percent Methane gas, (% vol.), $\Delta N_3 = \pm 0.03\%$

$$\frac{dQ_{cv}}{dx_1} = \frac{(CV)_{H_2}}{100}$$

$$\frac{dQ_{cv}}{dx_2} = \frac{(CV)_{CO}}{100}$$

$$\frac{dQ_{cv}}{dx_3} = \frac{(CV)_{CH_4}}{100}$$

The overall uncertainty is

$$\pm N = \left[\left(\frac{dQ_{cv}}{dx_1} \Delta N_1 \right)^2 + \left(\frac{dQ_{cv}}{dx_2} \Delta N_2 \right)^2 + \left(\frac{dQ_{cv}}{dx_3} \Delta N_3 \right)^2 \right]^{1/2}$$

$$= \left[\left(\frac{(CV)_{H_2}}{100} \times 0.02 \right)^2 + \left(\frac{(CV)_{CO}}{100} \times 0.03 \right)^2 + \left(\frac{(CV)_{CH_4}}{100} \times 0.03 \right)^2 \right]^{1/2}$$

$$= \left[\left(\frac{12.78}{100} \times 0.02 \right)^2 + \left(\frac{12.71}{100} \times 0.03 \right)^2 + \left(\frac{39.76}{100} \times 0.03 \right)^2 \right]^{1/2}$$

$$= \pm 0.012$$

The uncertainty analysis of the dependent parameters are tabulated below

Table-1. Uncertainty of experiment results

Sr No	Experimental parameter	Uncertainty magnitude
01	Mass flow rate of gas	± 0.086
02	Calorific value of producer gas	± 0.012
03	Gas conversion efficiency	± 0.064
04	Carbon conversion efficiency	± 0.045

APPENDIX – X

SPECIFICATION OF TAR CRACKING UNIT

The specification of Tar Cracking Liquid-Gas Bubbling Fluidized Unit is as given below.

TAR CRACKING UNIT(IITG MAKE)	
Tar Cracking Chamber diameter (mm)	101.6
Tar Cracking Chamber length (mm)	1020
Aeration pipe diameter (mm)	12.7
Pore diameter of aeration pipe (mm)	2
Tar residual pipe diameter (mm)	12.7
Air Inlet diameter (mm)	12.7
Tar-gas outlet diameter (mm)	12.7
ELEMENTAL HEATER	**230 V AC SINGLE PHASE**
kW	4
VERIAC	**VARIVOLT MAKE**
Voltage	0-270 V
amp	20
Size	3.5 inch
VOLTMETER	
Voltage	0-300
AMMETER	0-30
amp	
COMPRESOR	**INGERSOLL RAND (IR) MAKE** **MODEL: S-01480**
Litre	225
Maximum working pressure(kg/cm^2)	12.30
Motor (HP)	3
ROTAMETER	
Liter per minute	0-5

APPENDIX – XI
MEASUREMENT FACILITY

A) VISCOSITY MEASUREMENT

Viscosity is calculated with Rheometer as shown in Fig. 1.

Make- Anton Paar,
Model-Phsica MCR101

Fig.1 Rheometer

B) FESEM AND EDS

Field Emission Scanning Electron Microscope (FESEM) is microscope that works with electrons (particles with a negative charge). These electrons are liberated by a field emission source. The object is scanned by electrons according to a zig-zag pattern. Energy dispersive x-ray spectroscopy (EDS) is coupled with FESEM. It is used to determine chemical composition of micro-features. Figure 2 shows the Field Emission Scanning Electron Microscope (make-Zeiss and model- Sigma).

Make-Zeiss
Model- Sigma

Fig. 6.43. Field Emission Scanning Electron Microscope (FESEM)

C) FOURIER TRANSFORM INFRARED SPECTROSCOPY (FTIR) TECHNIQUE

Fourier transform infrared spectroscopy (FTIR) is a technique which is used to obtain an infrared spectrum of absorption or emission of a solid, liquid or gas. (Model: IR Affinity Make: SHIMADZU) as shown Fig. 6.48. FTIR spectrometer simultaneously collects high spectral resolution data over a wide spectral range.

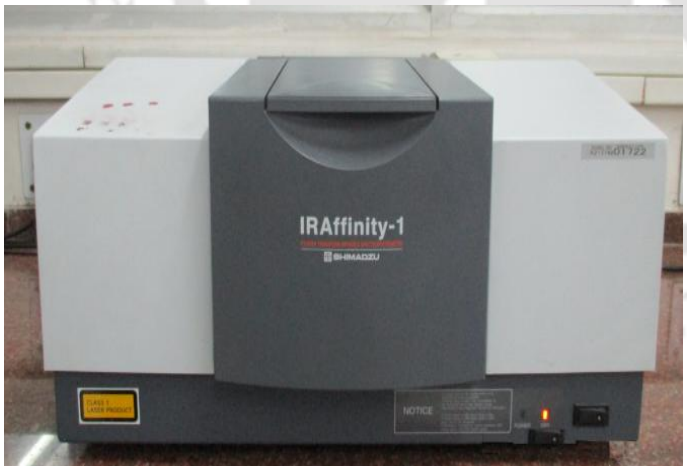

Model: IR Affinity

Make: SHIMADZU

Functional groups identified in FTIR spectra (Krishna and Pugazhenthi 2011)

The functional group identified by Krishna and Pugazhenthi (2011) are given in Table-1

Functional groups identified in FTIR spectra (Krishna and Pugazhenthi, 2011), (Blanco, 2012).

Frequency (cm^{-1})	Functional group (assignment)
3200–3600	Phenolic OH ,COOH & H_2O
3500	O–H stretching modes of interlayer water molecules and H-bonded OH groups
1630	Bending mode of water molecules
3070 - 3030	Aromatic C–H stretching vibration
2960-2930	Aliphatic C–H stretching vibration
3000-2850, 2848, 2920 and 2957	C−H stretching vibrations
1450-1350	C−Hde formation vibrations
1625-1575, 950-800	mono- and polycyclic aromatic compounds
1675-1352, 1504-1496	C = C stretching vibration from the alkene
1700	Phenol carboxylic acid and ketone
1100-1050	bonds (C−H) and long linear aromatic
1100-1200	ether and phenolic OH
1400–1600	Aromatic structures
757-698	CH out-of-plane bending of phenyl ring or mono substituted benzene

D) GC/MS

The GC–MS spectrum Chromatograph is as shown in Fig. 6.51.

Varian 450-GC

Varian 240- Mass Spectrometer

GCMS spectrum

Appendix – XII

List of Equipment/Instrument Used

List of instrument used

- Data acquisition system, Agilent 34970A (Data acquisition switch unit with multiplexer)
- Gas flow meter , manufacture by Chongqing Actaris metring system, Model: Gallus 2000
- Compressor: Capacity: 225 litres, Maximum working pressure: 12.30 kg/cm^2, run by a 3 hp motor, manufacture by Ingersoll Rand (IR), Model: S-01480
- Weighing balance: weighing scale panel, measuring range; max = 15 kg, min = 0.04 kg, error, error =2 gm, Model: SP/p1s-15-FLP, manufactured by Shyam Switchgears Pvt. Ltd.
- Variac, Make: VARIVOLT (0-270 V), 20 amp
- Pressure gauge, Make: Swagelok, Model: EN837-1
- Pressure regulator, Make: Swagelok
- Stop watch, Ball valve, Gate valve, one way valve, Flow control valve, Bye pass valve, Air control valve
- Water tube manometer
- Manometer board
- Pressure tapings
- Rotameter for the flow measurement
- Thermocouple sensor – K type and T type
- Non contact type thermo meter (infra red)
- Thermocouple calibrator with constant temperature bath.

List of Publications

JOURNAL PUBLICATIONS

(1) Shelke, G. N. and Mahanta, P. (2014). "Biomass briquette characterization for downdraft gasification," Applied Mechanics and Materials. Vols. 592-594: pp 2442-2446.

(2) Shelke, G. N. and Mahanta, P. (2016). "Feasibility Study on Utilization of Biomass Briquette in a Conventional Downdraft Gasifier," International Energy Journal 16 (2016) 157-166.

CONFERENCE PUBLICATIONS

(1) Shelke, G. N., Mahanta, P., Patil, R. S., (2014), "Experimental Studies on Thermal Behavior of Downdraft Gasifier," Proceedings of the World Congress on Engineering , London, U.K., 2 - 4, July, WCE, Vol II: pp 1356-1359.

(2) Shelke, G. N., Bora, D., Mahanta, P., (2015), Fibre analysis and estimation of heating value for biomass briquettes, Workshop on Frontier Energy Research with Industry-Academia partnership, Center for Energy IIT Guwahati, March 20-21 (2015).

(3) Shelke, G. N. and Mahanta P. (2015), "Performance analysis of downdraft gasification with biomass briquette," NTPC Energy Technical Journal, e-Compendium GETS (2015) 229.

(4) Shelke, G. N. and Mahanta, P. (2015). "Comparative analysis of downdraft gasification for woodchips and biomass briquette/pellets," CHMCON-2015, Chemical Engineering Department, IIT Guwahati, December 27-30 (2015).